

FAUSKE & ASSOCIATES, INC.  
CALCULATION NOTE COVER SHEET

SECTION TO BE COMPLETED BY AUTHOR(S):

Page i

Calc-Note Number FAI/99-77 Revision Number 2

Title Containment Sump Level Evaluations for the D.C. Cook Plant

Project Containment Sump Level Evaluations for the D.C. Cook Plant Shop Order AEP-009

Purpose: This set of analyses addresses the minimum levels in the D.C. Cook recirculation sump following a postulated Loss-Of-Coolant Accident (LOCA). In these analyses a spectrum of break sizes has been considered from 1/2 inch in diameter to the equivalent of a double-ended cold leg break. In addition, analyses have been performed for postulated main steam line breaks into the containment lower compartment. Moreover, analyses have been performed for postulated breaks associated with mode 3 operations with the initial Reactor Coolant System (RCS) temperature at or below 350°F. As part of these analyses, the MAAP4 models for ice melting and ice condenser containment response were benchmarked with available experiments for ice melting and global containment response for ice condenser containment geometries.

Results Summary: Compliance with the 602'10" Mode 1 vortexing limit is demonstrated. Sufficient sump level for Mode 3 and MSLB operations is also demonstrated. Revision 2 incorporates DIT-B-00011-04 which provides all of the final "Approved for Use" design input values. These design input values did not change the results or conclusions.

Author(s):

Completion  
Date

Name (Print or Type)

Signature

R. E. Henry

Robert E. Henry

Sept. 17, 1999

R. J. Hammersley

R. J. Hammersley

September 21, 1999

C. Y. Paik

Chan Young Paik

September 21, 1999

R. W. Reeves

R. W. Reeves

Sept. 21, 1999

SECTION TO BE COMPLETED BY VERIFIER(S):

Verifier(s):

Completion  
Date

Name (Print or Type)

Signature

W. Luangdilok

Alison Luangdilok

9/21/1999

Method of Verification: Design Review \_\_\_\_\_  
Other (Specify) \_\_\_\_\_

Independent Review or

Alternate Calculations ☒

Testing \_\_\_\_\_

SECTION TO BE COMPLETED BY MANAGER:

Responsible Manager:

Approval  
Date

Name (Print or Type)

Signature

R. J. Hammersley

R. J. Hammersley

September 22, 1999

9910060104 991001  
PDR ADDCK 05000315  
P PDR



CALC NOTE NUMBER FAI/99-77 REV. 2 PAGE ii

CALCULATION NOTE METHODOLOGY CHECKLIST

CHECKLIST TO BE COMPLETED BY AUTHOR(S) (CIRCLE APPROPRIATE RESPONSE)

1. Is the subject and/or the purpose of the design analysis clearly stated? ..... YES • NO
2. Are the required inputs and their sources provided? ..... YES • NO • N/A
3. Are the assumptions clearly identified and justified? ..... YES • NO • N/A
4. Are the methods and units clearly identified? ..... YES • NO • N/A
5. Have the limits of applicability been identified? ..... YES • NO • N/A  
(Is the analysis for a 3 or 4 loop plant or for a single application.)
6. Are the results of literature searches, if conducted, or other background data provided? ..... YES • NO • N/A
7. Are all the pages sequentially numbered and identified by the calculation note number? ..... YES • NO
8. Is the project or shop order clearly identified? ..... YES • NO
9. Has the required computer calculation information been provided? ..... YES • NO • N/A
10. Were the computer codes used under configuration control? ..... YES • NO • N/A
11. Were the computer code(s) used applicable for modeling the physical and/or computational problems identified? ..... YES • NO • N/A  
(Is the correct computer code being used for the intended purpose.)
12. Are the results and conclusions clearly stated? ..... YES • NO
13. Are Open Items properly identified ..... YES • NO • N/A
14. Were approved Design Control practices followed without exception? ..... YES • NO • N/A  
(Approved Design Control practices refers to guidance documents within WNATD that state how the work is to be performed, such as how to perform a LOCA analysis.)
15. Have all related contract requirements been met? ..... YES • NO • N/A

NOTE:

If NO to any of the above, Page Number containing justification \_\_\_\_\_





*FAI/99-77  
(Revision 2)*

***CONTAINMENT SUMP LEVEL  
EVALUATIONS FOR THE  
D.C. COOK PLANT***

Submitted To:

American Electric Power

Prepared By:

Fauske & Associates, Inc.  
16W070 West 83rd Street  
Burr Ridge, Illinois 60521  
Tel: (630) 323-8750  
Fax: (630) 986-5481

September, 1999

## PURPOSE

This set of analyses addresses the minimum levels in the D.C. Cook recirculation sump following a postulated Loss-Of-Coolant Accident (LOCA). In these analyses a spectrum of break sizes has been considered from 1/2 inch in diameter to the equivalent of a double-ended cold leg break. In addition, analyses have been performed for postulated main steam line breaks into the containment lower compartment. Moreover, analyses have been performed for postulated breaks associated with mode 3 operations with the initial Reactor Coolant System (RCS) temperature at or below 350°F. As part of these analyses, the MAA4 models for ice melting and ice condenser containment response were benchmarked with available experiments for ice melting and global containment response for ice condenser containment geometries.



## INPUT DATA AND ASSUMPTIONS

The input data and assumptions used in this report are derived from several references as listed below.

1. LOTIC-3 and NOTRUMP results - Westinghouse Electric Corporation letter NSD-SAE-ESI-97-555 from Donald E. Peck to Bob Henry dated October 1, 1997.
2. AEP document on recirculation sump inventory analysis - analysis input assumptions, transmitted to FAI by a letter from John Olvera to R.E. Henry, October 2, 1997. This includes items that are closed, which are treated as input and items that are classified as "opened" which are treated as assumptions unless they have been resolved by documents listed below.
3. Information related to stated values in the Donald C. Cook UFSAR which include:
  - performance of the ice condenser drain lines,
  - spray droplet size for the containment sprays,
  - water holdup in the refueling canal during spray operation is conservatively assumed to be UFSAR value.
4. Evaluations of operator responses during the post-LOCA cooldown and RCS depressurization are taken from the Donald C. Cook procedure number 02-OHP 4023.ES1.2, Rev. 5.
5. A series of Design Information Transmittals (DITS) which are included and discussed in this report as Appendix A.



6. Initial containment pressure is the highest allowed (0.3 psig) per Cook Technical Specifications Section 3/4.6-7 as this minimizes the time to spray initiation which reduces the melted ice mass.

## TABLE OF CONTENTS

	First Page	Last Page
CALC NOTE COVER SHEET	i	i
CALC NOTE CHECKLIST	ii	ii
TITLE PAGE	iii	iii
PURPOSE	iv	iv
INPUT DATA AND ASSUMPTIONS	v	vi
TABLE OF CONTENTS	vii	x
LIST OF FIGURES	xi	xv
LIST OF TABLES	xvi	xvi
1.0 INTRODUCTION	1-1	1-5
2.0 THE MAAP4 MODEL OF D.C. COOK AND COMPARISONS WITH DESIGN BASIS CALCULATIONS	2-1	2-21
2.1 Introduction	2-1	
2.2 MAAP4 Modeling of the D.C. Cook Plant	2-1	
2.2.1 Important Features in MAAP4.0.4	2-12	
2.2.2 Representation of Important Phenomena Related to the Accident Sequence	2-14	
2.2.3 MAAP4 Representation of Pump and Air Recirculation Fan Curves	2-17	
3.0 BENCHMARKING OF THE MAAP4 ICE CONDENSER CONTAINMENT MODEL	3-1	3-21
3.1 Introduction	3-1	

3.2	Comparison of the MAAP4 Containment Model With LOTIC-3 for a Six-Inch Cold Leg LOCA	3-4	
3.2.1	Boundary Conditions	3-4	
3.2.2	Results	3-6	
3.3	Comparison of the MAAP4 Containment Model with LOTIC-3 for a Two-Inch Cold Leg LOCA	3-6	
3.3.1	Boundary Conditions	3-6	
3.3.2	Results	3-8	
3.4	Comparison of the MAAP4 and NOTRUMP Mass and Energy Releases for a Two-Inch Cold Leg LOCA	3-8	
3.5	Westinghouse Waltz Mill Tests	3-12	
3.5.1	Boundary Conditions	3-17	
3.5.2	Results	3-17	
3.6	PNL Ice Condenser Experiments	3-18	
3.6.1	Boundary Conditions	3-18	
3.6.2	Results	3-18	
3.7	CSTF Ice Condenser Experiments	3-18	
3.7.1	Boundary Conditions	3-19	
3.7.2	Results	3-19	
3.8	Discussion of the McQuire Event	3-20	
3.9	Summary	3-20	
4.0	DESCRIPTION OF THE MOST LIMITING CONDITIONS FOR CONTAINMENT SUMP EVALUATIONS AND SENSITIVITY ANALYSES PERFORMED WITH MAAP4	4-1	4-13
4.1	Introduction	4-1	



4.2	Key Plant Parameters	4-2	
4.3	FMEA Conditions Used in the Analyses	4-9	
4.4	Modeling of the EOPs	4-9	
4.4.1	Transfer to Containment Recirculation	4-10	
4.4.2	Duration of the Containment Sprays	4-11	
4.4.3	Pressurizer Level Control	4-12	
4.4.4	RCS Cooldown	4-12	
4.4.5	Isolating the Accumulators	4-13	
5.0	ANALYTICAL RESULTS FOR THE COMPLETE SPECTRUM OF LOCA SIZES	5-1	5-49
5.1	Introduction	5-1	
5.2	Base Case Results	5-7	
5.2.1	RCS Break Location in the Lower Compartment	5-7	
5.2.2	Split Flow Pipe Breaks into the Sump and the Reactor Cavity	5-17	
5.2.3	Breaks Into the Reactor Cavity	5-27	
5.2.4	Summary of Minimum Sump Level	5-27	
5.3	Details of the Most Limiting Case	5-31	
5.4	Sensitivity Analyses for Mode 1 Evaluations	5-41	
5.5	Conservatisms in the Analyses	5-42	
6.0	ANALYTICAL RESULTS FOR THE CONTAINMENT SUMP INVENTORY FOLLOWING A LOCA UNDER MODE 3 CONDITIONS	6-1	6-12
7.0	ANALYTICAL RESULTS FOR THE CONTAINMENT SUMP INVENTORY FOLLOWING A MAIN STEAM LINE BREAK	7-1	7-3



8.0	CONCLUSIONS	8-1	8-3
9.0	REFERENCES	9-1	9-3
APPENDIX A:	Design Information Transmittals (DITs)	A-1	A-38
APPENDIX B:	Flow Split for Postulated Ruptures in the Cold Leg Near the RPV	B-1	B-7
APPENDIX C:	Ice Condenser Door Opening	C-1	C-9
APPENDIX D:	Representation of the Ice Condenser Outlet Temperature	D-1	D-9
APPENDIX E:	Benchmarking of the MAAP4-Ice Condenser Model With Waltz Mill Experiments	E-1	E-30
APPENDIX F:	Benchmarking of the MAAP ice Condenser Model With the PNL Ice Condenser Experiments	F-1	F-14
APPENDIX G:	Benchmarking of the CSTF	G-1	G-40
APPENDIX H:	Droplet Fall Velocity	H-1	H-3
APPENDIX I:	Water Film Drainage Analysis	I-1	I-2



## LIST OF FIGURES

Figure 2-1	Basic layout for an ice condenser containment . . . . .	2-2
Figure 2-2	D.C. Cook containment nodalization revision 4 MAAP4 parameter file (14 nodes/44 junctions) . . . . .	2-3
Figure 2-3	MAAP4 representation of the D. C. Cook reactor cavity (Node 1) . . . . .	2-8
Figure 2-4	PWR primary system nodalization for Westinghouse 4-loop design taken from the MAAP4 User's Manual (EPRI, 1999) . . . . .	2-10
Figure 2-5	MAAP4 functional behavior for a single high head injection pump (see Appendix A for vendor and system data) . . . . .	2-18
Figure 2-6	MAAP4 functional behavior for a single charging pump (see Appendix A for vendor and system data) . . . . .	2-19
Figure 2-7	MAAP4 functional behavior for a single air recirculation fan . . . . .	2-20
Figure 3-1	Comparison of the LOTIC-3 and MAAP4 ice depletion rate for a six-inch diameter cold leg LOCA (NOTRUMP) for the D.C. Cook Unit 2 . . . . .	3-7
Figure 3-2	Comparison of the LOTIC-3 ice depletion rate for a two-inch diameter cold leg LOCA with the MAAP4 calculation using the same mass and energy inputs from the NOTRUMP calculation . . . . .	3-10
Figure 3-3	Comparison of the upper and lower containment compartment temperatures for a LOTIC-3 calculated biased for maximum containment pressure and the MAAP4 representation with the accident initiator being a two-inch diameter cold leg LOCA as represented by NOTRUMP . . . . .	3-11
Figure 3-4	A comparison of the instantaneous mass flow rates for the MAAP4 primary system and NOTRUMP assuming a two- inch cold leg LOCA . . . . .	3-13



Figure 3-5	A comparison of the integral mass release to containment for NOTRUMP and the MAAP4 primary system model assuming a two-inch cold leg LOCA . . . . .	3-14
Figure 3-6	A comparison of the instantaneous energy release to the containment for NOTRUMP and the MAAP4 primary system model assuming a two-inch cold leg LOCA . . . . .	3-15
Figure 3-7	Primary system pressure for MAAP4 and NOTRUMP for a two-inch cold leg LOCA . . . . .	3-16
Figure 4-1	Water flow paths to the active and inactive sump regions . . . . .	4-5
Figure 4-2	Elevation view of an ice condenser including the drain line . . . . .	4-6
Figure 5-1	A description of the in-core instrument penetrations for the D.C. Cook design . . . . .	5-4
Figure 5-2	A summary of the primary system and containment response for a DECL break into the lower compartment . . . . .	5-8
Figure 5-3	A summary of the primary system and containment response for a 6 inch dia. cold leg break into the lower compartment . . . . .	5-10
Figure 5-4	A summary of the primary system and containment response for a 4 inch dia. cold leg break into the lower compartment . . . . .	5-11
Figure 5-5	A summary of the primary system and containment response for a 3 inch dia. cold leg break into the lower compartment . . . . .	5-12
Figure 5-6	A summary of the primary system and containment response for a 2 inch dia. cold leg break into the lower compartment . . . . .	5-14
Figure 5-7	A summary of the primary system and containment response for a 1.5 inch dia. cold leg break into the lower compartment . . . . .	5-15
Figure 5-8	A summary of the primary system and containment response for a 1 inch dia. cold leg break into the lower compartment . . . . .	5-16
Figure 5-9	A summary of the primary system and containment response for a 0.5 inch dia. cold leg break into the lower compartment . . . . .	5-18





Figure 5-10	A summary of the primary system and containment response for a 1 ft <sup>2</sup> area cold leg break into the reactor cavity and lower compartment . . . . .	5-20
Figure 5-11	A summary of the primary system and containment response for a 4 inch dia. cold leg break into the reactor cavity and lower compartment . . . . .	5-21
Figure 5-12	A summary of the primary system and containment response for a 3 inch dia. cold leg break into the reactor cavity and lower compartment . . . . .	5-22
Figure 5-13	A summary of the primary system and containment response for a 2 inch dia. cold leg break into the reactor cavity and lower compartment . . . . .	5-24
Figure 5-14	A summary of the primary system and containment response for a 1.5 inch dia. cold leg break into the reactor cavity and lower compartment . . . . .	5-25
Figure 5-15	A summary of the primary system and containment response for a 1 inch dia. cold leg break into the reactor cavity and lower compartment . . . . .	5-26
Figure 5-16	A summary of the primary system and containment response for a 2.75 inch dia. upper head break into the reactor cavity . . . . .	5-28
Figure 5-17	A summary of the primary system and containment response for a 0.61 inch dia. break in the bottom of the RPV . . . . .	5-29
Figure 5-18	A summary of the minimum sump water levels for the spectrum of breaks considered in the lower compartment and the reactor cavity for Mode 1 operation . . . . .	5-30
Figure 5-19	A summary of the melted ice mass for the spectrum of LOCAs considered into the lower compartment and the reactor cavity . . . . .	5-32
Figure 5-20a	Details of the primary system and containment response for the most limiting case of a 1 inch dia. break into the reactor cavity . . . . .	5-33
Figure 5-20b	Details of the primary system and containment response for the most limiting case of a 1 inch dia. break into the reactor cavity . . . . .	5-34



Figure 5-20c	Details of the primary system and containment response for the most limiting case of a 1 inch dia. break into the reactor cavity . . . . .	5-35
Figure 5-20d	Details of the primary system and containment response for the most limiting case of a 1 inch dia. break into the reactor cavity . . . . .	5-36
Figure 5-20e	Details of the primary system and containment response for the most limiting case of a 1 inch dia. break into the reactor cavity . . . . .	5-37
Figure 5-20f	Details of the primary system and containment response for the most limiting case of a 1 inch dia. break into the reactor cavity . . . . .	5-38
Figure 5-21	Comparison of the minimum water levels for a 1.5 inch break into the reactor cavity assuming (a) the failure of a single CEQ fan, (b) the failure of a complete train of ECCS and containment safeguards and (c) no failure of either ECCS/containment safeguard train . . . . .	5-43
Figure 5-22	Details of original sump taken from Padmanabhan (1978) . . . . .	5-47
Figure 5-23	A summary of the minimum sump water levels versus sump total suction flow rate for Mode 1 operation . . . . .	5-48
Figure 6-1	Summary of the results for a 6 inch LOCA into the lower compartment under Mode 3 conditions . . . . .	6-2
Figure 6-2	Summary of the results for a 2 inch LOCA into the reactor cavity under Mode 3 conditions . . . . .	6-3
Figure 6-3	Summary of the results for a 4 inch LOCA into the lower compartment under Mode 3 conditions . . . . .	6-4
Figure 6-4	Summary of the results for a 3 inch LOCA into the lower compartment under Mode 3 conditions . . . . .	6-5
Figure 6-5	Summary of the results for a 6 inch split flow LOCA under Mode 3 conditions . . . . .	6-7
Figure 6-6	Summary of the results for a 4 inch split flow LOCA under Mode 3 conditions . . . . .	6-8
Figure 6-7	Summary of the results for a 3 inch split flow LOCA under Mode 3 conditions . . . . .	6-9



Figure 6-8	Comparison of the minimum required sump level and the minimum calculated levels for the lowest RCS temperature in Mode 3 .....	6-11
Figure 7-1	Summary of the minimum sump inventory for a steam line break of 1.4 ft <sup>2</sup> into the lower compartment .....	7-2
Figure 7-2	Summary of the minimum sump inventory for a steam line break of 4.6 ft <sup>2</sup> into the lower compartment .....	7-3

## LIST OF TABLES

Table 2-1	D.C. Cook 14-Node Containment Nodalization . . . . .	2-4
Table 2-2	D.C. Cook 14-Node Containment Model Flow Junctions . . . . .	2-5
Table 2-3	D.C. Cook 14-Node Containment Fan Flow Rates . . . . .	2-7
Table 2-4	Pedigree of the D.C. Cook MAAP4 Parameter File . . . . .	2-11
Table 3-1	Mass and Energy Source Rates to the Containment From the NOTRUMP Analyses for a Six-Inch Cold Leg LOCA . . . . .	3-5
Table 3-2	NOTRUMP Mass and Energy Releases for a Two-Inch Cold Leg LOCA . . . . .	3-8
Table 3-3	Summary of the Benchmarks Related to the D.C. Cook Containment Sump Evaluations . . . . .	3-21
Table 4-1	Water Inventory Available . . . . .	4-3
Table 4-2	Volumes Controlling Water Accumulation in the Analysis . . . . .	4-3
Table 4-3	Potential Locations of Spray Water Holdup . . . . .	4-8
Table 5-1	Break Size/Location Matrix for Evaluating Minimum Level in the Containment Sump for a Mode 1 Operating Condition . . . . .	5-6
Table 5-2	Mass Balance at the Time of Minimum Sump Level for 1 Inch Small LOCA (50% to Cavity and 50% to Lower Compartment) . . . . .	5-41
Table 6-1	Summary of Mode 3 Results . . . . .	6-10



## 1.0 INTRODUCTION

This report evaluates the containment sump level history for postulated LOCA conditions, including the injection phase, the transfer from injection to recirculation and recirculation phase. As such, this integral analysis using the MAAP4 code 4.0.4.1 (FAI, 1999) addresses whether the containment sump level is above the licensing base limit for vortexing established at the 602'10" elevation (approximately 4 ft above the lower compartment floor) by D.C. Cook specific containment sump tests under maximum Emergency Core Cooling System (ECCS) and containment safeguard flow rates (Padmanabhan, 1978). (The last digit in the code designation indicates an enhancement to the official internationally distributed version of 4.0.4 to enable separate temperatures to be supplied on the cooling side of the containment spray heat exchangers and the RHR heat exchangers.) These scaled containment sump experiments are the licensing basis for protecting against vortexing/air ingress into the D.C. Cook recirculation piping. The necessary water level derived from these experiments, along with additional information derived from the experiments for less than full ECCS and containment safeguards flow rates, is used to evaluate the protection against air ingress for accident conditions. Since most of the accidents have relatively small breaks in the RCS, the demands on the containment sump are less than those for the design basis Double Ended Cold Leg (DECL) break.

The MAAP4 code was used since it provides an integral evaluation of the RCS and containment response. Both are necessary for this assessment since the water inventory in the sump is influenced by:

- the RWST injection and containment spray,
- the melted ice mass,
- the holdup in the RCS,
- the extent of accumulator injection, and
- the water flow between containment compartments.





The integral nature of the MAAP4 model for D.C. Cook, the nodalization of the various compartments of the ice condenser containment, the behavior of the ice condenser inlet doors, and the capability to consider that the break discharge flow may be simultaneously directed to two compartments are important code features. Moreover, the MAAP4 models describing ice melting and ice condenser containment response have been benchmarked with the large scale ice melting and containment response experiments performed to investigate the containment response.

These analyses were performed using the following computer system, operating system, and compiler.

Computer:	DEC ALPHA
Operating System:	Open VMS V6.2
FORTTRAN Compiler:	DEC FORTRAN V6.3-711

The version of the parameter file used for these analyses is:

\$6\$DKA0:[DCCOOK.AEP005.INPUT]COOK\_MAAP4\_REV4.PAR

The input and output files for these analyses are documented in FAI QA Report FAI/99-84 entitled "Input and Output Files for D.C. Cook Minimum Sump Level Analyses Reported in FAI/99-77," (FAI, 1999). The input and output files can be found in the record

\$6\$DKA0:[DCCOOK.JUL99.1CEQ.SUBMIT.SAVE].

A complete spectrum of RCS break sizes are evaluated for Mode 1 conditions beginning with the DECL and including all break sizes which are sufficient to initiate containment sprays. Also included are the operator actions associated with establishing recirculation and RCS cooldown. Furthermore, as a conservatism these analyses use the plant conditions that have been judged to be the most limiting in terms of the mass of ice melted since this water inventory is added to the containment sump and is an important element of the evaluation. These analyses also



include new plant modifications to the crane wall to permit open communication of water between the pipe annulus and the active sump as well as the earlier actuation of air recirculation fans.

These analyses also considered different system configurations, such as one train of ECCS/safeguards operating, two trains of ECCS/safeguards operating and two trains performing with an individual single failure. Through these integral analyses, the most limiting cases for the containment sump water level recirculation can be determined.

In addition to the Mode 1 LOCA evaluations, the containment response to breaks in the RCS pressure boundary conditions were also assessed for Mode 3 conditions, i.e., conditions inclusive of hot shutdown to a RCS temperature of 350°F. (During the cooldown, the RCS pressure is maintained at, or above 1000 psia.) These analyses considered the low end of Mode 3 at the time the break occurs since this is conservative with respect to ice melt and sump water level. With these conditions, the reactor coolant saturation pressure is 135 psia, and as a consequence, the steam flow to the containment is substantially reduced. As a result, these sequences are extended in time which has a substantial influence on the performance of the ice condenser containment.

Lastly, analyses were also performed for two main steam line break sizes with the reactor at 100% full power. These breaks discharge steam into the lower compartment and also are sufficient to pressurize the containment to the setpoints for the air recirculation fans (CEQ fans) and the containment sprays. Therefore, these sequences are also included in the evaluation matrix.

To document these analyses, this report is organized as follows.

- Section 2 - discusses a description of the MAAP4 model for D.C. Cook.
- Section 3 - provides the dynamic benchmarking information for the MAAP4 models with available design basis models and ice condenser experiments. These include:



- a comparison of the ice melting rates for the MAAP4 best estimate model and the LOTIC-3 Design Basis Analysis (DBA) approach,
  - a comparison of the MAAP4 mass and energy releases to the containment and those calculated for a small break LOCA using the licensing basis NOTRUMP code,
  - comparison with the Waltz Mill and PNL ice condenser experiments as well as the CSTF tests for mixing in ice condenser containments.
- 
- Section 4 - documents those conditions which are the most limiting for containment sump evaluations.
  - Section 5 - discusses the analytical results for the containment sump level with respect to the 602'10" licensing base limit for vortexing for the Mode 1 LOCAs.
  - Section 6 - discusses the results for the Mode 3 LOCAs.
  - Section 7 - discusses the results of the main steam line break analyses.
  - Section 8 - provides the conclusions from these evaluations.
  - Section 9 - lists the references for the text.

The list of appendices include:

- Appendix A - information documented in Design Information Transmittals.
- Appendix B - a discussion of the flow split for cold leg breaks near the reactor vessel.



- Appendix C - a discussion of how MAAP represents opening of the ice condenser doors.
- Appendix D - a description of the MAAP4 model for the ice condenser exit temperature.
- Appendix E - a summary of the MAAP4 benchmark with the Waltz Mill tests.
- Appendix F - a description of the MAAP4 benchmark with the PNL ice condenser tests.
- Appendix G - a discussion of the MAAP4 benchmark with the CSTF experiments.
- Appendix H - a discussion of the spray droplet fall velocity used for water holdup calculations.
- Appendix I - an assessment of water film drainage on vertical walls which is also used for estimating water holdup.





## 2.0 THE MAAP4 MODEL OF D.C. COOK AND COMPARISONS WITH DESIGN BASIS CALCULATIONS

### 2.1 Introduction

The MAAP4 integral characterization of D.C. Cook (FAI, 1997) includes models for the RCS, containment, ECCS, emergency safeguard systems, etc. This fast running, best-estimate model can explore the influence of variations in the accident, the initial conditions, tech spec allowable variations in key plant parameters, operator actions, etc. This section summarizes the MAAP4 model for D.C. Cook and also discusses some of the important modeling features that are important for assessing the minimum sump inventory.

### 2.2 MAAP4 Modeling of the D.C. Cook Plant

This MAAP4 model of D.C. Cook uses a 14 node containment model and 44 flow junctions coupling the various nodes. Both forced and natural convection flows are represented with the hydrogen skimmer flows being considered as part of the forced flow system. Figures 2-1 and 2-2 illustrate the containment and the 14 node scheme with Tables 2-1, 2-2 and 2-3 listing the containment nodes, the 44 flow junctions and the flow rates used for the hydrogen skimmer and CEQ flows to the various compartments. Typically each node is represented by a free volume versus height table. Since the reactor cavity is a major part of the containment sump analyses, this has a detailed volume versus height table as illustrated in Figure 2-3. It should also be noted in Table 2-2 that, in addition to the normal flow paths, two flow paths (junctions 43 and 44) are included to represent the flow area between the lower compartment and the reactor cavity due to holes in the biological shield wall to accommodate Nuclear Instrumentation System (NIS) reach rods. An additional node (number 15) was used to represent the containment spray header which distributed water to the upper and lower compartment sprays simultaneously. Note that this is only used for spray headers in the different compartments. The 14 nodes listed in Table 2-1

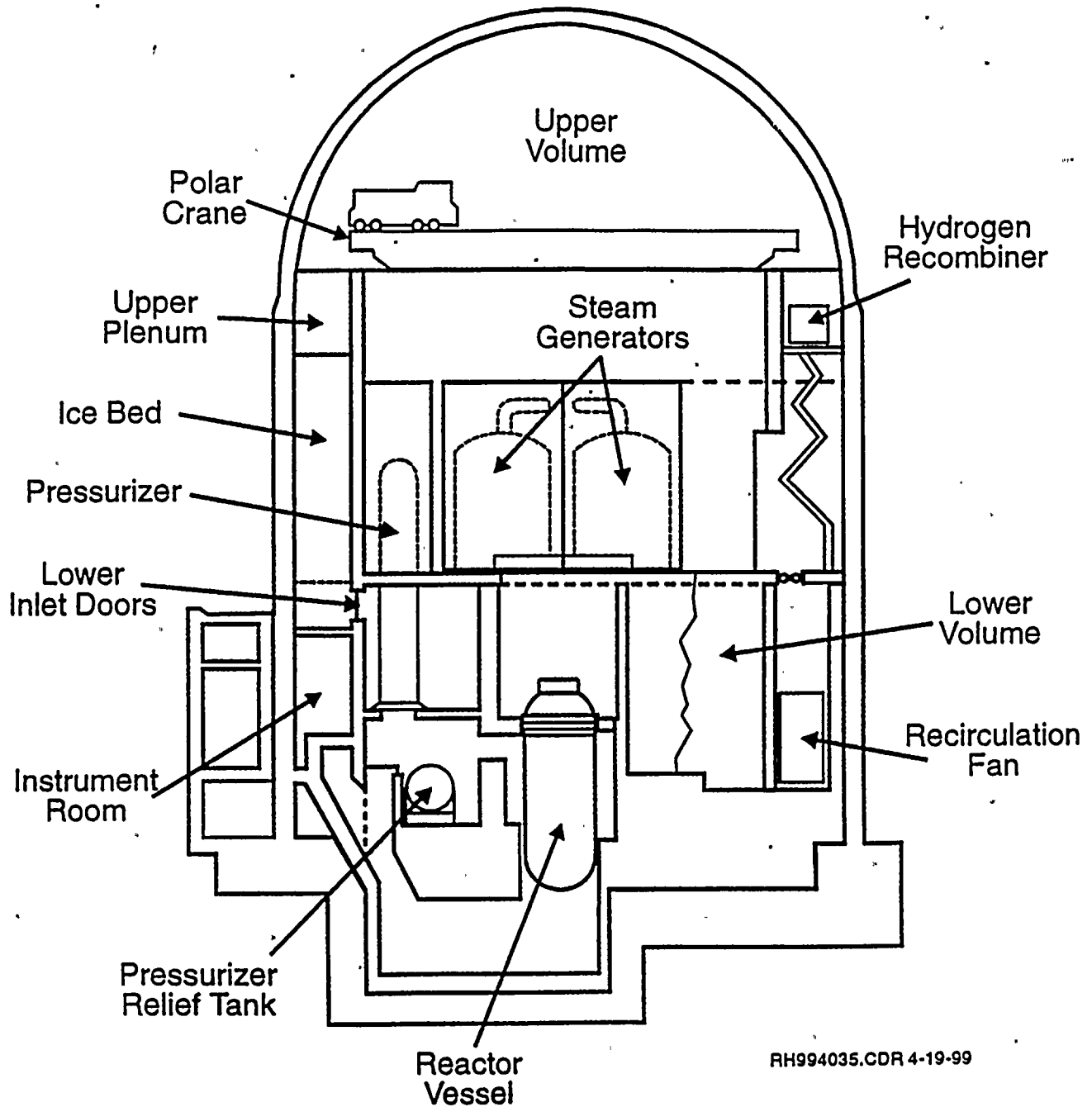
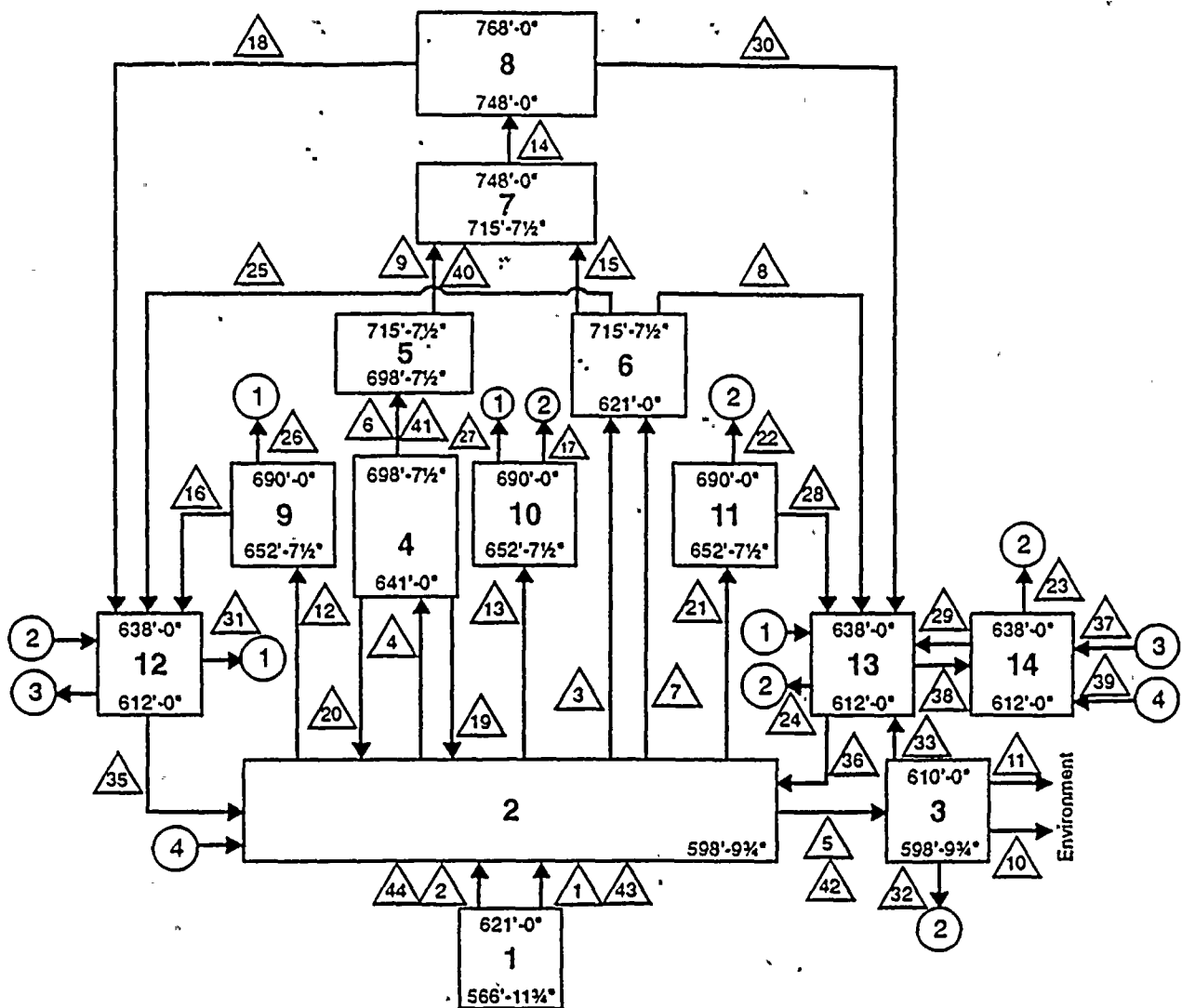


Figure 2-1 Basic layout for an ice condenser containment.



- |                                |                         |
|--------------------------------|-------------------------|
| 1 - Cavity                     | 8 - Upper Dome Region   |
| 2 - Lower Compartment          | 9 - PZR Enclosure       |
| 3 - Pipe Annular Region        | 10 - SG 1 & 4 Enclosure |
| 4 - Ice Condenser              | 11 - SG 2 & 3 Enclosure |
| 5 - Ice Upper Plenum           | 12 - East Fan Room      |
| 6 - Upper Compartment Cylinder | 13 - West Fan Room      |
| 7 - Lower Dome Region          | 14 - Instrument Room    |

△ - Junctions

○ - Indicates Connected Flow Paths

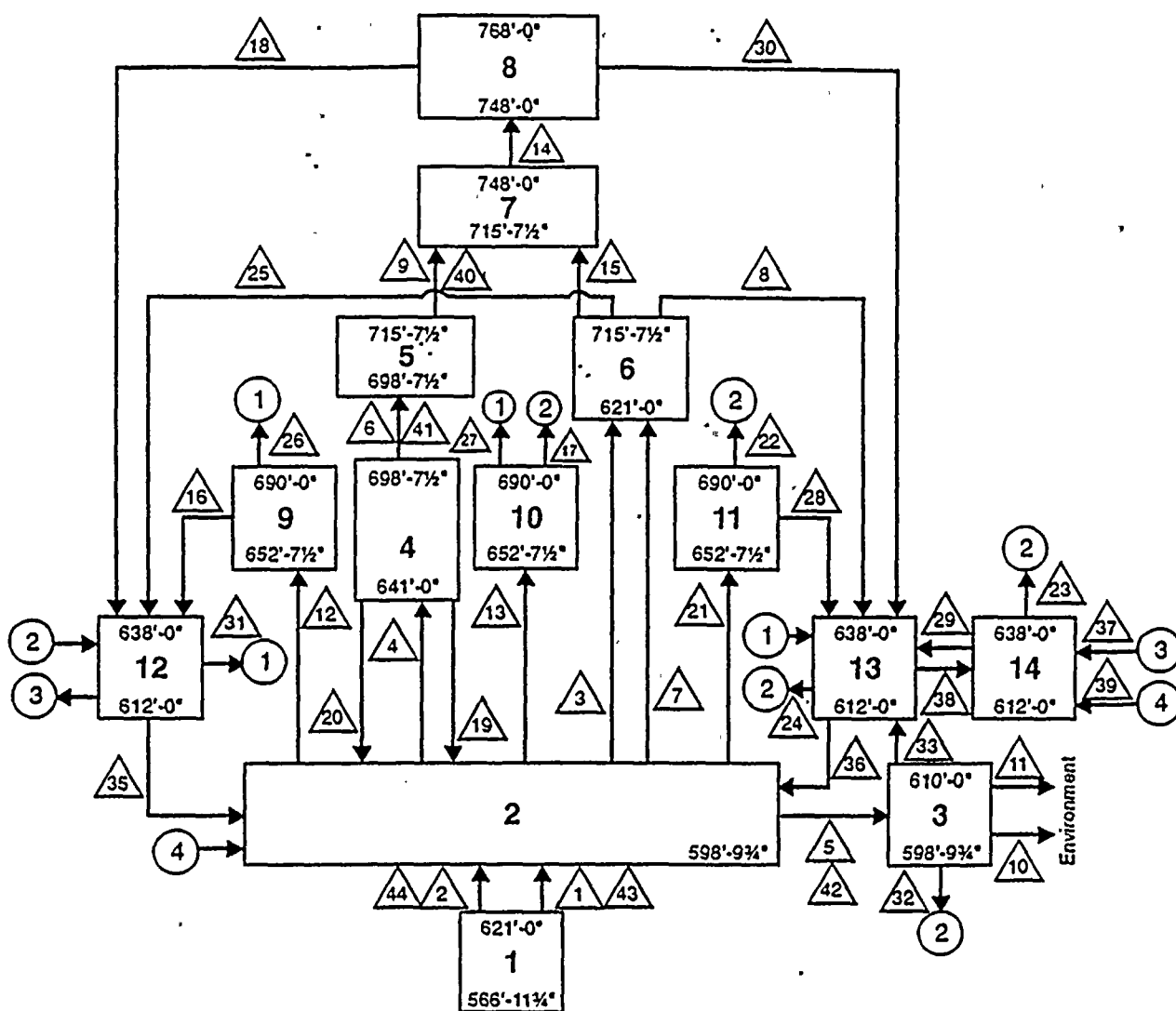
RR99A005.CDR 8-3-99

Figure 2-2 D.C. Cook containment nodalization revision 4 MAAP4 parameter file (14 nodes/44 junctions).

Table 2-1

**D.C. Cook 14-Node Containment Nodalization**

Node	Region
1	Cavity
2	Lower Compartment
3	Pipe Annulus Region
4	Ice Condenser
5	Ice Condenser Upper Plenum
6	Cylindrical Section of Upper Compartment
7	Lower Dome of Upper Compartment
8	Upper Dome of Upper Compartment
9	Pressurizer Enclosure
10	Steam Generator 1/4 Enclosure
11	Steam Generator 2/3 Enclosure
12	East Fan Room
13	West Fan Room
14	Instrument Room



- |                                |                         |
|--------------------------------|-------------------------|
| 1 - Cavity                     | 8 - Upper Dome Region   |
| 2 - Lower Compartment          | 9 - PZR Enclosure       |
| 3 - Pipe Annular Region        | 10 - SG 1 & 4 Enclosure |
| 4 - Ice Condenser              | 11 - SG 2 & 3 Enclosure |
| 5 - Ice Upper Plenum           | 12 - East Fan Room      |
| 6 - Upper Compartment Cylinder | 13 - West Fan Room      |
| 7 - Lower Dome Region          | 14 - Instrument Room    |

△ - Junctions

○ - Indicates Connected Flow Paths

RR99A005.CDR 8-3-99

Figure 2-2 D.C. Cook containment nodalization revision 4 MAAP4 parameter file (14 nodes/44 junctions).



Table 2-1

D.C. Cook 14-Node Containment Nodalization

Node	Region
1	Cavity
2	Lower Compartment
3	Pipe Annulus Region
4	Ice Condenser
5	Ice Condenser Upper Plenum
6	Cylindrical Section of Upper Compartment
7	Lower Dome of Upper Compartment
8	Upper Dome of Upper Compartment
9	Pressurizer Enclosure
10	Steam Generator 1/4 Enclosure
11	Steam Generator 2/3 Enclosure
12	East Fan Room
13	West Fan Room
14	Instrument Room





Table 2-2

D.C. Cook 14-Node Containment Model Flow Junctions

Junction	Type	Description
1	AO*	Cavity ~ Lower Compt. (Bypass Tunnel)
2	AO	Cavity ~ Lower Compt. (Annular Gap)
3	AO	Lower Compt. ~ Upper Cylindrical Sec. (Refueling Cavity Drains)
4	UD**	Lower Compt. ~ Ice Condenser (Door Model)
5	AO	Lower Compt. ~ Pipe Annulus (over Weir Wall)
6	UD	Ice Condenser ~ Ice Upper Plenum
7	AO	Lower Compt. ~ Upper Cylindrical Section (Bypass)
8	Fan	Upper Cylindrical Section ~ West Fan Room (Cont. Air Recirc.)
9	OOAO***	Ice Upper Plenum ~ Upper Compt. Lower Dome
10	AO	Normal Cont. Leakage (Pipe Annuls ~ Env.)
11	OOAO	Cont. Failure (Pipe Annulus ~ Env.)
12	AO	Lower Compt. ~ PZR Enclosure
13	AO	Lower Compt. ~ SG 1/4 Enclosure
14	AO	Upper Compt. Lower Dome ~ Upper Dome
15	AO	Upper Cylinder Section ~ Upper Compt. Lower Dome
16	Fan	PZR Enclosure ~ East Fan Room (H <sub>2</sub> Skimmer)
17	Fan	SG 1&4 Enclosure ~ East Fan Room (H <sub>2</sub> Skimmer)
18	Fan	Upper Dome ~ East Fan Room (H <sub>2</sub> Skimmer)
19	UD	Ice Condenser ~ Lower Compt. (Floppers)
20	AO	Ice Condenser ~ Lower Compt. (Drain Line)
21	AO	Lower Compt. ~ SG 2/3 Enclosure
22	Fan	SG 2/3 Enclosure ~ East Fan Room (H <sub>2</sub> Skimmer)
23	Fan	Instrument Room ~ East Fan Room (H <sub>2</sub> Skimmer)
24	Fan	West Fan Room ~ East Fan Room (H <sub>2</sub> Skimmer)

Junction	Type	Description
25	Fan	Upper Cylinder Section - East Fan Room (Containment Air Recirc.)
26	Fan	PZR - West Fan Room (H <sub>2</sub> Skimmer)
27	Fan	SG 1/4 Enclosure - West Fan Room (H <sub>2</sub> Skimmer)
28	Fan	SG 2/3 Enclosure - West Fan Room (H <sub>2</sub> Skimmer)
29	Fan	Instrument Room - West Fan Room (H <sub>2</sub> Skimmer)
30	Fan	Upper Dome - West Fan Room (H <sub>2</sub> Skimmer)
31	Fan	East Fan Room - West Fan Room (H <sub>2</sub> Skimmer)
32	AO	East Fan Room - Pipe Annulus (Floor Holes)
33	AO	West Fan Room - Pipe Annulus (Floor Holes)
34	AO	Instrument Room - Pipe Annulus (Floor Holes)
35	AO	East Fan Room - Lower Compt. (Fan Windows)
36	AO	West Fan Room - Lower Compt. (Fan Windows)
37	AO	East Fan Room - Instrument Room (Wall Openings)
38	AO	West Fan Room - Instrument Room (Wall Openings)
39	AO	Instrument Room - Lower Compt.
40	AO	Ice Upper Plenum - Upper Cylindrical Section (Bypass Area)
41	AO	Ice Condenser - Ice Upper Plenum (Bypass Area)
42	AO	Lower Compt. - Pipe Annulus (Holes in Weir Wall)
43	AO	Lower Compt. - Rx Cavity (NIS Holes)
44	AO	Lower Compt. - Rx Cavity (NIS Holes)

**Notes:****\*AO**

Always Open - means junction is always open and flow may occur in either direction as well as counter-current natural circulation flow when applicable.

**\*\*UD**

Uni-Directional - means that the junction performs like a check valve and only permits flow in one direction, as well as counter-current flow if the junction is open due to uni-directional flow.

**\*\*\*OOAO**

Once Opened Always Open - means that once a sufficient pressure differential is developed to open the junction, it remains open thereafter regardless of the pressure differential.



Table 2-3

**D.C. Cook 14-Node Containment Fan Flow Rates**

Main fan flow (suction from the upper volume).	39,000 cfm
Upper containment dome skimmer.	1,000 cfm
Steam generator 2&3 enclosure skimmer.	500 cfm
Steam generator 1&4 enclosure skimmer.	500 cfm
Pressurizer enclosure skimmer.	500 cfm
Instrument room skimmer.	100 cfm
Skimmer from East fan room to West fan room. (West train operation assumed. For East train, the skimmer is from West to East).	100 cfm



Volume of Node 1 (Cross Hatched Portion)  
 = 15,748 ft.<sup>3</sup> up to the 610' Elevation

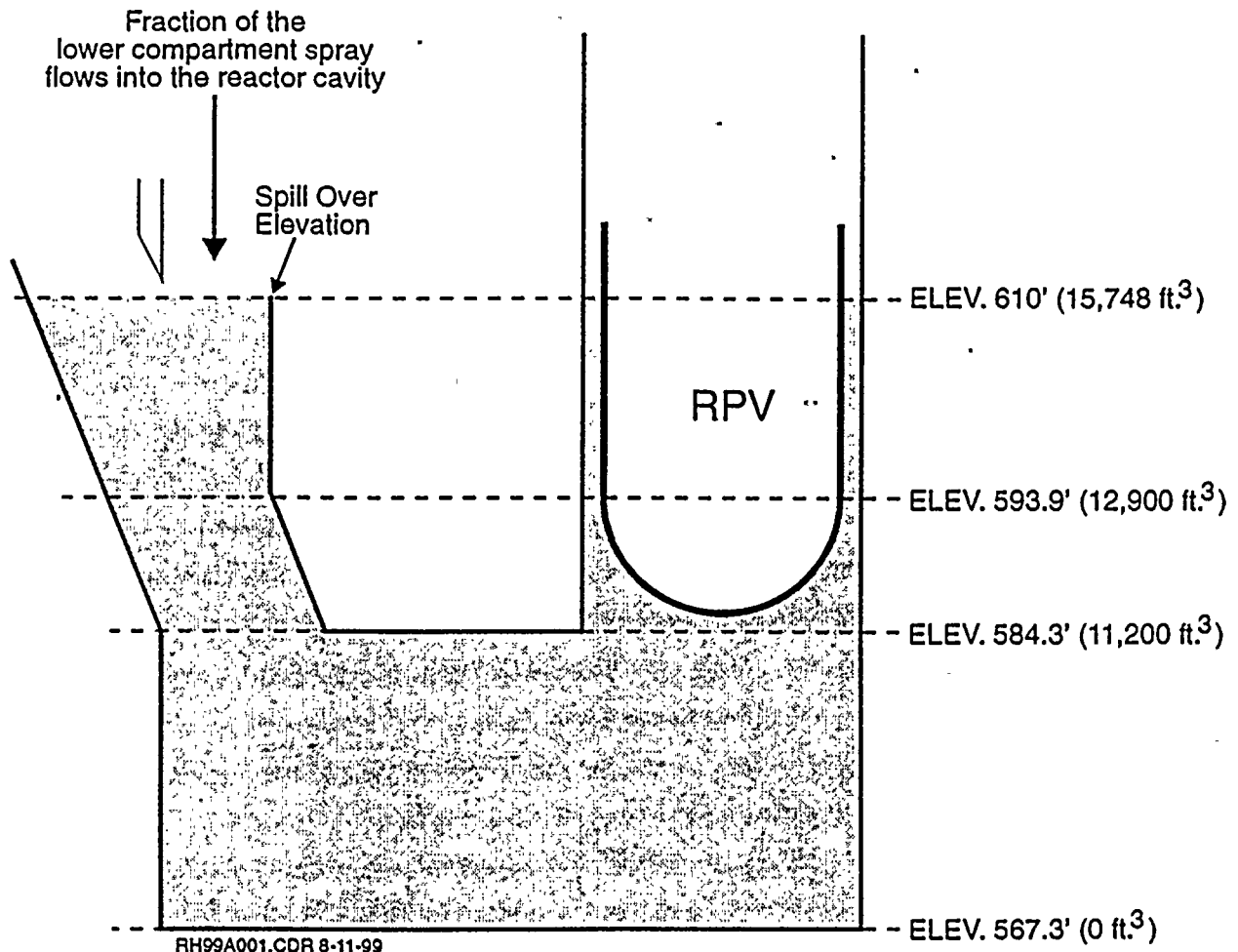


Figure 2-3 MAAP4 representation of the D.C. Cook reactor cavity (Node 1).





describe the physical arrangement of the containment. The spray flow calculations also consider that a small fraction of spray droplets in the active sump region will fall through the grated opening to the instrument tunnel and thereby influences the water mass held up in the reactor cavity. This fractional quantity is determined by ratioing the area of this opening to the cross-sectional area of the lower compartment.

The MAAP4 model of the D.C. Cook reactor coolant system is illustrated in Figure 2-4 and is a typical model for a Westinghouse 4-loop design. For the 2 loops considered, 1 loop represents a single steam generator while the other represents the composite behavior of 3 steam generators. The MAAP4 parameter file for the reactor coolant system has been upgraded at several stages beginning with the IPE process in 1992. Table 2-4 summarizes the pedigree of the parameter file and the reports/QA records which document this information. This parameter file was used, along with any specific changes identified through Design Information Transmittals (DITs) (see Appendix A) to evaluate the reactor coolant response for the spectrum of accident scenarios included in this analysis.

An important feature of the MAAP4 primary system model that is influential for these assessments is the representation of mass and energy releases leaving the reactor coolant system. For these analyses, the MAAP4 code sums the contribution of water and steam flows and assumes a thermodynamic equilibrium characterization for this mixture to determine the steam released to the containment atmosphere. As such, this maximizes the water enthalpy and minimizes the steam flow rate that would be available to melt ice. For an assessment of the minimum recirculation sump water level, an evaluation that minimizes the steam released to the containment atmosphere produces a conservative assessment of the ice melting phenomenon. Consequently, the MAAP4 representation of mass and energy release to the containment is appropriately biased for these specific analyses. For analyses that are directed towards containment integrity, a different characterization of the steam released to the atmosphere is desired, i.e., an evaluation which minimizes the water enthalpy and maximizes the steam mass flow rate. It is important to understand these differences related to different design basis evaluations since this directly influences the water contribution to the sump inventory due to ice melting.

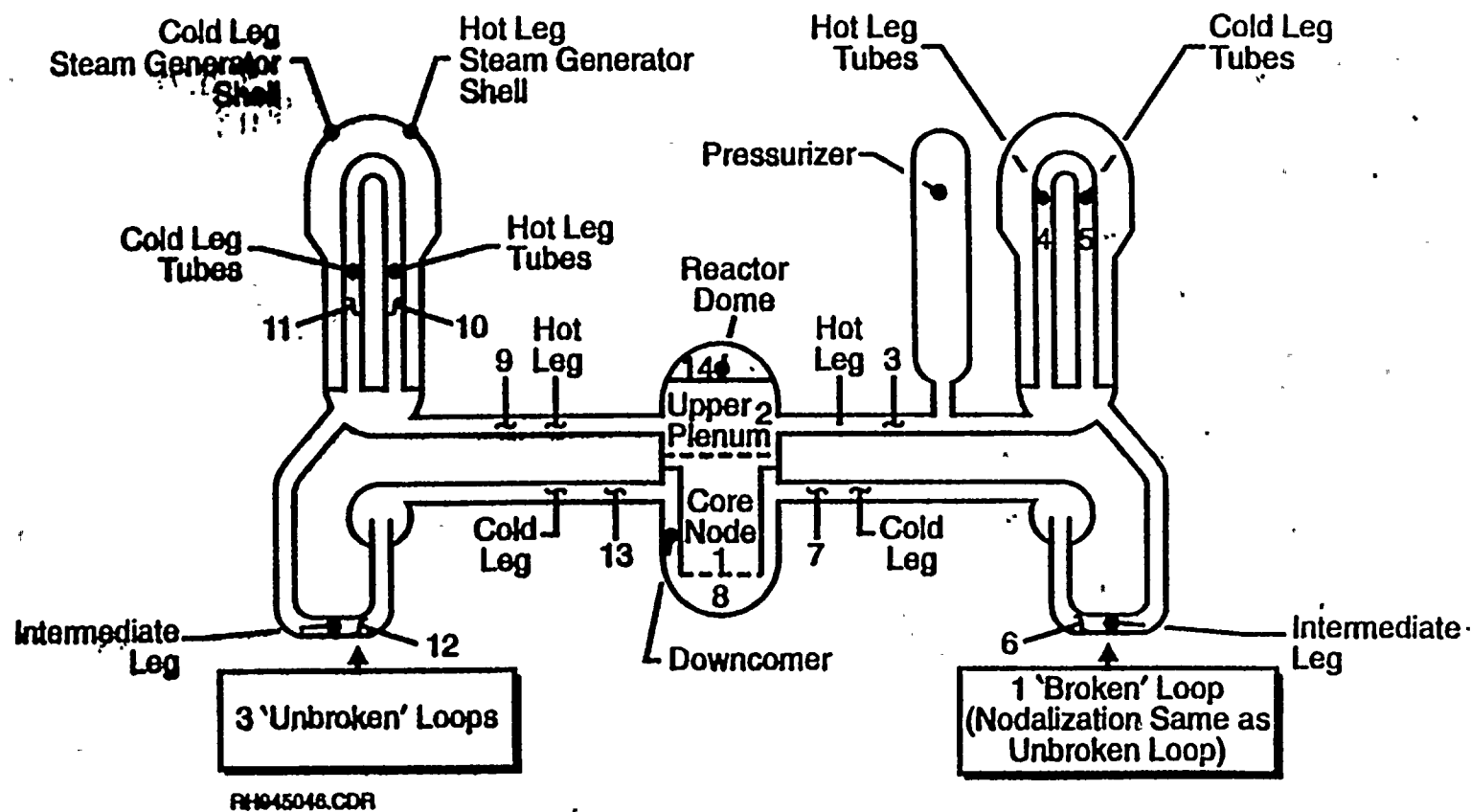


Figure 2-4 PWR primary system nodalization for Westinghouse 4-loop design taken from the MAAP4 User's Manual (EPRI, 1999).

Table 2-4

Pedigree of the D.C. Cook MAAP4 Parameter File

Parameter File Update	Year	Supporting Activities
Generic Ice Condenser Parameter File for MAAP3	1986	Generic ice condenser review associated with IDCOR issue resolution.
D.C. Cook MAAP3B Parameter File	1992	IPE evaluations supported by a containment walkdown and documented MAAP3B (Rev. 17) parameter file, FAI/92-42, FAI QA Record 5.38-6.
D. C. Cook MAAP4 Parameter File	1994	Updated hydrogen assessment for 75% clad oxidation evaluation, FAI/94-113, FAI QA Record 5.38-2.
Updated Containment Parameter File for MAAP 4.0.3	1997	Containment walkdown and resolution of input for containment parameters with AEP personnel, FAI/97-104 as well as FAI QA Records 5.16-52 and 5.16-66.
Updated MAAP4 Parameter File for Version 4.0.3 (several minor revisions)	1998	Review of drawings and walkdown information.
Update of the D.C. Cook Parameter File for MAAP 4.0.4	1999	Resolution of qualified input information from the AEP documents and visual checks by a containment walkdown, AEP DIT-B-00011-00 (June 28, 1999) and FAI QA File 5.38-7.



## 2.2.1 Important Features in MAAP4.0.4

### 2.2.1.1 Ice Condenser Door Models

#### Lower Inlet Door Models

The ice condenser inlet doors control the flow junction that enables steam to enter the ice condenser, be condensed and add the condensate and the melted ice inventories to the lower compartment. These doors and their characterization are a major element of the containment response. Consequently, the force to open each door is checked and recorded at each outage. Experiments to measure the forces necessary to open the containment doors and their opening interval was the subject of substantial efforts at the time that the plant was constructed and licensed (Newby, 1973). MAAP4 models the door response (degree of opening) as a function of the imposed flow rate. Appendix C is taken directly from the MAAP 4.0.4 User's Manual.

#### Intermediate and Top Deck Doors

These doors are essentially held in place by their own weight with a bypass ( $\sim 20 \text{ ft}^2$ ) around these doors that enables a small through-flow without forcing the doors to open. For the analyses performed in this set of calculations the intermediate doors are assumed to lift a sufficient amount to vent the through-flow with the initial opening being governed by the weight of the doors and their projected area. The top deck doors are assumed to fully open and remain fully open once the weight of the doors is exceeded by the force on their projected area. Since these doors and the bypass control the flow for a thermally stable environment (high temperature gas over low temperature gas) it is expected that these doors have a very small influence on the overall response of the ice condenser system and on these sump evaluations.

### 2.2.1.2 Ice Condenser Exit Temperature

The energy balance determining the extent of energy transfer in the ice condenser is based on a knowledge of the gas exit temperature. Previous versions of MAAP used a fixed, user specified value which was derived from the large scale Waltz Mill tests. This is sufficient for large break evaluations directed at containment integrity evaluations. However, the PNL experiments (Ligothke et al., 1991) showed a significant dependence of the exit temperature on the incoming steam mass fraction. Small break analyses have a large variation in the inlet steam fraction, especially when the lower compartment sprays are operating.

To address this, a mechanistic model was developed for calculating the ice condenser exit temperature. This model correctly describes the variations in the exit temperature as the inlet conditions change. Appendix D is the MAAP 4.0.4 User's Manual description.

### 2.2.1.3 Effect of Steam Condensation on Water Pool Surface and due to Drainage From Ice Condenser

The following two models have been included in the latest code (MAAP4 PWR Revision 4.0.4) to represent the potentially influential processes of condensation on the ice melt drainage and the agitated water pool in the sump region. Both of these tend to reduce the ice melt by increasing steam condensation in the lower compartment.

#### Steam Condensation on Water Pool Surface

When a water pool is stable, a hotter, lighter thermal layer develops at the water pool upper surface to prevent any significant condensation. However, when a water pool is continuously disturbed or agitated by inflows, it is possible to have steam condensation at the pool surface when the water temperature is lower than the saturation temperature based on the steam partial pressure. For example, the containment spray and the water drainage from the ice condenser drain pipes continuously disturb the lower compartment water pool in the D.C. Cook

plant. For the integral evaluations in this report, steam condensation is allowed on the water pools in the cavity, the lower compartment, and the annular compartment. If steam condensation can occur, the convective heat transfer coefficient is calculated based on the heat sink (water pool) facing downward (inherently unstable) instead of facing up. This approach increases the heat transfer coefficient, thereby mimicking the heat transfer enhancement factors due to agitated gas space. The mass transfer coefficient and subsequent steam condensation rate are evaluated using the Reynold's analogy between heat and mass transfer. Increasing heat transfer coefficient on the pool surface will increase steam condensation in the lower compartment and decrease potential ice melt in the ice condenser.

#### Steam Condensation Due to Drainage From Ice Condenser

The drainage from the ice condenser into lower compartment is calculated in a mechanistic manner. The drainage would be discharged from the flapper covered drains and fall through the gas space in the lower compartment. During this fall, the water would breakup into capillary size droplets and energy transfer between the gas and the water would occur. To represent this in MAAP, the initial capillary droplet size and the drainage flow rate are input to subroutine SPRAY to calculate the energy transfer between the gas and the drainage water, including steam condensation on the droplets.

### 2.2.2 Representation of Important Phenomena Related to the Accident Sequence

#### Break Location

To investigate the most demanding set of conditions for the recirculation sump water level inventory, the possible variations in the break location must be considered including the lower compartment and the reactor cavity. Possible locations of breaks in the cavity included the bottom of the RPV (instrument penetration), the vessel nozzles (cold leg and CRDM) and the reactor head vent (Westinghouse 1999b). Westinghouse evaluations of these possible locations (Kury, 1998) conclude that break sizes up to 0.6-inch diameter need to be considered in the bottom of the





vessel, sizes up to 1 ft<sup>2</sup> are to be evaluated for the RPV nozzles and break diameters of 2.75-inch for the Control Rod Drive Mechanisms (CRDM) and 0.6-inch for the head vent in the RPV upper head.

Another attractive feature of the MAAP4 integral analysis is that the discharge flow rate from a postulated RCS break can be directed simultaneously to two different containment compartments. This is important when considering potential breaks in the cold leg at the reactor vessel nozzles where a fraction of the discharge flow could be directed into the reactor cavity and the remainder into the lower compartment as a result of the tight configuration in the holes through the biological shield. The fraction of the flow diverted is evaluated principally through jet impingement considerations and is discussed in Appendix B. Functionally this is accomplished using the generalized opening in the MAAP4 RCS representation and using discharge coefficients to determine the extent of flow directed to each compartment. For example, a typical discharge coefficient of 0.7 for that flow rate directed to the reactor cavity and a value of 0.3 for the flow rate directed to a lower compartment means that 70% of the discharge is directed to the reactor cavity and 30% to the lower compartment. This capability is used in characterizing those postulated breaks in the cold leg at the reactor vessel nozzle level in the near vicinity to the RPV.

### Break Size

The variations in the postulated size of the RCS LOCA range from those which are considered to be small-small LOCAs (1/2 to 1 inch in effective diameter) to those which include large break conditions (6-inch equivalent diameter and DECL LOCAs). As expected, the large break LOCAs eventually transition to a condition in which the water injected to the RCS is discharged from the break with the RCS never being completely refilled. In these cases there is an additional water inventory from the RCS, in addition to that from the RWST, which accumulates on the containment floor. Moreover, when there is little potential for containment pressurization as a result of the partial pressure of the relatively cold water being discharged from the break once the RCS is cooled down, there is no significant continuous steam source to force continued containment spray operation. Therefore, the large break conditions typically have a

spray demand early in the accident sequence and then are secured for the remainder of the accident with respect to the containment pressurization given the assumptions controlling the mass and energy releases for minimum sump inventory evaluations. As a result, for long term spray operation and sump water level assessments, the small LOCAs typically result in a reduced sump water level compared to the large LOCAs. On the other hand, the small-small LOCAs can be so small that they cause ice melting and initiation of the CEQ fans but do not cause the containment sprays to be initiated. In this sense the very small LOCAs will have more water in containment when any long term recirculation will be demanded. Therefore a break size spectrum is considered from the large DECL to a size which is insufficient to initiate sprays.

#### Containment Spray and Recirculating Fan Setpoints

The setpoints for actuation of the recirculation fans (CEQ) and the containment sprays (CTS) for D.C. Cook are 1.1 psig and 2.9 psig respectively with the measurement location being in the lower compartment (MPR, 1999a). This is the basis for numerous containment analyses and provides the necessary characterization for the plant response given the spectrum of break sizes considered. Uncertainties in this setpoint must also be considered since this may also have some influence on the demands for containment sprays. An uncertainty of  $\pm 0.6$  psig is considered for this instrument with the lower pressure being conservative with respect to the mass of ice melted. A lower setpoint leads to earlier spray initiation which results in a decrease in the mass of ice melted. Hence, the respective setpoints considered, including instrument uncertainty, are 0.5 psig and 2.3 psig.

#### Containment Spray Reset Setpoint

Securing of containment sprays would be through the Emergency Operating Procedures (EOPs) by instructing the operators to take this action when the containment pressure has been decreased to an indicated value of 1.5 psig. An uncertainty evaluation shows that the combined uncertainties for the instrument and for the operators reading the instrument indicates this is  $\pm$



0.73 psi. Hence, the action to secure the sprays can be as low as 0.77 psig. This action is combined with the information regarding minimum spray duration.

### Recirculation Fans

To address the fundamental question for these analyses, the decision for the recirculating fan performance was based on that which would give the minimum ice melt and therefore the minimum inventory in the active sump. The flow rate generated by the recirculating fans pushes the atmosphere from the lower compartment through the ice condenser. An increase in the fan flow rate would increase the energy transferred to the ice and therefore increase the water inventory due to ice melting. Consequently, the nominal case investigated was for one train of recirculating fans with the variation considered as two trains operating once the recirculation fan setpoint is reached.

### External Bypass of the Ice Condenser Compartment

There are bypass flows around the ice condenser itself ( $\sim 5 \text{ ft}^2$ ). The results of this flow bypass are considered according to the values given in the D.C. Cook FSAR.

### 2.2.3 MAAP4 Representation of Pump and Air Recirculation Fan Curves

An integral model needs to represent the feedbacks associated with RCS pressure changes, as well as the pressure changes in containment, since this can influence the air circulation through the containment. The respective curves for the high head injection and charging pumps were developed from the vendor shutoff head (see DIT information in Appendix A) and the behavior under full recirculation, assuming that each system experiences a functional behavior that the flow rate varies as the square root of the available pressure difference. Figures 2-5 and 2-6 illustrate the functions used for the high head and charging pumps, respectively.

A similar approach was used for the air recirculation fans. Specifically, a stagnation pressure was used with a run out flow to determine a quadratic function. This is shown in Figure 2-7, along with vendor data, for the vanes opened  $45^\circ$  and fully opened. As shown, this

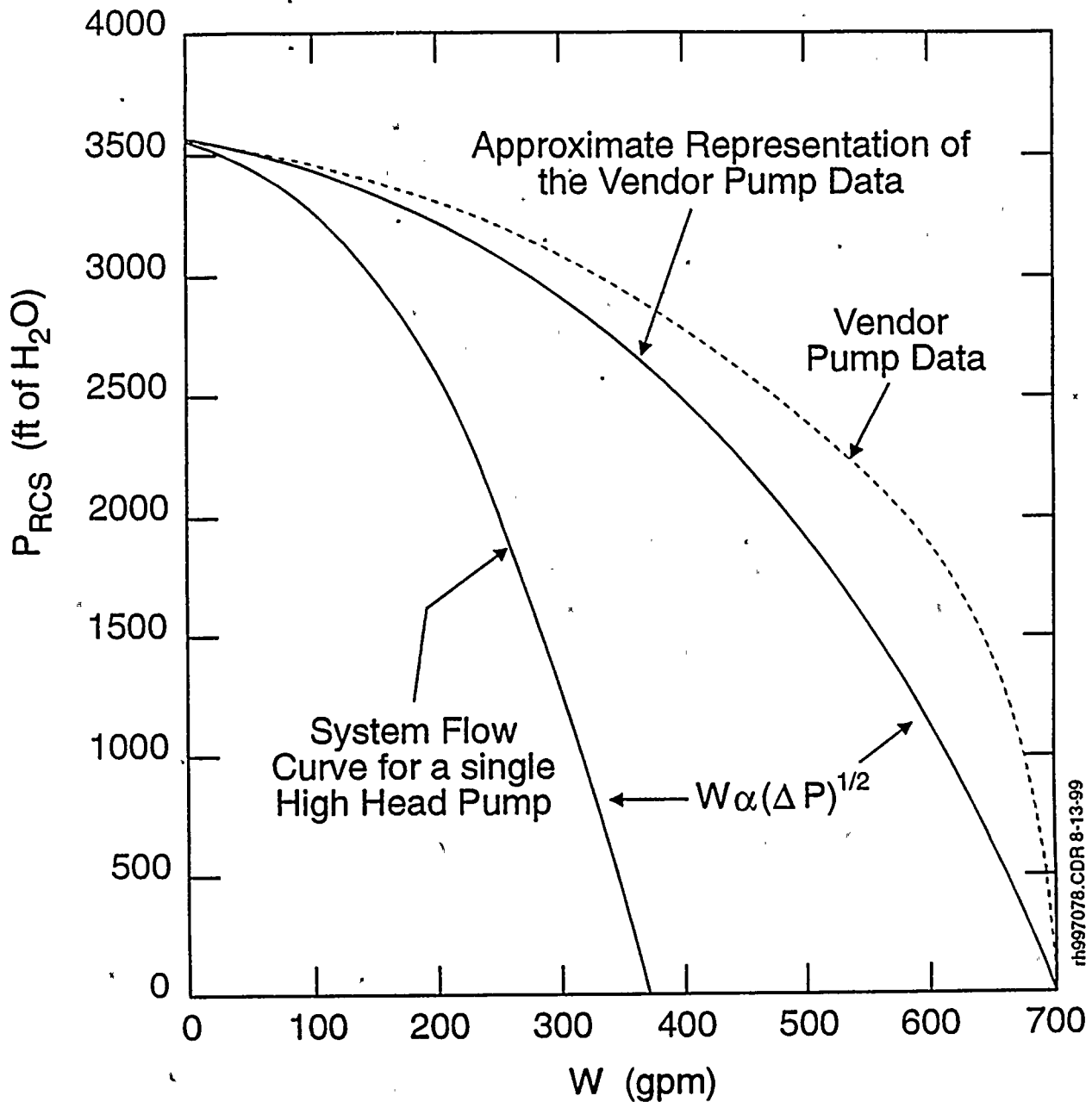


Figure 2-5 MAAP4 functional behavior for a single high head injection pump (see Appendix A for vendor and system data).



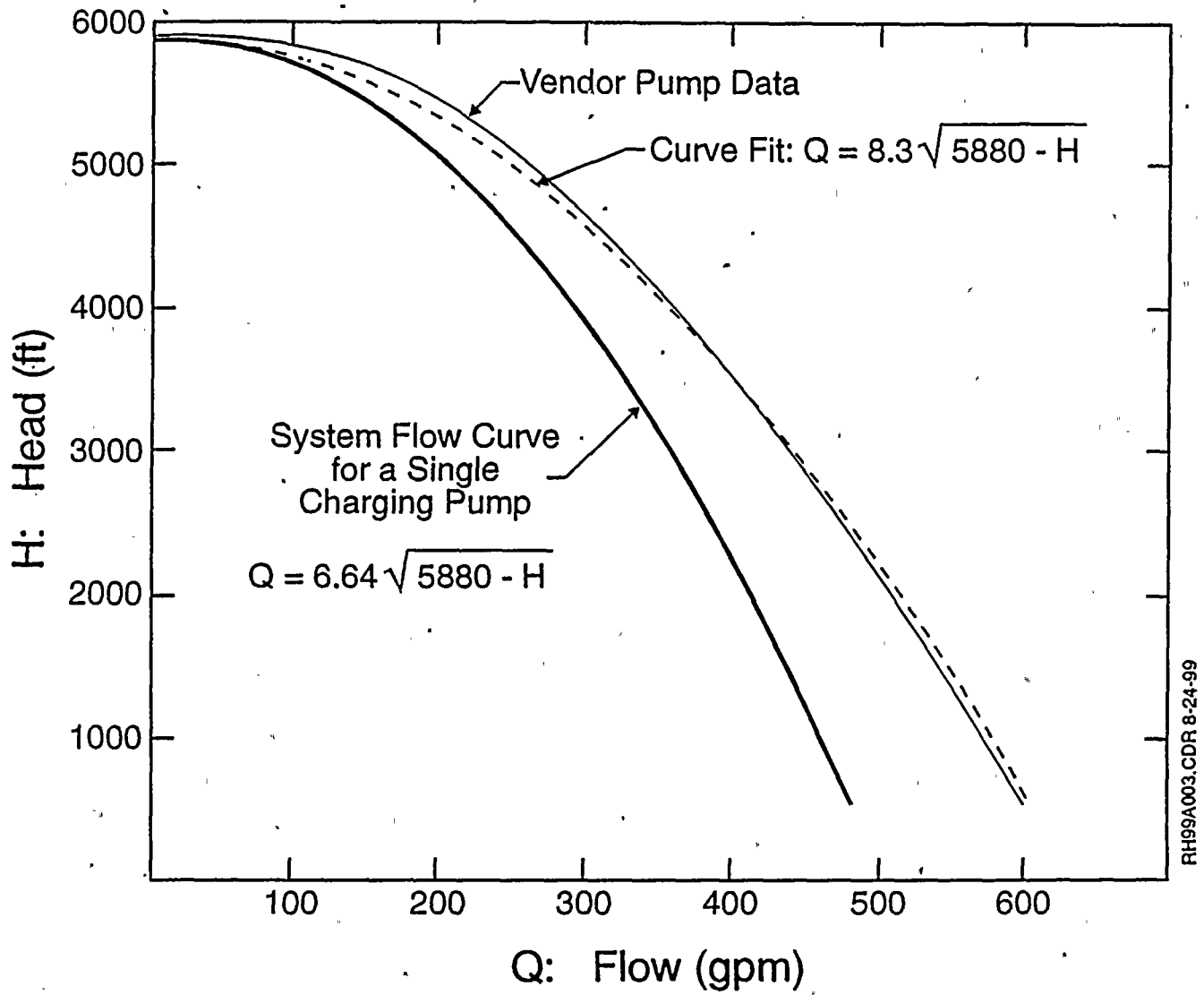


Figure 2-6 MAAP4 functional behavior for a single charging pump (see Appendix A for vendor and system data).





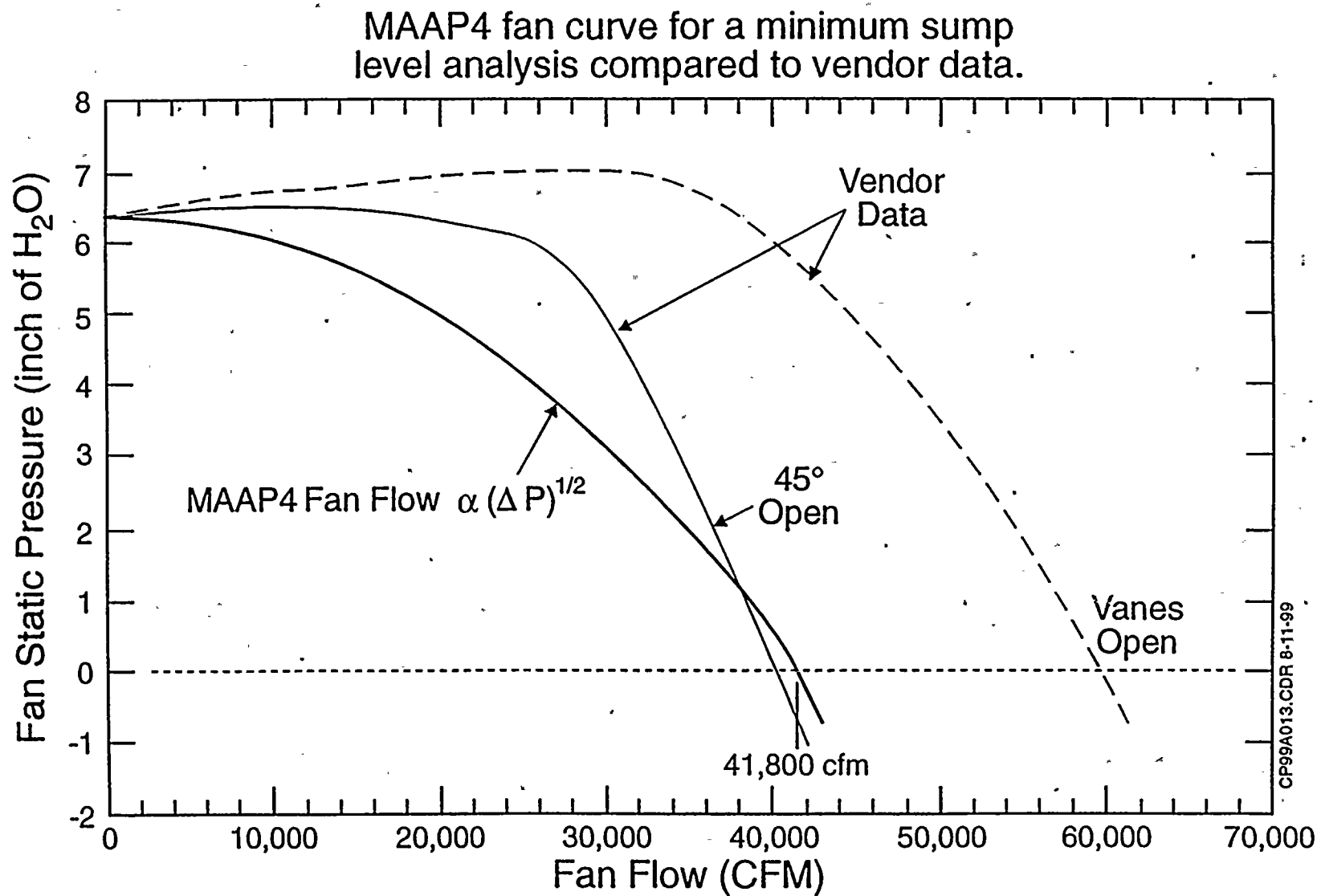


Figure 2-7 MAAP4 functional behavior for a single air recirculation fan.



functional description is conservative since an increased air flow through the ice condenser causes an increase in the ice melt.

### 3.0 BENCHMARKING OF MAAP4 ICE CONDENSER CONTAINMENT MODEL

#### 3.1 Introduction

It is essential that this approach be compared with the design basis assessment to assure that the calculations for the containment behavior are consistent and that the differences between the calculated results are also consistent with the differences in philosophies of best-estimate and design basis assessments. Therefore, before entering into a series of MAAP4 integral system calculations to investigate the influence of variations in the break area and key plant parameters, the best-estimate model for the integral system behavior is compared with several design basis Reactor Coolant System (RCS) and containment assessments. Through such a comparison, one can assure that there is consistency in the modeling of the containment response for the two different modeling approaches.

DBA containment evaluations for the D.C. Cook Units 1 and 2 have been performed using the LOTIC-3 (Westinghouse, 1997) code to describe the containment response, including the performance of the ice condenser compartment. Typically such analyses are performed by developing the mass and energy releases from the RCS to the containment using the Westinghouse design basis small LOCA code, NOTRUMP (Westinghouse, 1997). These mass and energy releases are then input to the LOTIC-3 computer code, which represents the containment as different nodes and also has the plant specific dimensions for D.C. Cook containment, to assess the transient pressure and temperature distributions throughout the containment, the ice melting rate, the depth of water accumulation in the lower compartment, etc.

Comparisons of the LOTIC-3 and MAAP4 ice melting rates calculations have been performed using mass and energy releases input from both a six-inch LOCA and a two-inch cold leg break as calculated by NOTRUMP. This provides a comparison between the MAAP4 and the LOTIC-3 calculations for a range of effective break diameters. Moreover, it provides an opportunity to establish the uncertainty bands that should be considered in the MAAP4



calculations to examine the possible influences of the minimum ice melting rate on the accident sequences in question.

MAAP4 also has a dynamic benchmarking capability (Henry, 1996) which enables major experimental observations to be captured (documented) in the code software and these benchmarks are updated with each new code version. Three types of benchmarks are considered. The first are nuclear power plant experiences and exercise the complete capabilities of the code (RCS and containment), such as the Davis-Besse loss of feedwater event. The second are large integral experiments which exercise a major part of the code computational capabilities but not the entire code (one such example is the full scale HDR containment experiments). The third category includes separate effects tests which exercise only a limited part of the codes computational capabilities. These benchmarks are used to test and verify numerous parts of the MAAP4 code and are discussed in Volume III of the MAAP4 User's Manual "Benchmarking" (EPRI, 1999).

Three benchmarking activities have been performed to test the modeling capabilities for representing ice melting and the flow patterns developed in ice condenser containment configurations. These include:

- the large scale ice condenser tests performed by Westinghouse at their Waltz Mill facility (Salvatori, 1974),
- the full length ice condenser basket experiment at Pacific Northwest Laboratories (Ligotke et al., 1991), and
- the ice condenser containment flow distribution tests at the Containment Systems Test Facility (CSTF) (Bloom et al., 1983).

Each of these is important in establishing a level of confidence that the MAAP4 code can represent the response of the D.C. Cook ice condenser containment system to a spectrum of postulated



accident sequences. These benchmarks provide insights into the modeling capabilities representing:

- the ice melting rate,
- the response of the ice condenser doors,
- the potential for single-phase countercurrent natural circulation flows given the substantial density differences between compartments of the ice condenser containment,
- the response and importance of the structural heat sinks as steam is introduced into containment compartments,
- the potential for condensation on agitated water pools collected in the various containment compartments, especially the lower compartment (active sump),
- the potential for condensation on containment sprays,
- the potential for condensation on the drainage of melted ice from the ice condenser compartment into the lower compartment, and
- the distribution of flow in the containment compartments when the air recirculation fans are operating.

Consequently, these dynamic benchmarks are an important part of the code qualification and testing of individual model capabilities. As such, these are reviewed through the dynamic benchmarking program and are also summarized here with the details for the various experiments given in Appendices E, F and G.





### 3.2 Comparison of the MAAP4 Containment Model With LOTIC-3 for a Six-Inch Cold Leg LOCA

#### 3.2.1 Boundary Conditions

As mentioned above, the element of principal interest for these integral plant analyses is the minimum sump water level which protects against vortexing (air ingression). An important contributor to this inventory is the mass of ice melted by condensing steam. Hence, a comparison of the MAAP4 containment model with the LOTIC-3 result for the transient ice melt rate is of particular interest. To accomplish this, the mass and energy releases from a 6-inch cold leg LOCA calculation using NOTRUMP results (FAI, 1997) were input to the MAAP4 containment model in the same manner as they are used for the LOTIC-3 analysis. This time dependent information is input as a transient boundary condition (see Table 3-1). It is assumed that there is no feedback from the containment to the RCS. To provide the same initial conditions, the following boundary conditions, which are different than those used in Sections 4 and 5, are specified in the MAAP4 calculations:

- the containment initial pressure is 14.7 psia,
- the lower compartment gas temperature is 120°F,
- the upper compartment gas temperature is 70°F,
- the RWST water temperature is 105°F,
- the cooling water for the containment spray heat exchanger is 86°F, and
- one train of containment spray is operating without the RHR spray.

This is performed as a dynamic benchmark for the MAAP4 code such that the comparison is with the containment modeling used for all of the analyses accompanying this small break assessment. In particular, the dynamic benchmarking assures that the comparison is directly with the appropriate MAAP4 containment software models and is not performed with a standalone, special code version. Also, these dynamic benchmarks for this activity are archived in the FAI QA files (FAI, 1999).

**Table 3-1**  
**Mass and Energy Source Rates to the Containment From**  
**the NOTRUMP Analyses For a Six-Inch Cold Leg LOCA**

Time (sec)	Mass Flow Rate	Rate of Energy Addition
	(lbm/sec)	(BTU/sec)
-1.	5600	3.0339E+06
0.	5600	3.0339E+06
10.	4279.4	2.3854E+06
20.	2417.7	1.3920E+06
30.1	1973.6	1.1310E+06
40.2	1830.6	1.0400E+06
50.2	1753.5	0.990247E+06
60.4	1720.3	0.968205E+06
70.5	1786.4	1.0018E+06
80.5	1789.2	1.004E+06
90.5	1778.8	0.993281E+06
100.5	1797.8	1.0026E+06
110.5	1906.9	1.05762E+06
120.5	1876.9	1.0426E+06
130.6	1971.5	1.0901E+06
140.7	2010.9	1.1102E+06
150.7	1865.5	1.096E+06
160.7	1663.2	0.920538E+06
170.7	871.3	674220.
180.7	994.8	713703.
190.8	802.1	636242.
200.8	795.	625980.
210.8	748.4	599745.
222.9	799.4	608020.
230.9	671.1	548867.
240.9	510.7	478961.
250.1	571.4	485297.
250.8	359.3	430991.
300.8	351.2	379299.
350.9	262.3	318283.
401.	195.1	240141.
451.	143.4	179459.
501.	130.8	163958.
551.	129.1	160324.
601.1	128.7	158092.
651.1	129.	157918.
700.	115.6	142295.
1500.	115.6	142295.



The values in Table 3-1 were input through subroutine EFECT using the dynamic benchmarking capability accessed through subroutine BENCH. With this approach, the comparison can be easily repeated for future code versions to examine the MAAP4 comparison with the DBA calculation.

### 3.2.2 Results

A comparison of the code predictions for the remaining ice mass during the two models for the first 1500 secs is shown in Figure 3-1. The best estimate calculation includes steam condensations in the lower compartment due to cold water pool and cold water drainage from the ice condenser drainage pipes as discussed in the previous section. These two MAAP4 models will reduce the ice melt in the ice condenser because of increased steam condensation in the lower compartment. As expected, the ice melt from the best estimate MAAP4 calculation is slightly less than the LOTIC-3 results. In this regard, the MAAP4 representation is the conservative representation for the minimum sump inventory.

## 3.3 Comparison of the MAAP4 Containment Model with LOTIC-3 for a Two-Inch Cold Leg LOCA

### 3.3.1 Boundary Conditions

This benchmarking comparison is carried out in the same manner as that described above. The mass and energy releases from a two-inch cold leg LOCA calculation using NOTRUMP results (FAI, 1997) were input to the MAAP4 containment model in the same way that was used for the LOTIC-3 analysis. The transient mass and energy releases for this calculation are illustrated in Table 3-2.

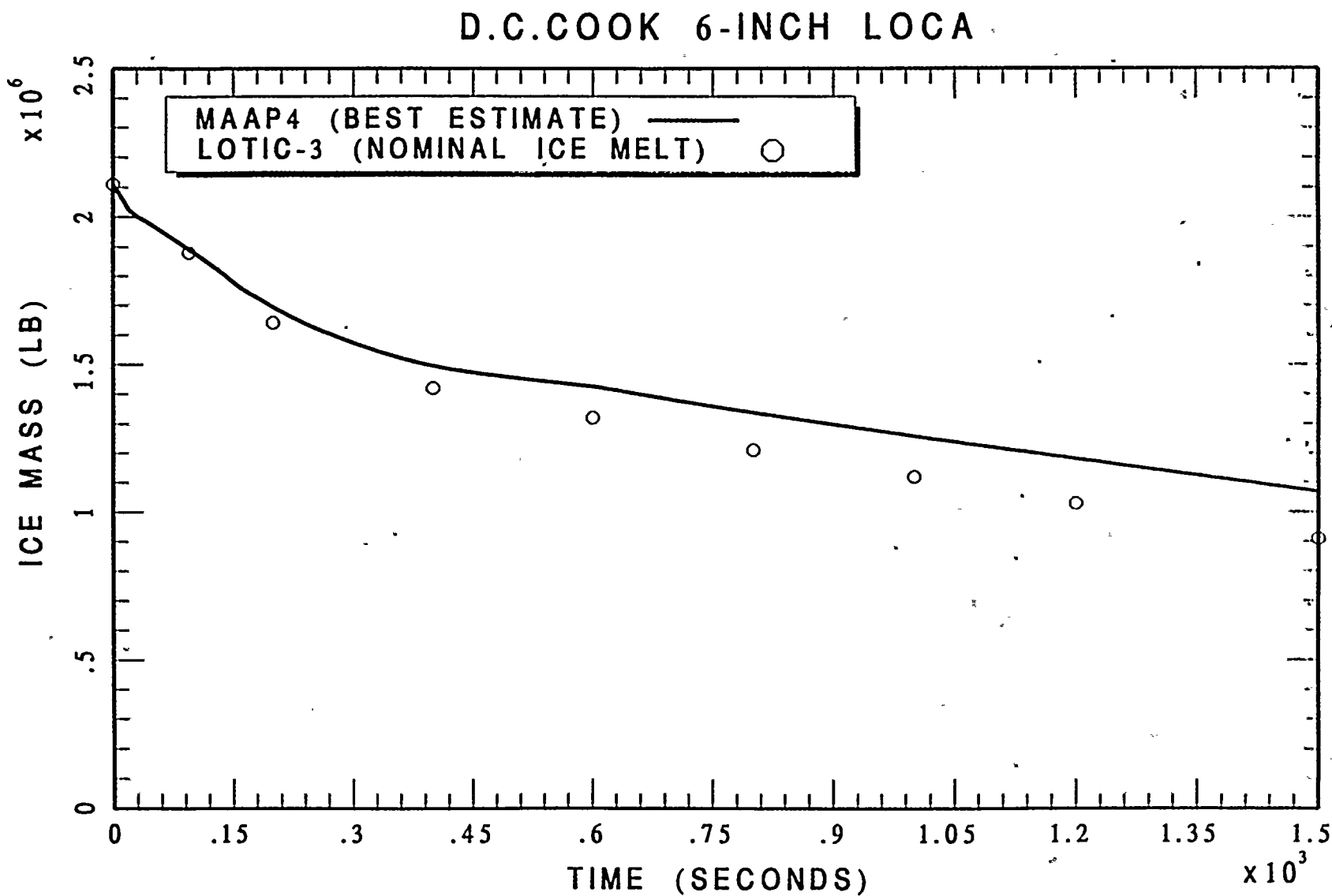


Figure 3-1 Comparison of the LOTIC-3 and MAAP4 ice depletion rate for a six-inch diameter cold leg LOCA (NOTRUMP) for the D.C. Cook Unit 2.

Table 3-2  
NOTRUMP Mass and Energy Releases for a Two-Inch Cold Leg LOCA

Time	Mass Flow Rate (lbm/sec)	Energy Flow Rate (BTU/sec)
0.01	672.32	343776.09
24.46	589.21	306724.84
50.59	467.2	252904.58
100.59	366.67	200798.7
163.37	303.18	166565.56
314.97	311.75	171573.41
433.91	234.63	129801.85
500.34	259.88	142323.66
600.34	302.73	161726.95
700.68	310.16	164810.02
800.52	333.74	174618.25
900.25	359.35	184711.30
1000.68	366.11	186407.45
2100.71	370.27	187081.73
1161.06	54.39	61667.56
1234.43	307.47	162575.5
1247.26	54.61	61388.5
1300.33	237.59	127066.84
1329.34	269.2	145428.66
1351.04	73.58	64738.06
1450.69	88.3	68026.2
1511.87	122.19	78115.33
1574.64	115.87	76351.45
1600.4	101.49	71851.73
1650.5	93.40	70239.51
1700.54	88.35	68337.6
1750.24	84.13	67021.08
1825.01	71.64	63029.41
1850.18	71.57	62858.77
1900.88	71.49	62587.18
1950.92	71.36	62197.95
2001.8	71.14	61609.86
3000.57	69.92	58521.9
4000.53	68.25	55160.46
6000.78	67.15	53195.57
8000.7	65.26	49330.02
10000.0	63.16	45410.11

### 3.3.2 Results

A comparison of the MAAP4 and LOTIC-3 predictions for the remaining ice mass is illustrated in Figure 3-2. As shown in the figure, MAAP4 calculates less ice melt compared to the nominal LOTIC-3 results (LOTIC-3 used an exit ice bed gas temperature of 105°F in this calculation). After 10,000 seconds, the remaining ice mass calculated by LOTIC-3 is about 380,000 lbm compared to about 700,000 lbm of the best estimate MAAP4 calculation. Thus, the best estimate MAAP4 calculation is conservative in terms of ice melt and is appropriate for sump level analysis.

Figure 3-3 illustrates a comparison of the upper and lower compartment temperatures from the LOTIC-3 analysis with those by the best estimate MAAP4 calculation. As illustrated, there is general agreement between the transient thermal history in these two compartments with the LOTIC-3 analysis.

### 3.4 Comparison of the MAAP4 and NOTRUMP Mass and Energy Releases for a Two-Inch Cold Leg LOCA

For this benchmark, the boundary conditions are the D.C. Cook primary system operating at 102% of 3250 MWt core power with a system pressure of 2033 psia and experiencing a two-inch cold leg break. To provide the same initial and boundary conditions in both NOTRUMP and MAAP4, some of the MAAP4 inputs such as initial conditions, ECCS flows and temperatures, and AFW temperature and flow rates are adjusted to the NOTRUMP values (Westinghouse, 1999). In addition, the initial core power is increased to 120% at 10 seconds after the reactor scram in the MAAP4 calculation to match the decay heat used in the NOTRUMP calculation (ANS + 20%). In this sequence, NOTRUMP calculates recirculation occurs at 2199 seconds into the transient. The operator action of 100°F/hr cool down was mimicked in the same manner in both codes.





# D.C. COOK 2-INCH LOCA

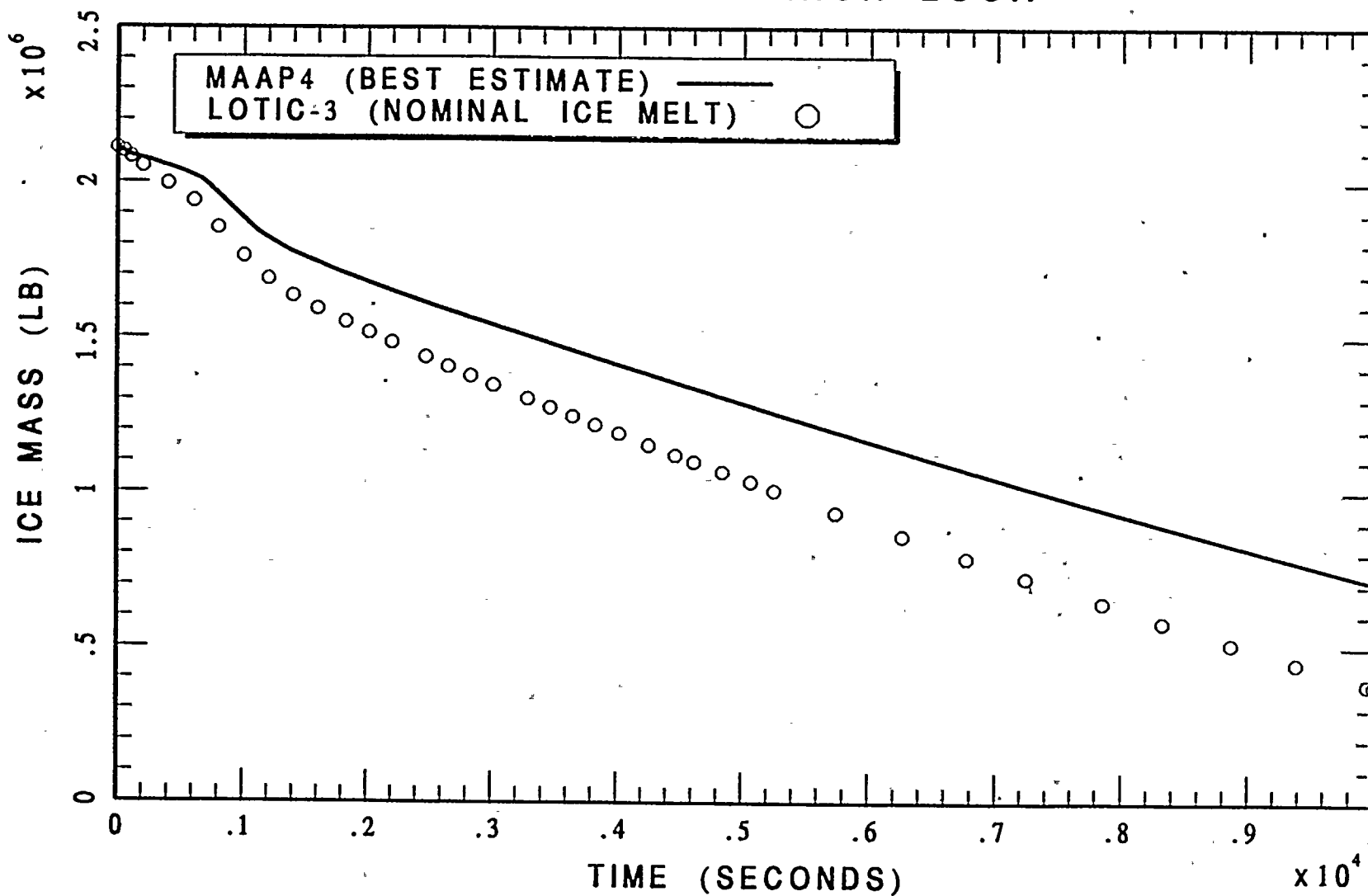


Figure 3-2 Comparison of the LOTIC-3 ice depletion rate for a two-inch diameter cold leg LOCA with the MAAP4 calculation using the same mass and energy inputs from the NOTRUMP calculation.



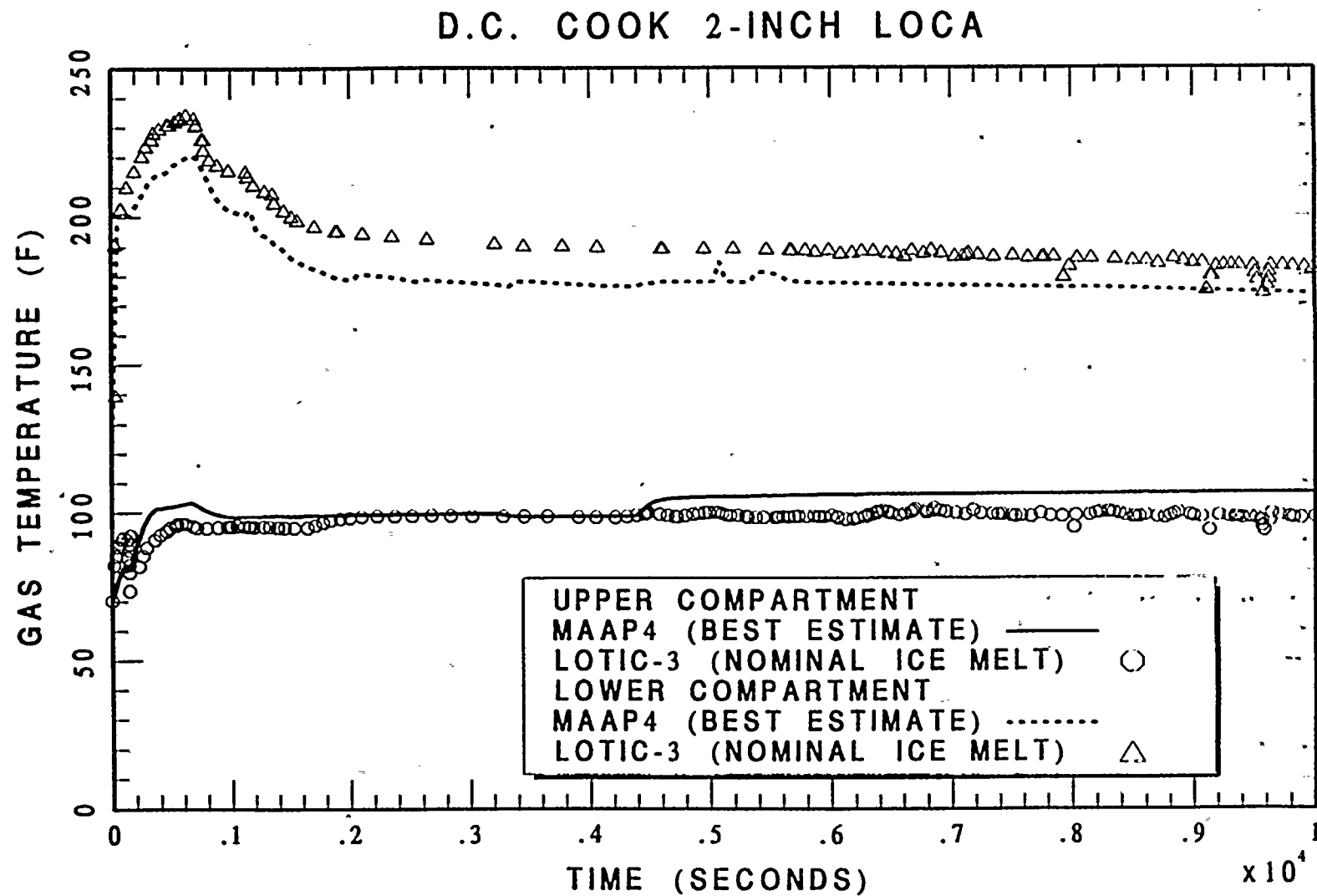


Figure 3-3

Comparison of the upper and lower containment compartment temperatures for a LOTIC-3 calculated biased for maximum containment pressure and the MAAP4 representation with the accident initiator being a two-inch diameter cold leg LOCA as represented by NOTRUMP.



The MAAP4 calculated instantaneous mass release rate is compared to the NOTRUMP value in Figure 3-4 along with the integrated mass and energy release in Figures 3-5 and 3-6. As shown in the figures, NOTRUMP discharge rates are higher early in the transient, i.e., within the first 1500 seconds. Between 1500 seconds and 4000 seconds, NOTRUMP calculates two-phase discharge from the primary system while MAAP4 calculates a subcooled (all water) two-phase critical flow discharge. Such differences are likely due to the different ways in which the primary system and the break flow model are modeled. For most of the transient, the average MAAP4 and NOTRUMP flow rates are in good agreement. Overall integrated mass and energy releases to the containment are in general agreement between MAAP4 and NOTRUMP with NOTRUMP having about 10% higher integrated mass and energy flow out of the break. In this regard the MAAP4 energy release is conservative in that it minimizes the ice melt for these analyses. The primary system pressure response is similar between MAAP4 and NOTRUMP as shown in Figure 3-7. These demonstrate that using the best estimate models in MAAP4 will provide a somewhat different history for the accident, but the integrated mass and energy releases to the containment, which is the principal issue regarding sump water level, will be very similar.

### 3.5 Westinghouse Waltz Mill Test

The Waltz Mill tests were performed with eight 36 ft long ice baskets in a facility set up to provide scaled steam delivery rates typical of large break LOCAs, medium size LOCAs, small break LOCAs as well as one test with a large LOCA followed by long term steaming from the decay heat in the reactor core. As such, these experiments provide an important test of the MAAP4 ice melting model to that observed in the various experiments covering the spectrum of LOCA sizes considered in the containment sump evaluations. Consequently, these are an important benchmark for the integral MAAP4 ice melting rate representation.

#### 3.5.1 Boundary Conditions

The important boundary conditions for the various experiments include the break size, the initial ice mass, whether long term steaming from core decay heat was represented (Test K only)

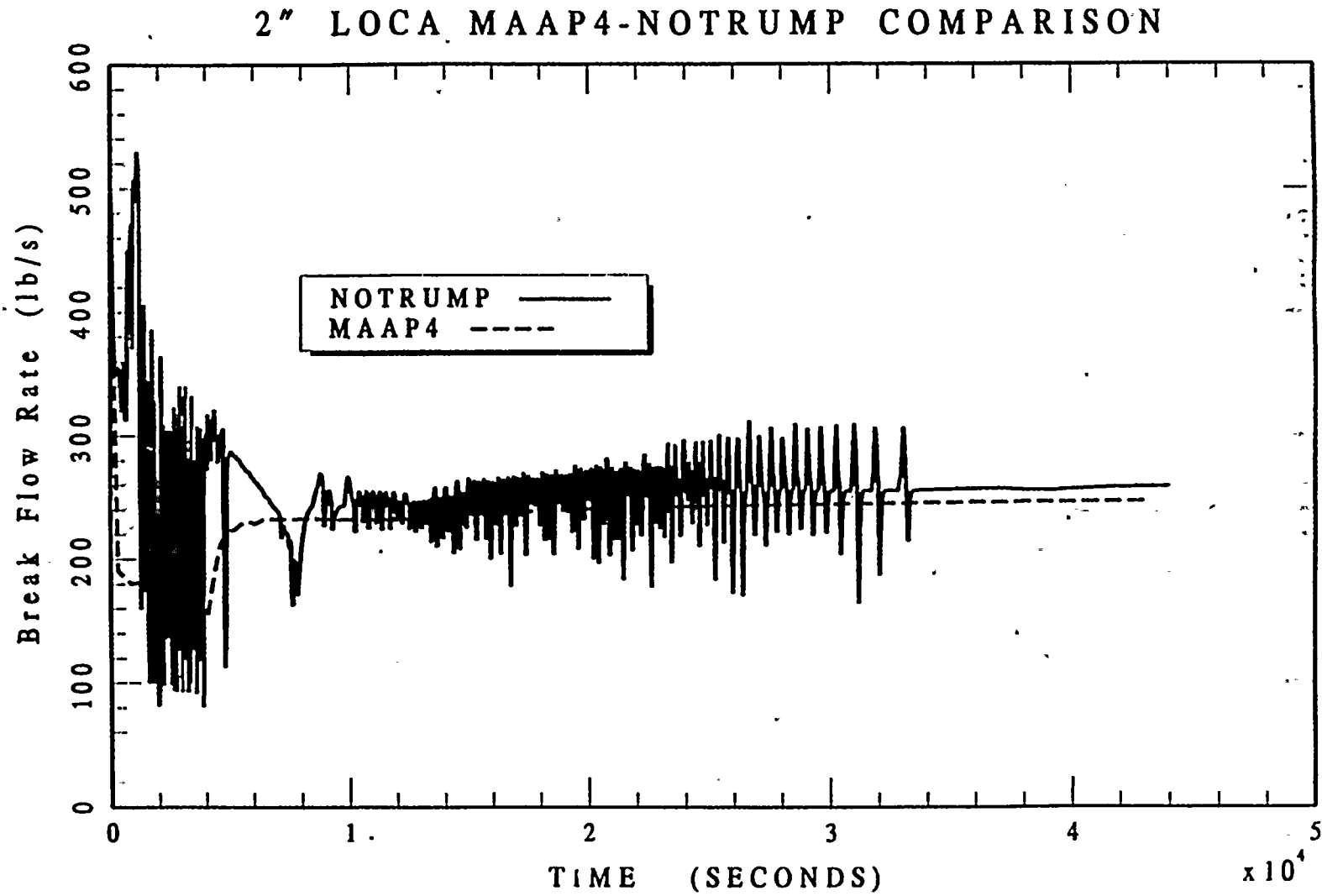


Figure 3-4 A comparison of the instantaneous mass flow rates for the MAAP4 primary system and NOTRUMP assuming a two-inch cold leg LOCA.





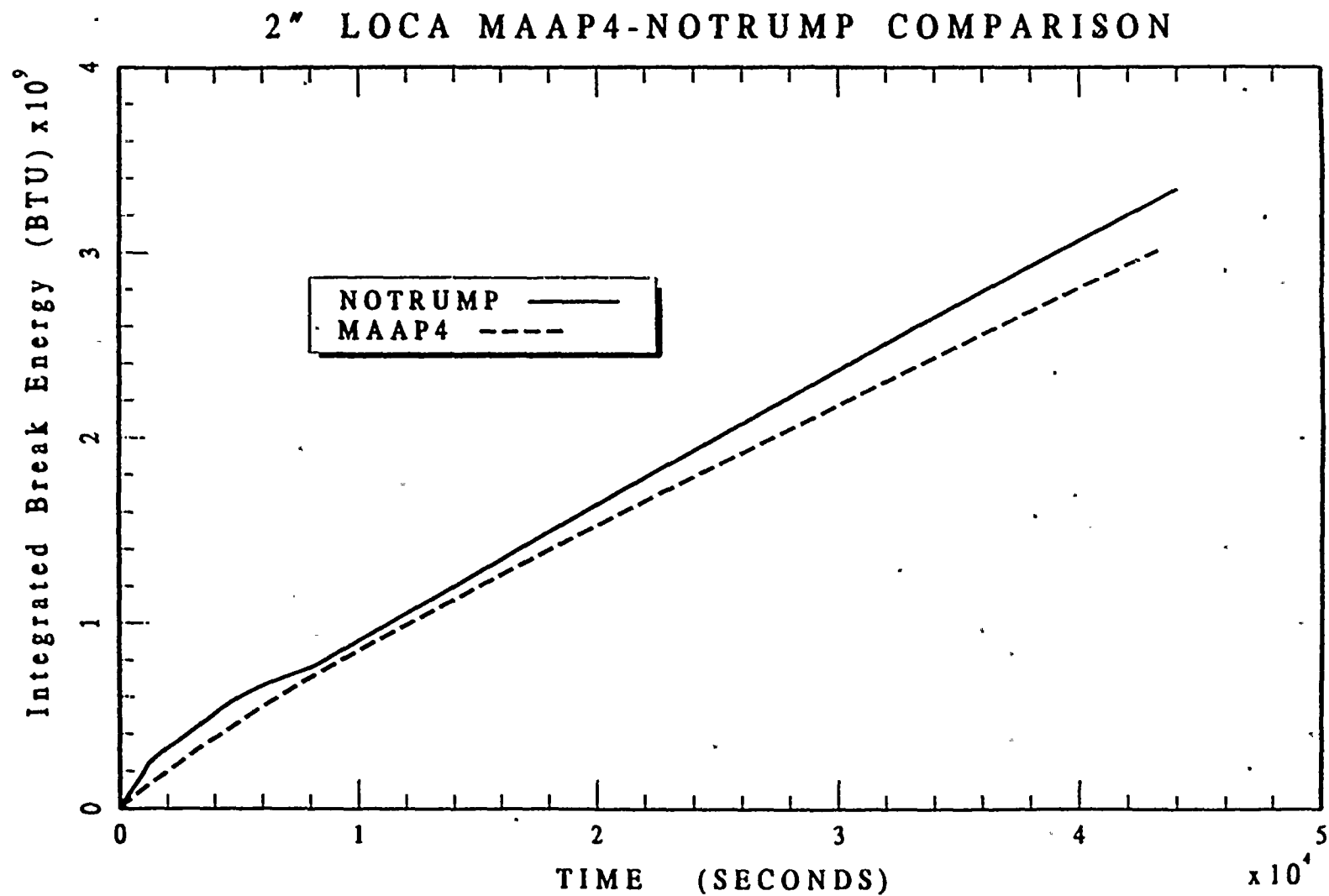


Figure 3-5 A comparison of the integral mass release to containment for NOTRUMP and the MAAP4 primary system model assuming a two-inch cold leg LOCA.

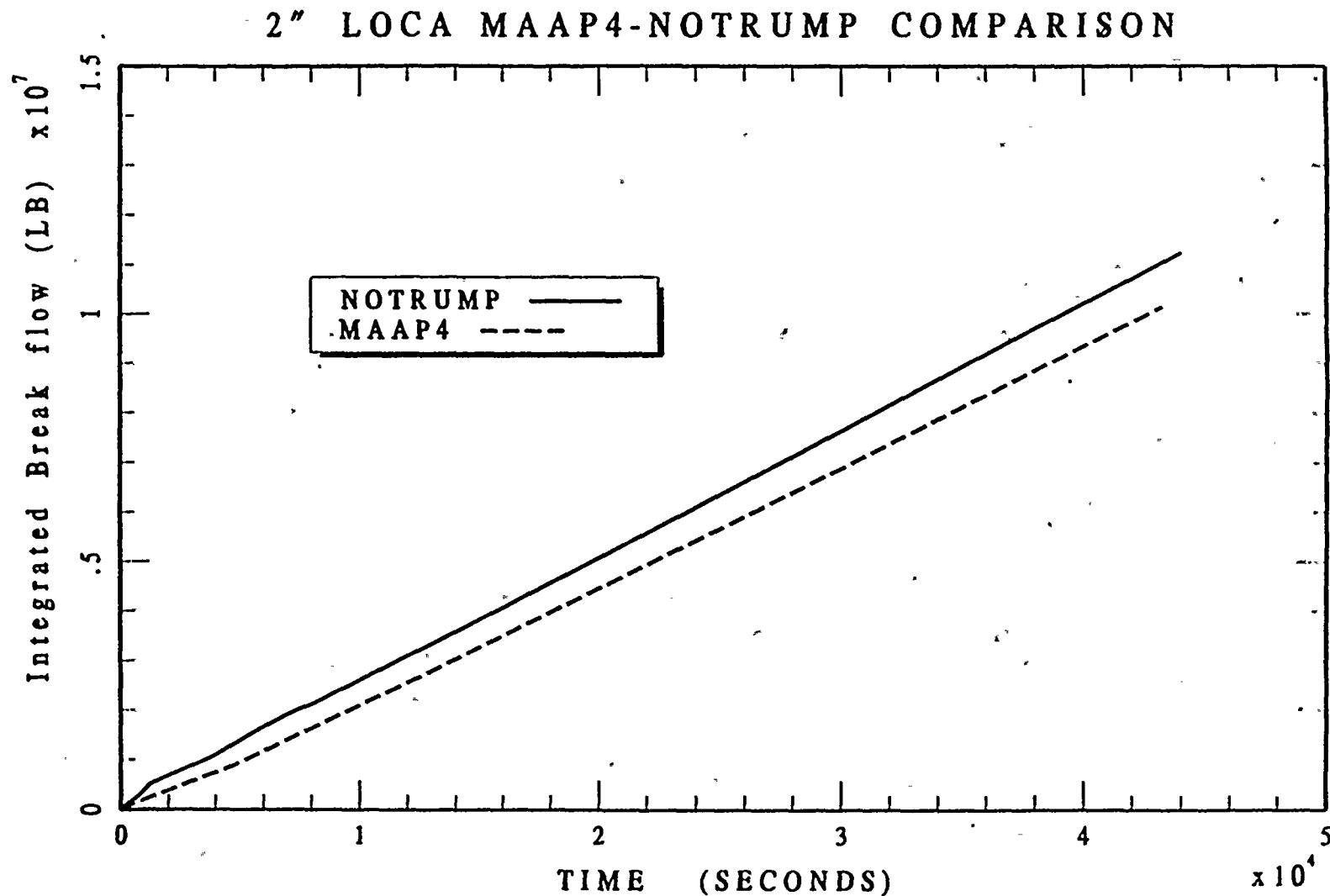


Figure 3-6 A comparison of the instantaneous energy release to the containment for NOTRUMP and the MAAP4 primary system model assuming a two-inch cold leg LOCA.

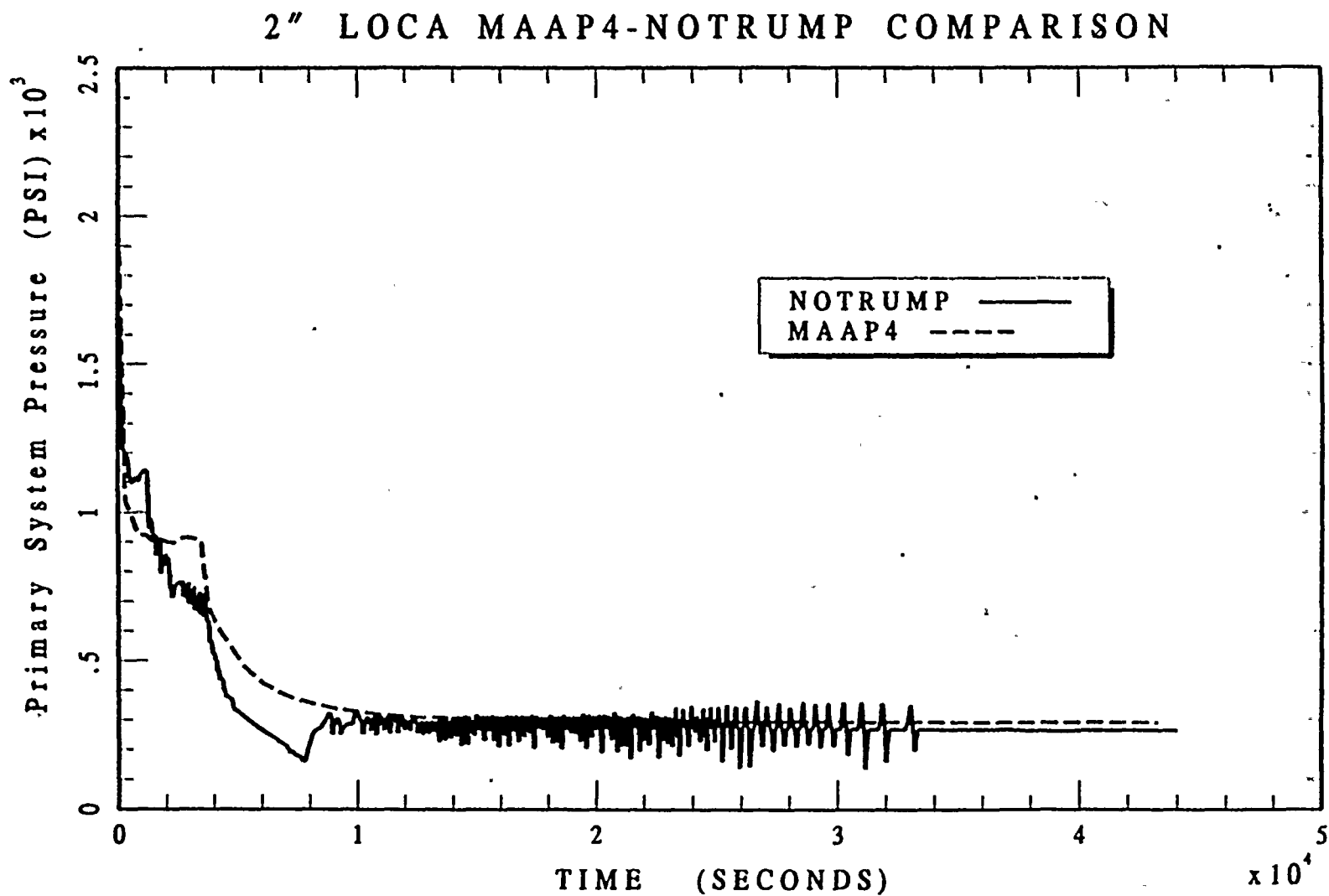


Figure 3-7 Primary system pressure for MAAP4 and NOTRUMP for a two-inch cold leg LOCA.



as well as the initial pressure and temperature of the blowdown vessel simulating the reactor coolant system water inventory. The various boundary conditions for the individual Waltz Mill tests are discussed in Appendix E.

### 3.5.2 Results

The results for the various benchmarks are comparisons of the following information:

- the transient simulated containment pressure history,
- the extent of ice melting for the different experiments,
- the temperature history of the water in the bottom of the ice condenser (Test K only), and
- the comparison of the temperature history in the simulated lower compartment for this scaled experiment (Test K only).

These comparisons are provided in Appendix E as the write-up used in Volume III of the MAAP4 User's Manual "Benchmarking". The conclusions derived from each of these comparisons are that the MAAP4 model provides a good characterization of the ice melted in each test and the water temperatures in the bottom of the ice condenser compartment and the lower compartment as well.

### 3.6 PNL Ice Condenser Experiments

The PNL experiments differ from the Waltz Mill tests in that the ice condenser baskets were full length but the experiment did not include the ice condenser inlet doors. Furthermore, the steaming rates for these experiments, as well as the noncondensable gas (air) flow rates were typical of the ice condenser response after the blowdown transient has been completed and the steam generation rate is due to decay heat steaming in the reactor core and is subsequently

discharged to the containment atmosphere. A spectrum of experiments were performed with similar noncondensable flow rates but different steam partial pressure which enables the MAAP4 ice condenser model to be compared with the PNL experiments over a variety of steam and air recirculation rates. Consequently, these experiments provide an important benchmark of the ice condenser/ice melt model for the range of conditions expected in the spectrum of break sizes considered in these analyses.

### 3.6.1 Boundary Conditions

Boundary conditions for the PNL experiments are described in Appendix F of this report, which is the write-up extracted from Volume III of the MAAP4 User's Manual "Benchmarking".

### 3.6.2 Results

The results from these comparisons are described in Appendix F along with the conclusions derived from the comparisons. In summary, the MAAP4 ice condenser model provides a good representation of ice melting rate and the exit temperature behavior observed for the different inlet conditions tested.

## 3.7 CSTF Ice Condenser Experiments

Large scale experiments were performed related to the flow distribution and mixing in ice condenser containment configurations. These were performed in the CSTF vessel as part of an EPRI funded program to examine the mixing in different regions of the ice condenser pressure suppression containment design. As part of this experimental program, the potential for single phase natural convection circulation between the upper and lower compartments through the simulated ice condenser doors was examined along with the potential for "flooding" of the gas-gas countercurrent natural circulation process by the imposed flow of the air recirculation fans. With these complex flow patterns, this is an important benchmark for the natural convection models in the MAAP4 code.

### 3.7.1 Boundary Conditions

The important boundary conditions for the CSTF ice condenser containment experiments are the initial temperatures in the upper and lower compartments, the steam addition rate to the lower compartment representative of the postulated LOCA condition and the imposed flow rate of light gases into the lower compartment to simulate the release of hydrogen under the postulated accident conditions. Furthermore, the boundary condition of the imposed air recirculation flow determines both the mixing potential between the upper and lower compartment as well as the potential for gas-gas "flooding" in the simulated ice condenser doors. These boundary conditions are discussed in Appendix G of this report.

### 3.7.2 Results

The results from the comparisons associated with the CSTF large scale flow distribution test show good agreement between MAAP4 model and the experimental data for mixing of the upper and lower compartment gas spaces. This agreement is obtained for those conditions in which the air recirculation fans are operating as well as for those where there is no forced circulation flow. The details of the comparisons are given in Appendix G of this report.

## 3.8 Discussion of the McGuire Event

In December of 1993, McGuire Unit 2 experienced a total loss of offsite power which led to a Safety Injection (SI) signal due to low pressurizer pressure and a consequential containment isolation. One of the Main Steam Containment Isolation Valves (secondary side) failed to isolate allowing the associated steam generator to depressurize. As a result an excessive steam generator differential pressure was observed and the pressurizer Power Operated Relief Valve (PORVs) were opened to reduce this differential. Subsequently, the Pressurizer Relief Tank (PRT) rupture disk was broken releasing steam to the containment lower compartment and causing the ice condenser inlet doors to open. Post event weighting of the ice baskets showed that ice melting occurred in the inboard baskets for all of the ice condenser bays. While these observations are more global

than the large scale experiments discussed above, this event provides a test for the integral model to determine if the calculated response would open the ice condenser lower inlet doors.

To perform this benchmark, the MAAP4 D.C. Cook model was initiated at full power and given a loss of offsite power and after the reactor scrammed, the RCS pressurized, and a safety valve was forced open. About 200 secs later the PRT rupture disk burst and steam was discharged to the containment lower compartment. This is sufficient to open the lower inlet doors and begin melting ice. Consequently, the integral model calculations are consistent with the McGuire experience. Equally important, the McGuire post incident observations show the uniformity of the inlet door response (all doors open) for this small break accident sequence.

### 3.9 Summary

Numerous benchmarks have been performed comparing the individual models of the MAAP integral RCS and containment representation with major experiments and other analytical approaches. All of these show that the MAAP4 representation (models) are in good agreement with the experimental observation and also the results of design basis computer codes. Table 3-3 summarizes the benchmarking activities and the conclusions.





**Table 3-3**  
**Summary of the Benchmarks Related to the**  
**D.C. Cook Containment Sump Evaluations**

Issue	MAAP4 Approach	Relevant Benchmarks
Representation of different conditions in different regions of the containment.	MAAP uses a 14 node containment model including the <ul style="list-style-type: none"> <li>• reactor cavity</li> <li>• lower compartment</li> <li>• annular compartment</li> <li>• ice condenser</li> <li>• fan rooms</li> <li>• instrument rooms</li> <li>• ice condenser upper plenum and</li> <li>• upper compartment (3 nodes),</li> </ul>	<ul style="list-style-type: none"> <li>• HDR tests have many rooms.</li> <li>• CSTF tests have the major rooms of an ice condenser containment.</li> <li>• Waltz Mill tests have the ice condenser compartments.</li> </ul>
Variations in break size and location.	14 node containment model with 0.5-inch to DECL breaks postulated in lower compartment and 0.5-inch to 2.75-inch in the reactor cavity.	<ul style="list-style-type: none"> <li>• Comparison with the NOTRUMP mass and energy releases for a 2-inch dia cold leg break.</li> <li>• HDR tests, T31.5 (large LOCA), and E11.2 (small LOCA).</li> </ul>
Structural heat sinks.	Each node has separate concrete and steel heat sinks, including the ice condenser node.	<ul style="list-style-type: none"> <li>• HDR tests, T31.5, and E11.2 has numerous rooms and both concrete and steel heat sinks.</li> <li>• CSTF includes steam addition and condensation of steel and wooden structures.</li> </ul>
Ice melt rate.	Mechanistic ice melt model.	<ul style="list-style-type: none"> <li>• Comparison with LOTIC-3 for the same mass and energy releases.</li> <li>• <u>W</u> Waltz Mill tests and PNL full length ice condenser tests.</li> <li>• McGuire ice melt due to rupture of pressurizer drain tank.</li> </ul>
CEQ fan flow.	Model for each train of fans and each fan room modeled separately.	<u>W</u> Waltz Mill test K, long term steam released to the containment with recirculation air flow.
Containment spray flow distribution.	Sprays are distributed to the upper, lower, and annular compartments.	Theoretical basis for spray droplet response.
Additional water for the RCS to remain full during cooldown for small LOCAs.	Integral model, including RCS and containment response for a spectrum of postulated LOCA sizes.	RCS response for Davis-Besse LOFW and Prairie Island SGTR during cooldown. Also McGuire for the drain tank rupture disk incident.

## 4.0 DESCRIPTION OF THE MOST LIMITING CONDITIONS FOR CONTAINMENT SUMP EVALUATIONS AND SENSITIVITY ANALYSES PERFORMED WITH MAAP4

### 4.1 Introduction

These evaluations focus on the minimum water level in the containment sump during recirculation. To perform such analyses, it is important to have an integral representation of the containment and the RCS since the water inventory retained in the RCS is an important component of the water distribution, i.e., it is not available to the containment sump. Furthermore, the extent of ice melting is an important contribution to the sump inventory and is influenced by the break discharge enthalpy and flow rate.

With an integral representation, the cooldown transient for the small break accidents represents the increased density of the RCS coolant and the capabilities to keep the reactor coolant system full as instructed by the EOPs. Moreover, the accumulators are also important since they could inject approximately 30,000 gallons into the RCS depending upon the pressure and the system status as defined through EOP decisions. They are a part of this analysis and are discussed further in this section.

Other influential components of the analysis that determine the minimum containment level are the initial containment temperature, (sets the initial steam partial pressure) and the cooling water temperatures for both the Emergency Service Water system (ESW) and the Component Cooling Water system (CCW) for the containment spray and RHR heat exchangers respectively. These, along with the UA product for the respective heat exchangers, determine the temperatures of the containment spray and RHR spray/RHR injection under recirculation condition and thus the potential for reducing the ice melt by condensing steam in the lower compartment. Similarly the RWST water temperature is important since this influences the potential for spray condensation in the lower compartment during injection phase. These limiting conditions are also discussed in this section.



## 4.2 Key Plant Parameters

For all LOCAs, there is no overpressure challenge to the containment as long as (a) ice is available, (b) the containment sprays are operating with water drawn from the RWST or (c) the containment sprays are operating in the recirculation mode with cooling provided by the containment spray heat exchangers. When investigating a spectrum of break sizes, there is a break size where the break discharge flow over the long term can have a significant vapor pressure, for example several psi. For such conditions, there will be steam released to the containment atmosphere that is condensed by the containment sprays. The sprays are assumed to remain on until the reset pressure (0.77 psig) is achieved, at which time the sprays are shut off. This is conservative with respect to the extent of ice melting.

The spray distribution for the D.C. Cook plant includes spray headers in the upper and lower compartments as well as in the pipe annulus. With the water flow paths between the various containment compartments described in Section 2, during long term containment spray operation, water would accumulate in the pipe annulus and lower compartment and with the communication (flow) through the crane wall, the level would be essentially the same in these regions. As noted in Section 2, a small fraction of the lower compartment spray flow would fall through the grated opening between the lower compartment and the reactor cavity which decreases the water inventory in the sump. Furthermore, the long term flow through the NI holes also enables water to flow from the lower compartment into the reactor cavity, or from the cavity to the lower compartment for a postulated break into the reactor cavity.

With this focus on the water inventory distribution, the basic analysis issue becomes one of the available water inventory. Therefore, there are several volumes of importance to the analysis since these control the water available in the sump. These are listed in Table 4-1. (This assumes that the pressurizer water level remains at the normal operating level.) Those RCS and containment volumes controlling the water distribution are listed in Table 4-2. Several other volumes are noted as reference volumes since they are calculated without including the volumes occupied by various pieces of equipment such as pipes, support structures, etc.



Table 4-1

Water Inventory Available

Volume Description	Volume/Mass
Available RWST Water Inventory	314,000 gal
Available Ice Mass	2.11 x 10 <sup>6</sup> lbm (253,089 gal)
TOTAL	567,089 gal
Accumulators (4)	230,252 lbm (27,618 gal)
TOTAL WITH ACCUMULATORS	594,707 gal

Table 4-2

Volumes Controlling Water Accumulation in the Analysis

Volume Description	Volume
Reactor Coolant System (including the pressurizer)	11,159 ft <sup>3</sup> (83,469 gal)
Volume of the Pressurizer	1800 ft <sup>3</sup> (13,464 gal)
Approximate Inventory Needed to Keep RCS Full During Cool Down	~ 20,000 gal
Inactive Sump Water Volume (pipe annulus)	334,950 gal
Net Volume for Water Accumulation in the Sump (active and inactive) to the 602'10" Level	220,300 gal
Water Volume for the Reactor Cavity Up to 610'0"	117,795 gal
TOTAL	572,795 gal





As illustrated by these two tables, the water distribution is determined by the water inventories in the RCS and containment. Of particular note, the RCS cooldown process requires a substantial water addition for the RCS to remain full, which may be the case for small break events. On the other hand, the large LOCA accidents do not keep the RCS full, i.e., there is a larger water inventory in the active sump to support ECCS operation.

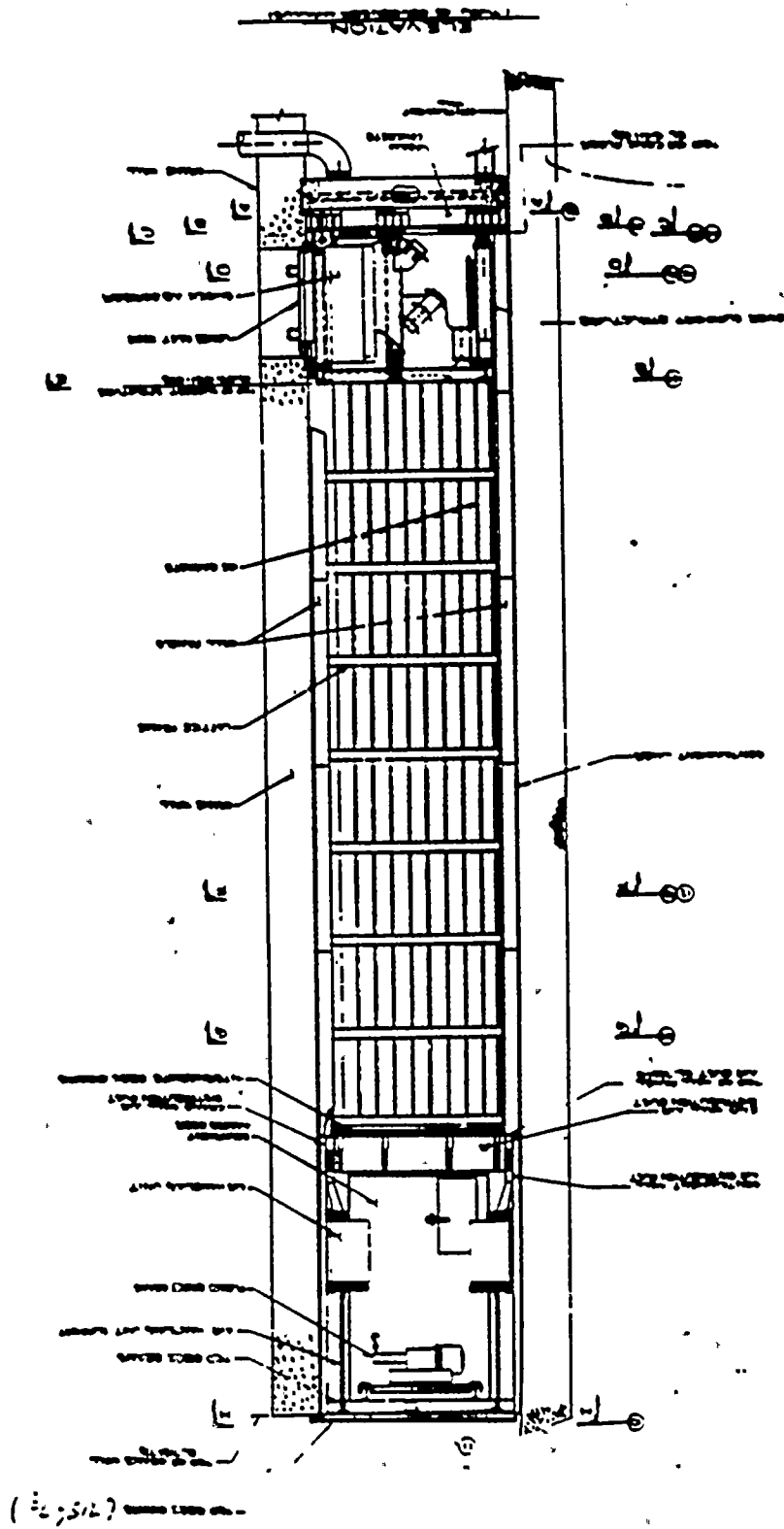
For very small breaks there are additional components to be considered such as the water stored in the pressurizer. Typically, the pressurizer drains and only partially refills, hence there is somewhat of a net contribution to the containment water inventory. This pressurizer response is determined by the EOPs which instruct the operator to keep the level between high and low level if possible. Maintaining the pressurizer level is unlikely for break sizes of 2-inch or greater. For these conditions the pressurizer drains and the accumulators remain unblocked and discharge as a result of the LOCA condition combined with a RCS cooldown (100°F/hr was used in this analysis since this maximizes the RCS water density increase). The accumulators contribute potentially another 27,618 gallons to the containment water inventory.

In these evaluations it is conservative for the reactor cavity to be filled with water, hence, sequences were analyzed assuming that the break discharge is into the reactor cavity, which ensures that the reactor cavity is flooded as well as the lower compartment. Furthermore, the base case analyses are performed following the system response and operator procedures for the containment sprays, i.e., the sprays actuate automatically at a containment pressure of 2.3 psig and are turned off, as stated in the procedures, when the indicated pressure is less than 1.5 psig which is 0.77 psig when the uncertainties for this instrument and reading the instrument are considered.

For the integral evaluations, the containment water distribution includes assessments of where water accumulates and flows into drains and thus into the lower compartment. The most important place for water accumulation and drainage is in the bottom of the ice condenser. Figure 4-1 shows an elevation view of an ice condenser with the drain pipe at the bottom passing through the crane wall such that the melted ice and condensate drain into the lower compartment. Figure 4-2 is a plan view for the bottom of the ice condensers showing the floor drains in the ice boxes.



**Figure 4-1** Water flow paths to the active and inactive sump regions.





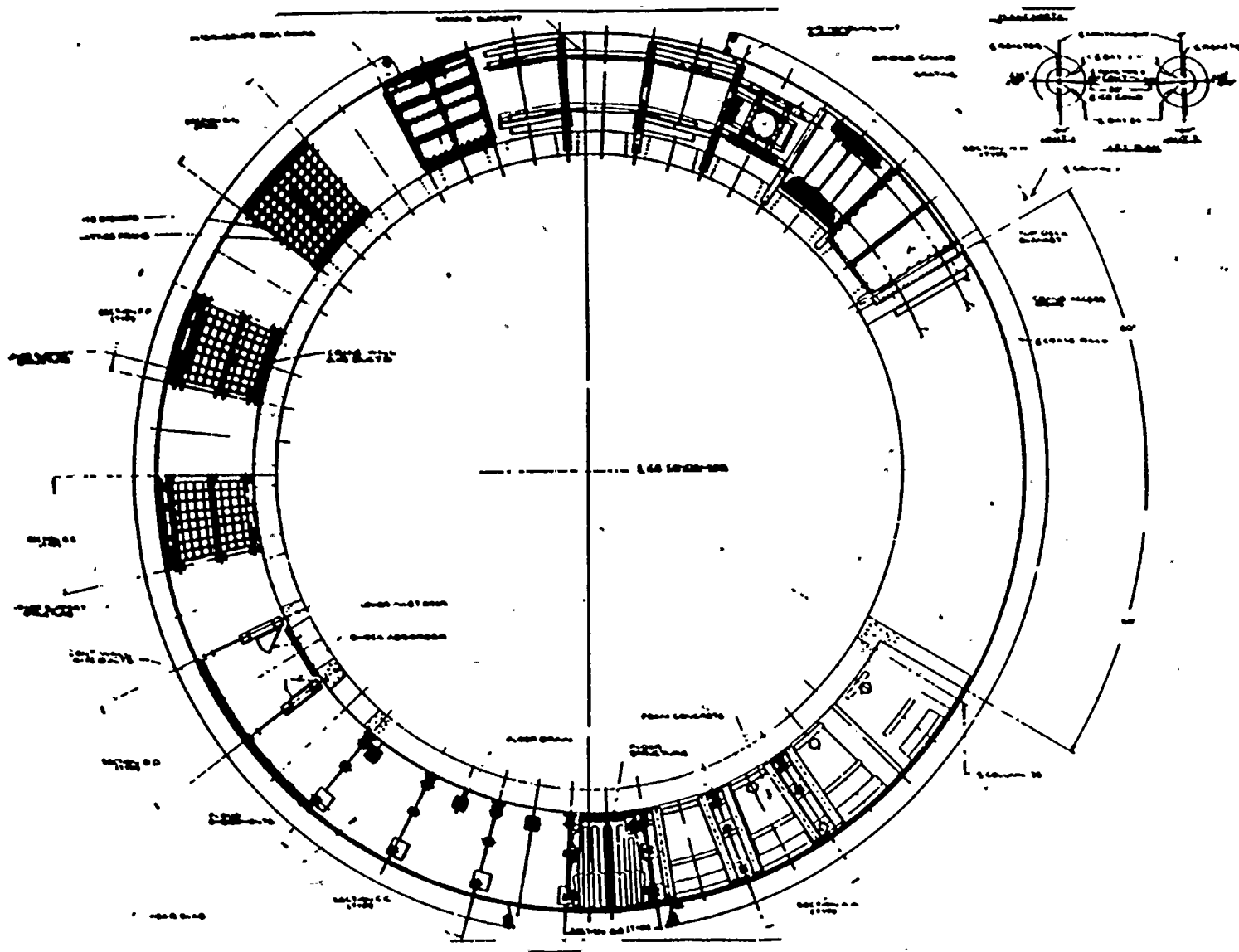


Figure 4-2 Elevation view of an ice condenser including the drain line.



As stated in the D.C. Cook FSAR, approximately 18 inches of water in this drain pipe is sufficient to open the flapper valve covering the drain exit into the lower compartment. In comparison, the height of the drain line is approximately 4 feet, hence, this flapper valve would open before the drain pipe would be filled with water. Like the previous MAAP4 analysis (FAI, 1997), this analysis also models this junction between the ice condenser and the lower compartment as a water only junction that does not allow reverse flow, i.e., the flapper valve closes. Hence, the drainage from the ice condenser into lower compartment is modeled in a mechanistic manner and includes a relatively small water mass that would exist on the ice condenser floor. This drainage is modeled with capillary size drops as the water falls through the lower compartment. (It is noted that each drain line has a small (1/2-inch) pipe which drains ice melted during normal operation and ducts the water to the sump. These are also modeled but have essentially a negligible influence on the containment response.)

Another location for water accumulation is the refueling pool, which has two 12 inch drains and one 10 inch drain into the lower compartment and requires water to be accumulated to a depth that would permit flow into these drains in the bottom of the refueling canal. The MAAP4 code provides a mechanistic spillover calculation for this region. However, a value of 9500 gallons is given in the D.C. Cook FSAR for the water retained in the refueling canal as a result of this spillage process and accumulation in the fuel transfer pit. Therefore, the MAAP4 "curb height" for this location was increased such that the depth to be accumulated before spilling could occur to match a value of 9500 gallons.

In addition there are several minor elements influencing the water distribution, which are modeled in terms of the thermal hydraulic containment response, but the water inventory is not calculated directly by MAAP. These include the water required to fill the various pipes for containment spray and RHR operation, the water inventory that is airborne during a steady-state operation of the containment sprays, that portion of the containment spray which impinges on walls in a given compartment and drains to the floor region as a film draining down the wall and water that accumulates on the top of the dog house following spray initiation. The various water volumes held up in these additional processes are listed in Table 4-3 for the readers reference.





Table 4-3  
Potential Locations of Spray Water Holdup

Location	Magnitude of Water Holdup
Water required to fill spray piping and S/G doghouse roof <ul style="list-style-type: none"> <li>• containment spray header,</li> <li>• RHR spray header,</li> <li>• top of S/G doghouses.</li> </ul>	7789 gal 1730 gal 5312 gal
Water in-flight during spray operation <ul style="list-style-type: none"> <li>• upper compartment (h = 80.2 ft),</li> <li>• lower compartment (h = 50.9 ft),</li> <li>• annular compartment (h = 36.75 ft).</li> </ul>	656 gal 155 gal 40 gal
Sprays impinging upon walls and draining as a film <ul style="list-style-type: none"> <li>• upper compartment (42,000 ft<sup>2</sup>),</li> <li>• lower compartment (15,000 ft<sup>2</sup>),</li> <li>• annular compartment (10,000 ft<sup>2</sup>).</li> </ul>	206 gal 74 gal 49 gal
<b>TOTAL</b>	<b>16056 gal</b>
* A conservative value of 50 ft <sup>3</sup> (374 gal) was used in the analysis.	

The first item was determined by summing the volumes of the respective piping configurations, the second is calculated using the spray fall height in the respective compartments (see Appendix H) with the third item being determined by the containment geometry and a methodology for approximating drainage films (see Appendix I). Since MAAP4 does not specifically represent these holdup volumes, these were accounted for by transferring from RWST injection to containment recirculation at a RWST level equal to that defined by the RWST low-low trip plus the sum of the volumes listed in Table 4-3. Therefore, the water inventory injected to the RCS and containment from the RWST is  $314,000 - 16,056 = 297,944$  gal. In this manner, the water involved in determining the water level history already has the sum of these volumes subtracted from the final distribution.



#### 4.3 FMEA Conditions Used in the Analyses

To support this effort a Failure Modes and Effects Analysis (FMEA) was performed to determine the most limiting conditions related to the containment sump inventory under the spectrum of LOCA conditions evaluated. Since the ice melt inventory is part of the containment sump evaluation, the FMEA conditions are directed toward minimizing the extent of ice melt with the particular focus being the lowest spray temperatures which produce the maximum steam condensation, i.e., minimize the ice melt. Specifically, these relate to the minimum RWST temperature, according to the D.C. Cook technical specifications, and the minimum lake temperature that is the cooling water for the ESW systems. In addition, there are other elements of the containment which cause the sprays to be initiated at the earliest time in the accident, etc. The results of this FMEA study are listed below:

- RWST temperature of 70°F,
- initial containment pressure 15 psia,
- initial containment temperature in all compartments 60°F (this minimizes the steam partial pressure to be condensed),
- lake water temperature used for cooling the ESW system is 33°F,
- the CCW heat exchanger inlet temperature is 60°F,
- the initiation signal including uncertainty for the CEQ fans is 0.5 psig, and
- the setpoint including uncertainty for initiation of containment sprays is 2.3 psig.

#### 4.4 Modeling of the EOPs

Several operator actions directed by the EOPs are important to this analysis. These relate to the RWST water level at which transfer to recirculation is started, the shutdown of containment sprays to transfer to recirculation, the use of the RHR sprays, the instructions for refilling the RCS to obtain and maintain a water level in the pressurizer, cooldown of the RCS with the maximum rate of 100°F/hr, the isolation of the accumulators depending upon the specific response developed



in the RCS, and the termination of containment sprays once initiated. Each of these has an influence on the accident behavior and the modeling of each is discussed below.

#### 4.4.1 Transfer to Containment Recirculation

For the D. C. Cook Units 1 and 2 design, transfer from the injection mode to containment recirculation is a manual operation. As represented in the DIT values presented in Appendix A, this transfer begins when 280,000 gallons have been taken from the RWST with the initial action being to transfer the suction of the large pumps (containment spray and RHR) from the RWST to the recirculation sump. The assumption of two trains of ECCS injection and spray operation is conservative for the sump water level analysis. Transfer to recirculation of both trains is accomplished by shutting down both trains of containment sprays and RHR, aligning the valves to recirculation and restarting the pumps. These actions are performed within a five minute interval; hence, this is modeled as five minutes without containment spray once the RWST transfer level is reached.

Once these high volume pumping systems have been transferred, the operators then transfer the smaller systems, such as the high head injection pumps and charging pumps from the RWST to the containment recirculation sump. This is completed when 314,000 gallons have been taken from the RWST.

The above values are the calculated deliverable volumes. Holdups in the spray piping, the airborne water in the containment and the film drainage on the containment walls are all represented in the analysis as water which remained in the RWST. Consequently, the actual amount of water injected to the RCS and containment are the above values minus the individual holdup contributions.



#### 4.4.2 Duration of the Containment Sprays

Containment sprays are initiated when the lower compartment pressure reaches 2.3 psig. Water is initially taken from the RWST and takes a few tens of seconds before the spray is injected to the containment gas spaces.

The duration of the containment spraying, once initiated, is determined in this analysis by the pressure in the containment lower compartment, which is monitored by the control room operators. The RHR sprays (this system only sprays to the containment upper compartment) are initiated by the operators given the following three conditions are met:

- 50 minutes or more have elapsed since the SI signal was received, and
- a single train of containment sprays is operating.

Note that the RHR sprays would not be initiated if both trains of containment sprays are operating. It should also be noted that RHR sprays take their suction from the containment sump and influence the overall containment thermal hydraulic conditions (some reduction of ice melt), but do not, by themselves, increase or decrease the water level in the containment sump since the water sprayed into the upper compartment returns to the sump through the refueling pool drains.

Control room dose evaluations have suggested that the containment sprays may operate for a significant period before the dose associated with the postulated design basis accident source term (Soffer et al., 1995) would be reduced by containment spray operation. Currently, these analyses consider the sprays are terminated when the containment pressure is reduced to 0.77 psig. This is the minimum containment pressure corresponding to an indicated pressure of 1.5 psig, the operator set point for terminating containment spray. Generally this results in a time which is comparable to the 6 hr. duration. However, no specific time duration has been imposed on these calculations.

#### 4.4.3 Pressurizer Level Control

For small break LOCA conditions, the capability of injection systems to restore the RCS inventory (pressurizer level) determines the ECCS injection rate. The EOPs instruct the operators to establish pressurizer level and to control the level between 30% and 47% of the full inventory. In these evaluations, this is represented by a throttling of the injection flow if the pressurizer inventory approaches the 47% full limit. Since this is the upper limit that the operators are instructed to maintain, this represents the maximum holdup in the pressurizer and is a conservatism in the analysis:

#### 4.4.4 RCS Cooldown

RCS depressurization and cooldown is based on the conditions following transfer to recirculation. Since the initiation of two trains of containment sprays is a key element of this assessment, the LOCA conditions evaluated are those which would initiate containment sprays. Typically, these are LOCAs for break sizes which are 1 inch in diameter or larger. Once the containment sprays initiate, which is generally within a few minutes of the postulated LOCA transient under Mode 1 conditions, the containment sprays actuate automatically with two trains operating and this determines that the operators attention would be directed towards recirculation since this occurs approximately 1/2 hr after the sprays have been initiated. Given the importance of transferring from RWST injection to taking suction from the containment sump, this is the highest priority for the operators. Hence, cooldown would be deferred until transfer to recirculation was completed. This is modeled as taking 15 mins which for this high priority activity is an underestimate (conservative) of the time over which the operators would have devoted their attention to actions other than RCS cooldown. Therefore, RCS cooldown is evaluated as beginning 15 mins after the start of the transfer to containment recirculation.

Once cooldown is initiated, it is evaluated at the maximum rate described in the EOPs of 100°F/hr. In the analysis this is represented as 10 steps of 10°F over each hour and is accomplished in the MAAP4 model by resetting the secondary side PORVs to sequentially lower



values corresponding to the 10°F steps. The steam generator secondary side saturation temperature follows this cooldown as long as the generators can blowdown at a sufficient rate through the PORVs controlling the secondary side depressurization. Early in the depressurization the cooldown is about 100°F/hr, but at reduced secondary side pressures later in the transient, the blowdown cannot produce 100°F/hr.

#### 4.4.5 Isolating the Accumulators

One of the actions in the EOPs is to isolate the accumulators during RCS depressurization. Reviewing the procedure ES-1.2 for RCS cooldown and discussions with D.C. Cook control room operators, the accumulators would only be isolated if the pressurizer level could be maintained with normal charging flow. For the break sizes sufficient to initiate containment sprays, which is discussed in Section 5, the pressurizer level is not capable of being maintained with normal charging. As a result, the accumulators will not be isolated for any of the LOCA conditions considered and are modeled as being available for injection during the entire transient history.

## 5.0 ANALYTICAL RESULTS FOR THE COMPLETE SPECTRUM OF LOCA SIZES

### 5.1 Introduction

In assessing the minimum containment sump level for a spectrum of potential LOCA conditions, the two most influential boundary conditions are the size of the LOCA and its location. As mentioned previously, the assessment for the minimum level is compared to the licensing base limit for vortexing established at an elevation of 602'10" through D.C. Cook specific scaled experiments performed at Alden Laboratories (Padmanabhan, 1978). This level was developed for injection flow rates typical of maximum ECCS and containment safeguard flows and is the licensing basis for all LOCAs initiating from a Mode 1 state begin even though the sump demand flowrate may be substantially reduced for smaller break accident initiators. Mode 3 analyses have less stored energy in the RCS and have smaller break sizes and therefore smaller sump demands.

For very small LOCA conditions, the steam entering the lower compartment pressurizes the region and opens the ice condenser doors. Continued steam delivery to the lower compartment displaces noncondensable gases from the lower compartment to the upper compartment and increases the containment pressure sufficiently that the setpoint is reached for actuating the air recirculation fans. Until this time, the normal containment ventilation system is operating but the cooling water for this system is isolated once the CEQ fan setpoint is reached. Since this occurs early in the accident sequence for the spectrum of LOCAs examined, the influence of the normal ventilation system is considered insignificant and neglected.

Forced flow from the CEQ fan(s) increases the condensation in the ice condenser and begins to mitigate the containment pressurization. As the lower compartment pressure increases, the steam condensation rate in the ice condenser also increases. If the containment pressure remains below the containment spray setpoint, the minimum sump inventory is assured since the transfer to recirculation occurs after many hours and there is sufficient ice melt to assure that the



minimum sump inventory is always above the licensing base limit for vortexing. However, for a somewhat larger break size, the containment pressure reaches the containment spray setpoint even though the recirculation fans are operating. At this juncture, the containment sprays are initiated and the spray flow rate into the lower compartment condenses steam such that the ice melt is substantially reduced from that immediately prior to the sprays being initiated. These conditions result in minimal steam partial pressure in the lower compartment to be forced through the ice condenser by the air recirculation fans. Moreover, the limiting case of two trains of containment sprays operating results in the minimal time to the transfer point from injection to recirculation. Consequently, the ice melt contribution to the sump inventory at the time of minimum sump level is further decreased by the relatively short interval available to melt ice.

As the break size is further increased, the steam partial pressure in the lower compartment is increased even with the actuation of containment sprays. Consequently, an increased steam partial pressure causes more ice melt and the minimum sump inventory during recirculation will increase compared to the smaller break sequence where the sprays were also initiated. With these general considerations, it is apparent that the minimal sump inventory results from that postulated LOCA size, which is large enough to actuate the containment sprays but also results in minimal steam partial pressure in the lower compartment once the sprays are actuated.

The second element addressed is the break location with two general locations considered, i.e., the lower compartment and the reactor cavity. If the break is postulated to occur in the lower compartment, the accumulated water inventory in the reactor cavity is only due to the flow between the lower compartment and the reactor cavity through the small nuclear instrumentation (NIS) holes and the spillover which occurs if the active sump water level reaches the 610' elevation. As a result, most of the water inventory is accumulated in the active sump and the pipe annulus, both of which have essentially the same water level as a result of the water flow (communication) through the holes in the crane wall. Conversely, if the postulated break is into the reactor cavity, the same steam discharge flows into the lower compartment but the water from the postulated break is discharged, at least partially, into the reactor cavity. If the break is in the bottom of the RPV, all of the break liquid discharge is deposited in the reactor cavity. If the

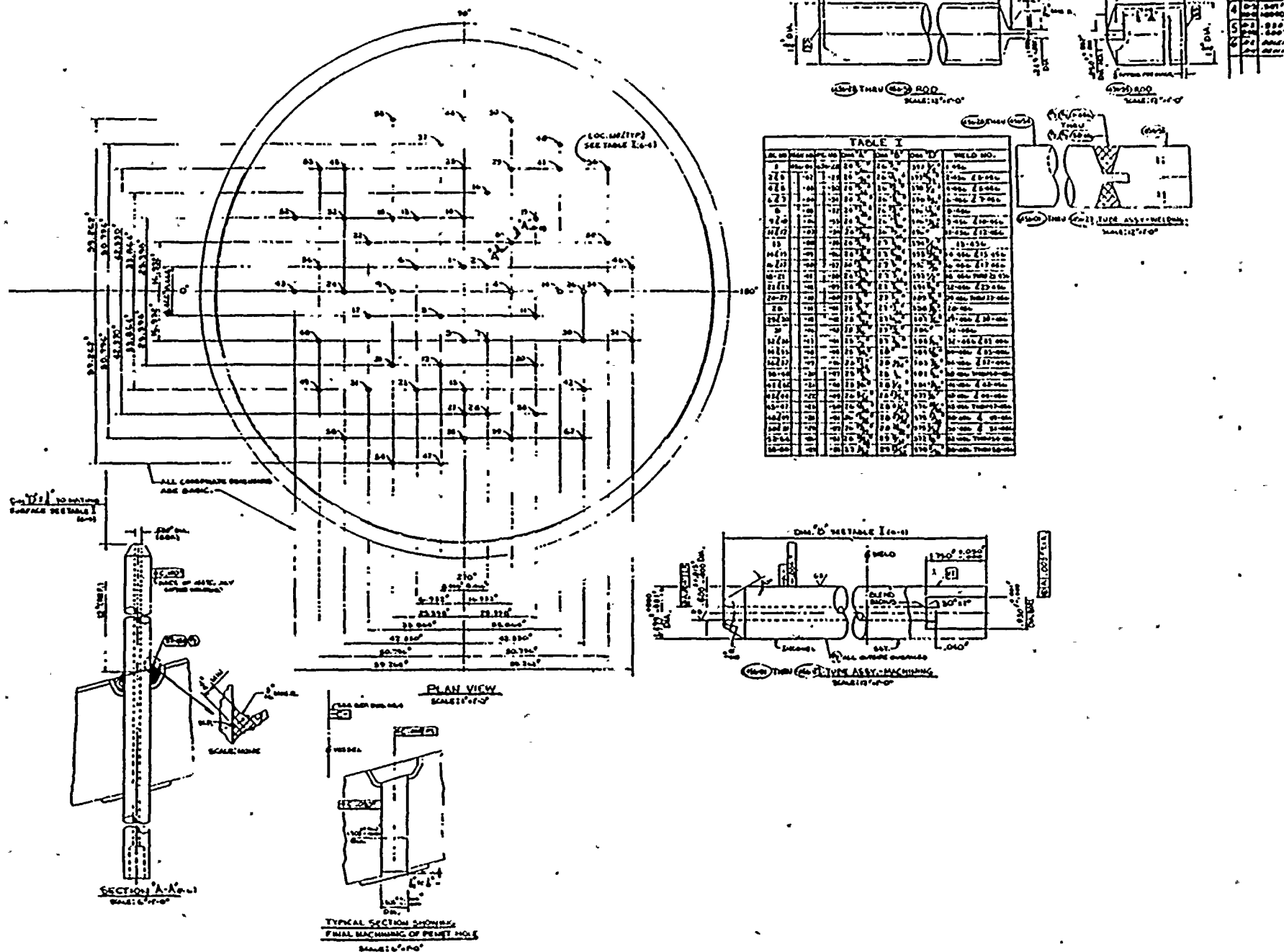
break is in the cavity at the cold leg nozzle elevation, the water discharge would be split between the reactor cavity and the lower compartment (see Appendix B). Hence, there may be a substantial water holdup in the reactor cavity until spillover occurs at the 610' elevation.

Several different break sizes have been evaluated for the reactor cavity with the breaks in the bottom of the reactor vessel being considered as a severing of an in-core instrument penetrations with a diameter potentially as large as 0.61 inches (Kury, 1998). The penetration diameter for the in-vessel instruments is illustrated in Figure 5-1. Severing of an in-core instrument with the thimble tube ejected leaves the full inner diameter of the penetration for a discharge of the reactor coolant inventory. The penetration structure remains in the lower plenum and this results in a flow path for the discharge of about 2 ft. Hence, for the D.C. Cook penetration design this results in a break geometry with an effective length of 40 to 50 L/Ds. Given this configuration, the effective discharge coefficient is 0.6 or less as illustrated by several experiments with saturated and subcooled liquid discharge through similar configurations as summarized and modeled by Henry (1970). With this significant L/D ratio, a discharge coefficient of 0.4 to 0.5 is the expected range. In the MAAP4 analyses discussed here, a discharge coefficient of 0.61 was used and is a conservatism in that it overstates the break discharge flow rate into the reactor cavity.

Break sizes larger than 0.61 inch diameter are also considered but these are into the upper regions of the reactor cavity, specifically at the cold leg nozzle location. In these locations the postulated break is in the weld between the safe end (RPV nozzle) and the reactor coolant piping with a spectrum of break sizes considered ranging from an effective diameter of 1 inch to an area of 1 ft<sup>2</sup>. This large break size is the largest that could occur in the vicinity of the RPV considering the vessel mounts and the pipe restraints. Evaluations of the critical flow discharge from the break and the secondary choking at locations in the downstream passages results in a flow split of 28% to the reactor cavity and 72% to the lower compartment (McCurdy et al., 1968).

Because of the tight geometry in this locale and the possibility of the break discharge being delivered to both the reactor cavity and the lower compartment, the split of the discharge flow for









the smaller breaks is evaluated in Appendix B. A best estimate of the flow split is 50/50 based on the analysis of the two-phase jet impinging on the wall of the biological shield. Westinghouse GOTHIC analyses (Westinghouse, 1999c) concluded that even more than 50% of the water discharge would flow to the lower compartment. These split break flow analyses have been performed with a 50/50 split of the water discharged from the postulated break. Since the break is never submerged at this elevation, the steam discharge flows from the cavity to the lower compartment as a natural consequence of the MAAP4 generalized containment model.

Lastly, break sizes in the reactor cavity are also considered in the top of the reactor vessel in the control rod drives. Considerations of possible ruptures in the top of the reactor pressure vessel included assessments for the CRDMs and the reactor head vent. Assessments for the CRDM behavior (Westinghouse, 1999b) conclude that rupture of the CRDM would either be very small leaks or a rupture and ejection of the entire mechanism. This was represented in the spectrum of accident sequences by considering a 2.75 inch break in the top of the reactor vessel with a discharge coefficient of 0.75. While this is the default coefficient in the MAAP4 code, it is also a typical value given the entry into the break location and the length of the flow break location. As will be discussed this break size initiates containment sprays and is analyzed as having 100% of the break water flow into the reactor cavity. An increase in this discharge coefficient would tend to actuate the sprays slightly earlier but would not significantly change the minimum level in the sump. Hence, there is no significant influence of the discharge coefficient for these analyses. The representation for a postulated severing of the reactor head vent considers that the effective discharge coefficient for the upper head is 0.61 as determined from the length-to-diameter ratio ( $> 7$ ) and the composite set of two-phase critical flow experiments for the discharge of saturated subcooled liquids as summarized and evaluated by Henry (1970).

Given the sensitivities to the break size and the break location, an evaluation matrix was developed (Table 5-1) to assess the influence for variations in both of these parameters given a Mode 1 operating state.



Table 5-1

**Break Size/Location Matrix for Evaluating Minimum Level  
in the Containment Sump for a Mode 1 Operating Condition**

Break Size	Location
DECL <sup>a</sup>	Lower Compartment (Sump)
6 inch	Lower Compartment (Sump)
4 inch	Lower Compartment (Sump)
3 inch	Lower Compartment (Sump)
2 inch	Lower Compartment (Sump)
1.5 inch	Lower Compartment (Sump)
1 inch	Lower Compartment (Sump)
0.5 inch	Lower Compartment (Sump)
1 inch <sup>b</sup>	Cavity/LC (Split Break)
1.5 inch <sup>b</sup>	Cavity/LC (Split Break)
2 inch <sup>b</sup>	Cavity/LC (Split Break)
3 inch <sup>b</sup>	Cavity/LC (Split Break)
4 inch <sup>b</sup>	Cavity/LC (Split Break)
1 ft <sup>2</sup> <sup>c</sup>	Cavity/LC (Split Break)
0.61 inch <sup>d</sup>	Cavity
2.75 inch <sup>e</sup>	Cavity
<sup>a</sup> This break represents a Double-Ended Rupture on the Cold Leg. <sup>b</sup> The break occurs in the cold leg and 50% of the water flows to the sump. <sup>c</sup> The break occurs in the cold leg and 30% of the water flows to the reactor cavity. <sup>d</sup> The break occurs at the bottom of the reactor vessel. <sup>e</sup> The break occurs in the top of the reactor vessel.	

## 5.2 Base Case Results

### 5.2.1 RCS Break Location in the Lower Compartment

Given the size of the piping configurations in the lower compartment, a complete break spectrum from an effective diameter of 0.5 inch to a Double-Ended Cold Leg break (DECL) were considered for this region. Figure 5-2 summarizes the response for the DECL condition which is the break sized used in the design basis assessment for the ECCS and containment systems. In this sump inventory analysis the mass and energy releases from the RCS to the containment are produced by the MAAP4 code. The resulting steam discharge to the containment is determined by the thermodynamic equilibrium of the water and steam discharged from the break during a blowdown. Using this assumption results in the minimum steam flow rate to the lower compartment gas space and hence results in the minimum potential for ice melting. This conservative representation for the ice melt behavior is consistent with the structure of evaluations for the minimum sump inventory. It is to be noted that this thermodynamic equilibrium representation differs from that used in design basis assessments related to containment integrity which maximize the steam flow rate from the break into the lower compartment.

As illustrated by this composite plot of the four variables depicted in Figure 5-2, the water level history in the sump increases rapidly due to the break discharge and ice melt as well as the water added by the containment sprays once the spray setpoint pressure is reached. Furthermore, with a large break, the reactor coolant system cannot be refilled and the containment sump inventory includes essentially half of the RCS inventory as well as the accumulator inventory. This results in a water level at recirculation of approximately 7.7 ft (an elevation of 606.5') with a minimum level of 604.7' at 9.1 hours into the accident. This lower level is due to long term flow into the reactor cavity through the NIS holes. Therefore, for this accident sequence the minimum water level is well above the 602'10" licensing basis limit for vortexing.

Note that these four plots summarize the integral plant response represented by the MAAP4 code and in particular illustrate the ice melt history, the sump water level, the water inventory in

# DECL BREAK INTO LOWER COMPARTMENT

FAI\99-77; Rev. 0

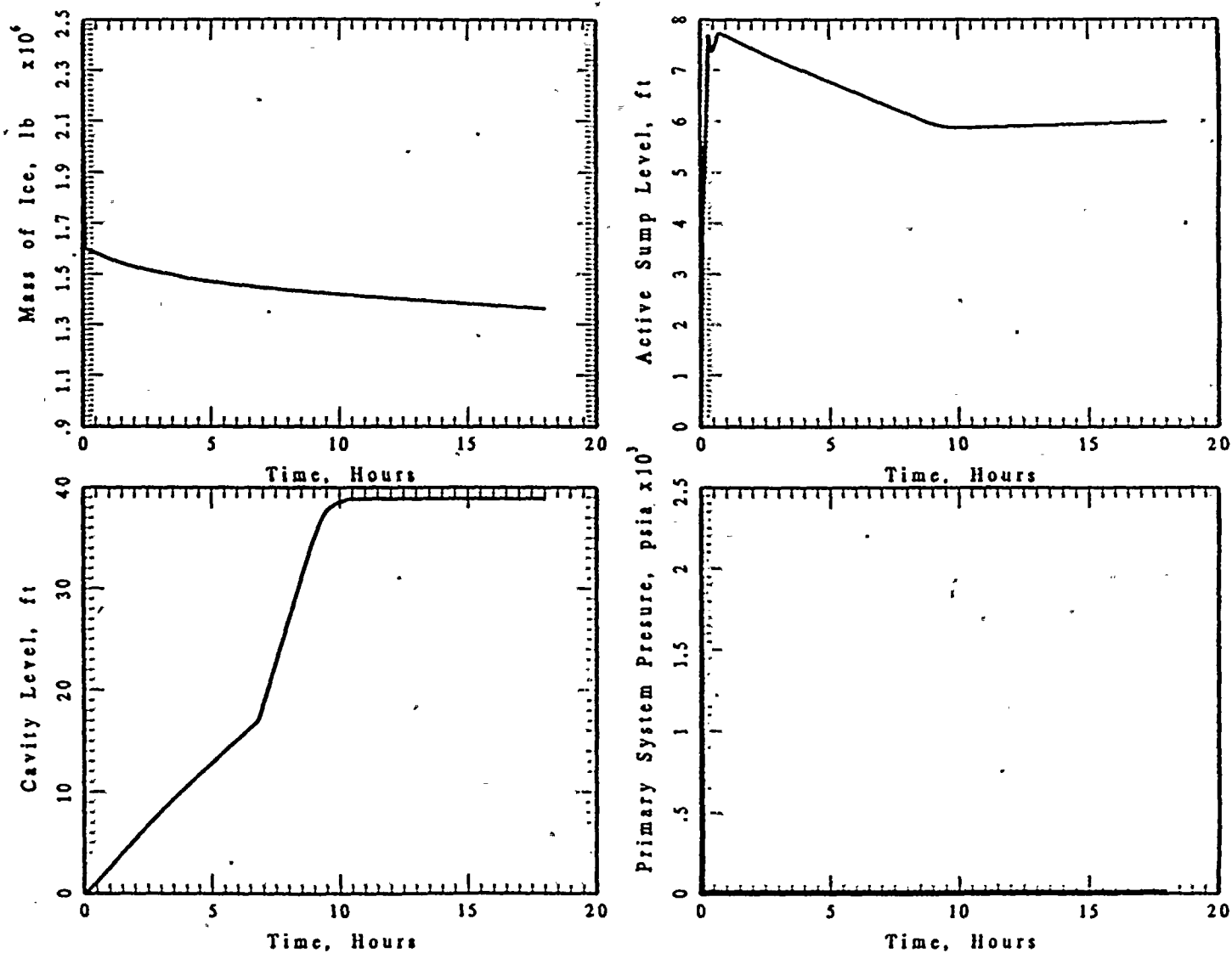


Figure 5-2 A summary of the primary system and containment response for a DECL break into the lower compartment



the reactor cavity and the RCS pressure which indicates whether the RCS is essentially half full (depressurized) or completely full (pressurized by the injection flow). Interactions between the RCS and containment are important for this evaluation and can only be tracked with an integral model. This set of plots are used to illustrate the integral response as a function of the LOCA size and location.

Figure 5-3 illustrates the calculated results for a LOCA into the lower compartment with an effective diameter of 6 inch. This accident sequence progresses in a similar manner to the DECL case except that the RCS refill is somewhat more effective such that some additional water is held up in the reactor coolant system. However, the pressurizer is not refilled and accumulators inject early in the accident. Consequently, the water level in the active sump at recirculation is 6.8 ft (an elevation of 605.6') and, like the DECL assessment the minimum water level occurs at 9.2 hours and is 604.1' which is above the 602'10" licensing basis limit for vortexing.

Figure 5-4 summarizes the results for a 4 inch dia. LOCA into the lower compartment. In comparison to the 6 inch dia. break, this sequence can have more water held up in the RCS. The water level in the sump at recirculation is 6.5' (an elevation of 605.3') with the minimum level being 603.9' at 9.7 hrs. This is above the 602'10" licensing basis limit for vortexing.

The results for a postulated break into the lower compartment with an equivalent diameter of 3 inch is illustrated in Figure 5-5. For this intermediate size break, two trains of ECCS injection are sufficient to eventually begin refilling of the pressurizer after the reactor coolant system has been substantially depressurized. Therefore, there is additional holdup of water in the RCS but the accumulators have injected completely by the time that the minimum level occurs in the sump. With this smaller break diameter, the steam released to the lower compartment atmosphere is substantially less than that which was calculated for both the 6 inch and the DECL break and consequently results in a smaller mass of ice melt added to the lower compartment. As illustrated in Figure 5-5 the water level in the active sump at recirculation is 6.1 ft (elevation of 604.9'), with the minimum level occurring at 10 hrs. with a value of 604.3'. This is less than that of large breaks but above the licensing basis limit for vortexing of 602'10".

# 6.0 IN BREAK INTO LOWER COMPARTMENT

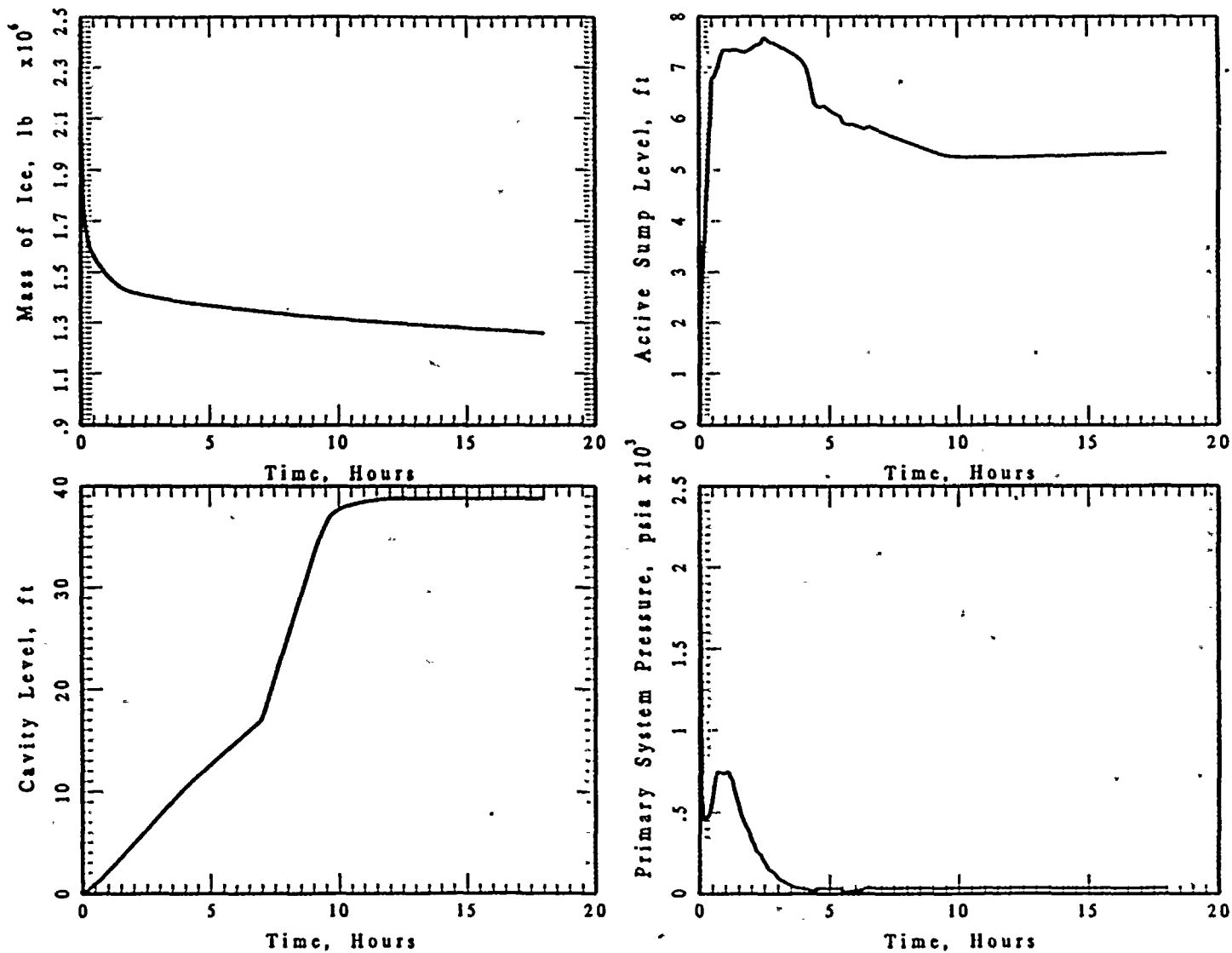


Figure 5-3 A summary of the primary system and containment response for a 6 inch dia. cold leg break into the lower compartment.



# 4.0 IN BREAK INTO LOWER COMPARTMENT

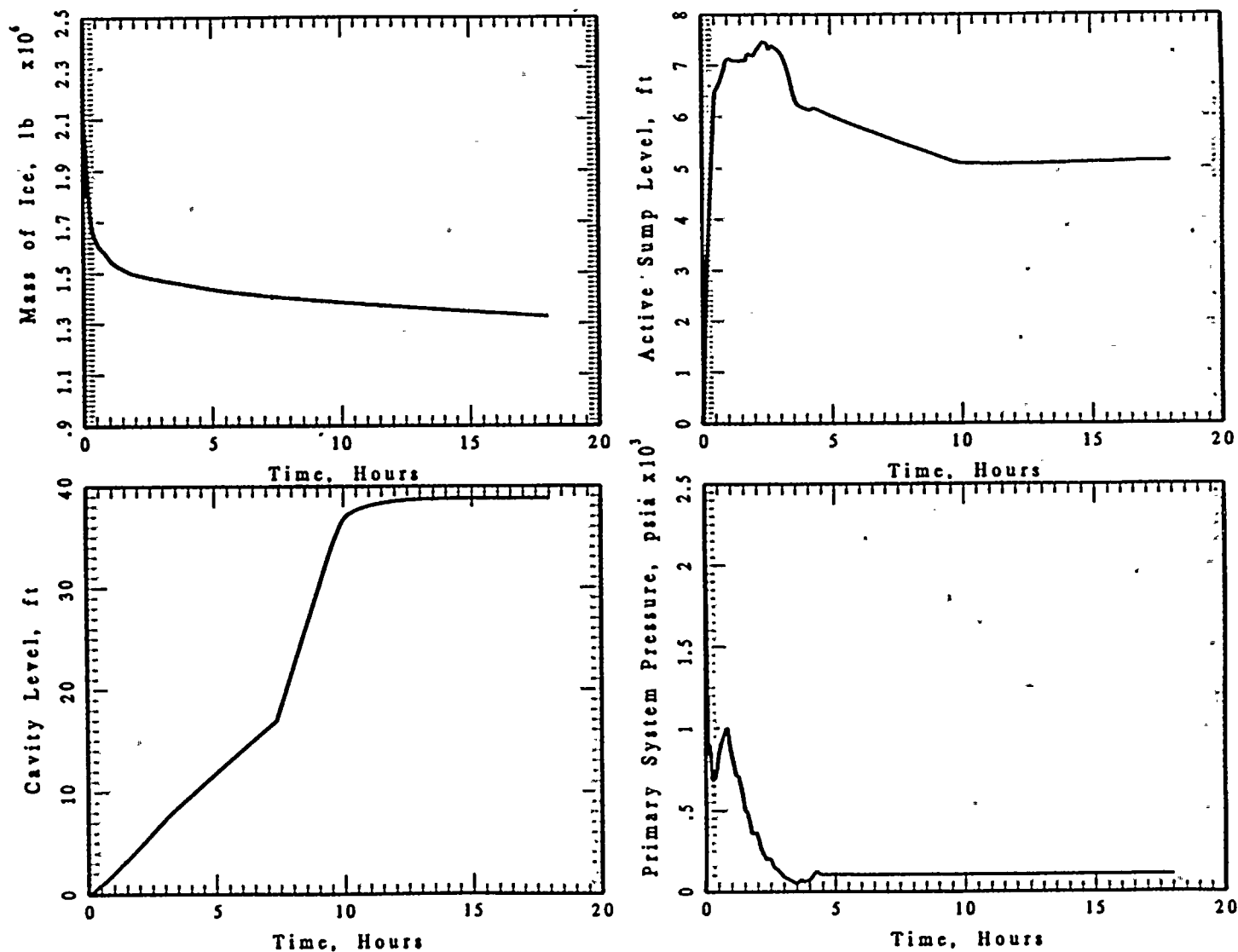


Figure 5-4 A summary of the primary system and containment response for a 4 inch dia. cold leg break into the lower compartment.

### 3.0 IN BREAK INTO LOWER COMPARTMENT

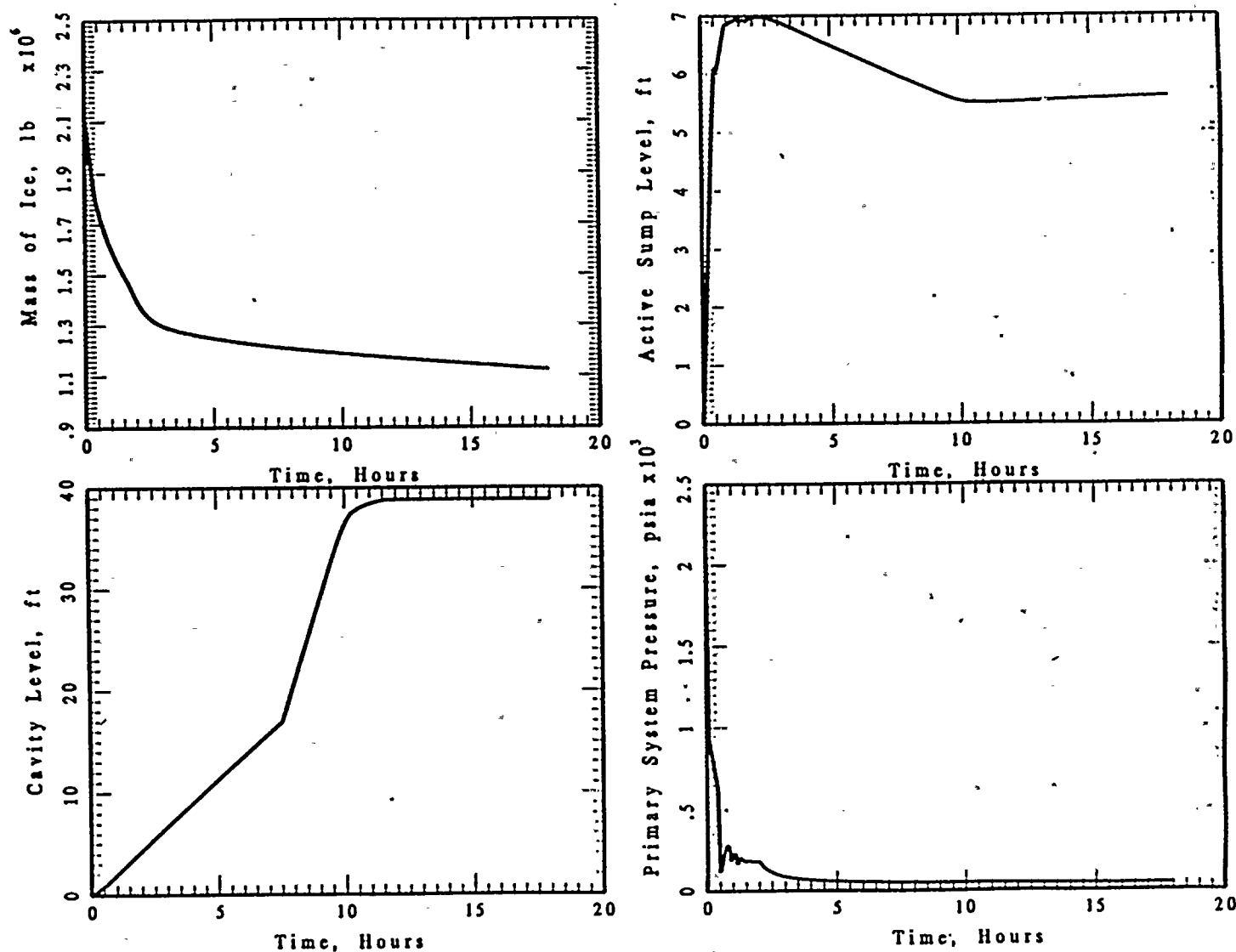


Figure 5-5 A summary of the primary system and containment response for a 3 inch dia. cold leg break into the lower compartment.



Continuing the analysis to a smaller break with an equivalent diameter of 2 inches further reduces the steam flow to the lower compartment. However, this steam flow is sufficient to actuate both the CEQ fan (with a 150 sec delay) and the containment sprays. With the smaller steam release to the lower compartment atmosphere, after condensation by the containment spray flow rate, there is a reduced contribution of ice melt for this smaller break case. Also, two trains of ECCS injection are sufficient to eventually recover the pressurizer level after the RCS cooldown begins. The accumulators inject during the accident as a result of the RCS cooldown and this inventory is added to that accumulated in the active sump. As illustrated in Figure 5-6, the minimum water level for this LOCA at recirculation is 5.1 ft (an elevation of 603.9') which is less than that calculated for the 3 inch dia case but above the licensing basis limit for vortexing.

A MAAP4 analysis was also performed for a 1.5 inch dia. effective break into the lower compartment. The results of this accident sequence are illustrated in Figure 5-7. The reduced steam discharge into the lower compartment is sufficient to pressurize the containment to the CEQ fan setpoint as well as to the containment spray setpoint. Actuation of the containment sprays in the lower compartment is sufficient to substantially decrease the ice melt rate and therefore decrease the contribution of the ice melt to the sump inventory. As illustrated, the minimum sump level is approximately 5.1' (an elevation of 603'9") which is above the licensing basis limit for vortexing of 602'10".

For the minimum sump water inventory assessment, the analyses also considered a small-small LOCA with an effective diameter of 1 inch. The results for this calculation are illustrated in Figure 5-8 and show that the steam released to the lower compartment is sufficient to again actuate both the CEQ fans and the containment sprays with the spray initiation being approximately 800 secs into the accident. During this time, there has been a significant amount of ice melted which has drained to the lower compartment. Once the containment sprays are initiated, the ice melt rate is reduced and the water addition by the sprays to the lower compartment results in a significant water level in the active sump. As was the case for the other LOCA conditions into the lower compartment there is some loss of water to the reactor cavity through the nuclear instrumentation holes in the biological shield which continues to decrease the



# 2.0 IN BREAK INTO LOWER COMPARTMENT

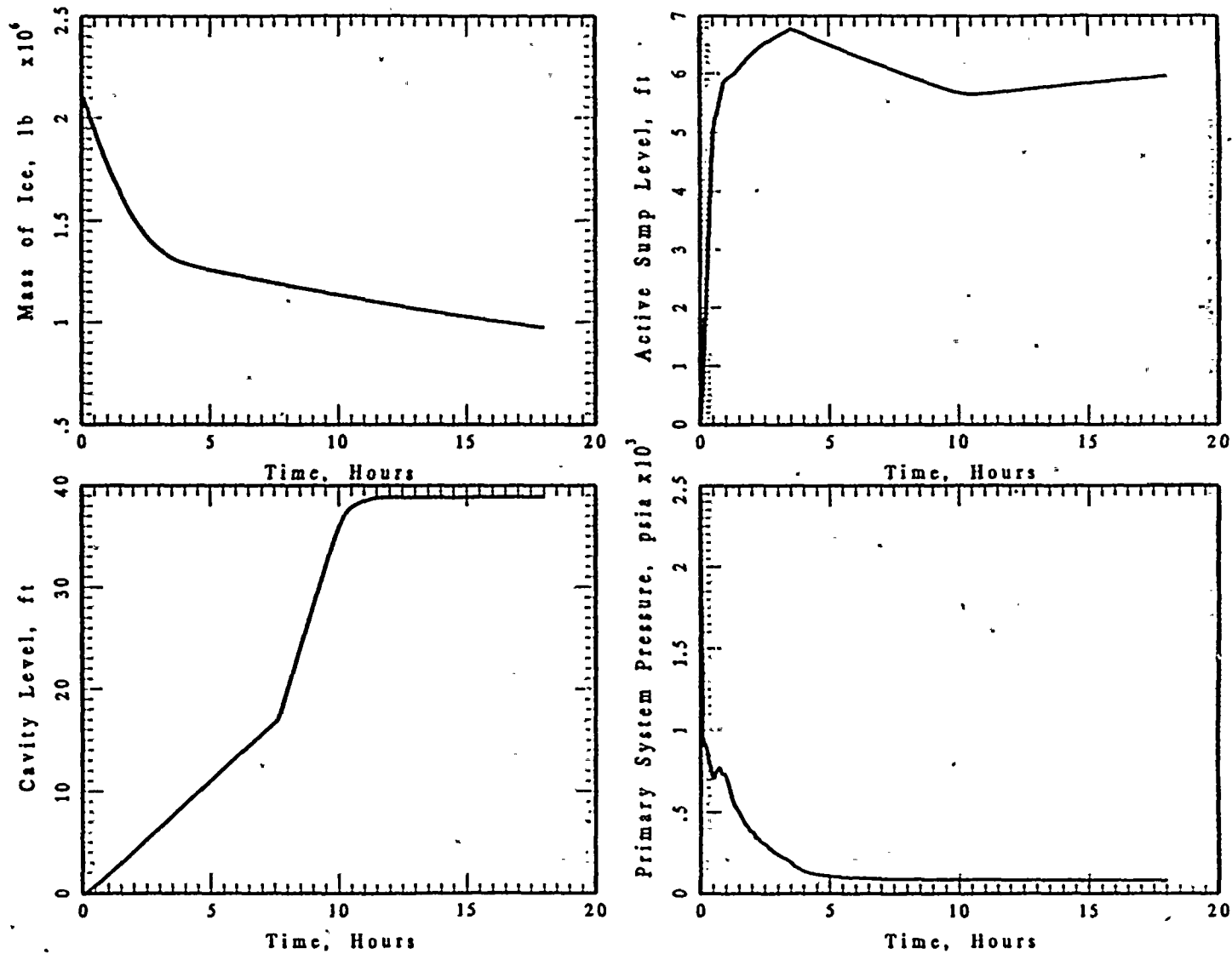


Figure 5-6 A summary of the primary system and containment response for a 2 inch dia. cold leg break into the lower compartment.

# 1.5 IN BREAK INTO LOWER COMPARTMENT

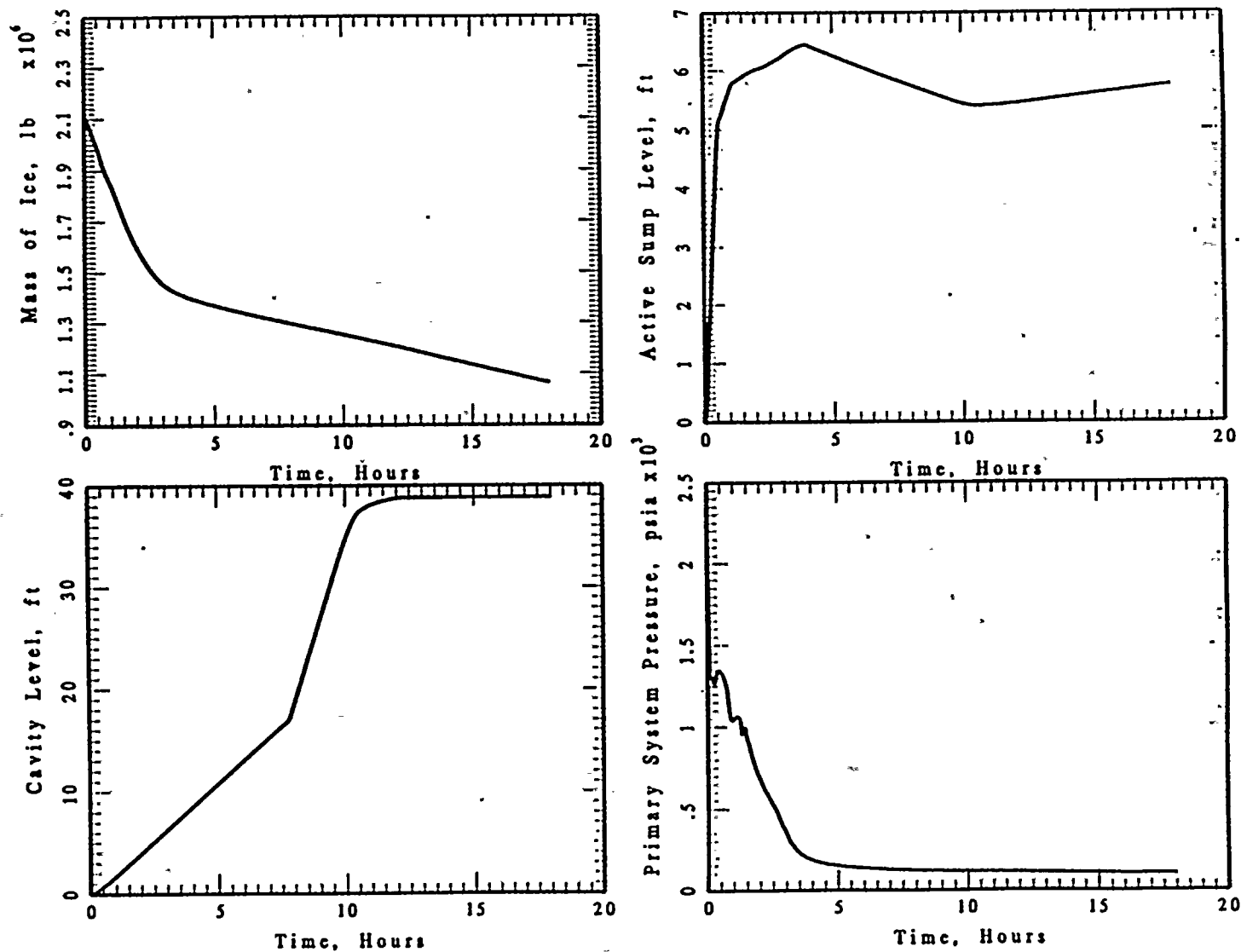


Figure 5-7 A summary of the primary system and containment response for a 1.5 inch dia. cold leg break into the lower compartment.





# 1.0 IN BREAK INTO LOWER COMPARTMENT

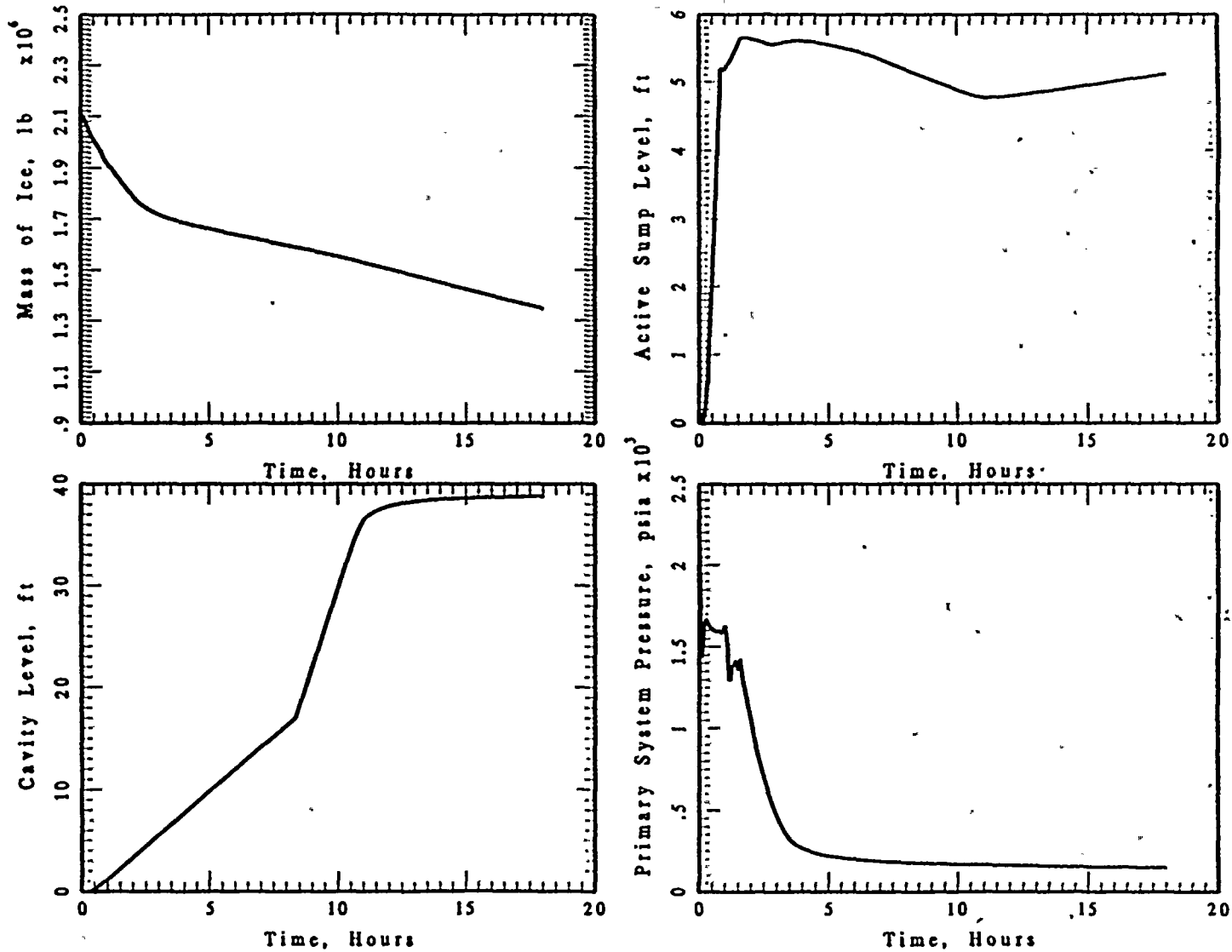


Figure 5-8 A summary of the primary system and containment response for a 1 inch dia. cold leg break into the lower compartment.



water level in the active sump over the duration of the containment sprays. However, once the sprays are secured, this loss of water to the reactor cavity is offset by the existing ice melt rate. Throughout this transient the minimum water level in the active sump is 4.8' (an elevation of 604') which is above the licensing basis limit for vortexing of 602'10".

A LOCA into the lower compartment with an effective diameter of 1/2 inch was also investigated in this assessment, as illustrated in Figure 5-9. This very small LOCA does not initiate containment sprays. This is manifested by the extended time to recirculation and the large mass of ice melted at this time. Consequently, during the time that this release occurs into the lower compartment atmosphere, the CEQ fans are initiated and circulate the air-steam mixture through the ice condenser sufficiently to prevent the pressure from increasing to the containment spray setpoint of 2.3 psig. Therefore, this represents a condition in which there is substantial ice melt and a very long time (greater than 36 hours) before recirculation is required. (At 36 hours, the sump water level is at 604.8'.) Hence, the water level in the active sump is always above the licensing basis limit for vortexing.

### 5.2.2 Split Flow Pipe Breaks into the Sump and the Reactor Cavity

Because a break in the reactor vessel piping inside the biological shield could cause some of the break discharge to collect in the cavity and some in the sump, these possible break locations need to also be investigated. In this region, the spectrum of small breaks considered is the same as that considered for the lower compartment. The largest break associated with the vessel nozzles and piping is a postulated break at the vessel safe end which has an effective area of 1 ft<sup>2</sup> (McCurdy et al., 1968). A spectrum of smaller break sizes are addressed for this locale including those which do not initiate the containment sprays, i.e., the same analytical approach used in the lower compartment.

Figure 5-10 illustrates the system response to the postulated break of 1 ft<sup>2</sup> into the reactor cavity at the elevation of the reactor nozzles. Because of the relatively large break in this confined configuration, 30% of water is added to the reactor cavity and 70% of the water is discharged to

0.5 IN BREAK INTO LOWER COMPARTMENT

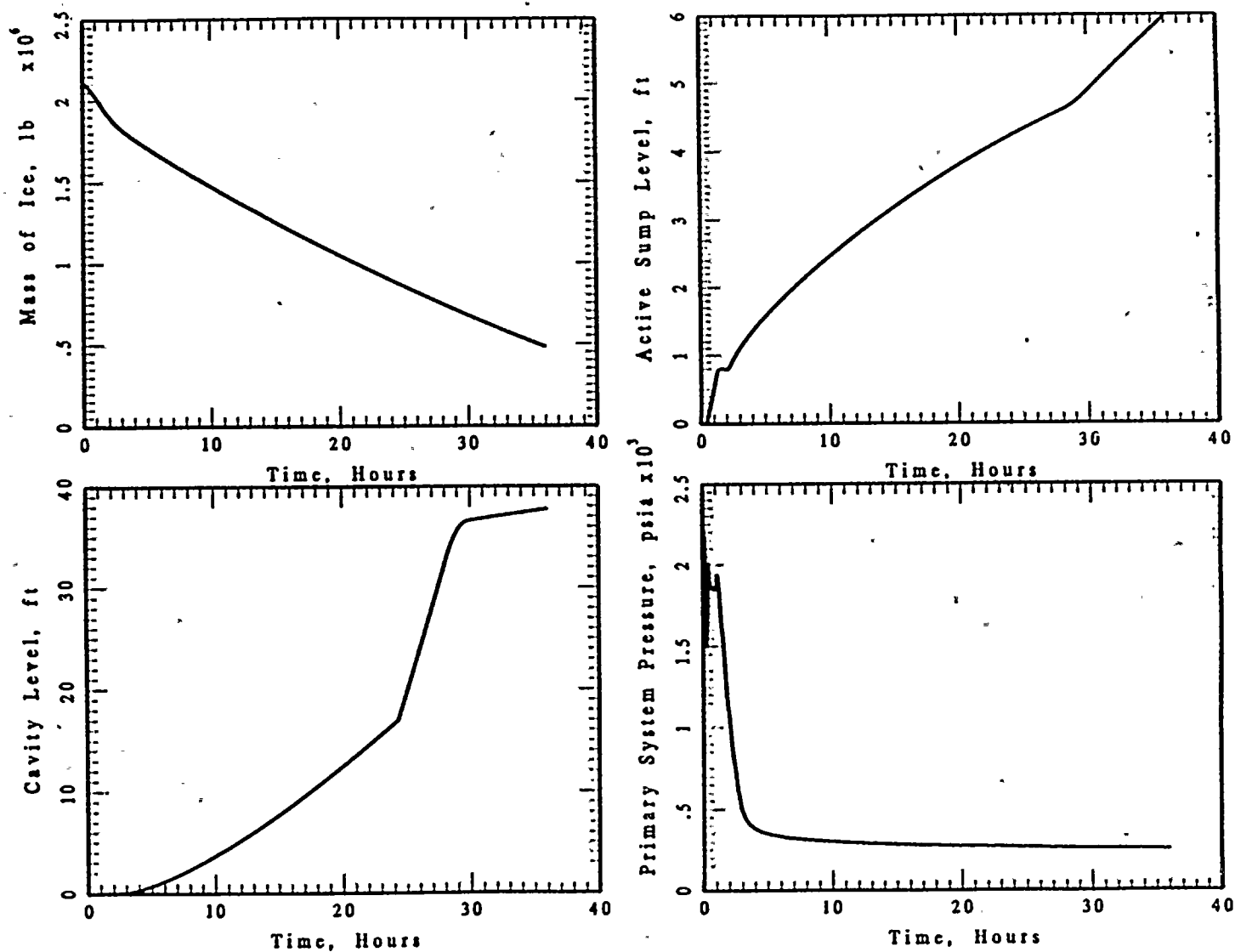


Figure 5-9 A summary of the primary system and containment response for a 0.5 inch dia. cold leg break into the lower compartment.



1.0 FT<sup>2</sup> BREAK INTO LC & RC

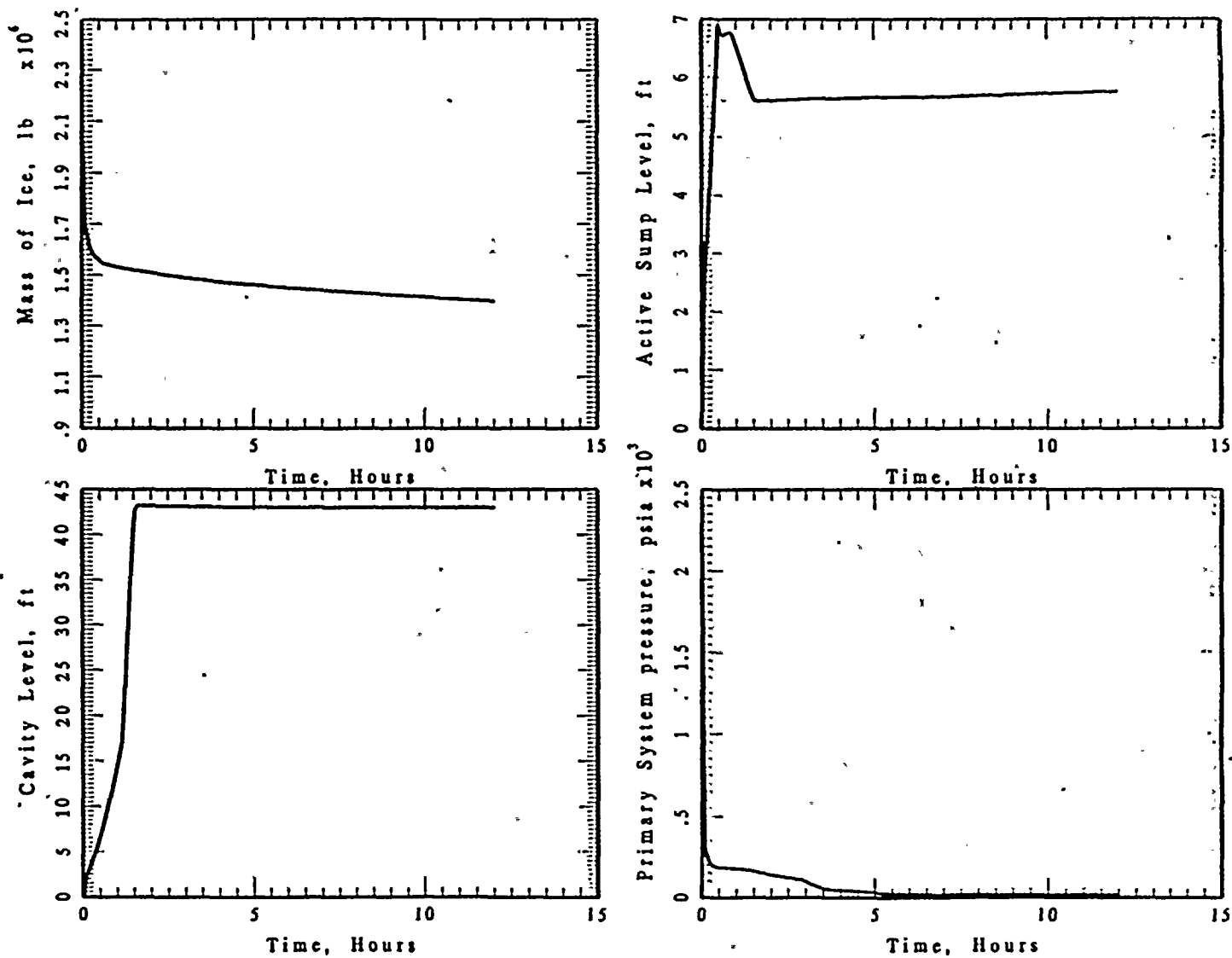


Figure 5-10 A summary of the primary system and containment response for a 1 ft<sup>2</sup> area cold leg break into the reactor cavity and lower compartment.

the lower compartment (Westinghouse, 1988). The steam, is released to the reactor cavity but is calculated to flow through connecting flow paths to the lower compartment by the MAAP4 containment model. Given the elevation of the reactor cavity, the break location is never submerged. As was the case for breaks into the lower compartment, the initiation of the single CEQ fan and two trains of containment sprays occurs for this accident sequence with the lower compartment sprays condensing steam thereby minimizing the steam partial pressure circulated into the ice condenser. With this break size, two trains of ECCS injection are not sufficient to refill the reactor coolant system, hence, the water inventory in the containment sump includes some of the water from the RCS (primary system is not refilled) as well as the accumulators which have injected prior to the minimum water level. As illustrated in Figure 5-10, the minimum water level for this condition is 5.6 ft (elevation of 604.4'), which is greater than the licensing base limit for vortexing of 602'10".

A effective break size of 4 inch dia. into the reactor cavity was also considered with the location being at the cold leg nozzles as previously discussed. With this size break, the water discharged into the reactor cavity and the lower compartment follows the guidance in Appendix B. Specifically, the best estimate would suggest that this break flow rate is split 50/50 between the reactor cavity and the lower compartment as a result of the flow due to the jet impingement on the biological shield wall. Figure 5-11 summarizes the behavior for this accident sequence and illustrates that there is substantial ice melt resulting from the steam discharged during the accident. This ice melt in combination with the water lost from the reactor coolant system, including accumulated discharge, and that discharged by the containment sprays into the lower compartment results in a minimum sump level of 4.71 ft., or an elevation of 603.5' which is greater than the licensing base limit for vortexing.

A similar accident sequence was assessed for a 3 inch dia. break in the cold leg with the water discharge simultaneously directed to the reactor cavity and the lower compartment as discussed above. Figure 5-12 summarizes the observations from this accident sequence. This break is sufficient to initiate the CEQ fans and the containment sprays. For this postulated break

# 4.0 IN BREAK INTO REACTOR CAVITY

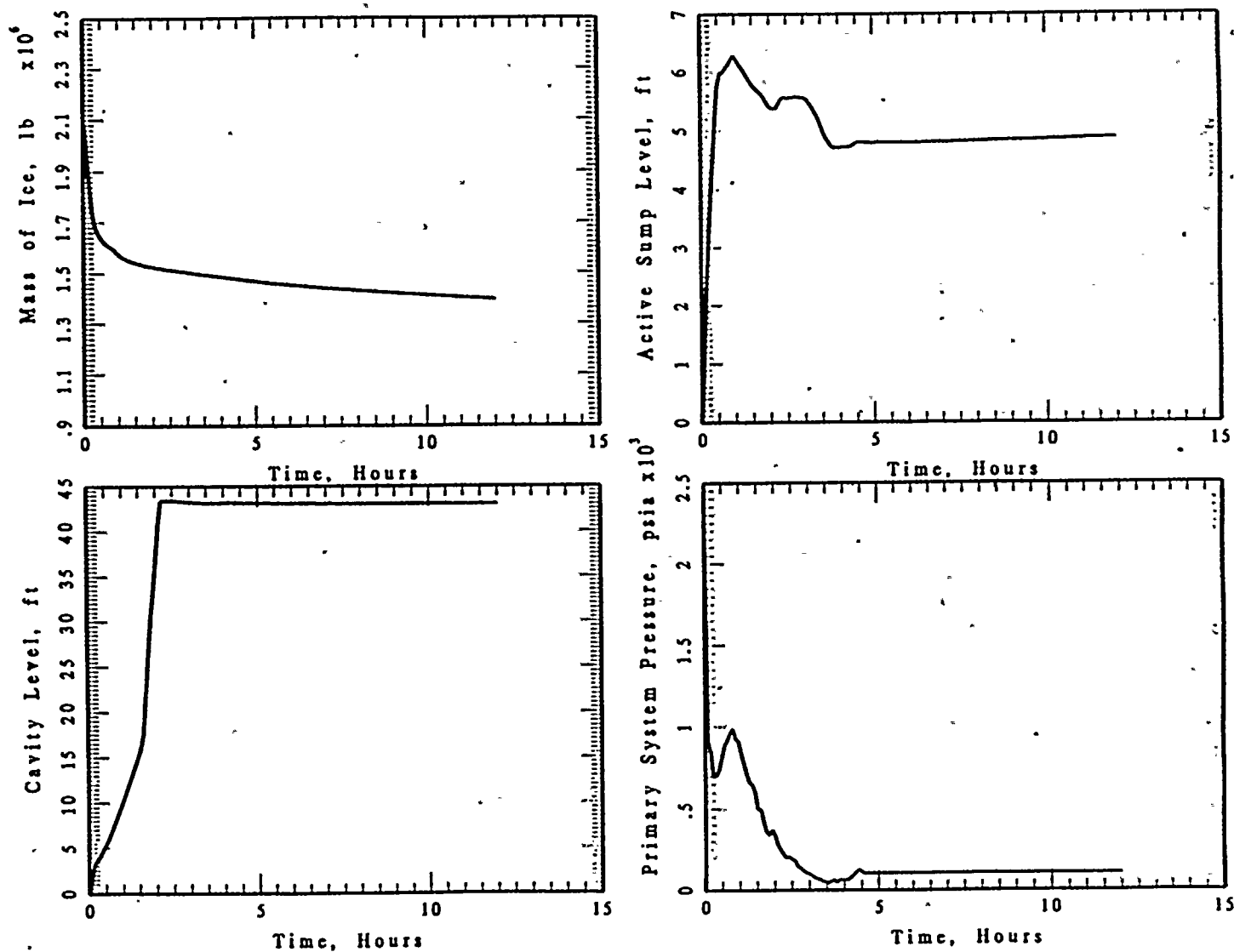


Figure 5-11 A summary of the primary system and containment response for a 4 inch dia. cold leg break into the reactor cavity and lower compartment.



### 3.0 IN BREAK INTO REACTOR CAVITY

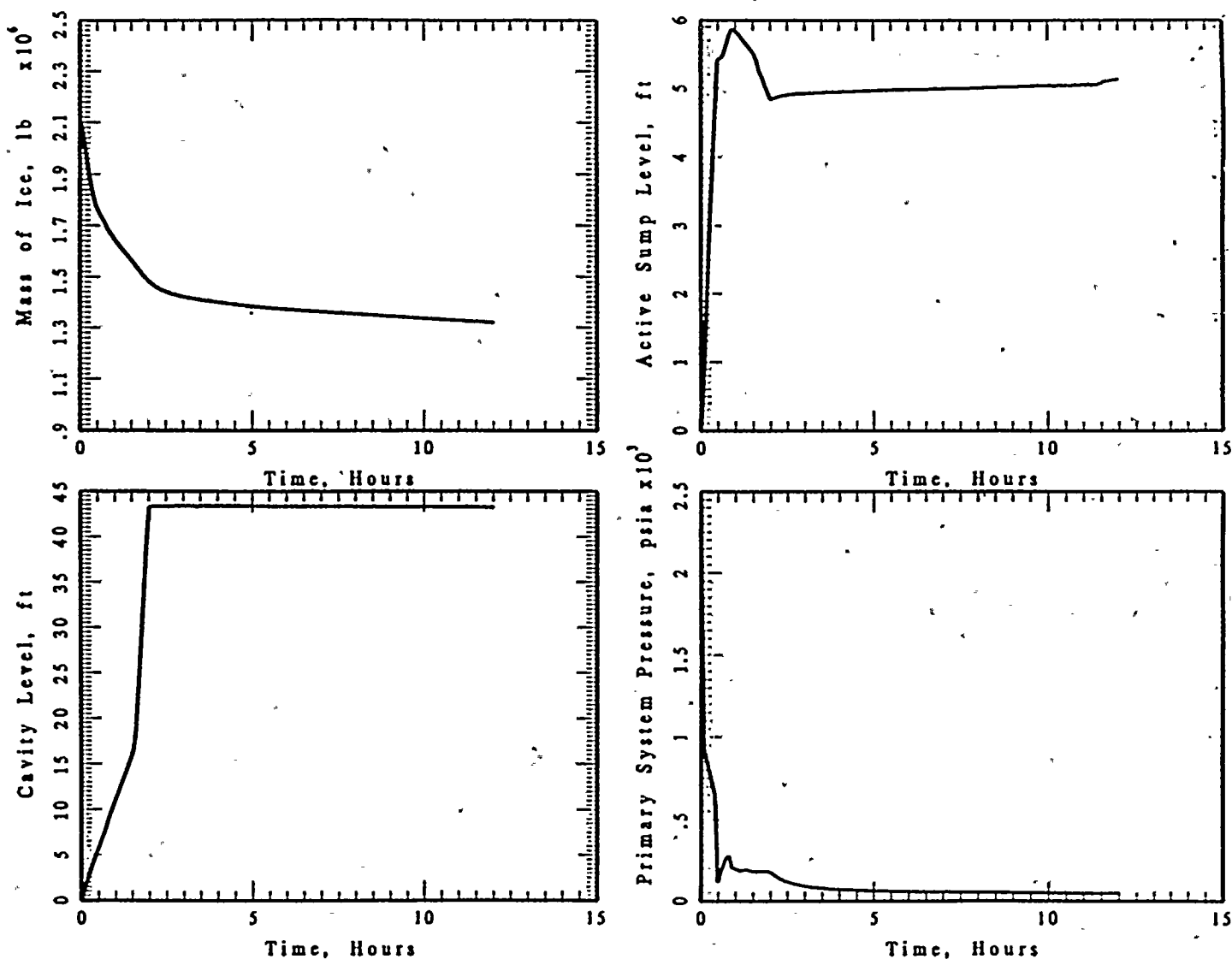


Figure 5-12 A summary of the primary system and containment response for a 3 inch dia. cold leg break into the reactor cavity and lower compartment.



size, the minimum sump level observed is 4.84 ft. (an elevation of 603.6') which is above the 602'10" licensing basis limit for vortexing.

The break spectrum into the reactor cavity also considered a 2 inch effective diameter break in the cold leg/RPV nozzle region. As was the case with other breaks in this locale, the flow split of the water discharge follows the guidance given in Appendix B. Figure 5-13 illustrates the results from this analysis and shows that the containment sprays were initiated early in the accident sequence and that the minimum water level occurs after several hours and reaches a value of 4.63 ft. (elevation of 603.4') which is above the licensing basis limit for vortexing.

The results for a postulated break with an effective diameter of 1.5 inch at the cold leg-RPV nozzle weld is illustrated in Figure 5-14. As was the case with the smaller breaks in the lower compartment, there is a reduced steam inventory released to the lower compartment but this is sufficient to actuate both the single CEQ fan and the containment sprays. This results in a reduced ice melt contribution to the containment sump and the RCS inventory can be established by two trains of injection. As shown in this figure, the minimum water level in the containment sump is 4.57 ft (an elevation of 603.4'), which is above the licensing basis limit for vortexing.

The results for a very small LOCA with an effective diameter of 1 inch at the nozzle safe end is illustrated in Figure 5-15. The steam released is very small but is sufficient to increase the lower compartment pressure such that both the CEQ fan and the containment sprays actuate. Once the sprays have been initiated with the assumption that two trains are initiated and sustained, the system progresses to recirculation at approximately 45 mins into the accident sequence. The active sump water level decreases until about 5 hrs into the accident sequence. At this time the water level in the sump reaches a minimum of 4.35 ft (elevation of 603.13') which is 3.5 inch above the licensing basis limit for vortexing.

# 2.0 IN BREAK INTO REACTOR CAVITY

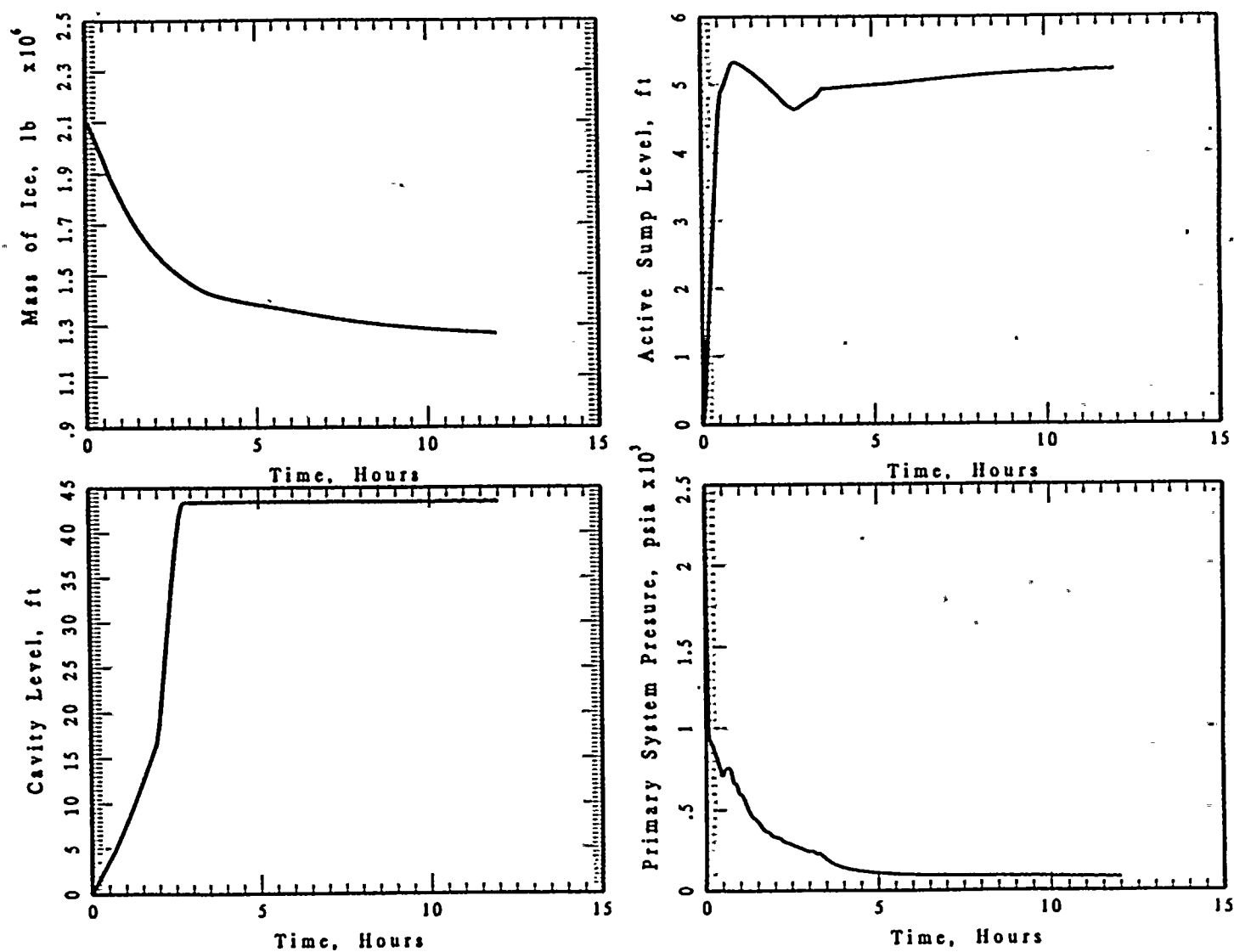


Figure 5-13 A summary of the primary system and containment response for a 2 inch dia. cold leg break into the reactor cavity and lower compartment.

# 1.5 IN BREAK INTO REACTOR CAVITY

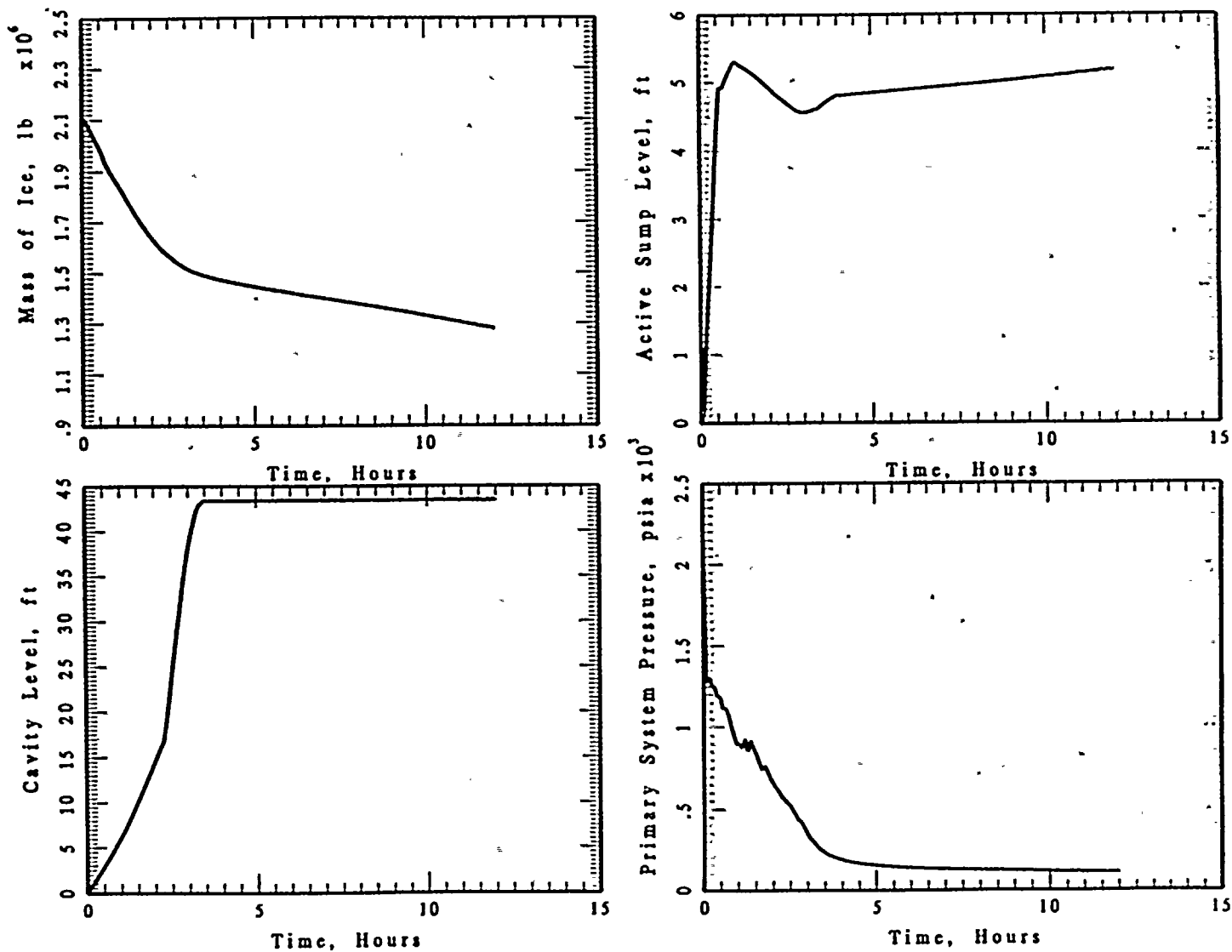


Figure 5-14 A summary of the primary system and containment response for a 1.5 inch dia. cold leg break into the reactor cavity and lower compartment.

# 1.0 IN BREAK INTO REACTOR CAVITY

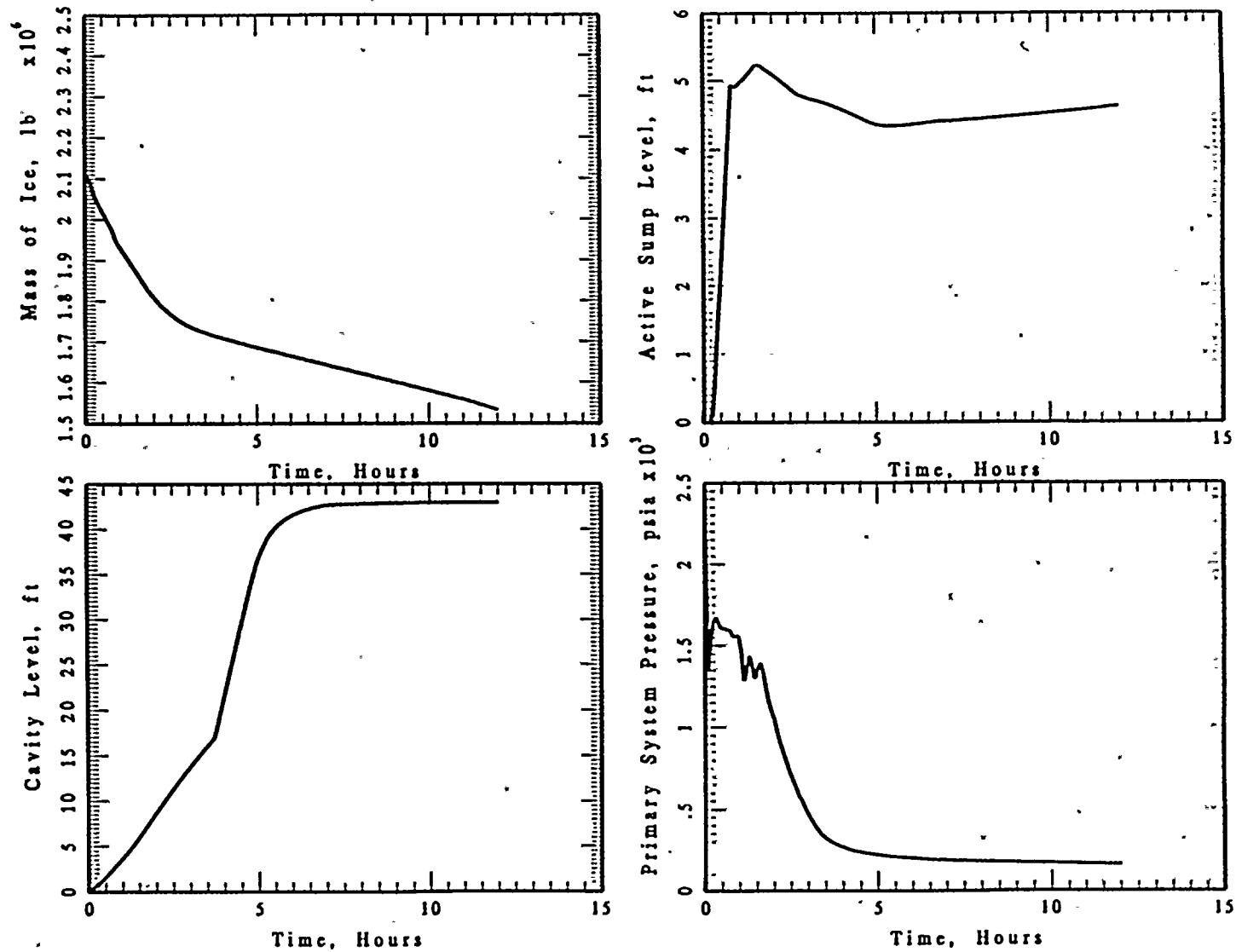


Figure 5-15 A summary of the primary system and containment response for a 1 inch dia. cold leg break into the reactor cavity and lower compartment.

### 5.2.3 Breaks Into the Reactor Cavity

Analysis for a postulated ejection of a CRDM due to weld-failure is illustrated in Figure 5-16. A rupture in this location may have an increased steam discharge due to two-phase separation within the reactor vessel. MAAP4 does not represent phase separation in the RPV upper plenum and as a result provides for a mass and energy release to the containment which minimizes ice melt for this postulated accident sequence. In contrast to the split flow break locations considered above, this postulated break in the RPV upper head is assumed to discharge all of the break flow to the reactor cavity. With this LOCA size, the RCS is eventually refilled by two trains of ECCS injection and is essentially full at the time the minimum level is calculated in the containment sump. However, during the blowdown and cooldown transient, the accumulators have partially injected and this inventory is discharged to the reactor cavity. As illustrated in Figure 5-16 the minimum water level during the transient is 4.41 ft (an elevation of 603.2') which is above the licensing basis limit for vortexing.

Figure 5-17 illustrates the results from a postulated break of 0.61 inch in the bottom of the reactor vessel. A break of this size is sufficiently small that the containment sprays are not actuated, which is the expected behavior given the results previously discussed for very very small LOCAs into the lower compartment. As long as the containment sprays do not actuate the time, to recirculation is determined by the ECCS injection which is in excess of 36 hrs. Consequently, the sump inventory includes a substantial amount of ice melt and the sump water level at recirculation is of no concern with respect to the licensing basis limit for vortexing. This result also characterizes a similar break size in the RPV upper head, which is the severing of the reactor head vent. Therefore, the containment sprays would not initiate for this postulated event.

### 5.2.4 Summary of Minimum Sump Level

Compiling the information from the various size postulated LOCAs into the lower compartment results in a characteristic behavior demonstrating the minimum active sump level as a function of the LOCA sizes for break location for these Mode 1 initiation cases. Figure 5-18

# 2.75 IN BREAK INTO REACTOR CAVITY

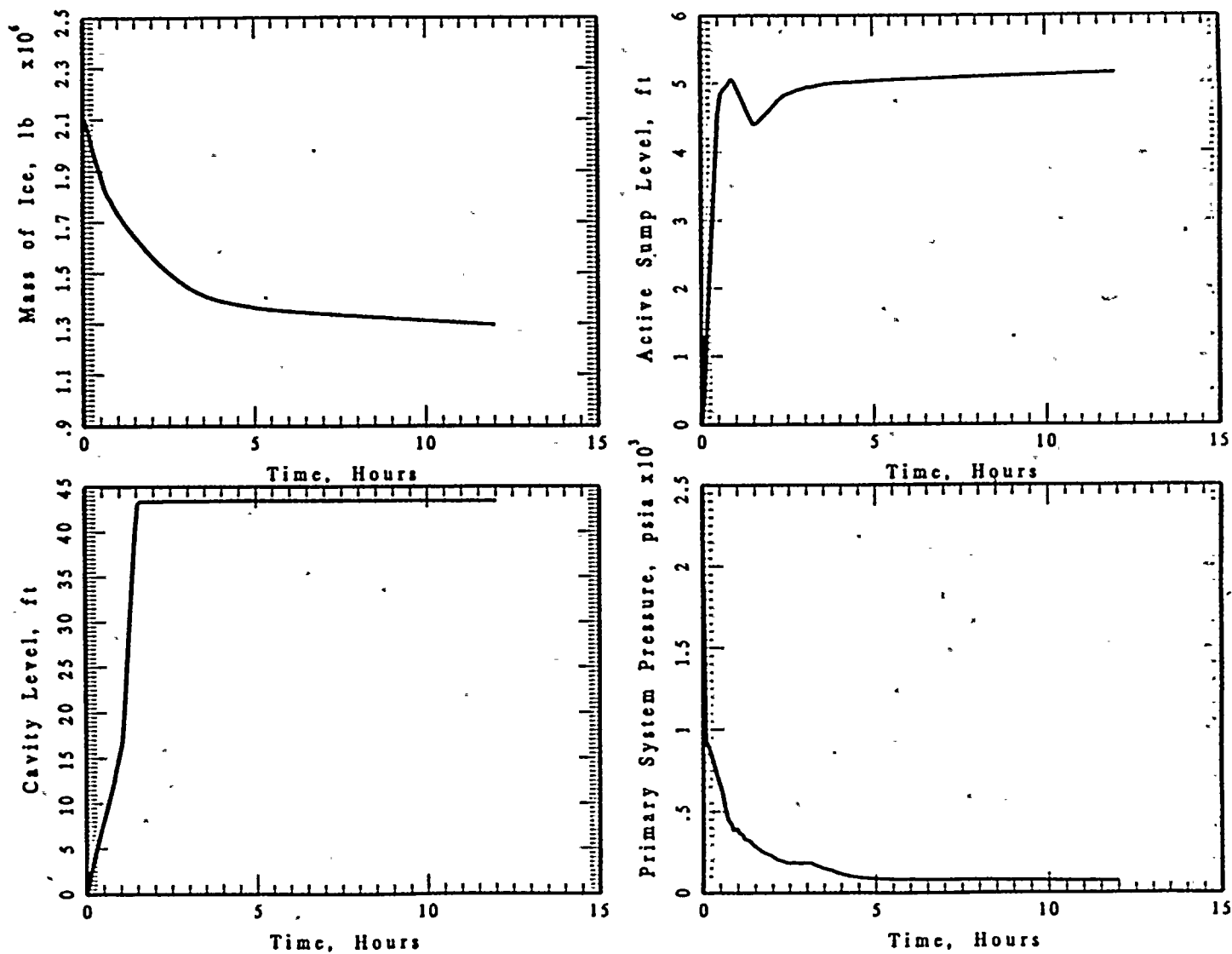


Figure 5-16 A summary of the primary system and containment response for a 2.75 inch dia. upper head break into the reactor cavity.



0.61 IN BREAK INTO REACTOR CAVITY

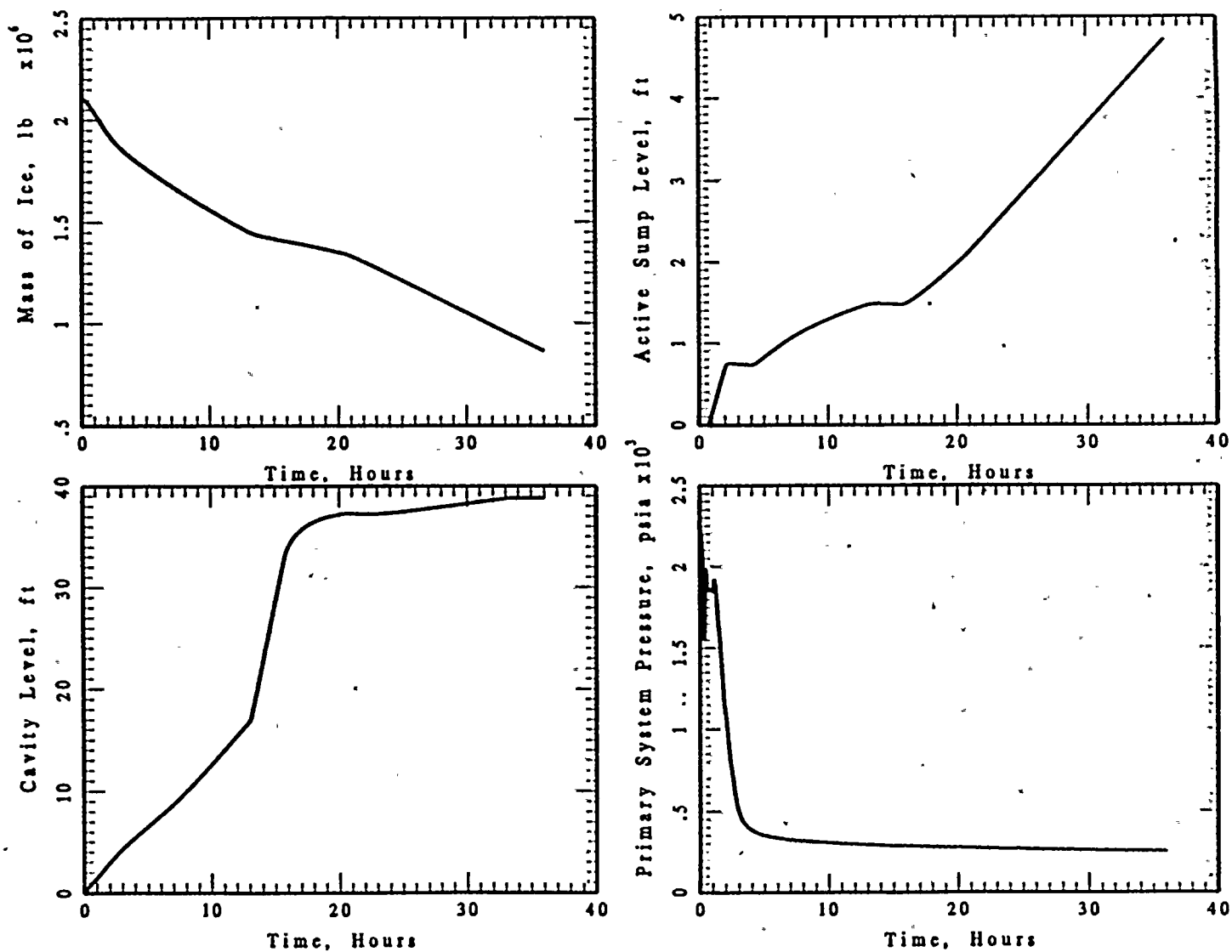


Figure 5-17 A summary of the primary system and containment response for a 0.61 inch dia. break in the bottom of the RPV.

- \* Break in the RPV Upper Head
- Break in the RPV Lower Head
- △ Break into the Lower Compartment (Min. if different than the level @ Recirc.)
- Break into the Lower Compartment (@ Recirc.)
- 50/50 Split Flow Reactor Cavity/Sump (Min.)
- 30/70 Split Flow Reactor Cavity/Sump (Min.)

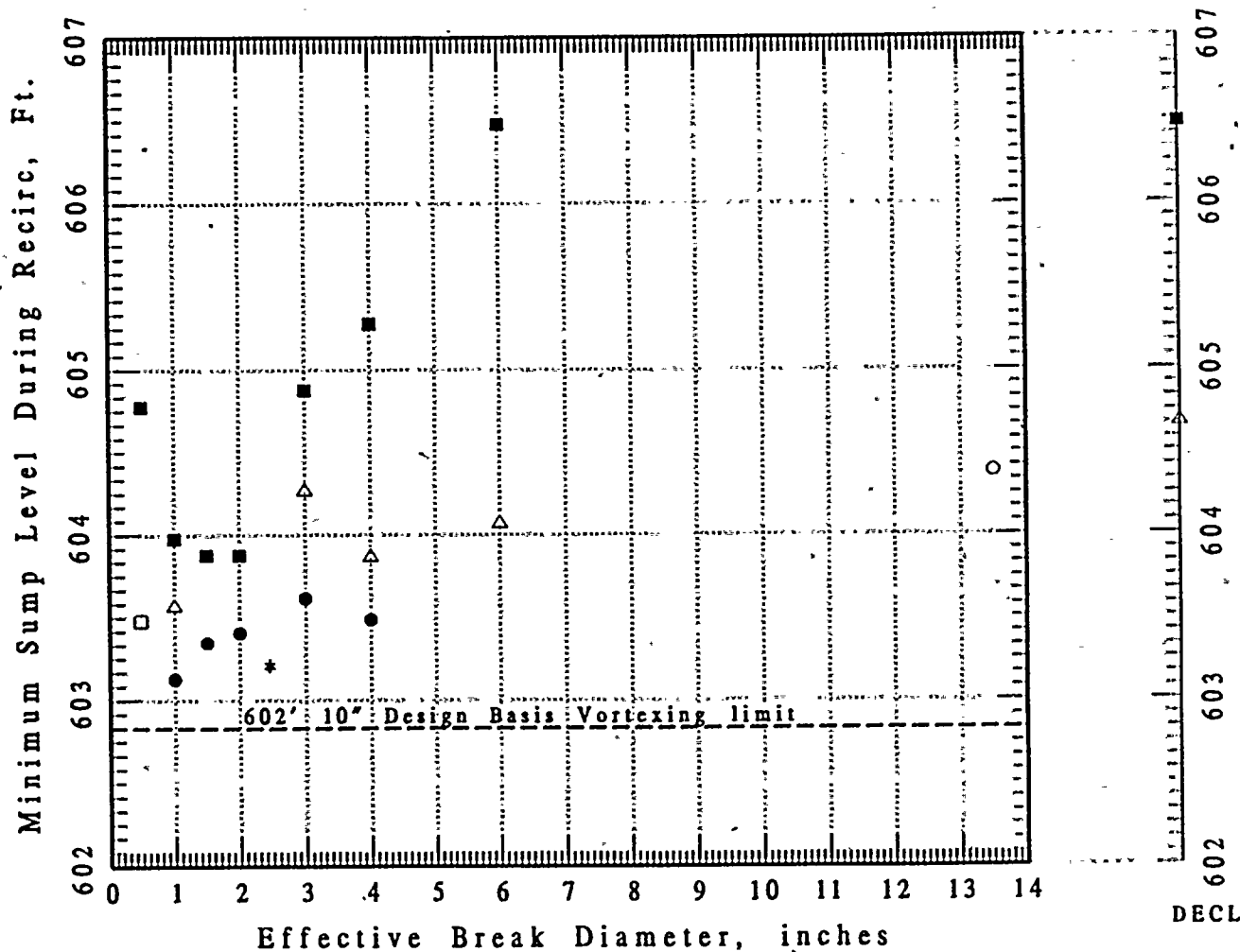


Figure 5-18 A summary of the minimum sump water levels for the spectrum of breaks considered in the lower compartment and the reactor cavity for Mode 1 operation.

shows the minimum sump water level for the spectrum of breaks into the lower compartment and the reactor cavity and Figure 5-19 shows the mass of ice melted at the minimum level for the different accident sequences. As illustrated, the water level in the active sump follows the expected trend of decreasing with a decreasing break size and results in a minimum value of 4.35 ft (elevation of 603.13') for the smallest split flow LOCA which is sufficient to actuate the containment sprays. For completeness, the 2.75 inch LOCA in the RPV upper head is included here as having an effective diameter of 2.4 inches. For effective LOCA sizes less than 1 inch, the containment sprays are not initiated and the minimum sump level is the level at recirculation which takes many hours and includes a substantial mass of water due to ice melting. Hence, these analyses demonstrate that the postulated LOCAs into either the lower compartment or the reactor cavity have a minimum sump level that is above the licensing basis limit for vortexing regardless of the LOCA size postulated.

### 5.3 Details of the Most Limiting Case

The information from the most limiting case was examined to provide the necessary details of the RCS and containment behavior to clearly illustrate the integral behavior of the system under this condition. These are documented in Figure 5-20 with the information in Figure 5-20a showing that the water level in the active sump (the lower compartment) is above the 602'10" licensing base limit for vortexing. This also shows that the reactor cavity reaches the spillover condition after approximately 6 hrs. into the accident and that the water level in the pipe annulus (inactive sump) is the same as that in the active sump region (lower compartment). For these analyses the containment sprays were secured when the lower compartment pressure is decreased to 0.77 psig.

Figure 5-20b shows the respective break flow rates to the sump and the reactor cavity and these follow the flow split evaluated in Appendix B. This figure also illustrates the required safety injection flow to the RCS eventually is reduced when the RCS is cooled down and the pressurizer level reaches the upper limit indicated in the EOPs. Injection flows were throttled in these analyses to maximize the water inventory in the pressurizer. This is different from the plant

- \* Break in the RPV Upper Head
- Break in the RPV Lower Head
- △ Break into the Lower Compartment (Min. if different than the level @ Recirc.)
- Break into the Lower Compartment (@ Recirc.)
- 50/50 Split Flow Reactor Cavity/Sump (Min.)
- 30/70 Split Flow Reactor Cavity/Sump (Min.)

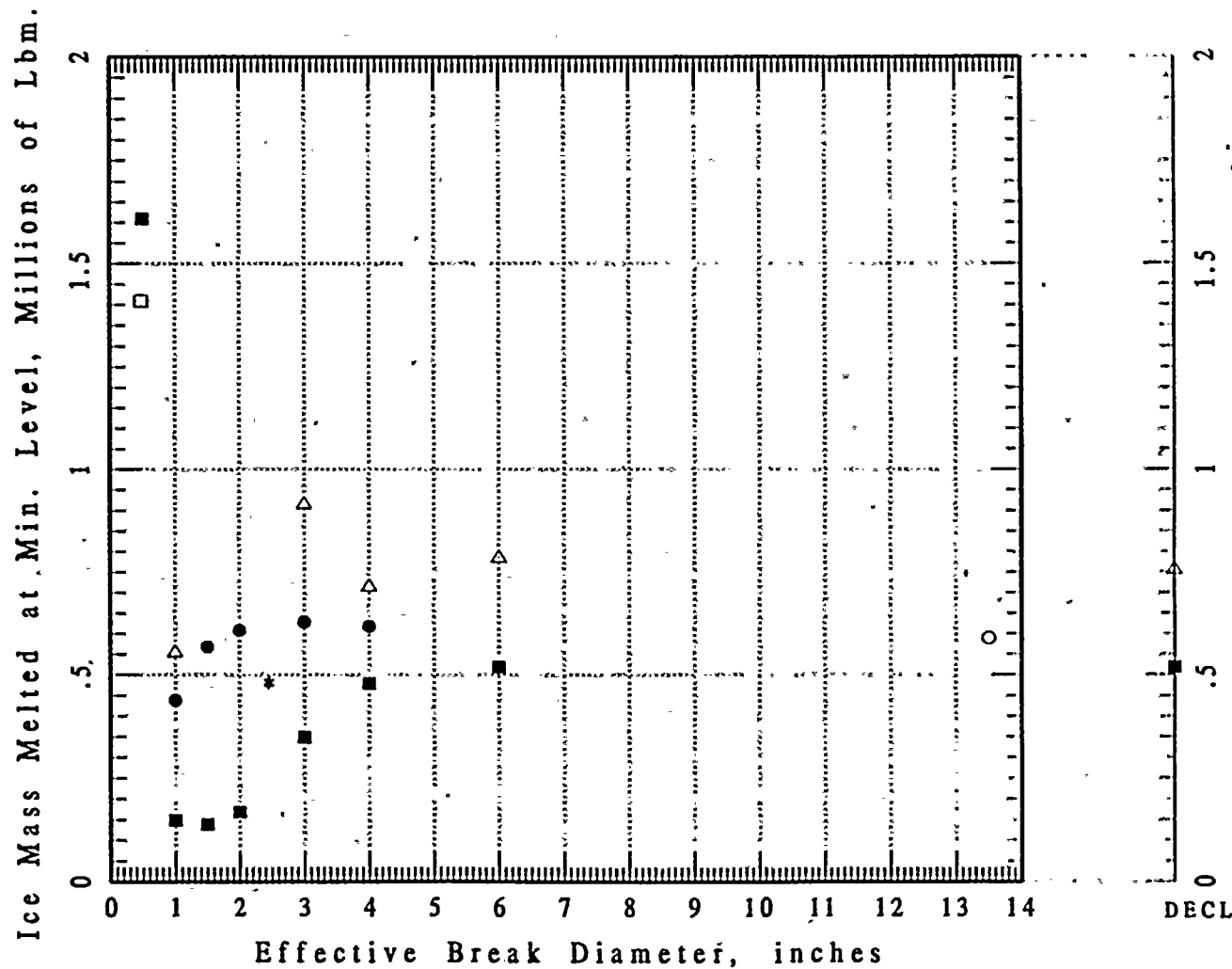


Figure 5-19 A summary of the melted ice mass for the spectrum of LOCAs considered into the lower compartment and the reactor cavity.

1" LOCA INTO RX - 2 TRAINS ECCS/SPRAY  
(50% TO RX 50% TO LOWER COMPT)

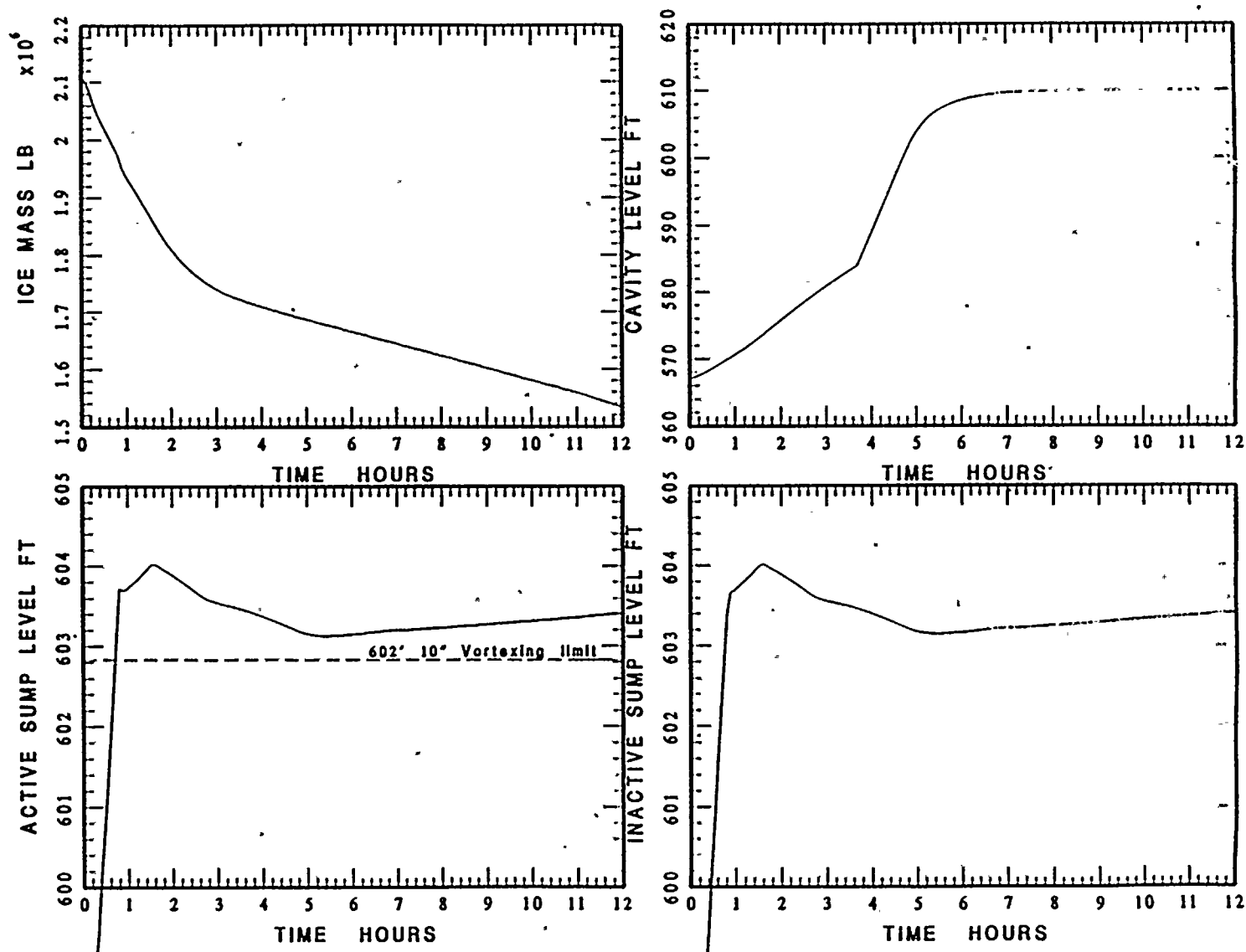


Figure 5-20a Details of the primary system and containment response for the most limiting case of a 1 inch dia. break into the reactor cavity.

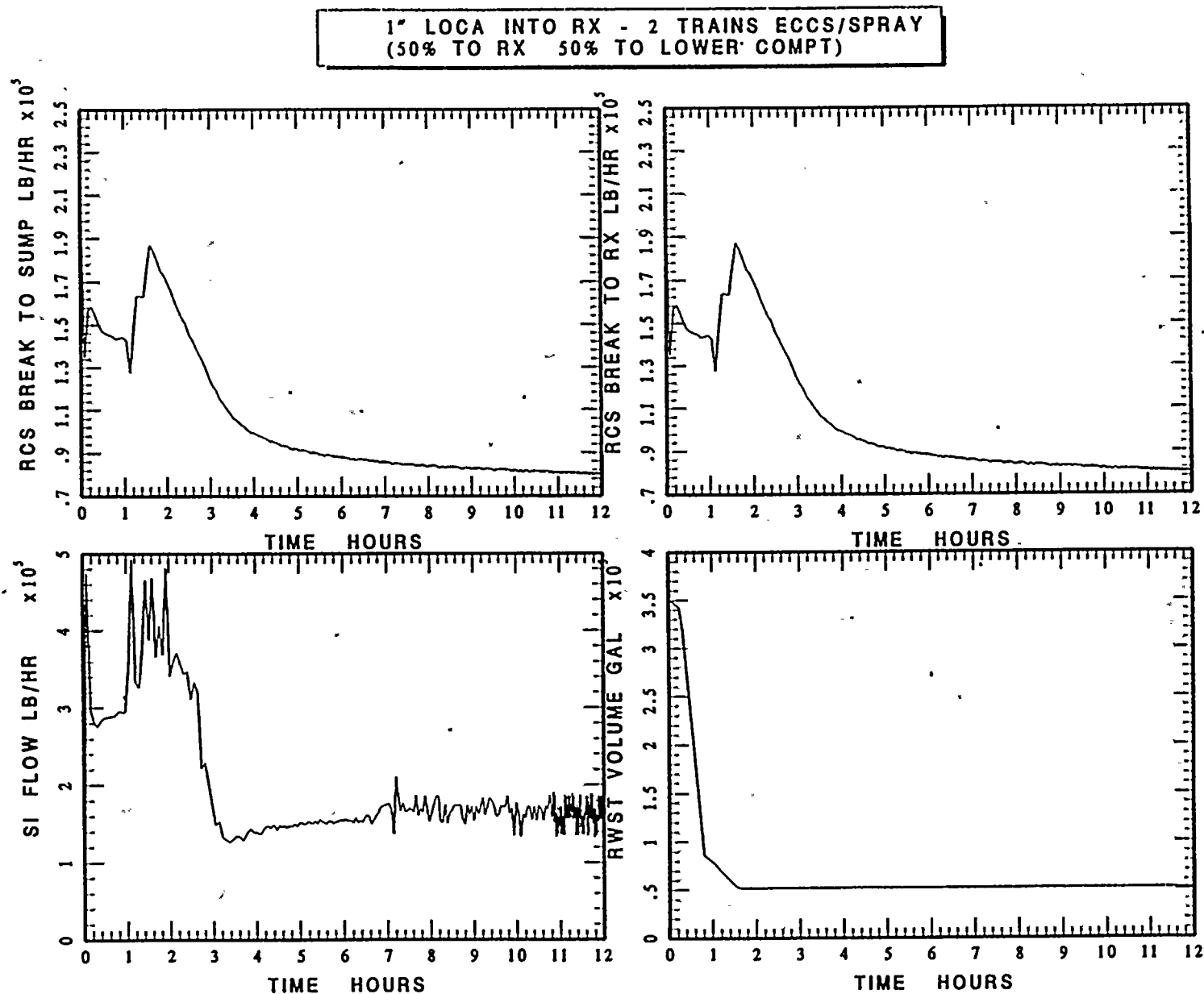


Figure 5-20b Details of the primary system and containment response for the most limiting case of a 1 inch dia. break into the reactor cavity.

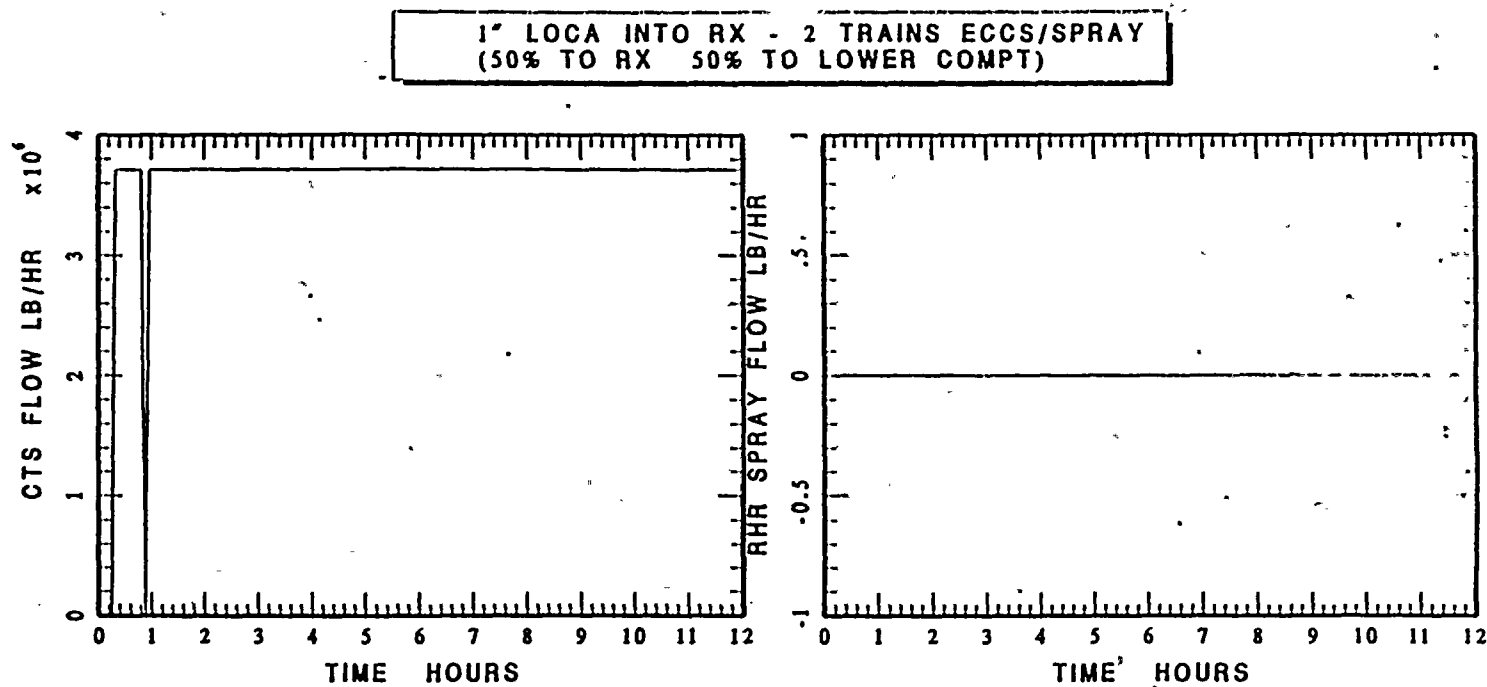


Figure 5-20c Details of the primary system and containment response for the most limiting case of a 1 inch dia. break into the reactor cavity.

1" LOCA INTO RX - 2 TRAINS ECCS/SPRAY  
(50% TO RX 50% TO LOWER COMPT)

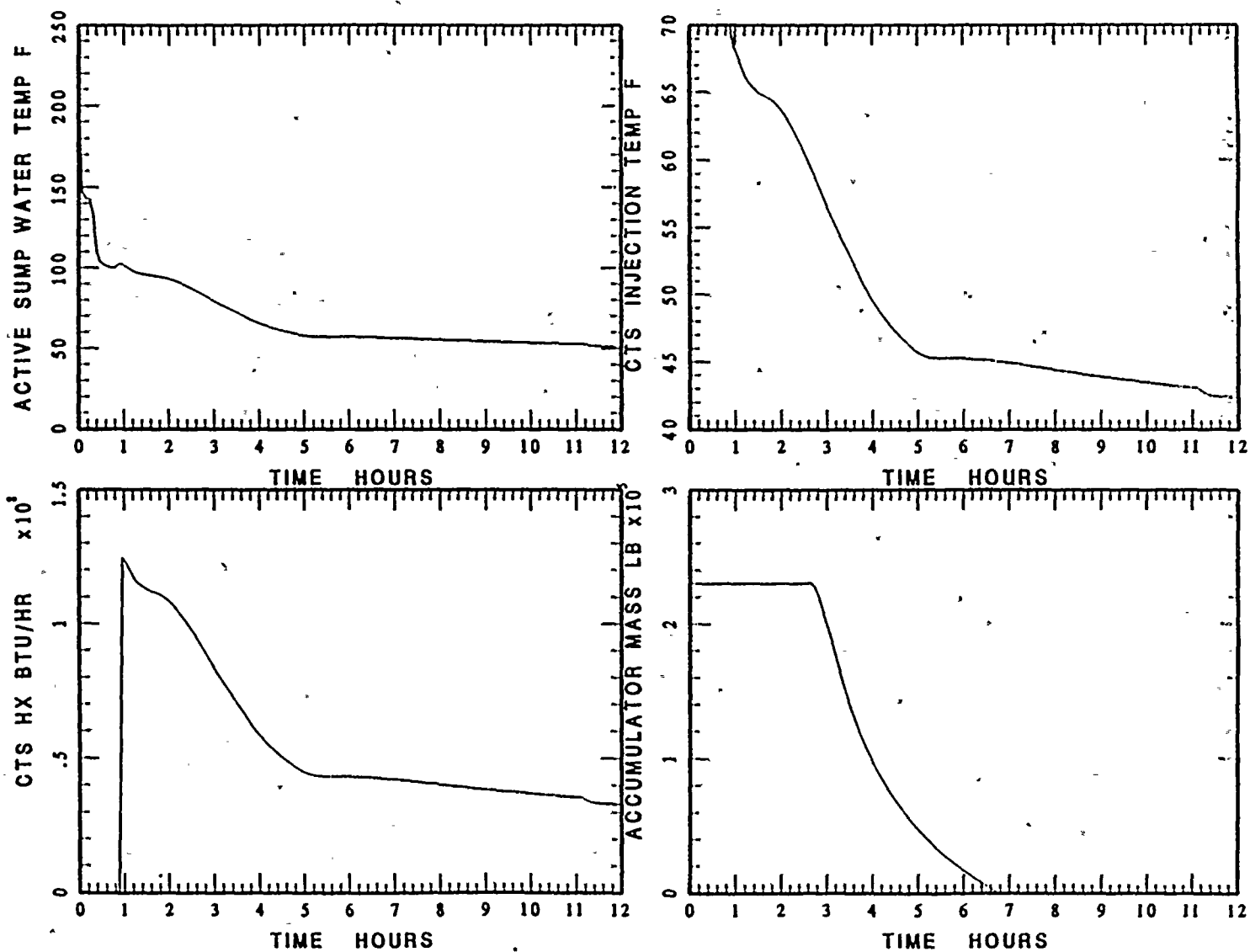


Figure 5-20d Details of the primary system and containment response for the most limiting case of a 1 inch dia. break into the reactor cavity.



1" LOCA INTO RX - 2 TRAINS ECCS/SPRAY  
(50% TO RX 50% TO LOWER COMPT)

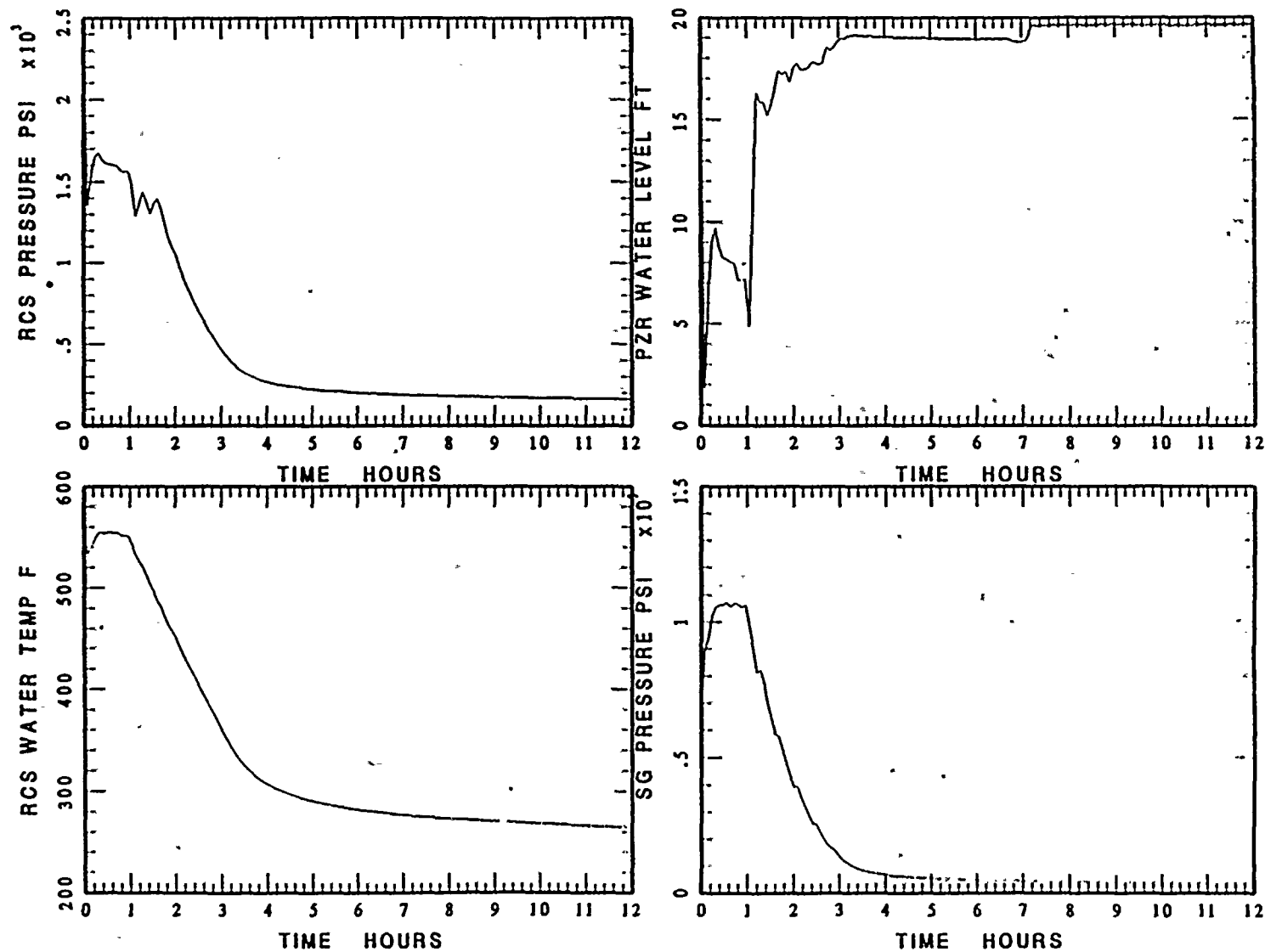


Figure 5-20e Details of the primary system and containment response for the most limiting case of a 1 inch dia. break into the reactor cavity.

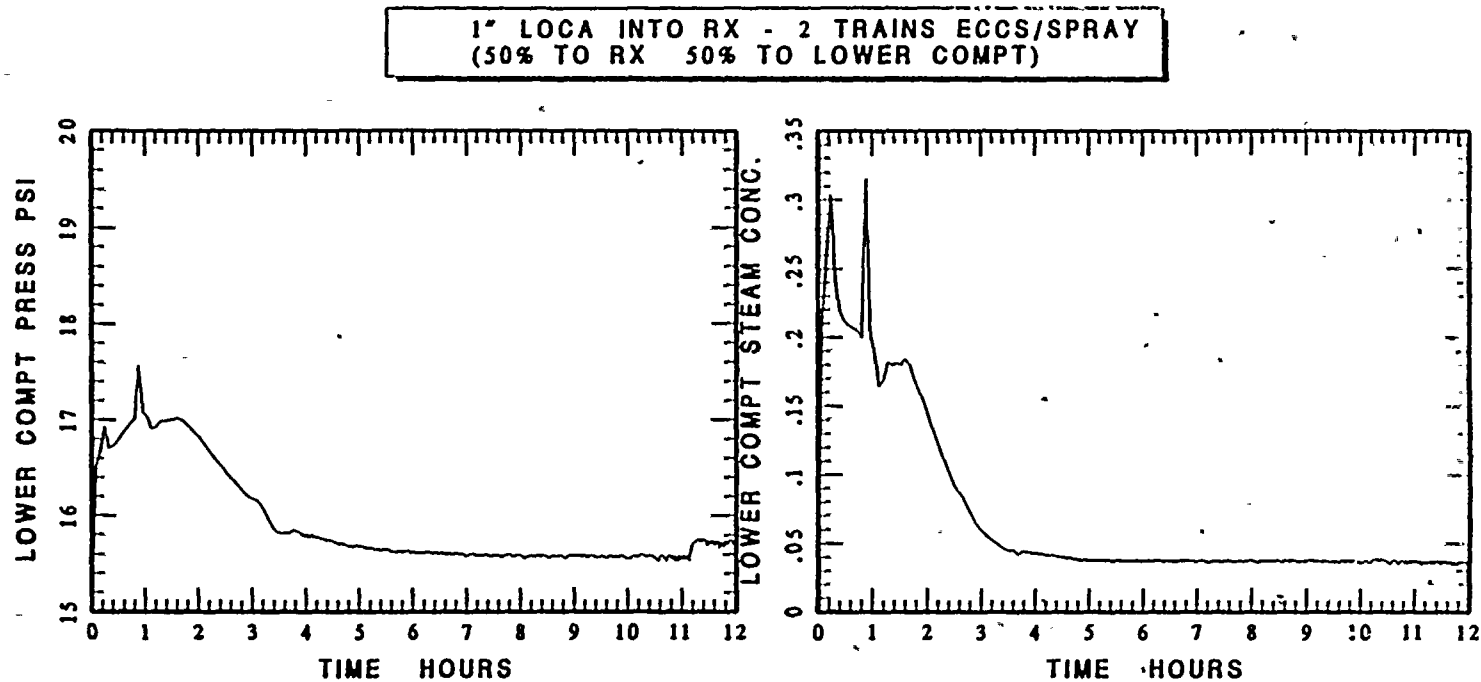


Figure 5-20f Details of the primary system and containment response for the most limiting case of a 1 inch dia. break into the reactor cavity.

behavior since the high head flows can not be throttled. Such an assumption is a conservatism in the analysis.

The flow rates of the containment sprays and RHR sprays are indicated in Figure 5-20c. It is particularly important to note that the RHR sprays were not actuated, which is consistent with the conditions input to the calculation requiring that the RHR sprays would only be used when both trains of containment sprays are not operating. Also, this figure shows that the containment sprays are actuated early in the accident progression with the injection phase terminating at about 3/4 hr. Once transfer to recirculation has been completed, both trains of sprays are restarted, i.e., the same flow rate as the injection phase.

The sump water temperature and the containment spray injection temperature are illustrated in Figure 5-20d which shows the influence of long term spray operation with containment heat removal through the containment sprays. Also, the heat removed by the containment spray heat exchangers is shown in this figure and as expected, the heat removal rate is highest early in the transient and decreases as the sump water temperature decreases. It should also be noted that the containment spray injection temperature changes substantially over the accident with the initial temperature being that set for the RWST and the final temperature approaching 42°F. This figure also shows the discharge of the accumulator mass, which begins at about 3 hrs. into the accident and is slowly discharged over the next 3-1/2 hrs. Hence, the accumulators provide most of their inventory to the containment sump at the time of the minimum level, i.e., at 5-1/2 hours.

Another important part of the system response is the RCS behavior, including the pressurizer and the secondary side transient response as illustrated in Figure 5-20e. With this small initial break size, the pressurizer does not drain completely and this level is restored once the cooldown begins. This figure also illustrates the influence of the cooldown process on the RCS water temperature. As discussed previously, a cooldown rate of 100°F/hr was used which is the maximum rate allowed in the EOPs and the maximum rate results in the minimum sump inventory. Once the cooldown process is initiated, the RCS water temperature decreases 200°F in 2 hrs, consequently, the cooldown effected by control of the secondary side pressure

accomplished the desired influence on the reactor coolant system. It should be noted that this cooldown and depressurization has the integral influence of enabling the pressurizer to be refilled, initiating accumulator injection and requiring additional water mass in the RCS as the coolant density increases.

Figure 5-20f illustrates the lower compartment pressure and the steam mass fraction in the lower compartment gas space during the accident sequence. This demonstrates that the pressure increases to the containment spray setpoint (17 psia) early in the accident sequence. This also shows that once the injection phase is completed and the containment sprays are shut down for 5 mins. during the transfer to recirculation, both the steam mass fraction and containment pressure increase during this interval which is the expected behavior. Once transfer to recirculation has been completed and the two trains of containment sprays are re-established with suction from the containment sump, the containment pressure and the steam concentration decrease rapidly to a quasi-steady value until the RCS cooldown begins to decrease the break flow rate and the steam flow rate to the containment.

In summary, the details of this most limiting case follow the expected behavior from the integral analysis. In addition to examining these details, a mass balance check was performed for this case. The water mass balance is examined for the most limiting break size (i.e., 1 inch small LOCA with a 50/50 flow split of saturated water from the break to the cavity the lower compartment). In this 1 inch small LOCA case, the minimum sump level occurs at around 5.4 hours. At the time of minimum sump level, the water level (referenced to the lower compartment floor; 598'9-3/8") in the active sump is 4.35 ft.

In these MAAP run analyses, it is assumed that 280,000 gallon - 16,100 gallon (assumed holdup volume) of RWST water will be injected into RCS and containment before switching from injection to recirculation. After the recirculation is completed, an additional 34,000 gallons of RWST water will be injected into the RCS. Thus, the total available RWST water to the RCS and the containment is 297,900 gallons (~ 2.48E6 lb). The additional water can be supplied from the accumulators and melted ice. At the time of the minimum sump level, 1.97E5 lb of accumulator

water has been injected into the RCS and 4.3E5 lb of ice melt has occurred. Table 5-2 shows a detailed mass balance of the entire system at the time of the minimum sump level. As illustrated, there is a check on the water inventory at the time of minimum sump level.

**Table 5-2**  
**Mass Balance at the Time of Minimum Sump Level for 1 Inch Small LOCA**  
**(50% to Cavity and 50% to Lower Compartment)**

Initial Water Mass in RCS + Pressurizer	5.230E5 lb
RWST Water Available (all injected)	2.48E6 lb
Accumulator Water Injected at 5.4 hour	1.97E5 lb
Ice Melted at 5.4 hour	4.3E5 lb
<b>TOTAL</b>	<b>3.63E6 lb</b>
Water Masses in RCS + Pressurizer at 5.4 hour	6.40E5 lb
Water Masses in Containment at 5.4 hours	
in Cavity	0.93E6
in Lower Compartment	1.03E6
in Annular Compartment	0.94E6
in the Rest of Containment	0.9E5
<b>TOTAL</b>	<b>3.63E6 lb</b>

#### 5.4 Sensitivity Analyses for Mode 1 Evaluations

As discussed previously, the most limiting containment conditions for a loss-of-coolant accident in the containment with respect to the containment sump inventory were addressed through a Failure Modes and Effects Analysis (FMEA). In general, these conditions are those which minimize the ice melt through the earliest spray initiation for a given break size combined with the minimum steam mass in the lower containment compartment and the coldest spray water temperature. Since the most limiting cases for this evaluation had already been established, these were not a subject of sensitivity analyses.

One aspect of the containment evaluation to be assessed through an integral model is the sensitivity to the ECCS and containment safeguards configuration. The base case for the sump evaluation was performed with two trains of ECCS and a single train of air recirculation fans in operation. Hence, the single active failure is a single CEQ fan failed with the remainder of that train operating as designed. To address the sensitivity to this assumed failure, two additional configurations were considered:

- failure of a complete ECCS train and containment safeguards (one CEQ fan is in operation along with one injection train and one train of containment sprays);
- the single active failure was not in the ECCS and containment safeguards such that two trains of all the systems were available.

Figure 5-21 illustrates the response to a 1.5 inch LOCA into the reactor cavity using a 50/50 split flow to the reactor cavity and the lower compartment (the limiting case) for these three different cases. As illustrated, the failure of a single CEQ fan is more limiting in terms of the minimum sump level by several inches with the principal reason for this difference being increased ice melt for the two conditions considered in addition to the base case. This demonstrates that the system configuration evaluated for these assessments is the single most limiting case in terms of presenting the minimum containment sump level for the spectrum of LOCA conditions.

### 5.5 Conservatisms in the Analyses

Several of the conservatisms can be quantified. These are detailed below.

The free volumes assumed in the pipe annulus and lower compartment regions are documented in the DIT information in Appendix A. This analysis represents the total volumes in these compartments and no assessment has presently been made for the volume occupied by internal structures such as pipes, valves, etc. In the previous analyses (FAI, 1997) an allowance of 5% was given for structure in the pipe annulus. Given the large pipe annulus volume, a 5%

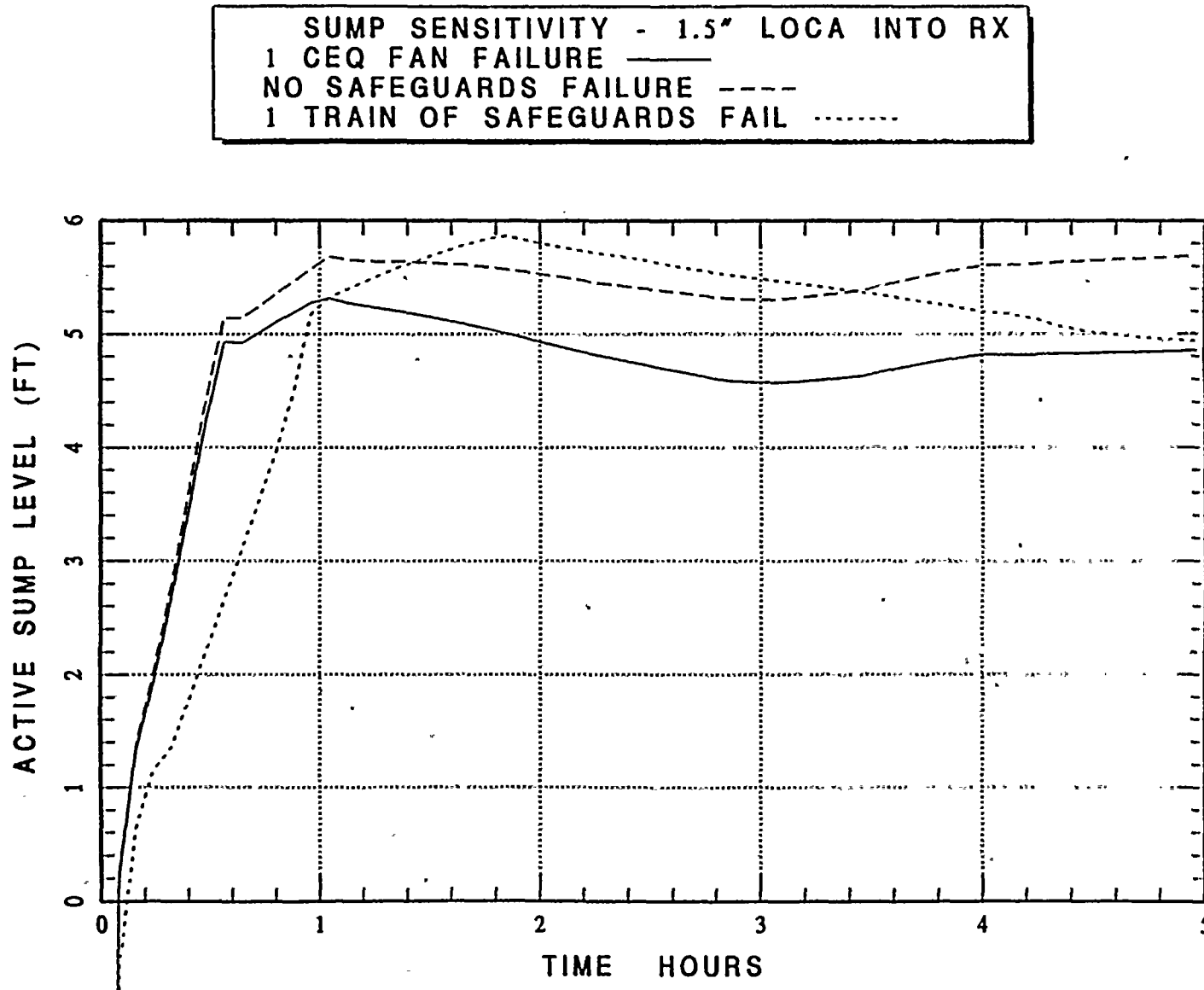


Figure 5-21 Comparison of the minimum water levels for a 1.5 inch break into the reactor cavity assuming (a) the failure of a single CEQ fan, (b) the failure of a complete train of ECCS and containment safeguards and (c) no failure of either ECCS/containment safeguard train.

value for the internal equipment represents about 16,000 gals. Approximately half of this blocked volume could become submerged. The blocked volume in the submergible portion of the lower compartment is given as 507.6 ft<sup>3</sup> (3800 gals). The combined submerged blocked volume is approximately 11,800 gals or a sump level increase of about 2.2 inches. This influence is not included in the evaluations documented in Section 5 and therefore is a conservatism in these analyses.

These assessments assumed the maximum cooldown rate of 100°F/hr. Slower cooldown rates, such as 30°F/hr or 50°F/hr would increase the energy discharged into the containment and therefore increase the ice melt inventory. Therefore, using the maximum cooldown rate in this assessment is a conservatism in the analysis.

Other parts of the analysis are conservatisms but cannot be directly quantified. The influence of these assumptions are discussed in the following paragraphs.

These split flow breaks postulated very small ruptures in the reactor coolant piping inside the biological shield. Such small breaks which are smaller than the piping thickness are highly unlikely. In particular, a postulate of cracks in the RCS piping would be demonstrated as leaks but not ruptures of this size and those ruptures which are postulated as a result of other events, such as seismically induced movement of the piping would result in larger break sizes if such a rupture would occur. Consequently, postulating very small ruptures of the RCS piping inside the biological shield is a substantial conservatism in these analyses.

For the assessments provided in this section, the most limiting conditions with respect to containment conditions, ECCS/containment safeguard configurations, postulated break sizes, break location, etc. have been considered. As discussed for each of these issues, the most limiting case is that which results in the earliest actuation of containment sprays combined with the smallest steam discharge rate to the lower compartment atmosphere. Hence, each of these parameters that has been examined through the FMEA calculations or specific MAAP4 analyses tends to provide for minimal ice melting which therefore translates to a minimal ice melting inventory to the



containment sump. Therefore, these are all individually conservatisms in the analysis since it is skewed towards the most conservative boundary of each parameter.

The mass and energy releases to the containment, regardless of the break size, are provided by MAAP4 using the assumption that the steam and water discharged from the break are in thermodynamic equilibrium. This results in the maximum water enthalpy and therefore the minimum steam mass produced as the mixture flashes into the containment. Therefore, the use of the MAAP4 mass and energy releases produces the minimal ice melt for a given postulated break size.

Another conservatism is the invariance of the licensing base limit for vortexing with the flow rates demanded by the ECCS and containment spray systems. The information in the literature with respect to changes in flow rate indicate that the water depth necessary to protect against substantial air ingress varies as the square of the velocity and therefore as the square of the flow rate (Weigand et al., 1982). For the most limiting cases examined, the ECCS injection flow is only a few hundred gpm and the containment spray flow is 3700 gpm per train. This is well below the 9500 gpm through a single section pipe that was considered in the Alden scaled test for the D.C. Cook sump. The value of 9500 gpm was considered as the runout condition for one ECCS train given complete failure of the other train. Another case considered was 7700 gpm flow for each suction pipe with both trains operating which is more representative of the conditions used in this analysis. This 7700 gpm flow rate simulated the runout condition of ECCS pumps with both trains operating. As mentioned earlier, the Alden Laboratory scaled experiments observed that a level of 602'10" was sufficient to protect both of these cases. Moreover, the parametric sump studies performed by Sandia National Laboratories and Alden Laboratories for the Nuclear Regulatory Commission (Weigand et al., 1982) show that a reduced injection rate could have sufficient protection for air ingress by a much lower water level. The guidance from the parametric study suggest that a Froude number of 0.55 can be used to describe the submergence sufficient to protect against air ingress up to 2.5% void fraction. This extent of ingested void would not result in damage to large pumping systems during long term operation. The Froude number in this context is defined as



$$Fr = \frac{U}{\sqrt{gs}}$$

where  $U$  is the water velocity in the pipe inlet,  $g$  is the acceleration of gravity and  $s$  is the submergence depth of the pipe inlet.

In the D.C. Cook specific scaled experiments the observation of no air ingress for a suction flow of 9500 gpm and a sump level of 602'10" can be used to formulate a Froude number function for such protection at lower suction flow rates. In the D.C. Cook sump, the vortex must be pulled below the bottom of the crane wall 593'9-3/4" (Figure 5-22) before air could be ingested into the suction piping. Combining this submergence (9'1/4") and flow rate with an 18 inch suction pipe diameter results in a Froude number of 0.7. Water levels necessary to prevent air ingress can be assessed using this characterization.

An additional observation was made by Padmanabhan (1978) for the D.C. Cook sump tests, i.e., "Preliminary tests indicated that the minimum water level in the sump should not be less than EL 602 ft, 3 inches so that the necessary head over the curb to effect the needed inflow balancing the outflow from the sump was available." This is the only reference to this elevation and there is insufficient data reported to check this against standard weir flow models. Furthermore, there is no such limitation noted for the same suction flow with the water level at a scaled height of 602'10" and a 50% blockage of the entry to the sump. Nevertheless, this observation provides a means of determining a bounding condition for characterizing the water supply flow to the sump. From standard weir flow theory (Vennard, 1954), the volumetric flow rate ( $\dot{Q}_v$ ) is proportional to the water height differential ( $H$ ) as given by

$$\dot{Q}_v \propto H^{3/2}$$

The appropriate height in this calculation is the distance above the curb which has an elevation of 599'4-3/8" (Figure 5-22). Solving for the constant of proportionality for a differential height of 2.89 ft. with a total flow rate of 15,400 gpm provides the functional behavior shown in Figure 5-23: Note that this is displayed on a per train basis and has a value very close to 602'10" for

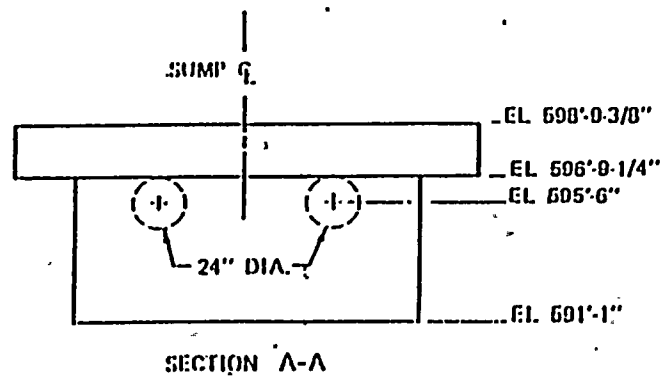
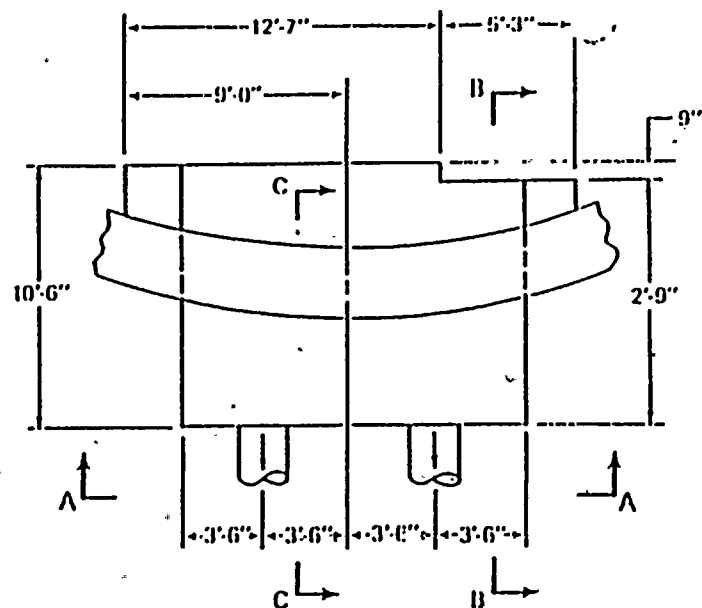
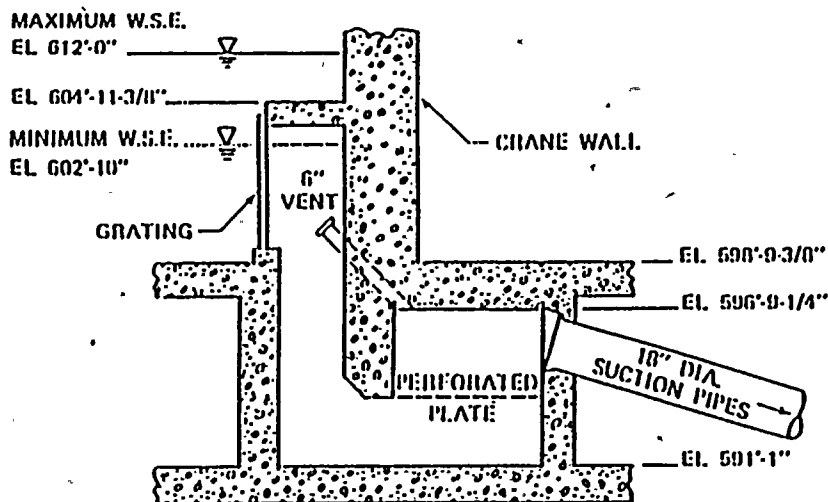
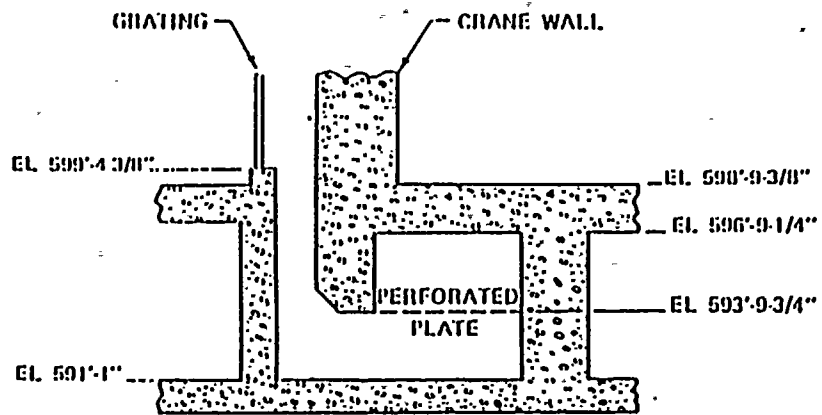


Figure 5-22 Details of original sump taken from Padmanabhan (1978).



## MODE 1: Necessary Sump Water Level for Reduced Suction Flow Rates

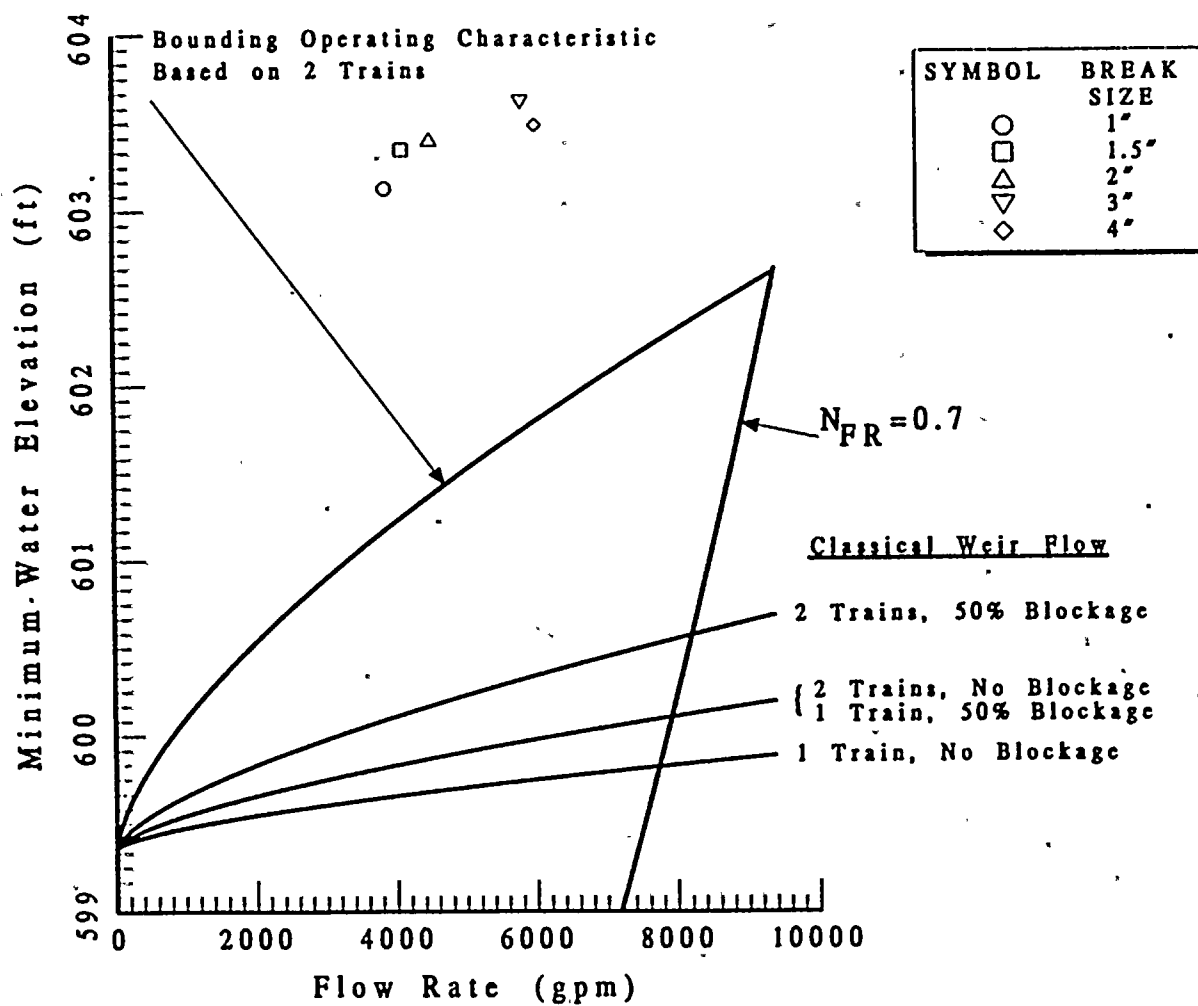


Figure 5-23 A summary of the minimum sump water levels versus sump total suction flow rate for Mode 1 operation (note that the flow rates are on a per train basis).



a flow rate of 9500 gpm. Thus, this curve can be used to bound the behavior for air ingression as well as supply flow to the sump.

To illustrate the conservatism in this representation, Figure 5-23 includes the air ingression boundary ( $N_{Fr} = 0.7$ ) as well as classical weir flow results for one and two trains of ECCS and containment safeguards operating including conditions for no blockage and 50% blockage of the sump inlet periphery. There is substantial margin between the bounding representation and these more mechanistic analyses.

Figure 5-23 also shows the results of the split flow Mode 1 analyses, which are the most limiting cases. These minimum levels are all above the 602'10" design basis limit for vortexing. Moreover, these postulated accident conditions also have the smallest suction demand. Hence, there is additional margin for these smaller break sizes than represented by the submergence above 602'10". This is an added conservatism for the Mode 1 analyses.

Lastly, the most limiting containment configuration is evaluated with respect to the ECCS/containment safeguards available in the accident response. In particular, the configuration selected, the failure of a single CEQ fan, results in the lowest gas flow through the ice condenser and therefore the minimal ice melt during the transient evaluated. No credit is taken for termination of a single train of sprays for these very small LOCAs or for shutting down one of the injection trains to the RCS. Each of these would slow the time to recirculation and would also increase the ice melt without creating any challenge to containment integrity. Neglecting such operator actions in very long transients is a conservatism in the assessments.





## 6.0 ANALYTICAL RESULTS FOR THE CONTAINMENT SUMP INVENTORY FOLLOWING A LOCA UNDER MODE 3 CONDITIONS

The assessment for the minimum sump inventory considered accident sequences other than the spectrum of possible ruptures in the RCS under Mode 1 conditions. One such set of conditions considered were the integral RCS and containment behavior following a postulated break in the reactor coolant system when the RCS had been cooled to a temperature of 350°F. (In these cases the break is initiated at 3 hours which is the interval required to cool down the RCS.) Several cases were examined, with the bounding cases being a 6 inch equivalent diameter break discharging to the lower compartment and a 2 inch diameter break in the cold leg near the reactor vessel nozzle which discharges water into both the lower compartment and the reactor cavity. The results for the first case are illustrated in Figure 6-1 and show that the accident is initiated after the RCS is cooled down to the temperature of interest. Note that this lower bound of the Mode 3 temperature range was used since this results in the minimum steam production due to flashing and therefore the minimum ice melt contribution to the sump. A LOCA of this size is sufficient to actuate the CEQ fans and the containment sprays with the water level in the sump being greater than the licensing base limit for vortexing at all times after recirculation which occurs at about 4 hrs. The results for the second case are illustrated in Figure 6-2. Such a small LOCA would not initiate containment sprays for the conditions defined. Consequently the location of a break of this size, or smaller, has no influence on the sump level since the sprays would not actuate.

Other effective break sizes were considered for locations in the lower compartment and the split flow cases since these are the limiting set of conditions. Break sizes larger than 2 inches release sufficient steam to increase the containment pressure to the 2.3 psig spray setpoint considered for these evaluations. Consequently, with the reduced energy inventory in the RCS, the net steam produced by these breaks results in a reduced water level in the active sump compared to the Mode 1 analyses. Figures 6-3 and 6-4 respectively illustrate the Mode 3 results assuming 4 inch and 3 inch effective diameter breaks into the lower compartment. As shown by these two figures, the water level at the initiation of recirculation, which occurs at approximately

MODE 3 - 6.0 IN BREAK INTO LOWER COMPARTMENT

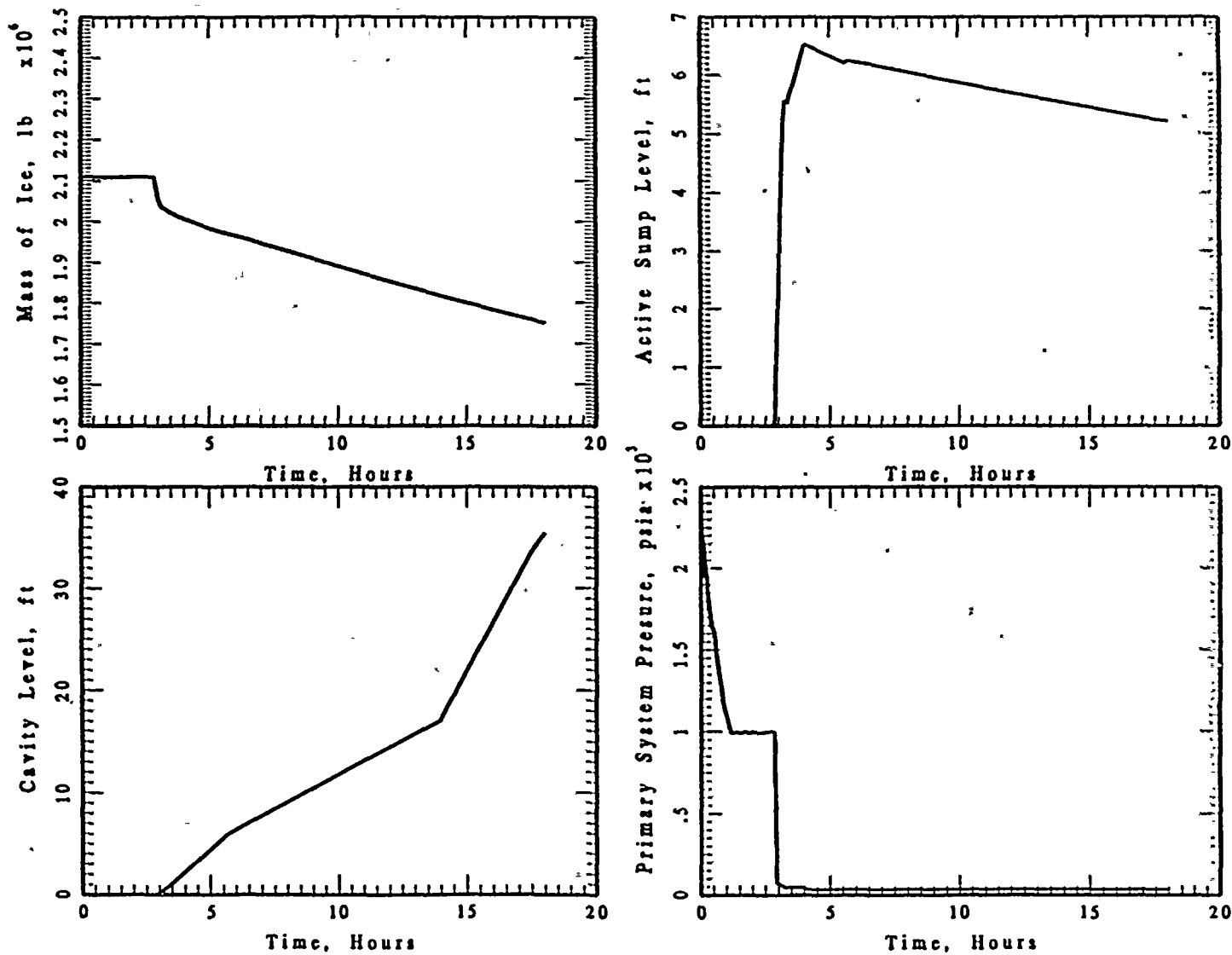


Figure 6-1 Summary of the results for a 6 inch LOCA into the lower compartment under Mode 3 conditions.

MODE 3 - 2.0 IN BREAK INTO REACTOR CAVITY

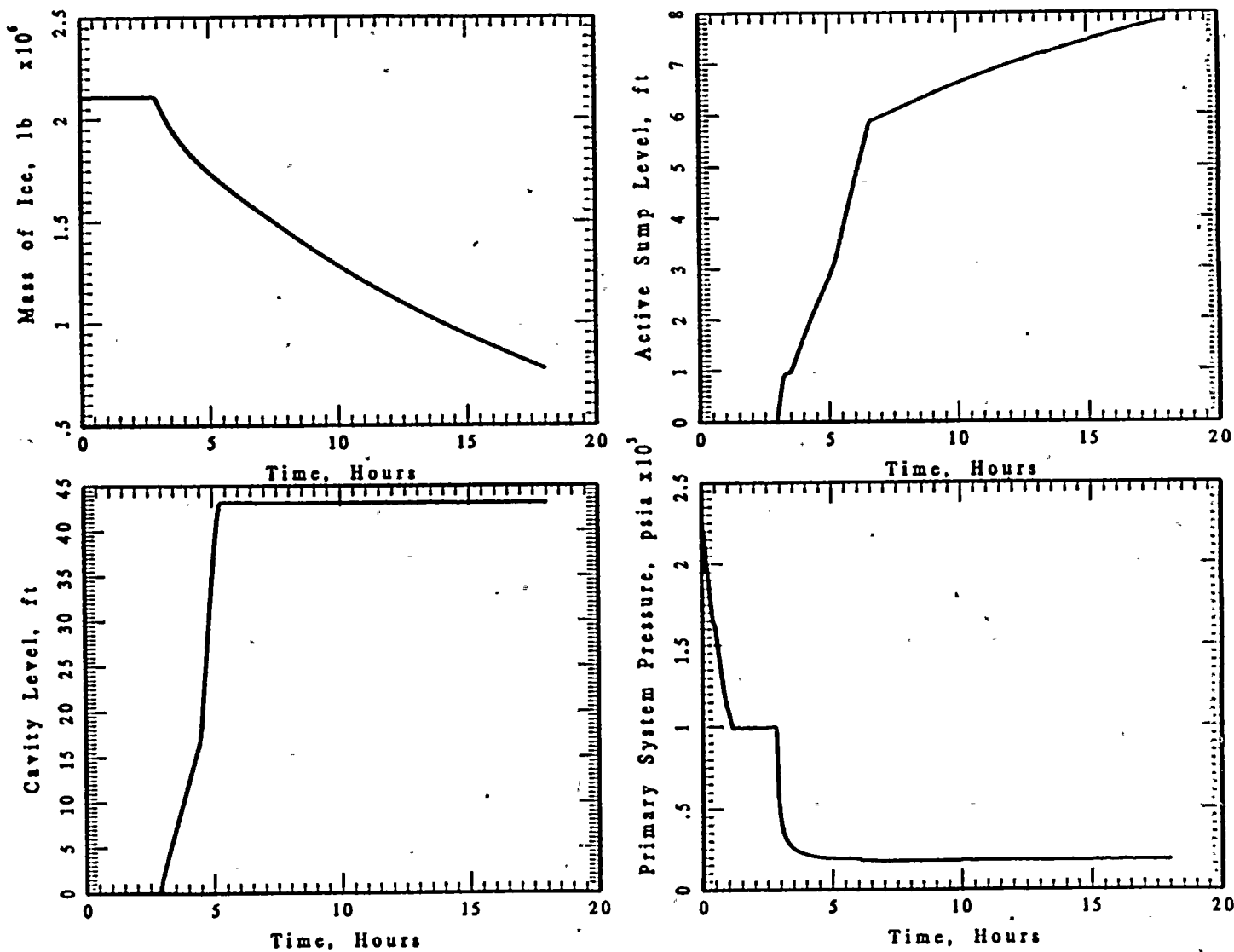


Figure 6-2 Summary of the results for a 2 inch LOCA into the reactor cavity under Mode 3 conditions.

MODE 3 - 4.0 IN BREAK INTO LOWER COMPARTMENT

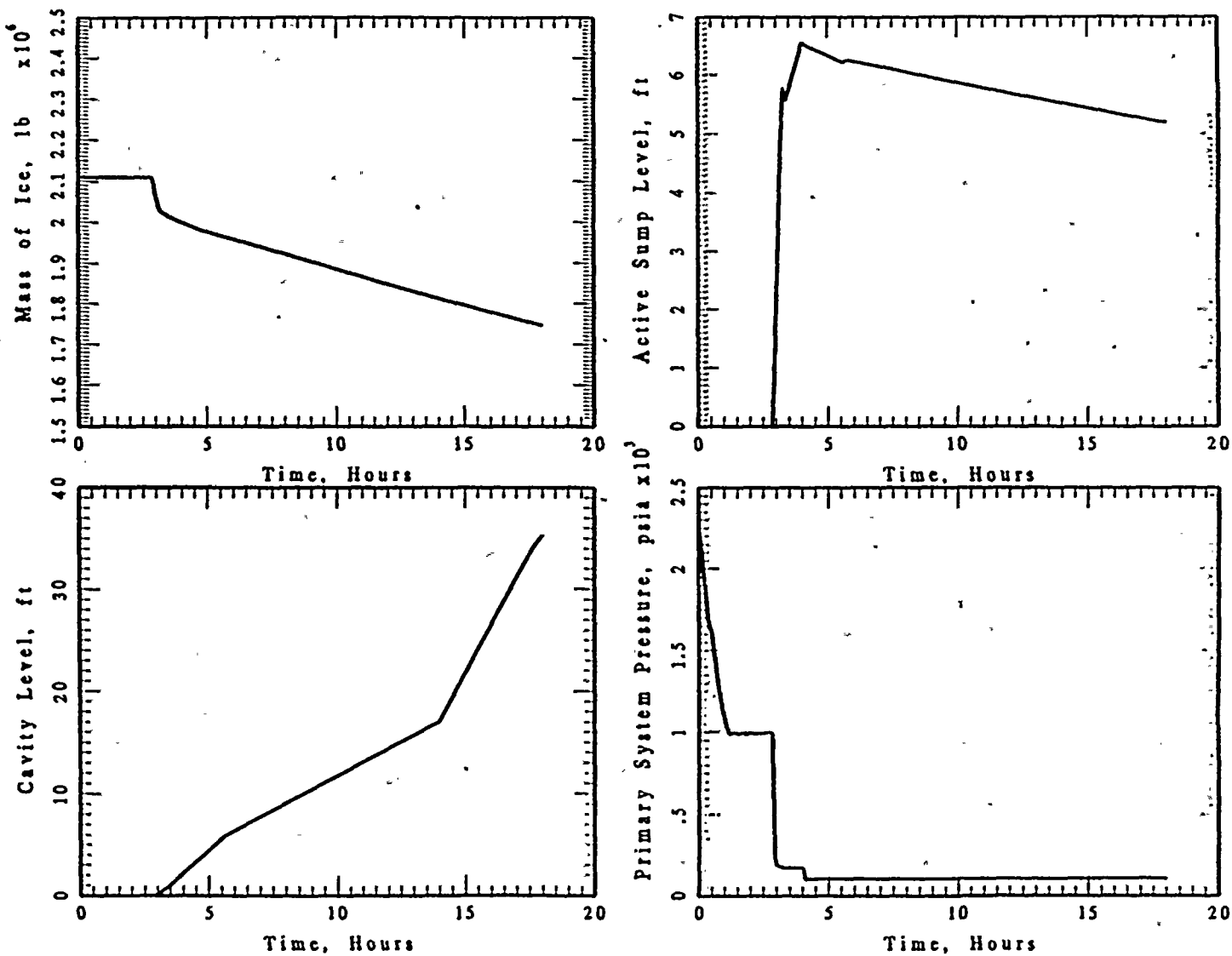


Figure 6-3 Summary of the results for a 4 inch LOCA into the lower compartment under Mode 3 conditions.

MODE 3 - 3.0 IN BREAK INTO LOWER COMPARTMENT

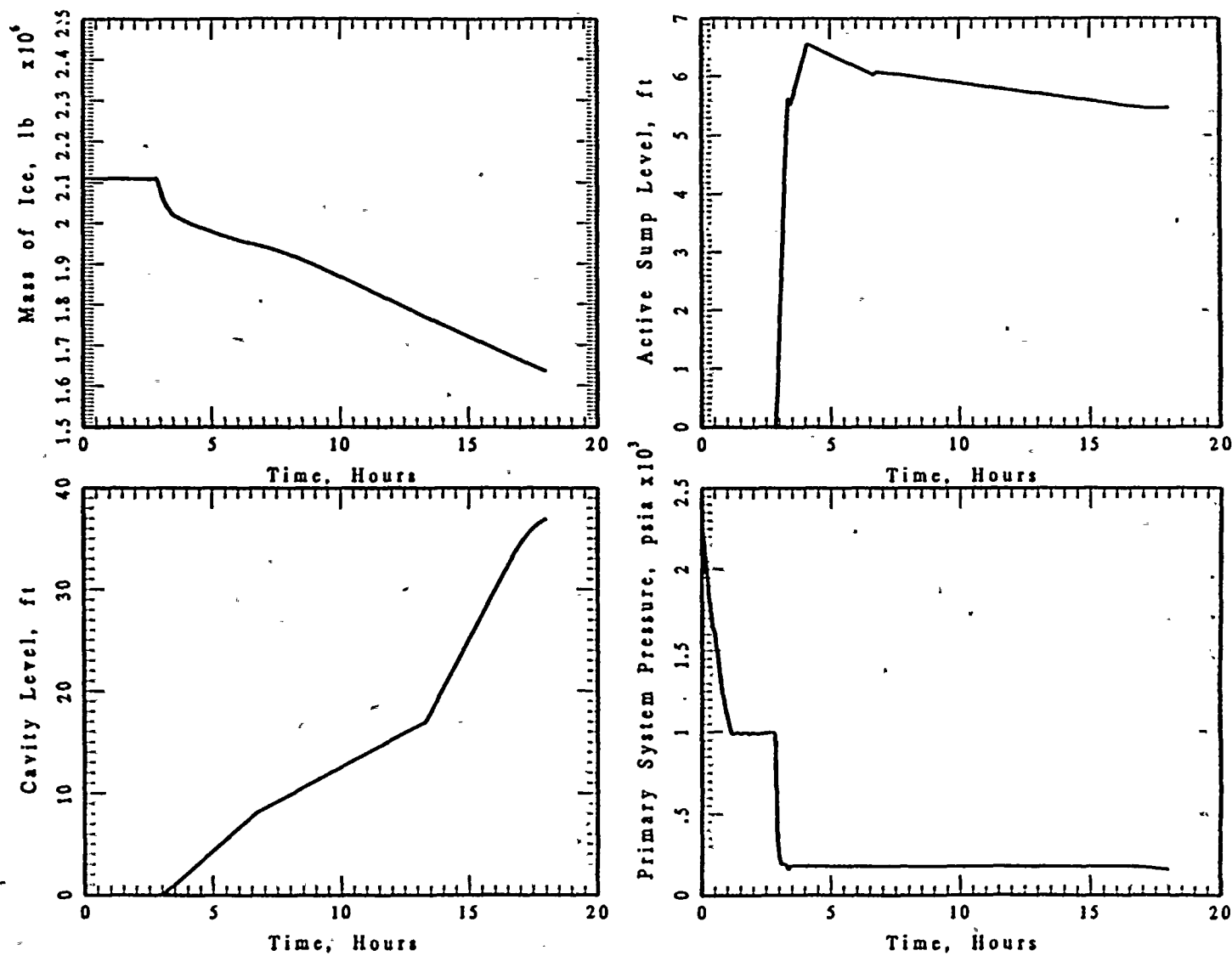


Figure 6-4 Summary of the results for a 3 inch LOCA into the lower compartment under Mode 3 conditions.

4 hours into the evaluation, is approximately 2-1/2 feet above the 4 foot level which corresponds to an elevation of 602'10". With the long term flow through the NIS holes and the potential for containment spray to fall through the entry to the instrument tunnel, this slowly decreases to a minimum value which is above the 5 foot level, i.e., an elevation of 604 feet.

The response of postulated split flow breaks in the cold leg piping as analyzed for the Mode 1 analyses is illustrated in Figures 6-5, 6-6 and 6-7 for respective effective break diameters of 6 inches, 4 inches and 3 inches. These cases experience a substantial flow rate to the reactor cavity early in the accident sequence and as a result less water accumulated in the sump. With the reduced contribution of ice melt for the initial RCS temperature condition, there is insufficient inventory in the sump at the time of recirculation to remain above the 602'10" condition. However, this is for a very short time and the level recovers to a value above the 602'10" condition which corresponds to 4.05 feet in these figures. The Mode 3 sump level results are summarized in Table 6-1.

With these smaller break sizes, the water demand from the containment sump is substantially reduced since the ECCS flow rates are well below those associated with the DECL design basis condition. Consequently, the information produced from these integral analyses can be integrated with that reported in the Alden Laboratory studies (Padmanabahn, 1978) as well as those integrated through the MPR evaluation of meaningful requirements for the recirculation sump based on the Alden Laboratory data. Similar to the analyses performed for the Mode 1 cases and shown in Figure 5-23, Figure 6-8 compares the minimum required sump level for these reduced suction flow rates on a per train basis with that resulting from the Mode 3 assessments. As illustrated, with the reduced sump demand flow, the minimum sump level is above the bounding limit characterizing both vortexing and the critical depth to support flow into the sump. Hence, while the level may be below 602'10" for postulated break sizes in the reactor coolant system piping inside the biological shield, the reduced recirculation flow has a correspondingly reduced demand with respect to vortexing (air ingress) and the flow rate into the sump (weir flow) to assure that the inflow equals the outflow. Consequently, there is also sufficient inventory

MODE 3 - 6.0 IN BREAK INTO RX CAVITY

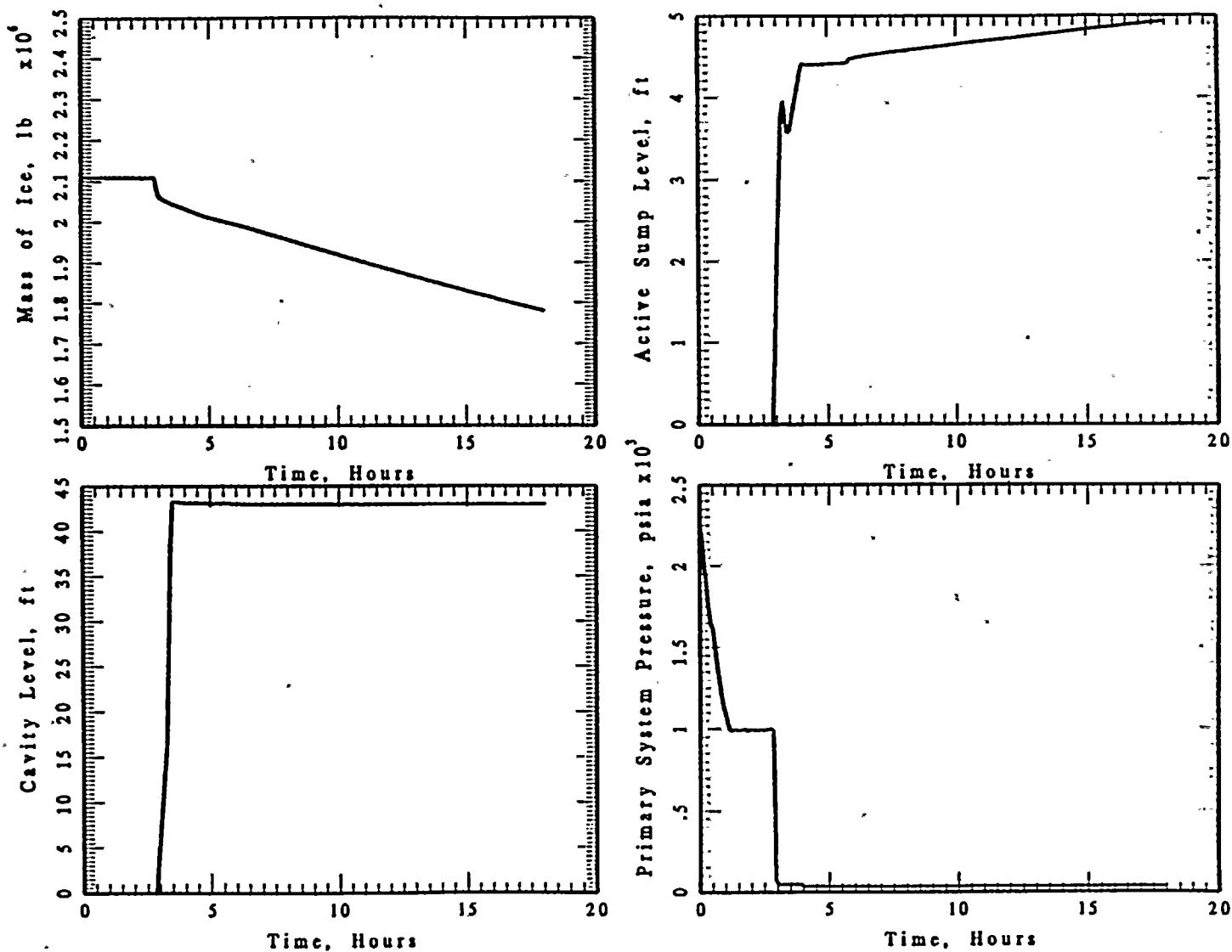


Figure 6-5 Summary of the results for a 6 inch split flow LOCA under Mode 3 conditions.



MODE 3 - 4.0 IN BREAK INTO RX CAVITY

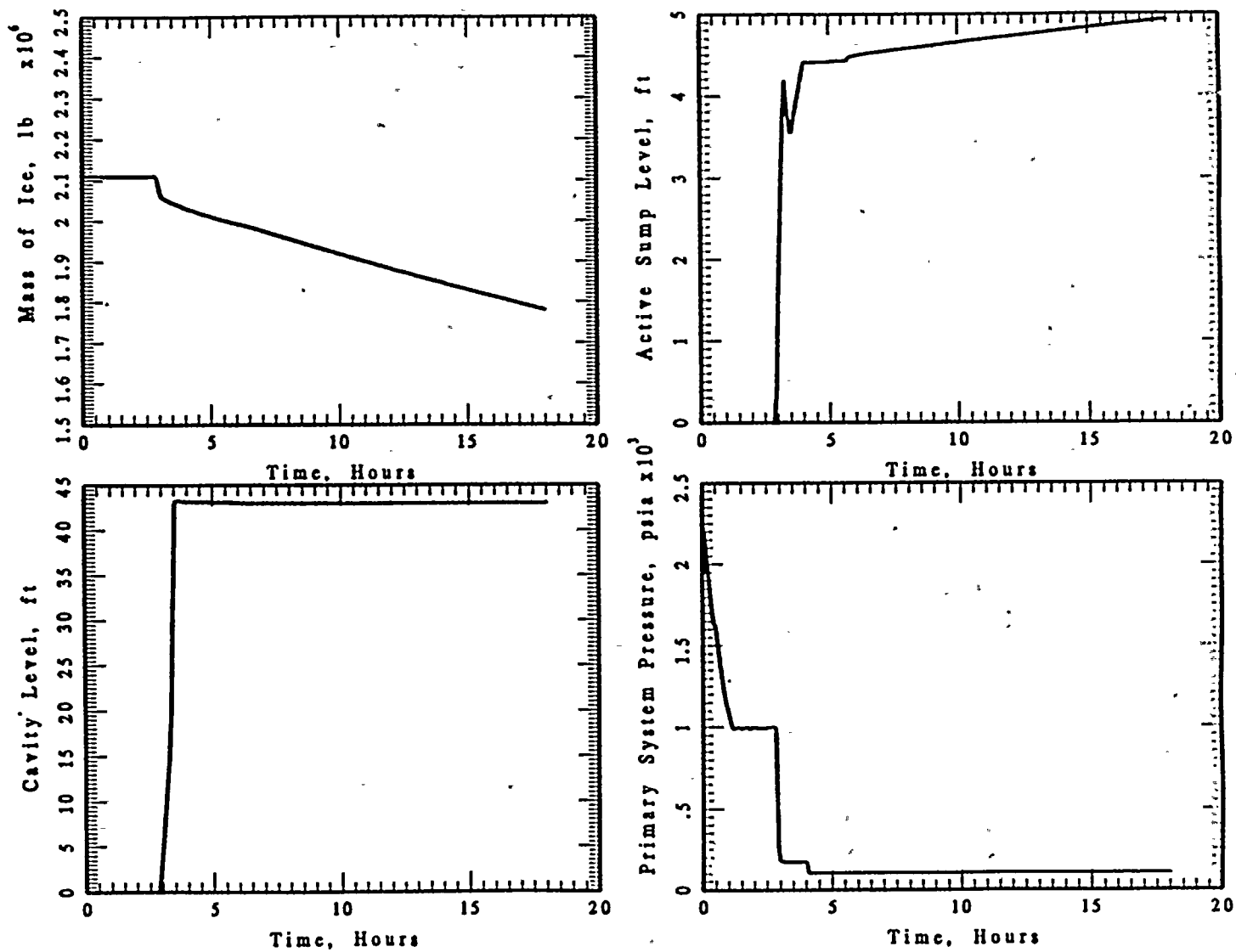


Figure 6-6 Summary of the results for a 4 inch split flow LOCA under Mode 3 conditions.



# MODE 3 - 3.0 IN BREAK INTO RX CAVITY

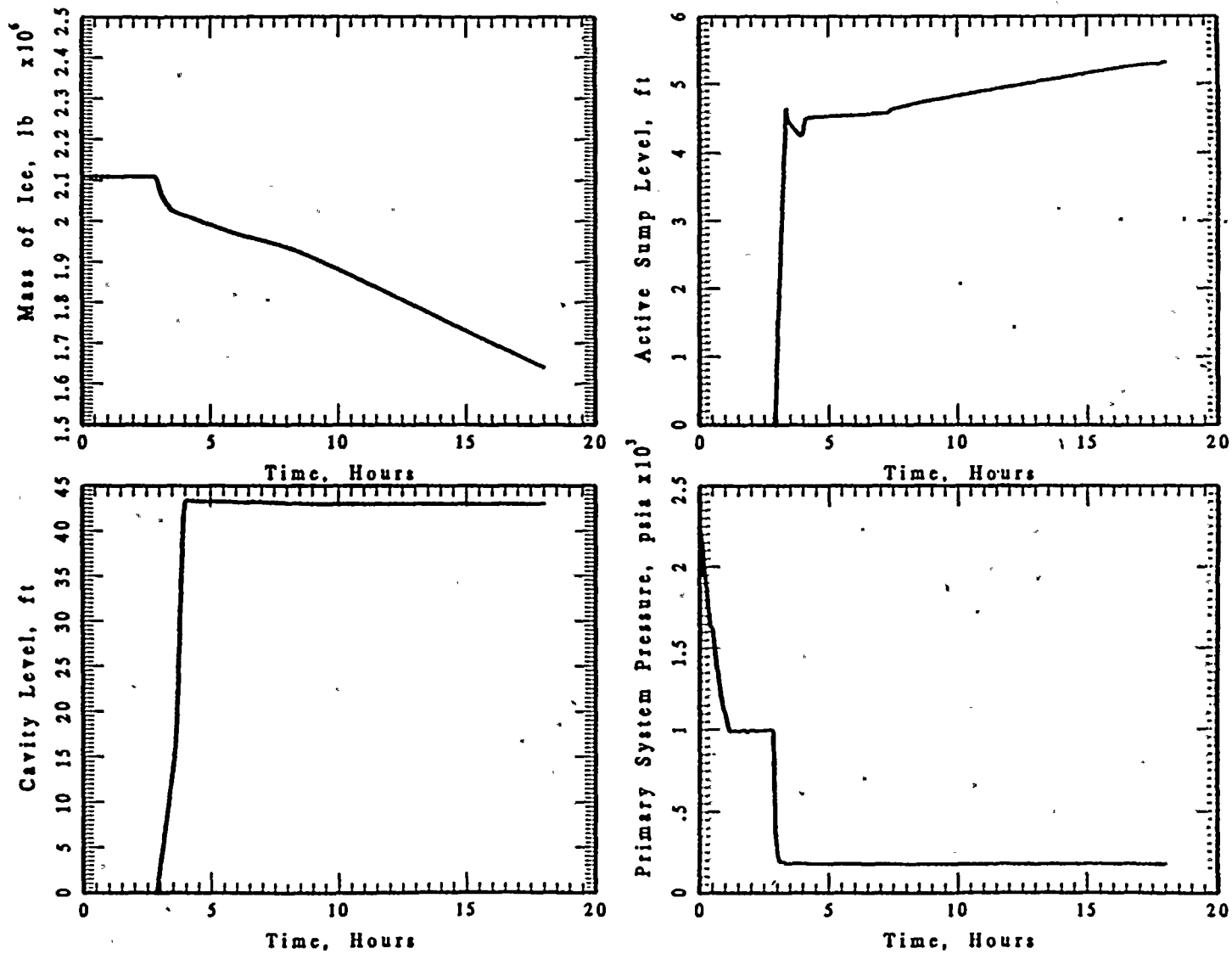


Figure 6-7 Summary of the results for a 3 inch split flow LOCA under Mode 3 conditions.

Table 6-1

Summary of Mode 3 Results

Break Size (inch)	Break Location <sup>(1)</sup>	Switch to Recirculation		Minimum Sump Level		Containment Spray Operation	
		Time <sup>(2)</sup> (seconds/hr)	Sump Level (ft)	Time <sup>(2)</sup> (seconds/hr)	Sump Level (ft)	Start Time <sup>(2)</sup> (seconds/hr)	Shut-Off Time <sup>(2)</sup> (seconds/hr)
2	LC	21037/5.84	6.4	21037/5.84	6.4	Not Initiated	N/A
3	LC	12048/3.35	5.5	12048/3.35	5.5	10440/2.9	24109/6.7
4	LC	11724/3.26	5.5	11724/3.26	5.5	10409/2.9	20228/5.6
6	LC	11639/3.23	5.5	61200/17.0	5.2	10387/2.9	20297/5.6
2	RX	21033/5.84	4.3	21033/5.84	4.3	Not Initiated	N/A
3	RX	12045/3.35	4.6	13860/3.85	4.25	10430/2.9	26470/7.35
4	RX	11709/3.25	4.0	12600/3.5	3.55	10404/2.9	20741/5.8
6	RX	11627/3.23	4.3	12200/3.4	3.55	10386/2.9	20874/5.8
<sup>(1)</sup> Lower compartment designated LC and reactor cavity designated RX. <sup>(2)</sup> All times referenced to start of cooldown from normal operating conditions which is time of 0 seconds. The Mode 3 LOCA is initiated when the primary water temperature reaches 350°F which occurs at 10,375 seconds (2.9 hours).							

MODE 3: Necessary Sump Water Level for Reduced Suction Flow Rates

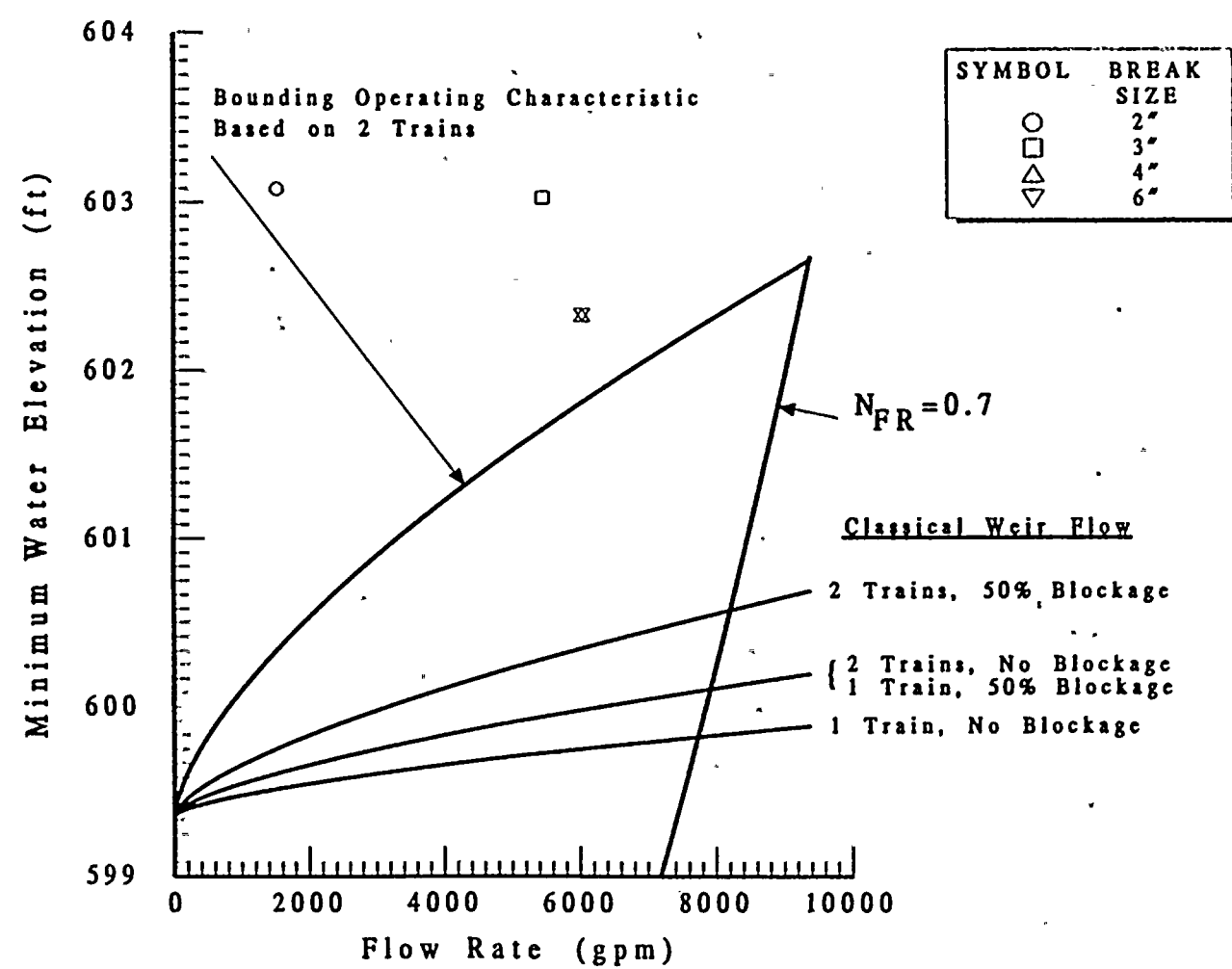


Figure 6-8 Comparison of the minimum required sump level and the minimum calculated levels for the lowest RCS temperature in Mode 3.

in the active sump during recirculation for the lowest RCS temperature in Mode 3. Other Mode 3 conditions (RCS temperatures between hot standby and the 350°F value used in these analyses) are bounded by the Mode 1 and Mode 3 results given here for the minimum sump level.

## 7.0 ANALYTICAL RESULTS FOR THE CONTAINMENT SUMP INVENTORY FOLLOWING A MAIN STEAM LINE BREAK

As with the cases addressed for a break in the reactor coolant system, the spectrum of conditions also considers the potential break in the secondary side, i.e., a main steam line break. This type of accident is different from those with a break in the RCS since there is no continuing need to inject to the RCS. The containment sprays can be actuated by the steam generator blowdown into the lower compartment and the RWST would be drained to the recirc condition but little injection is needed to the RCS. Also, there would be a substantial ice melt associated with the steam generator blowdown and this inventory would drain to the sump. Figures 7-1 and 7-2 illustrate the integral response for postulated break diameters of 1.4 ft<sup>2</sup> and 4.6 ft<sup>2</sup> respectively. There is essentially no difference in the global accident behavior. In both cases the failed steam generator is isolated 600 seconds after the postulated main steam line break. As illustrated in these figures, there is a substantial amount of ice mass melted early in the transient (approximately 400,000 lbs) and the water level in the sump increases to about 5.7 ft (an elevation of 604'6") due to the activation of containment sprays and the ice mass melted. There is flow into the reactor cavity through the nuclear instrumentation ports in the biological shield and by the spray flow into the entrance to the instrument tunnel which slowly increases the level in the reactor cavity and decreases the level in the sump. In this calculation the containment sprays were secured after about 8 hours when the containment pressure reached the reset condition. At this time the RCS is full and undergoing cooldown with very little ice melting. Hence, there is virtually no demand on the containment sump. During the time at which there was a suction demand from the sump, the level was well above the licensing base limit for vortexing of 602'10", which is approximately 4 ft. of level in the active sump. Consequently, neither of these steam line break initiating events resulted in any challenge to recirculation flows.

1.4 FT\*\*2 MSLB INTO LOWER COMPARTMENT

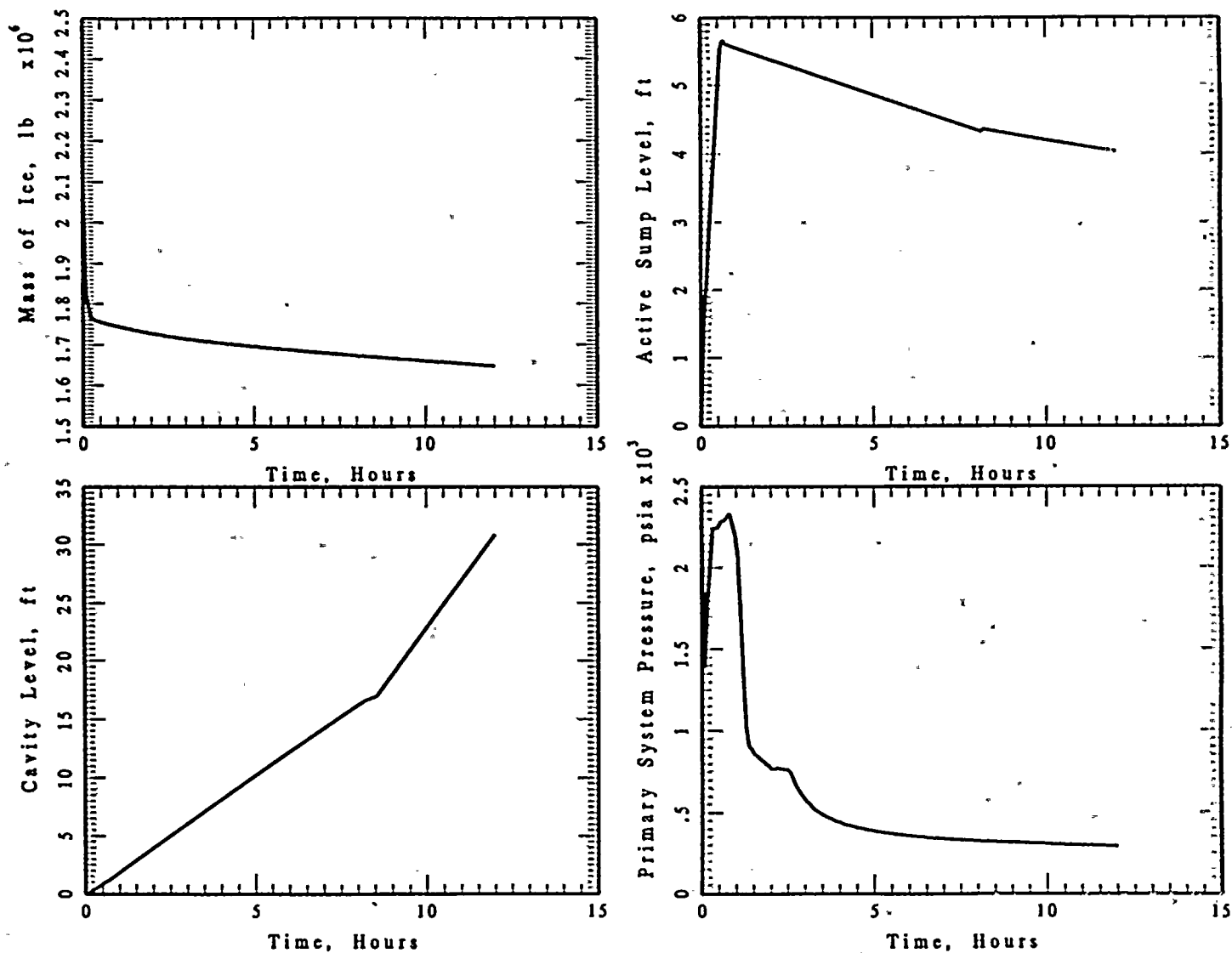


Figure 7-1 Summary of the minimum sump inventory for a steam line break of 1.4 ft<sup>2</sup> into the lower compartment.





4.6 FT<sup>2</sup> MSLB INTO LOWER COMPARTMENT

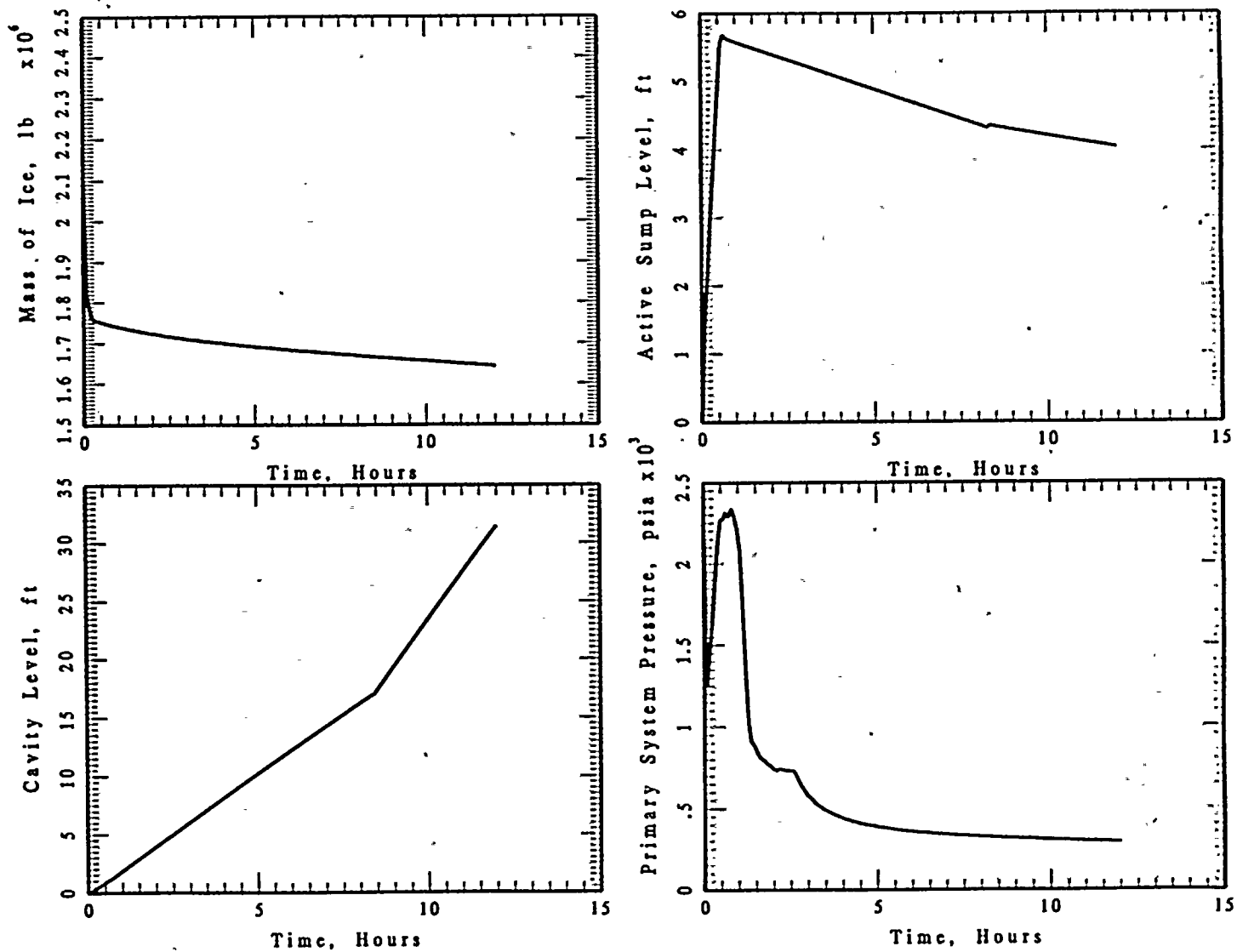


Figure 7-2 Summary of the minimum sump inventory for a steam line break of 4.6 ft<sup>2</sup> into the lower compartment.

## 8.0 CONCLUSIONS

The conclusions from these analyses are as follows.

1. With the changes in the containment design to assure adequate communication between the pipe annulus and the sump, as well as the change in the CEQ fan setpoint, there is sufficient sump level for the complete spectrum of RCS and secondary side breaks to protect against vortexing and air ingress. Hence, there is no need for additional plant modifications or changes to the EOPs.
2. The assessment of the minimum sump inventory requires an integral analysis which includes representations of the RCS and containment as well as the system performance of the ECCS and containment safeguards.
3. The containment building model needs to provide sufficient nodalization to represent water inventories in the sump (lower compartment), the pipe annulus and the reactor cavity as well as to model the flow connections between these different compartments. Furthermore, the assessment must provide a mechanistic description of the ice melt behavior such that the complete spectrum of LOCA conditions can be evaluated.
4. The MAAP4 models for the ice condenser, ice condenser containments and the inlet door characterization are in good agreement with the available experimental results from large scale experiments and plant observations, i.e., the forces required to open the ice condenser lower inlet doors.
5. The most limiting case for the minimum sump level during recirculation are those conditions in which the containment sprays are initiated but there is minimal ice melting when the sprays are operating. These are situations in which the steam

partial pressure in the lower compartment is minimized (small-small LOCA) and the potential for condensation is maximized (the coldest spray temperature). These conditions were developed through an independent FMEA assessment and applied in this analysis.

6. For the spectrum of LOCA conditions evaluated into the lower compartment, a LOCA with an effective diameter of 1" represents the minimum condition where sprays would be initiated and the steam partial pressure in the lower compartment the lowest. This represents the most limiting case for a break into the lower compartment and the minimum level in the sump for this most limiting transient is 9 inches above the licensing base limit for vortexing of 602'10".
7. For postulated breaks in the cold leg inside the biological shield, the water discharge from the break is represented as having a 50/50 split between the reactor cavity and the lower compartment based on jet impingement analyses of the two-phase discharge. For these types of breaks, the most limiting case of a 1 inch effective break diameter results in a minimum level in the sump of 603'1-1/2" which is 3-1/2 inches above the licensing base limit for vortexing of 602'10".
8. Possible break locations were also considered for the RPV lower and upper heads. The maximum break size in the lower head is a rupture (severing) of an in-core instrument penetration tube which provides a break diameter of 0.61 inches with a discharge coefficient of less than 0.6. This is not sufficient to actuate the containment sprays. Thus, the sump water level is well above the 602'10" at the time of recirculation which is in excess of 36 hours. A review of possible upper head breaks concludes that two size ruptures should be considered, a failure of a CRDM and the severing of the 0.6 inch diameter reactor head vent. The former initiates the containment sprays and has a minimum level of 603.2' and the latter, like the instrument line break, does not result in the sprays being actuated.



Therefore, the Mode 1 LOCAs into the reactor cavity result in water levels during recirculation which are greater than the design basis limit for vortexing.

9. Several Mode 3 cases were examined, the largest was a 6 inch break and the smallest has an effective diameter of 2 inches. The 6 inch break into the lower compartment results in a water level above the licensing base limit for vortexing and a 2 inch break does not actuate the sprays. This break size spectrum was examined for breaks into the lower compartment as well as for the split flow conditions. While some of these resulted in minimum levels below 602'10", considering the reduced sump demand flows for these LOCAs which are smaller than the design basis DECL, there is a sufficient water level to prevent vortexing based on the D.C. Cook specific sump tests.
10. The assessment of main steam line breaks into the containment for two different size breaks result in a water level in the sump that is above the licensing base limit for vortexing. Furthermore, since there is no break in the RCS there is no long term need for the containment sprays and the injection to the RCS is only that needed to maintain the pressurizer level as the RCS cools down, i.e., approximately 20,000 gals. Hence, the level in these sequences is always above the licensing basis limit for vortexing.

## 9.0 REFERENCES

- American Nuclear Society (ANS), 1988, "Design Basis for Protection of Nuclear Power Plants Against Effects of Postulated Pipe Rupture," ANSI-ANS-58.2-1988.
- AEP, 1999, EOP ES-1.2 Rev. 5, Emergency Operating Procedure "Post LOCA Cooldown and Depressurization".
- Bloom, G. R. et al., 1983, "Hydrogen Mixing and Distribution in Containment Atmospheres," EPRI Report NP-2669.
- Electric Power Research Institute (EPRI), 1999, "MAAP4 User's Manual Version 4.0.4," EPRI Report prepared by Fauske & Associates, Inc.
- Epstein, M. et al., 1983, "One-Dimensional Modeling of Two-Phase Jet Expansion and Impingement," Thermal-Hydraulics of Nuclear Reactors, Volume II, 2nd Int'l Topical Meeting on Nuclear Reactor Thermal-Hydraulics, Santa Barbara, California, January 11-14, pp. 769-777.
- Fauske & Associates, Inc. (FAI), 1997, "MAAP4 Small Break LOCA Analyses for the D. C. Cook Plant," Fauske & Associates Report FAI/97-104.
- Fauske & Associates, Inc. (FAI), 1997, "Source Code MAAP 4.0.3.2 and Input Files".
- Fauske & Associates, Inc. (FAI), 1997, Archived MAAP4 minor revision 4.0.4.1, FAI QA Record 5.13.7.
- Fauske & Associates, Inc. (FAI), 1999, "Input and Output Files for D.C. Cook Minimum Sump Level Analyses Reported in FAI/99-77," Fauske & Associates Report FAI/99-84.
- Henry, R. E., 1970, "The Two-Phase Critical Discharge of Initially Saturated Subcooled Liquid," Nuclear Science and Engineering, Volume 41, pp. 336-342.
- Henry, R. E. and Fauske, H. K., 1971, "The Two-Phase Critical Flow of One-Component Mixtures and Nozzles, Orifices and Short Tubes," ASME Journal of Heat Transfer, pp. 179, May, 1971.
- Kastner, W. et al., 1978, "Experimental Studies on Forces of Critical Two-Phase Jets for Transverse and Longitudinal Cracks in Pipelines," NRC-478, U.S. Nuclear Regulatory Commission, Washington, D.C.

Kury, N., 1998, "Potential for Break Flow Into the Reactor Cavity During a LOCA," Letter from N. Kury to J. Olvera, AEP98-02, NSD-SAE-PSI-98-071, February 17.

Kutateladze, S. S., 1972, "Elements of the Hydrodynamics of Gas-Liquid System," Fluid Mechanics/Soviet Research, No. 1, Vol. 4, p. 29.

Ligotke, M. W. et al., 1991, "Ice-Condenser Aerosol Test," NUREG/CR-5768, PNL-7765.

McCurdy et al., 1968, "Supplementary Information to WCAP-7183, Design and Performance Evaluation of the Ice Condenser Reactor Containment System for the Donald C. Cook Nuclear Plant," WCAP-7183, Supplement 1, Westinghouse Proprietary Report.

MPR, 1999a, "Containment Sump Level Design Condition and Failure Effects Analysis for Potential Draindown Scenarios," MPR Associates, Inc. report submitted to AEP dated July 16, 1999.

MPR, 1999b, "Evaluation of Cook Recirculation Sump Level for Reduced Pump Flow Rates," MPR Associates, Inc. report submitted to AEP.

Newby, D., 1973, "Test Plans and Results for the Ice Condenser System," WCAP-8110, Supplement 1.

Nguyen, D. M. and Forrest, C. F., 1980, "Ontario Hydro Jet Test: Results of Impingement Plate Tests Performed With a 25.4 mm ID Nozzle," Westinghouse Canada, Inc., Atomic Power Division, Tech Memo CWTM-066-FD.

Padmanabhan, M., 1978, "Hydraulic Model Investigation of Vortexing and Swirl Within a Reactor Containment Recirculation Sump, Donald C. Cook Nuclear Power Station," Alden Research Laboratory Report 108-78/M178PF to American Electric Power Service Corporation.

Salvatori, R., 1974, "Final Report: Ice Condenser Full-Scale Section Test at the Waltz Mill Facility," Westinghouse Proprietary Class 2 Report, WCAP-8282.

Soffer, L. et al., 1995, "Accident Source Terms for the Light-Water Nuclear Power Plants," NUREG/1465.

Vennard, J. K., 1954, Elementary Fluid Mechanics, 3rd Edition, John Wiley and Sons, Inc., New York.

Weigand, G. G. et al., 1982, "A Parametric Study of Containment Emergency Sump Performance," NUREG/CR-2758, SAND82-0624, ARL-46-82.



Westinghouse Electric Corporation, 1988, "Input and Output Parameters for the Accident Analyses Performed for Reduced Temperature and Pressure Operation for the Donald C. Cook Nuclear Plant Unit 1," Westinghouse Electric Corporation Proprietary Report, WCAP-12078.

Westinghouse Electric Corporation, 1997, Letter NSD-SAE-ESI-97-555 from Donald E. Peck to Bob Henry dated October 1, 1997.

Westinghouse Electric Corporation, 1999a, "Unit 1 (AEP) SBLOCA Mass and Energy Releases," Westinghouse Calculation Note CN-LIS-99-128, Rev. 0 transmitted to AEP via letter AEP-99-243.

Westinghouse Electric Corporation, 1999b, "Potential for Break Flow into the Reactor Cavity During a LOCA," Westinghouse Letter AEP-99-244 dated August 4, 1999, from E. Dzenis to J. Hawley.

Westinghouse Electric Corporation, 1999c, Calculation CN-CRA-99-064 describing the flow split for a LOCA into the reactor cavity, transmitted to American Electric Power.

Westinghouse Electric Corporation, 1999d, "Preliminary Indications of Spray Usage for LOCA Doses," Westinghouse Letter AEP-99-245 dated August 4, 1999, from E. Dzenis to J. Hawley.

**APPENDIX A**  
**Design Information Transmittals (DITs)**

# AEP DESIGN INFORMATION TRANSMITTALS (DIT)

## DIT Form, Part 1

<input checked="" type="checkbox"/> SAFETY-RELATED <input type="checkbox"/> NON-SAFETY-RELATED		Originating Organization <input checked="" type="checkbox"/> AEP <input type="checkbox"/> Other (specify)	DIT No. DIT-B-00011-03
D.C. Cook Unit (Circle applicable): <input type="checkbox"/> 1 <input type="checkbox"/> 2 <input checked="" type="checkbox"/> BOTH			Page 1 of 2
System Designation: Containment			To Fauske & Associates, Inc.
Subject: Accident analysis input assumptions for sump water level analyses.			
James T. Hawley Preparer	ENSA Engineer Position	James T. Hawley Preparer's Signature	Date 7/29/99
Raymond F. Sartor Reviewer	ENSA Engineer Position	Raymond F. Sartor Reviewer's Signature	Date 7/29/99
Donald R. Hafer Approver	Asst. Dir.- Design Engrg. Position	Donald R. Hafer Approver's Signature	Date 7/29/99
Status of Information: <input checked="" type="checkbox"/> Approved for Use <input type="checkbox"/> Unverified <input type="checkbox"/> Engineering Judgement			
Method and Schedule of Verification for Unverified DITs: _____ CR # _____			
Holds Associated with Unverified DITs: None			
Description of Information: Drawings showing containment geometry in the vicinity of the reactor vessel nozzles.			
Purpose of Issuance (Including any Precautions or Limitations): For FAI to perform sump water level analyses. Within the intended applications there are no precautions or limitations.			
Source of Information: As identified on DIT Form Part 2.			
Distribution: NRM, A. M. Mock (for DIT file), J. C. Bass, V. VanderBurg, R. Sartor, J. T. Hawley			
File No: DC-N-6452.7			




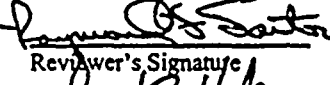
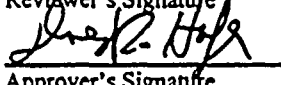
## AEP DESIGN INFORMATION TRANSMITTALS (DIT)

### DIT Form, Part 2

<p style="text-align: center;">AEP Design Information Transmittal</p>	<p>DIT No. <u>      </u> DIT-B-00011-03</p> <p>Page <u>  2  </u> of <u>  2  </u></p>
<p>There are 29 drawings provided by this DIT. The list of drawing numbers follows:</p> <p>AEP Drawings</p> <ul style="list-style-type: none"><li>2-3181-3</li><li>1-2-3182-10</li><li>1-2-3182A-10</li><li>1-2-3184-15</li><li>1-2-3192-15</li><li>1-2-3192A-13</li><li>1-2-3193-1</li><li>1-2-3193A-2</li><li>1-2-3193B-1</li><li>1-2-3193C-3</li><li>1-2-3193D-1</li><li>1-2-3193E-1</li><li>1-5321-3</li><li>2-5321-2</li><li>1-5330-9</li><li>2-5330-5</li><li>1-5343-20</li><li>2-5343-7</li><li>1-5344-13</li><li>2-5344-7</li><li>1-5358-2</li><li>2-5358-2</li><li>1-5484-11</li><li>2-5484-9</li></ul> <p>TRANSCO Drawings</p> <ul style="list-style-type: none"><li>3790D-1</li><li>3790D-3</li><li>3790D-5</li><li>3790L-3</li><li>3790L-5</li></ul>	

# AEP DESIGN INFORMATION TRANSMITTAL (DIT)

DIT Form, Part 1

<input checked="" type="checkbox"/> SAFETY-RELATED  <input type="checkbox"/> NON-SAFETY-RELATED	Originating Organization  <input checked="" type="checkbox"/> AEP <input type="checkbox"/> Other (specify)	DIT No DIT-B-00011-04  Page <u>1</u> of <u>13</u>  To Fauske & Associates, Inc.
D.C. Cook Unit: <input type="checkbox"/> 1 <input type="checkbox"/> 2 <input checked="" type="checkbox"/> BOTH  System Designation: <u>Containment</u>		
Subject: Accident analysis input assumptions for sump water level analyses.		
James T. Hawley Preparer	 Preparer's Signature	ENSA Engineer Position  9/15/99 Date
Raymond F. Sartor Reviewer	 Reviewer's Signature	ENSA Engineer Position  9/15/99 Date
Donald R. Hafer Approver	 Approver's Signature	Asst. Director, Design Eng. Position  9/15/99 Date
Status of Information: <input checked="" type="checkbox"/> Approved for Use <input type="checkbox"/> Unverified  Method and Schedule of Verification for Unverified DIT: .....  Holds Associated with Unverified DITs: ..... CR #.....		
Description of Information: Input values for all parameters previously provided by AEP to FAI for use in the containment sump inventory analyses. The values herein supersede all parameter values previously sent to FAI by Design Input Transmittals DIT-B-00011-00, DIT-B-00011-01, and DIT-B-00011-02. Parameter values were selected consistently with the biases identified in their descriptions. In this case, parameter biases are provided that minimize recirc sump water level by minimizing ice melting.		
Purpose of Issuance (Including any Precautions or Limitations): For FAI to perform sump water level analyses. Within the intended applications there are no precautions or limitations.  In addition, the values contained herein may be used as Design Inputs for other calculations, accident analyses, etc., as long as the biases identified for each parameter are appropriate for the intended use. There are no other precautions or limitations on this wider use of these values.		
Source of Information: As identified on DIT Form Part 2.		
Engineering Judgement Used? <input checked="" type="checkbox"/> Yes <input type="checkbox"/> No		
Distribution: Copy to Requestor: <u>J. C. Bass, R. Sartor, J. Hawley, V. VanderBurg, DCN 6452.7</u> Copy to DIT Administrator File Original to NRM (Transmitted by DIT Administrator)		

Note: This or other similar form may be used, provided the content is consistent with the currently approved 12 EHP 5040.DES.001, Attachment 6



# AEP DESIGN INFORMATION TRANSMITTAL (DIT)

## DIT-Form, Part 2

AEP Design Information Transmittal	DIT No. DIT-B-00011-04  Page <u>2</u> of <u>13</u>
<p>Attachments to this DIT are as follows:</p> <p>Attachment 1: Excerpts from DIT-B-00128-00, Subject: Design information for Proto-Power Corporation calculation, 99-064, Rev. 0 for D. C. Cook Unit-1 Containment Air Recirculation / Hydrogen Skinner System Proto-HVAC TM model development, Approved on 8/18/99. The excerpts provided herein are comprised of the following pages: Page 2 of 2 (1 page), Attachment B (3 pages) and Attachment C (1 page), for a total of 6 pages including cover sheet.</p> <p>Attachment 2: Excerpts from WCAP-14286, "American Electric Power Service Corporation Donald C. Cook Nuclear Plant Unit1 Steam Generator Tube Plugging Program Analysis Input Assumptions," Revision 7, 12/29/95. The excerpts consist of the following pages: Report Cover Sheet; Table 4.4-15 "D. C. Cook Maximum Safeguards 2 HHSI and 2 RHR All Lines Injecting," and Table 4.4-19 "D. C. Cook Maximum Safeguards 2 Charging/SI Pumps All Lines Injecting," for a total of 4 pages including cover sheet.</p> <p>Attachment 3: Two memos from Operations Department to ENSA. The first memo is 4 pages, dated 7/12/99 from Jim Abshire, EOP Project Manager to Gary Brassart, ENSA and Vance Vanderburg, ENSA, re: ES-1.3. The second memo is one page, dated 9/17/98 from Paul Cooper, EOP Coordinator to James Feinstein, subject: ECCS Switchover Times. There are 6 pages including the cover sheet in this attachment.</p> <p>Attachment 4: A tabulation of the cases to be analyzed for the Containment Sump Water Level Analyses, titled "Break Size/Location Matrix for the Resolution of the Containment Sump Issues Program"</p> <p>Attachment 5: A discussion of the application of the single failure criterion to the Containment Sump Water Level Analysis, titled "Single Failure Configuration For DC Cook Containment Sump Analyses"</p>	

Note: This or other similar form may be used, provided the content is consistent with the currently approved 12 EHP 5040.DES.001, Attachment 6



# AEP DESIGN INFORMATION TRANSMITTALS (DIT)

## DIT Form, Part 2

AEP Design Information Transmittal			DIT No. DIT-B-00011-04  Page 3 of 13	
Item #	Description	Value Provided	Source	Status
1	Definition of Scenarios Postulated for Recirculation Sump Inventory Behavior Analysis	See Attachment 4	Engineering Judgment. Information identifies combinations of LOCA / MSLB break size, location, and plant mode that address Chapter 14 cases or result in minimum sump water level at recirc switch-over. The latter cases consider guidance in "Containment Sump Level Design Conditions & Failure Effects Analysis for Potential Draindown Scenarios," Rev. 0, MPR Associates, Inc., 7/16/99.	Approved for Use
2	Single Failure Considerations for Determining Equipment Operation Following LOCA Initiation	See Attachment 5	Engineering Judgment. Information included providing guidance on application of single failure criterion.	Approved for Use
3a	Containment Volume vs. Height for Fill-up - Gross Lower Containment Volume up to elevation 598'- 9.375" (i.e., recirculation sump filled up to floor) (cu. Ft.)	1,005	DIT-B-00033-00	Approved for Use
3b	Containment Volume vs. Height for Fill-up - Gross Lower Containment Volume up to elevation 604'- 8.75" (i.e., recirculation sump plus active sump filled up to 604'- 8.75") (cu. Ft.)	22,657	DIT-B-00033-00	Approved for Use
3c	Containment Volume vs. Height for Fill-up - Gross Lower Containment Volume up to elevation up to 610' (i.e., recirculation sump plus active sump filled up to 610') (cu. Ft.)	40,740	DIT-B-00033-00	Approved for Use
3d	Containment Volume vs. Height for Fill-up - Volume Blocked by Equipment and Piping Inside Crane Wall up to elevation 602'- 10" (cu. Ft.)	507.6	DIT-B-00033-00	Approved for Use
3e	Containment Volume vs. Height for Fill-up - Volume Blocked by Equipment and Piping Inside Crane Wall up to elevation 610'-0" (cu. Ft.)	2651.1	DIT-B-00033-00	Approved for Use
3f	Containment Volume vs. Height for Fill-up - Gross Lower Compartment Volume up to elevation 610' 1st weir overflow (i.e., recirculation sump plus active sump filled to 610' plus reactor cavity filled to 610') (cu. Ft.)	56,488	DIT-B-00033-00	Approved for Use
3g	Containment Volume vs. Height for Fill-up - Gross Lower Containment Volume up to elevation 612' (i.e., recirculation sump plus active sump filled to 612' plus reactor cavity filled to 612') (cu. Ft.)	65,582	DIT-B-00033-00	Approved for Use
3h	Containment Volume vs. Height for Fill-up - Volume Blocked by Equipment and Piping Inside Crane Wall up to elevation 612'- 0" (cu. Ft.)	3079.8	DIT-B-00033-00	Approved for Use



# AEP DESIGN INFORMATION TRANSMITTALS (DIT)

## DIT Form, Part 2

AEP Design Information Transmittal			DIT No. DIT-B-00011-04	
			Page 4 of 13	
Item #	Description	Value Provided	Source	Status
3i	Containment Volume vs. Height for Fill-up - Gross Lower Containment Volume up to elevation 612' 2nd weir overflow (i.e., recirculation sump plus active sump filled to 612' plus reactor cavity filled to 612' plus inactive sump filled to 612') (cu. Ft.)	110,361	DIT-B-00033-00	Approved for Use
3j	Containment Volume vs. Height for Fill-up - Gross Lower Containment Volume up to 612'-5.5" (i.e., recirculation sump plus active sump filled to 612'-5.5" plus reactor cavity filled to 612'-5.5" plus inactive sump filled to 612'-5.5") (cu. Ft.)	114,127	DIT-B-00033-00	Approved for Use
4a	RWST - Delivered Volume at End of Recirculation (gal)	314,000	Design Requirement tracked by CR-99-21216.	Approved for Use
4b	RWST - Delivered Volume at Start of Recirculation (gal)	280,000	Design Requirement tracked by CR-99-21216.	Approved for Use
5	Minimum Containment Spray Flow rate - Upper Header (gpm)	1960	AEP Calculation TH-98-09, Revision 2	Approved for Use
6	Minimum Containment Spray Flow rate - Lower Header Inside Crane Wall (gpm)	706	AEP Calculation TH-98-09, Revision 2	Approved for Use
7	Minimum Containment Spray Flow rate - Lower Header Outside Crane Wall (gpm)	259	AEP Calculation TH-98-09, Revision 2	Approved for Use
8	Maximum Lower Compartment Containment Spray Flow rate with 1 Train - Upper Header (gpm)	2486	AEP Calculation TH-98-09, Revision 2	Approved for Use
9	Maximum Lower Compartment Containment Spray Flow rate with 1 Train - Lower Header Inside Crane Wall (gpm)	892	AEP Calculation TH-98-09, Revision 2	Approved for Use
10	Maximum Lower Compartment Containment Spray Flow rate with 1 Train - Lower Outside Crane Wall (gpm)	322	AEP Calculation TH-98-09, Revision 2	Approved for Use
11	Maximum Containment Spray Flow rate with 2 Trains - Upper Header (gpm)	5002	AEP Calculation TH-98-09, Revision 2	Approved for Use
12	Maximum Containment Spray Flow rate with 2 Trains - Lower Header Inside Crane Wall (gpm)	1760	AEP Calculation TH-98-09, Revision 2	Approved for Use
13	Maximum Containment Spray Flow rate with 2 Trains - Lower Header Outside Crane Wall (gpm)	638	AEP Calculation TH-98-09, Revision 2	Approved for Use
14	Containment Spray - Fall Height through Upper Compartment (Ft.)	80.167	DIT-B-00014-00	Approved for Use
15	Containment Spray - Fall Height through active sump (Ft.)	50.0	DIT-B-00014-00	Approved for Use
16a	Containment Spray Termination Criteria - Nominal Containment Pressure to Terminate CTS (psig)	1.5	Design Requirement tracked by CR-99-21182	Approved for Use
16b	Containment Spray Termination Criteria - Lower Compartment Indicated Pressure Total Loop Uncertainty (psig)	0.73	Design Requirement tracked by CR-99-21194	Approved for Use

# AEP DESIGN INFORMATION TRANSMITTALS (DIT)

## DIT Form, Part 2

AEP Design Information Transmittal				DIT No. DIT-B-00011-04
				Page 5 of 13
Item #	Description	Value Provided	Source	Status
17a	RHR Spray Initiation Criteria	50 min. after SI signal if less than 2 CTS pumps are operating	Design Requirement implemented by EOP Project acceptance of CRA-9 for CR-98-0913	Approved for Use
17b	RHR Spray Termination Criteria	Terminate when CTS pumps are secured	Design Requirement tracked by CR-99-22783.	Approved for Use
18	Minimum Containment Humidity (%)	15	Engineering Judgment supported by write-up included in this DIT	Approved for Use
19	Minimum Containment Ice Bed Mass (Mlbm)	2.2	Westinghouse Safety Evaluation SECL 99-076, Revision 2, "Containment Modifications Evaluation"	Approved for Use
20	Minimum Containment Ice Bed Temperature (°F)	10	Engineering Judgment supported by write-up included in this DIT	Approved for Use
21a	Openings in Crane Wall Between Active Sump and Piping annulus - Number of Openings	6	DIT-B-00016-00	Approved for Use
21b	Openings in Crane Wall Between Active Sump and Piping annulus - Height vs. Width	7.5" x 7.5" min.	DIT-B-00016-00	Approved for Use
21c	Openings in Crane Wall Between Active Sump and Piping annulus - Length	19.25" max.	DIT-B-00016-00	Approved for Use
21d	Openings in Crane Wall Between Active Sump and Piping annulus - Centerline elevation	599'-9.375" ± 3"	DIT-B-00016-00	Approved for Use
22	Containment Air Recirculation - Latest Fan Start Time (sec)	150 after High-I signal	Design Requirement tracked by CR-99-16842.	Approved for Use
23	Containment Air Recirculation - CEQ Fan Capacity Curve	Various (See Attachment 1)	DIT-B-00128-00	Approved for Use
24	Containment Spray - Normally Voided Piping Volume for Both Trains (gal.)	7789	DIT-B-00023-01	Approved for Use
25a	RHR Spray - 1E Normally Voided Piping Volume (cu. Ft.)	217.11	DIT-B-00005-01	Approved for Use
25b	RHR Spray - 1W Normally Voided Piping Volume (cu. Ft.)	227.46	DIT-B-00005-01	Approved for Use
25c	RHR Spray - 2E Normally Voided Piping Volume (cu. Ft.)	223.14	DIT-B-00005-01	Approved for Use
25d	RHR Spray - 2W Normally Voided Piping Volume (cu. Ft.)	231.26	DIT-B-00005-01	Approved for Use
26	Maximum ECCS Pump Two-Train Flow Rate as a function of RCS pressure (gpm)	Various (See Attachment 2)	WCAP-14286, Donald C. Cook Nuclear Plant Unit 1, Steam Generator Tube Plugging Program Engineering report, Volume 2, Tables 4.4-15 and 4.4-19	Approved for Use
27a	Maximum Containment Spray Heat Exchanger UA (MBTU/hr-°F)	2.5	AEP Calculation MD-12-CTS-008-N, Rev. 0; [Engineering Judgment for case selected is included in this DIT.]	Approved for Use
27b	Containment Spray Heat Exchanger Configuration for UA Calculation	U-tube, Counterflow	Yuba Heat Transfer Division, Exchanger Specification Sheet, Donald C. Cook Containment Spray Cooler, 9-18-70	Approved for Use
27c	ESW Flow to Containment Spray Heat Exchanger for Maximum UA Case (gpm)	3300	Engineering Judgment supported by write-up included in this DIT. Value is consistent with AEP calc. MD-12-CTS-008-N, Rev. 0.	Approved for Use



# AEP DESIGN INFORMATION TRANSMITTALS (DIT)

## DIT Form, Part 2

AEP Design Information Transmittal				DIT No. DIT-B-00011-04
				Page 6 of 13
Item #	Description	Value Provided	Source	Status
27d	Minimum ESW Cooling Water Temperature to Containment Spray Heat Exchanger (°F)	33	Engineering Judgment supported by write-up included in this DIT	Approved for Use
28a	Maximum RHR Heat Exchanger UA (MBTU/hr-°F)	3.1	AEP Calculation MD-12-CTS-008-N, Rev. 0; [Engineering Judgment for case selected is included in this DIT.]	Approved for Use
28b	RHR Spray Heat Exchanger Configuration for UA Calculation	U-tube, Counterflow	Engineers & Fabricators, Inc., Exchanger Specification Sheet, Westinghouse Electric Corp., Atomic Power division, Residual Heat Exchanger, 6-23-69	Approved for Use
28c	CCW Flow to RHR Heat Exchanger for Maximum UA Case (gpm)	5500	Engineering Judgment supported by write-up included in this DIT. Value is consistent with AEP calc. MD-12-CTS-008-N, Rev. 0.	Approved for Use
28d	Minimum CCW Cooling Water Temperature to RHR Heat Exchanger (°F)	60	OHP 4021.016.003, Unit 1 - Rev. 14; Unit 2 - Rev. 9	Approved for Use
29a	Openings in Biological Shield Wall Between Active Sump and Reactor Cavity - Orientation	Horizontal	AEP Drawings: 1-5343-13; 2-5344-7	Approved for Use
29b	Openings in Biological Shield Wall Between Active Sump and Reactor Cavity - Number of Openings at Elevation 599'-9 3/8"	8	AEP Drawings: 1-5343-13; 2-5344-7	Approved for Use
29c	Openings in Biological Shield Wall Between Active Sump and Reactor Cavity - Number of Openings at Elevation 605'-9 3/8"	8	AEP Drawings: 1-5343-13; 2-5344-7	Approved for Use
29d	Openings in Biological Shield Wall Between Active Sump and Reactor Cavity - Largest Outer Diameter of Penetration Liner (in.) / Liner Thickness (in.)	2.50 / 0.187	AEP Drawings: 1-5343-13; 2-5344-7	Approved for Use
29e	Openings in Biological Shield Wall Between Active Sump and Reactor Cavity - Largest Shaft Outer Diameter within Penetration (in.)	2.00	Westinghouse Drawing 618F235	Approved for Use
29f	Openings in Biological Shield Wall Between Active Sump and Reactor Cavity - Shortest Flow Length Through Smallest Annular Area (in.)	13.86	AEP Drawings: 1-5343-13; 2-5344-7; Westinghouse Drawings 618F235, 113E421	Approved for Use
30a	EOP Valve Manipulation Sequence Initiate and Complete Recirculation Switchover	See Attachment 3	7/12/99 Memo to Gary Brassart and Vance VanderBurg from Jim Abshire, EOP Prog. Mgr, re: ES-1.3; 6/17/98 Memo to J. G. Feinstein from P. Cooper and G. Tollas	Approved for Use
30b	Duration of RHR/CTS Flow Interruption During Recirculation Switchover (min)	5 (See Attachment 3)	7/12/99 Memo to Gary Brassart and Vance VanderBurg from Jim Abshire, EOP Program Manager, re: ES-1.3	Approved for Use
31	ECCS Leakage following recirculation switchover (gpm)	1	Design Requirement tracked by CR-99-21213	Approved for Use
32a	Initial Reactor Coolant System Pressure (psia)	2250	Engineering Judgment. This value is consistent with the previous analysis of record (i.e., WCAP-14286).	Approved for Use
32b	Initial Reactor Coolant System Temperature (°F)	556	Engineering Judgment. This value is consistent with the range of values in the previous analysis of record (i.e., WCAP-14286)	Approved for Use

# AEP DESIGN INFORMATION TRANSMITTALS (DIT)

## DIT Form, Part 2

AEP Design Information Transmittal			DIT No. DIT-B-00011-04  Page 7 of 13	
Item #	Description	Value Provided	Source	Status
32c	Initial Reactor Power (MWt) - Mode 1 Hot Full Power (HFP) / Mode 3	3250 / 0	Engineering Judgment. This value is consistent with the previous analysis of record (i.e., WCAP-14286) and a lower power level is conservative.	Approved for Use
33a	Minimum Accumulator Water Temperature (°F)	60	Engineering Judgment supported by write-up included in this DIT	Approved for Use
33b	Minimum Accumulator Pressure (psia)	600	Engineering Judgment supported by write-up included in this DIT	Approved for Use
33c	Minimum Water Mass per Accumulator (lbm)	57,563	Engineering Judgment supported by write-up included in this DIT	Approved for Use
34	Maximum Divider Barrier Bypass Area (sq. ft.)	5	Historical value established in original FSAR. LERs 98-004-01 (Unit 2) and 98-037-01 (Unit 1) reported that this design basis value was exceeded and committed to restoring and maintaining this value for divider barrier leakage area. Procedure 12 EHP 6040.PER.154, "Containment Divider Barrier Survey" was implemented to "... determine the operability of the containment divider barrier by demonstrating that the actual bypass area is less than the design bypass area of 5 ft <sup>2</sup> ."	Approved for Use

# AEP DESIGN INFORMATION TRANSMITTALS (DIT)

## DIT Form, Part 2

AEP Design Information Transmittal	DIT No. DIT-B-00011-04  Page 8 of 13
---------------------------------------	---

### Minimum Containment Humidity Outside of Ice Condenser for Minimum Containment Temperature Conditions

Old Value: 15% (Reference 1)

New value: 15%

References: 1. Engineering Judgment based on a consensus of attendees at a Steam Generator Tube Plugging program meeting on 4/27/94 to discuss design inputs.

Reason: Since containment relative humidity is not a monitored parameter, a typical value is not readily available. This lack of data precludes identifying a physically-based estimate for the lower-bound containment relative humidity. Although a relative humidity value of zero is an obvious analytical lower bound for relative humidity, this value is not a reasonable lower bound given that:

- The RCS and containment are normally open during refueling outages, which leads to a high relative humidity in containment at these times; and
- There is always some water present in the recirculation sump during normal operation due to the requirement to maintain the recirculation suction piping water-filled.

Following RCS and containment closure, however, it is possible that containment relative humidity will decrease due to operation of the containment purge system, condensation of steam vapor if containment temperature decreases, etc. However, it is unlikely that the containment relative humidity outside of the ice condenser could actually decrease to zero. Based on recent conversations with a system engineer and a licensed operator, there is always a shallow pool of water in the recirculation sump to maintain the recirculation suction piping water-filled. Consequently, the low value of 15% relative humidity is considered a reasonable estimate for a lower-bound on containment relative humidity.

### Minimum Containment Ice Bed Temperature

Old Value: 10°F (Reference 1)

New value: 10°F

References: 1. 10/7/98 Letter from V. VanderBurg documenting Engineering Judgment based on a consensus of attendees at a Steam Generator Tube Plugging program meeting on 4/27/94 to discuss design inputs.

2. NRM Archive Boxes #8037 and 9076, Chart Recorder Records for Unit 1 (Dates: 3/30/96 - 5/23/96 and 7/16/96 - 9/2/96 contained in Box # 9076) and Unit 2 (Dates: 1/28/96 - 2/12/96 and 3/27/96 - 4/10/96 contained in Box # 8037; 5/7/96 - 6/30/96 contained in Box # 9076)

Reason: Although the ice bed temperature is a monitored parameter and there is a High/Low temperature alarm, there are no operator actions required by the occurrence of a low temperature alarm. Informal discussions suggest that the low-end temperature is maintained above 10°F. This lower-bound temperature is based on



# AEP DESIGN INFORMATION TRANSMITTALS (DIT)

## DIT Form, Part 2

AEP Design Information Transmittal		DIT No. DIT-B-00011-04  Page 9 of 13															
<p>operational considerations related to the glycol cooling system, specifically that the cooling system operation becomes more difficult as glycol properties change with decreasing temperature.</p> <p>To establish whether the 10°F temperature is in fact a reasonable lower-bound ice bed temperature, chart recorder data were reviewed as documented in Reference 2. The data are summarized as follows:</p> <table border="0"> <tr> <td>Unit 1</td> <td>3/30/96 to 5/23/96</td> <td>All ice bed temperature channel readings fell between 8°F and 20°F. Values below 10°F occurred for only two channels and persisted only during three days. During that time frame, the rest of the channels were above 10°F.</td> </tr> <tr> <td>Unit 1</td> <td>7/16/96 to 9/2/96</td> <td>All ice bed temperature channel readings fell between 12°F and 20°F.</td> </tr> <tr> <td>Unit 2</td> <td>1/28/96 to 2/12/96</td> <td>All ice bed temperature channel readings fell between 12°F and 16°F.</td> </tr> <tr> <td>Unit 2</td> <td>3/27/96 to 4/10/96</td> <td>All ice bed temperature channel readings fell between 13°F and 32°F.</td> </tr> <tr> <td>Unit 2</td> <td>5/7/96 to 6/30/96</td> <td>All ice bed temperature channel readings fell between 10°F and 20°F.</td> </tr> </table> <p>While the above data are not comprehensive, they do show that over relatively long historical periods of time the ice bed temperature has been maintained above 10°F. On this basis, a minimum ice bed temperature of 10°F will be adopted for analysis purposes.</p>			Unit 1	3/30/96 to 5/23/96	All ice bed temperature channel readings fell between 8°F and 20°F. Values below 10°F occurred for only two channels and persisted only during three days. During that time frame, the rest of the channels were above 10°F.	Unit 1	7/16/96 to 9/2/96	All ice bed temperature channel readings fell between 12°F and 20°F.	Unit 2	1/28/96 to 2/12/96	All ice bed temperature channel readings fell between 12°F and 16°F.	Unit 2	3/27/96 to 4/10/96	All ice bed temperature channel readings fell between 13°F and 32°F.	Unit 2	5/7/96 to 6/30/96	All ice bed temperature channel readings fell between 10°F and 20°F.
Unit 1	3/30/96 to 5/23/96	All ice bed temperature channel readings fell between 8°F and 20°F. Values below 10°F occurred for only two channels and persisted only during three days. During that time frame, the rest of the channels were above 10°F.															
Unit 1	7/16/96 to 9/2/96	All ice bed temperature channel readings fell between 12°F and 20°F.															
Unit 2	1/28/96 to 2/12/96	All ice bed temperature channel readings fell between 12°F and 16°F.															
Unit 2	3/27/96 to 4/10/96	All ice bed temperature channel readings fell between 13°F and 32°F.															
Unit 2	5/7/96 to 6/30/96	All ice bed temperature channel readings fell between 10°F and 20°F.															
<p><u>ESW Flow to Containment Spray Heat Exchanger for Maximum UA Case</u></p> <p>Old Value: None (New parameter)</p> <p>New value: 3300 gpm</p> <p>References:</p> <ol style="list-style-type: none"> <li>1 / 2 EHP 4030.STP.241 "ESW Flow Balance"</li> <li>Yuba Industries, Yuba Heat Transfer Division, Exchanger Specification Sheet for American Electric Power Containment Spray Cooler</li> <li>Excerpts from surveillances documented by completing 1 / 2 EHP 4030.STP.241; surveillances performed on 9/21/95 (U1), 4/26/96 (U2), and 4/2/97 (U1)</li> </ol> <p>Reason:</p> <p>Reference 1 contains acceptance criteria for minimum ESW flow to each Containment Spray (CTS) heat exchanger of <math>\geq 2472</math> gpm (2476 gpm for the pre-1997 versions of Reference 1). However, the procedure does not contain acceptance criteria for maximum allowable ESW flow to the CTS heat exchangers. Since UA values typically increase with increasing shell-side flow, determining an appropriate, upper-bound shell-side flow is necessary.</p> <p>The design shell-side flow identified on Reference 2 for a CTS heat exchanger is 3300 gpm. Since this design shell-side flow value is significantly larger than the acceptable value for ESW flow to the CTS heat exchanger contained in Reference 1, it was expected to represent a conservative upper-bound for ESW flow through the CTS heat exchanger. Consequently, information was obtained as identified in Reference 3 to determine whether the design shell-side flow could in fact be established</p>																	

# AEP DESIGN INFORMATION TRANSMITTALS (DIT)

## DIT Form, Part 2

AEP Design Information Transmittal		DIT No. DIT-B-00011-04  Page 10 of 13																		
<p>as a conservative flow for use in determining the maximum CTS heat exchanger UA. The Reference 3 values for measured ESW flows to the CTS heat exchangers are as follows.</p> <table> <tr> <td>East CTS Heat Exchanger:</td> <td>2940.7 gpm (as-found)</td> <td>2768.8 gpm (as-left)</td> </tr> <tr> <td></td> <td>2691.5 gpm (as-found)</td> <td>2705.8 gpm (as-left)</td> </tr> <tr> <td></td> <td>2773.9 gpm (as-found)</td> <td>as-left not reported</td> </tr> <tr> <td>West CTS Heat Exchanger:</td> <td>2640.5 gpm (as-found)</td> <td>2552.7 gpm (as-left)</td> </tr> <tr> <td></td> <td>2487.2 gpm (as-found)</td> <td>2571.4 gpm (as-left)</td> </tr> <tr> <td></td> <td>2536.7 gpm (as-found)</td> <td>as-left not reported</td> </tr> </table> <p>The above data substantiate that the heat exchanger specification data sheet design value for shell-side flow of 3300 gpm provides a conservative upper-bound value for this parameter.</p>			East CTS Heat Exchanger:	2940.7 gpm (as-found)	2768.8 gpm (as-left)		2691.5 gpm (as-found)	2705.8 gpm (as-left)		2773.9 gpm (as-found)	as-left not reported	West CTS Heat Exchanger:	2640.5 gpm (as-found)	2552.7 gpm (as-left)		2487.2 gpm (as-found)	2571.4 gpm (as-left)		2536.7 gpm (as-found)	as-left not reported
East CTS Heat Exchanger:	2940.7 gpm (as-found)	2768.8 gpm (as-left)																		
	2691.5 gpm (as-found)	2705.8 gpm (as-left)																		
	2773.9 gpm (as-found)	as-left not reported																		
West CTS Heat Exchanger:	2640.5 gpm (as-found)	2552.7 gpm (as-left)																		
	2487.2 gpm (as-found)	2571.4 gpm (as-left)																		
	2536.7 gpm (as-found)	as-left not reported																		
<u>Minimum ESW Cooling Water Temperature to Containment Spray Heat Exchanger</u>																				
Old Value:	None (New parameter)																			
New value:	33°F																			
References:	None																			
Reason:	<p>The coldest possible temperature for lake water that can brought into the plant via the ESW system is 32°F. This water would absorb heat from the ESW pumps and the piping walls as it passes through the plant on its way to the containment spray heat exchangers. As a result, some pre-heating of the ESW cooling water is expected to occur prior to its entry into the shell-side of the containment spray heat exchanger. Since such a low ESW minimum water temperature yields very large temperature differences across the containment spray heat exchangers, a precise quantification of ESW cooling water pre-heating was not made. Instead, the ESW pre-heating was judged to be at least 1°F, and this value was added to the theoretical minimum water temperature that could exist in the ESW system.</p>																			
<u>CCW Flow to Residual Heat Removal Heat Exchanger for Maximum UA Case</u>																				
Old Value:	None (New parameter)																			
New value:	5500 gpm																			
References:	<ol style="list-style-type: none"> <li>1 / 2 EHP 4030.STP.248 "ESW Flow Balance"</li> <li>Engineers &amp; Fabricators Inc., Exchanger Specification Sheet for Westinghouse Electric Corp., Atomic Power Div., Residual Heat Exchanger</li> <li>Excerpts from surveillance documented by completing 12 EHP 4030.STP.248; surveillance performed on 4/4/97 (U1)</li> </ol>																			

# AEP DESIGN INFORMATION TRANSMITTALS (DIT)

## DIT Form, Part 2

AEP Design Information Transmittal	DIT No. DIT-B-00011-04  Page 11 of 13								
<p><b>Reason:</b> Reference 1 contains acceptance criteria for minimum CCW flow to each Residual Heat Removal (RHR) heat exchanger of <math>\geq 5000</math> gpm for recirculation alignment. However, the procedure does not contain acceptance criteria for maximum allowable CCW flow to the RHR heat exchangers. Since UA values typically increase with increasing shell-side flow, determining an appropriate, upper-bound shell-side flow is necessary.</p> <p>The design shell-side flow identified on Reference 2 for an RHR heat exchanger is 4950 gpm. Since this design shell-side flow value is less than the minimum acceptable value for CCW flow to the RHR heat exchanger contained in Reference 1, it cannot be used to provide any insight into the magnitude of a reasonable upper-bound for CCW flow through the RHR heat exchanger. Consequently, information was obtained as identified in Reference 3 to determine a conservative CCW flow for use in determining the maximum RHR CTS heat exchanger UA. The Reference 3 values for measured CCW flows to the RHR heat exchangers are as follows.</p> <table style="margin-left: auto; margin-right: auto;"> <tr> <td style="padding-right: 20px;">East RHR Heat Exchanger:</td> <td>5353.4 gpm (as-found)</td> </tr> <tr> <td></td> <td>5310.8 gpm (as-found)</td> </tr> <tr> <td style="padding-top: 10px;">West RHR Heat Exchanger:</td> <td>5467.1 gpm (as-found)</td> </tr> <tr> <td></td> <td>5279.9 gpm (as-found)</td> </tr> </table> <p>The above data suggest that a value for RHR shell-side flow of 5500 gpm provides a conservative upper-bound for this parameter.</p>		East RHR Heat Exchanger:	5353.4 gpm (as-found)		5310.8 gpm (as-found)	West RHR Heat Exchanger:	5467.1 gpm (as-found)		5279.9 gpm (as-found)
East RHR Heat Exchanger:	5353.4 gpm (as-found)								
	5310.8 gpm (as-found)								
West RHR Heat Exchanger:	5467.1 gpm (as-found)								
	5279.9 gpm (as-found)								
<p><b>Parameter:</b> <u>Minimum Accumulator Water Temperature</u></p> <p><b>Value:</b> 60°F</p> <p><b>Reference:</b></p> <ol style="list-style-type: none"> <li>1. D. C. Cook Nuclear Plant Unit 1 Technical Specifications, through Amendment 225</li> <li>2. D. C. Cook Nuclear Plant Unit 2 Technical Specifications, through Amendment 210</li> </ol> <p><b>Comments:</b> This is the minimum accumulator temperature based on the minimum lower containment air temperature per Technical Specification 3.6.1.5 (Ref. 1 and 2). The minimum value is used to minimize the break flow energy and ice melt addition to the containment sump.</p>									
<p><b>Parameter:</b> <u>Minimum accumulator pressure</u></p> <p><b>Value:</b> 600 psia</p> <p><b>Reference:</b> Technical Specification 3.5.1.</p> <p><b>Comments:</b> This is the minimum value per Technical Specification 3.5.1. The minimum pressure provides the least force to injecting water into the RCS. This minimizes the accumulator water injected into the RCS, which can spill to the containment sump.</p>									



# AEP DESIGN INFORMATION TRANSMITTALS (DIT)

## DIT Form, Part 2

AEP Design Information Transmittal	DIT No. DIT-B-00011-04  Page 12 of 13
---------------------------------------	--

Parameter: Minimum water mass per accumulator

Value: 57,563 lbm

Reference:

1. D. C. Cook Nuclear Plant Unit 1 Technical Specifications, through Amendment 225
2. D. C. Cook Nuclear Plant Unit 2 Technical Specifications, through Amendment 210
3. ASME Steam Tables, Sixth Edition, ASME Press, reprinted 1997

Comments: This value is based on the minimum water volume of 921 cu. ft. per accumulator in Technical Specification 3.5.1 (Ref. 1 and 2). The minimum volume minimizes the accumulator water injected into the RCS, which can spill to the containment sump. The specific volume for the temperature and pressure given above is 0.01600 ft<sup>3</sup>/lbm (Ref. 3). Then,

$$m_{\text{accum}} = \frac{921 \text{ ft}^3}{0.01600 \text{ ft}^3 / \text{lbm}} = 57,563 \text{ lbm}$$

## Basis for Maximum CTS Heat Exchanger UA Case Selected

# of Tubes Plugged: 16

Tube-side Fouling Factor: Design

Shell-side Fouling Factor: Design

Sump water temperature (°F) 160

Reference:

1. AEP Calculation MD-12-CTS-008-N, "CTS & RHR Heat Exchanger UA Determination for Containment Sump Analysis," Rev. 0.
2. FAI/99-77, "Containment Sump Level Evaluations for the D. C. Cook Plant," Rev. 0, Figure 5-20d.

Per Reference 1, the number of plugged tubes is chosen as the mean of the number of plugged tubes in the existing Unit 1 East CTS heat exchanger (33 tubes) and a new Unit 1 West CTS heat exchanger (0 tubes). Based on information provided in Reference 1, the average number of plugged tubes in the Unit 2 CTS heat exchangers is 25 (East 23; West 27). For this analysis, the conservative direction is that which minimizes ice melt. Thus, a larger UA value is conservative. Since both trains of CTS are assumed to operate for these analyses, use of a value slightly less than the average number of tubes plugged is conservative.

Per Reference 1, the use of design fouling factors is reasonable for these heat exchangers. For the recirc sump inventory analysis, more heat transfer through the CTS heat exchangers will minimize ice melt. More heat transfer is

# AEP DESIGN INFORMATION TRANSMITTALS (DIT)

## DIT Form, Part 2

AEP Design Information Transmittal	DIT No. DIT-B-00011-04  Page 13 of 13
<p>obtained from the CTS heat exchangers if a higher UA is used. A higher UA is determined if smaller fouling factors are assumed. For this case, according to Reference 1, the design fouling factors represent a realistic value for tube fouling. Specifically, the design fouling factors specified on the heat exchanger spec sheet are consistent with the relatively clean raw water on the shell side (i.e., Lake Michigan) and the relatively clean tube-side condition observed during recent inspections.</p> <p>Per Reference 2, the recirculation sump water temperature may be seen to reach about 100 °F prior to the switchover to recirculation. Since Reference 1 shows that CTS heat exchanger UA increases with increasing sump temperature, a conservatively high value of 160 °F was chosen to represent the recirculation sump temperature for the sump water level analysis.</p>	
<p><u>Basis for Maximum RHR Heat Exchanger UA Case Selected</u></p> <p># of Tubes Plugged: 0</p> <p>Tube-side Fouling Factor: 0 (i.e., clean)</p> <p>Shell-side Fouling Factor: 0 (i.e., clean)</p> <p>Sump water temperature (°F) 160</p> <p>Reference: 1. AEP Calculation MD-12-CTS-008-N, "CTS &amp; RHR Heat Exchanger UA Determination for Containment Sump Analysis," Rev. 0.</p> <p>2. FAI/99-77, "Containment Sump Level Evaluations for the D. C. Cook Plant," Rev. 0, Figure 5-20d.</p> <p>Per Reference 1, there are no plugged tubes in the existing RHR heat exchangers at Cook Plant. For the recirc sump inventory analysis, more heat transfer through the RHR heat exchangers will minimize ice melt, which is the appropriate conservative direction. More heat transfer is obtained from the RHR heat exchangers if a higher UA is used. A higher UA is determined if fewer plugged tubes are assumed. As a result, the realistic value of plugged tubes is appropriate for this analysis.</p> <p>Per Reference 1, the use of clean conditions is reasonable for these heat exchangers due to the high purity water that flows through both the shell and tubes. For the recirc sump inventory analysis, more heat transfer through the RHR heat exchangers will minimize ice melt. More heat transfer is obtained from the RHR heat exchangers if a higher UA is used. A higher UA is determined if smaller fouling factors are assumed. As a result, the fouling factor values chosen are appropriately conservative for this analysis.</p> <p>Per Reference 2, the recirculation sump water temperature may be seen to reach about 100 °F prior to the switchover to recirculation. Since Reference 1 shows that RHR heat exchanger UA increases with increasing sump temperature, a conservatively high value of 160 °F was chosen to represent the recirculation sump temperature for the sump water level analysis.</p>	

**Attachment 1 to DIT-B-00011-04:**

Excerpts from DIT-B-00128-00, Subject: Design information for Proto-Power Corporation calculation, 99-064, Rev. 0 for D. C. Cook Unit-1 Containment Air Recirculation / Hydrogen Skimmer System Proto-HVAC TM model development, Approved on 8/18/99. The excerpts provided herein are comprised of the following pages: Page 2 of 2 (1 page), Attachment B (3 pages) and Attachment C (1 page), for a total of 6 pages including cover sheet.

**AEP DESIGN INFORMATION TRANSMITTALS (DIT)**

**DIT Form, Part 2**

<p>AEP Design Information Transmittal</p>	<p>DIT No. <u>B-00128-00</u> Page <u>2</u> of <u>2</u></p>
<p><b>Description of Change (continuation):</b></p> <ol style="list-style-type: none"><li>1. Latest revision no. for flow diagram and isometric drawings are as noted in the Attachment A (Ref. 2).</li><li>2. Latest revision for American Warming and Ventilating, Inc. drawing no. DAA-D-9823 is "G" (Ref. 3).</li><li>3. Flow vs. Pressure curve for fan 1-HV-CEQ-1 and 1-HV-CEQ-2 is provided in Attachment "B". This curve is with inlet box and inlet vanes closed at 20°. Also, noted in this Attachment is the fan outlet area which is 13.91 ft<sup>2</sup> (Ref. 1).</li><li>4. Flow vs. Pressure curve for fan 1-HV-CEQ-1 and 1-HV-CEQ-2 is provided in Attachment "C". These curves are based on Westinghouse fan model 3049 SWSI 49" diameter at various inlet positions. Fan model no. is the same as the model no. used for the fan performance test curve with inlet box and vane closed at 20° as noted in item 3. Also, based on flow comparison at vanes closed at 20°, the curves compare fairly well. Therefore, based on engineering judgement, the flow/pressure fan curve at different vane position is correct.</li><li>5. Model no. for the butterfly valve used is Fischer Control butterfly valve series 9100 (Ref. 4). C<sub>v</sub> values used should be consistent with this. Proto-Power Inc. to obtain these values.</li><li>6. See attachment "D" for the physical data for the fans (1-HV-CEQ-1 &amp; 1-HV-CEQ-2) intake grills. This is based on walkdown.</li></ol> <p><b>Attachments:</b></p> <p>A - Latest revision no. for flow diagram and isometric drawings, Pages A1 thru A10 B - Flow vs. Pressure curve for fans 1-HV-CEQ-1 and 1-HV-CEQ-2 with inlet box and inlet vanes at 20°, Pages B1 thru B3 C - Flow vs. Pressure curve for fans 1-HV-CEQ-1 and 1-HV-CEQ-2 without inlet box, Page C1 thru C1 D - Fans (1-HV-CEQ-1 and 1-HV-CEQ-2) Intake grills physical data, D1 thru D2</p> <p><b>Source of Information (continuation):</b></p> <ol style="list-style-type: none"><li>1. Westinghouse submittal dated July 31, 1974 for fan performance test with inlet box and vanes control at 20° for fan model 3049 SWSI silent vane.</li><li>2. NDIS controlled document Query search results, dated August 11, 1999.</li><li>3. American Warming And Ventilating Inc. Vendor Technical Manual, VTM-AMVI-0001, Rev. 1</li><li>4. Fischer Controls Vendor Technical Manual, VTM-FISC-0001, Rev. 3</li></ol>	



3.24(30) A-19

ATTACHMENT "B"

Westinghouse Electric Corporation

Power Systems

Mr. R. S. Hunter  
Vice President  
AMERICAN ELECTRIC POWER SERVICE CORP.  
2 Broadway  
New York, New York 10004

AEW-5860

LETTER NO.

DIT No. B-20128-00

Page 21 of 83

PAR 3, Series D-1001

Doc 1:0

Doc 1:0

DT-B-00011-04  
Attach. 1, p. 3 of 6

Date July 31, 1974

S.O. No. AEP-AMP-313

Engr. Ltr. TO-JRP-415

Reference

W NES DOCUMENT TRANSMITTAL - AMERICAN ELECTRIC POWER CORPORATION  
DONALD C. COOK NUCLEAR PLANT

The following documents are transmitted herewith for your use. The status of each document is one of the following as noted below:

Preliminary (PRE)

Approved For Layout (AFL)

Certified For Construction (CFC)

Certified For Construction With Comments (CC)  
As Manufactured (AM)

SPIN No.	Document No.	Sht.	Rev.	Status	Unit	Document Title
-	-	-	-	CFC	AEP/AMP	Laboratory Performance Test for Westinghouse Nuclear Energy Systems and American Electric Power Co.

REMARKS:

R. S. Hunter SL  
R. F. Haring IL  
S. H. Horowitz IL

SA

WESTINGHOUSE NUCLEAR ENERGY SYSTEMS

J. W. Irons, Lead Engineer  
Service Equipment

J. J. Budkis, Project Manager  
American Electric Power Project

U 001



~~Aerodynamic performance test was~~ conducted at the Sturtevant Division laboratory, Hyde Park, Massachusetts on August 16, 1972 to confirm the performance of a 30/9 SMO Silentvane fan with inlet box and vane control furnished on order No. PKZ-2050.

DIT-B-00011-04  
Attach. 1; page 4 of 6

The standard APCA air performance and sound tests were performed per APCA Standards No. 210-67 and 300-67. Static and velocity pressures were measured in the discharge duct by means of a twenty point pitot tube traverse. Readings were taken on two precision inclined manometers. Prior to the test these manometers were calibrated with a precision Dwyer Beck Gage reading in thousandths of an inch of water. A laboratory dynamometer was used to drive the fan and measure the horsepower input.

Sound measurements were taken with a Bruel and Kjaer precision sound level meter and octave filter set. Prior to the test the meter was calibrated using the Bruel and Kjaer calibrating pistonphone.

The air performance test results are converted to 850 RPM and .075 PCF air density. The report contains performance curves, air and sound test results, test duct details, manometer calibration sheet and photographs.

J. R. Dine, Engineer

0 002

10x10 101 INCH 4U 1323  
 20 18 INCH 101  
 101 INCH 101

1-12A22

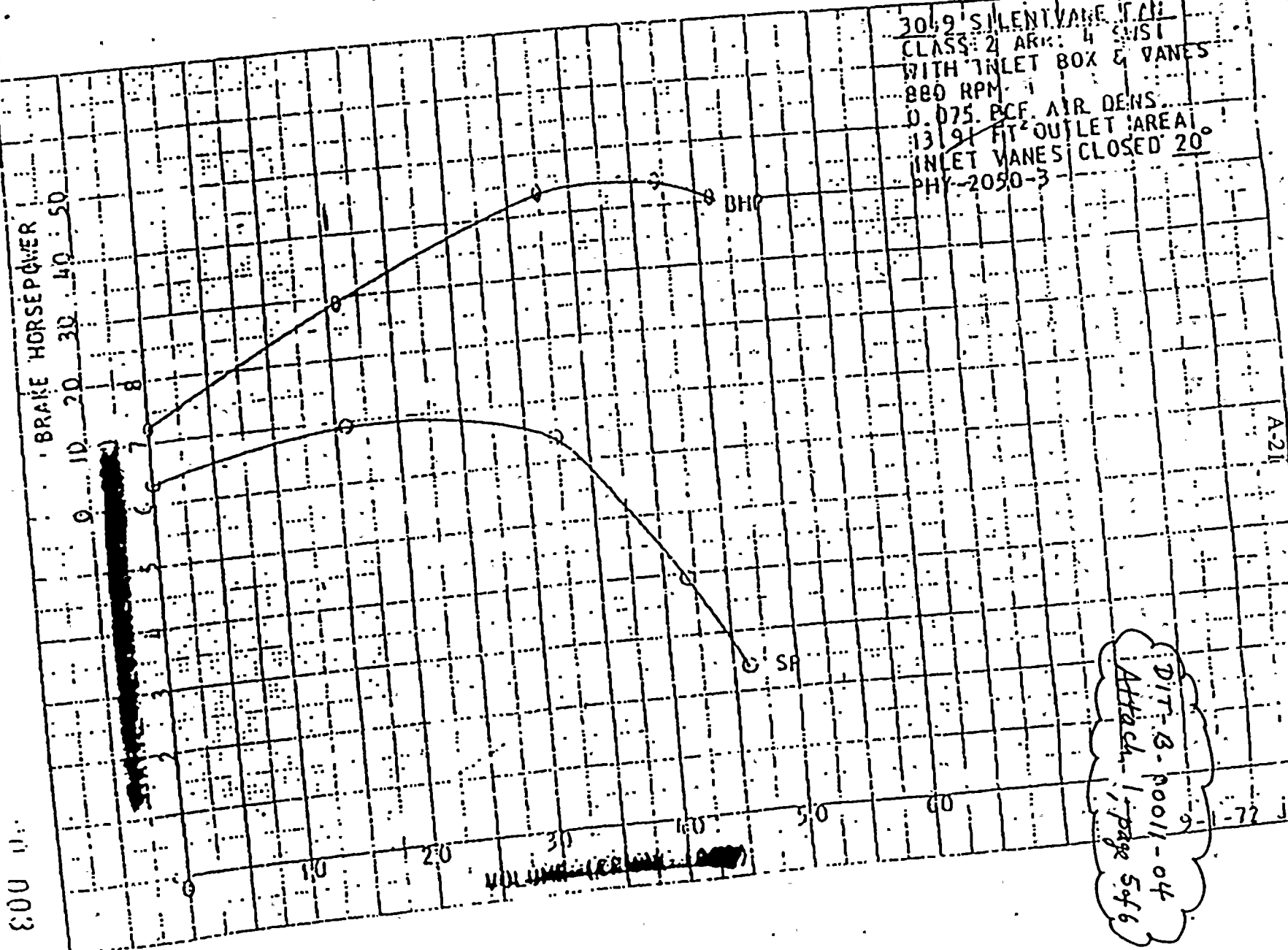
30.9 SILENT VANE FAN  
 CLASS 2 ARK 4  
 WITH INLET BOX & VANES  
 880 RPM  
 0.075 PCF AIR DENS  
 131.91 FT<sup>2</sup> OUTLET AREA  
 INLET VANES CLOSED 20  
 PHY-2050-3

ATTACHMENT B Page B3 of 6

A-211

50 40 30 20 10 0  
 BRAKE HORSEPOWER

003



DIT-B-00011-04  
 Attach 1, page 5 of 6

DIT NO-B-00011-04

1-72 JR

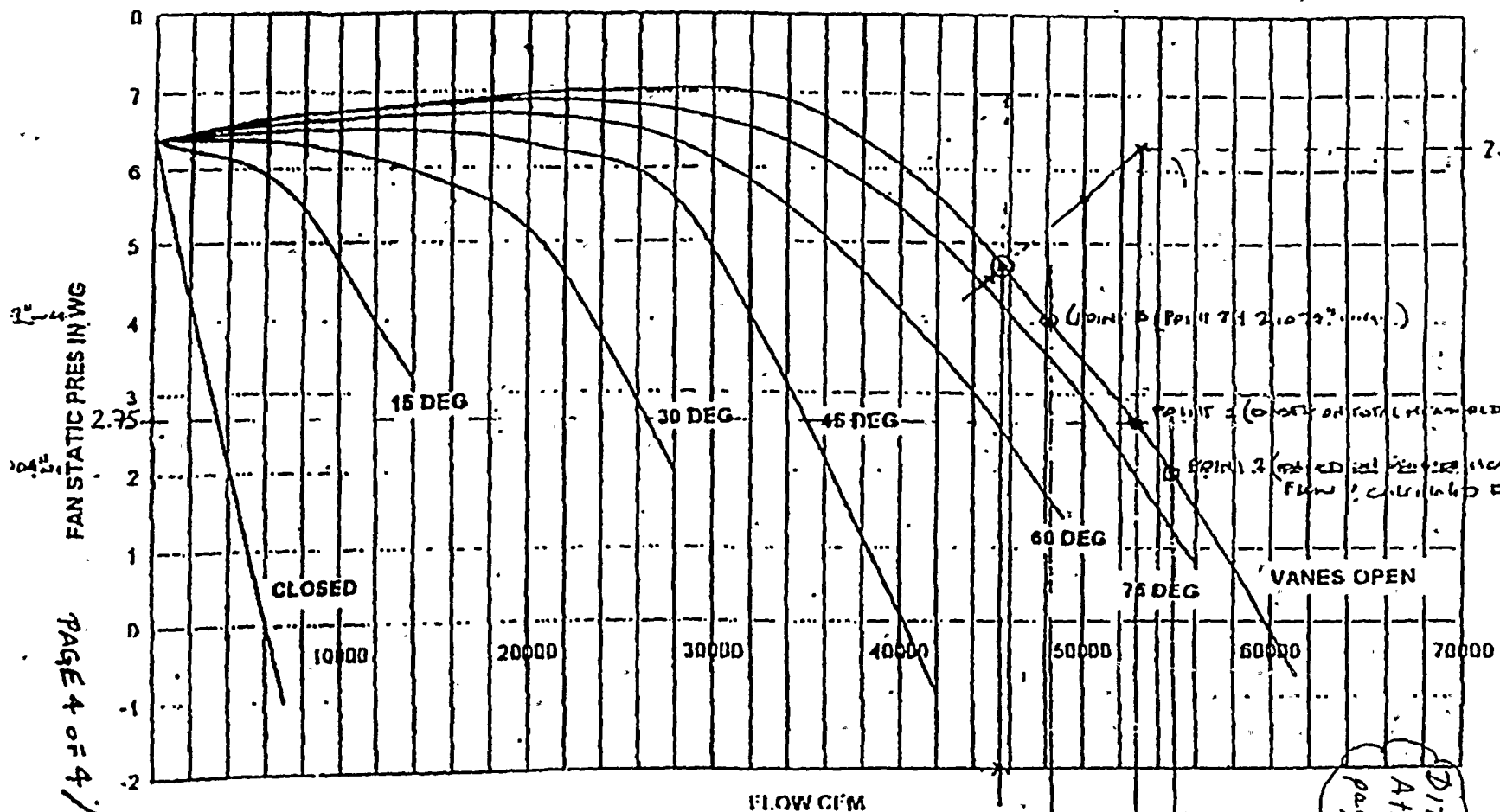


# ATTACHMENT "C"

PAGE 4 OF 4

DIT NO. B-00011-04

AEP DC COOK NUCLEAR PLANT W3049 SWSI 49" DIA 1110 RPM 0.075 lb/cu ft



FAN STATIC PRES IN WG

PAGE 4 OF 4/FINAL

FLOW CFM

2-HY-1000-2

45,400 CFM

54,500 CFM

52,900 CFM

DIT-B-00011-04  
Attachment 1  
page 6 of 6

**Attachment 2 to DIT-B-00011-04:**

Excerpts from WCAP-14286, "American Electric Power Service Corporation Donald C. Cook Nuclear Plant Unit 1 Steam Generator Tube Plugging Program Analysis Input Assumptions," Revision 7, 12/29/95. The excerpts consist of the following pages: Report Cover Sheet; Table 4.4-15 "D. C. Cook Maximum Safeguards 2 HHSI and 2 RHR All Lines Injecting," and Table 4.4-19 "D. C. Cook Maximum Safeguards 2 Charging/SI Pumps All Lines Injecting," for a total of 4 pages including cover sheet.





DIT-B-00011-04  
Attach. 2  
pg. 2 of 4

AMERICAN ELECTRIC POWER SERVICE CORPORATION  
DONALD C. COOK NUCLEAR PLANT UNIT 1

STEAM GENERATOR TUBE PLUGGING PROGRAM  
ANALYSIS INPUT ASSUMPTIONS

REVISION 7

DECEMBER 29, 1995

This document is the property of and contains Proprietary Information owned by Westinghouse Electric Corporation and/or its subcontractors and suppliers. It is transmitted to you in confidence and trust, and you agree to treat this document in strict accordance with the terms and conditions of the agreement under which it was provided to you.

WESTINGHOUSE ELECTRIC CORPORATION  
Nuclear Technology Division  
P.O. Box 355  
Pittsburgh, PA 15230

Copyright 1995, Westinghouse Electric Corporation, all rights reserved.



## WESTINGHOUSE PROPRIETARY CLASS 2C

TABLE 4.4-15

D.C. COOK MAXIMUM SAFEGUARDS  
2 HHSI AND 2 RHR  
ALL LINES INJECTING

DIT-B-00011-04

Attach. 2

pg. 3 of 4

<u>RCS Pressure</u> <u>(psig)</u>	<u>Flow</u> <u>(gpm)</u>
0	7565
100	5580
200	1409
300	851
400	817
500	783
600	747
700	708
800	666
900	623
1000	585
1100	527
1200	468
1300	402
1400	326
1500	214
1600	68
1700	0

## WESTINGHOUSE PROPRIETARY CLASS 2C

TABLE 4.4-19

D.C. COOK MAXIMUM SAFEGUARDS  
2 CHARGING/SI PUMPS  
ALL LINES INJECTING

DIT-B-00011-04

Attach. 2

pg. 4 of 4

Pressure (psig)	Total Flow Into Core	
	(lbs/sec)	(gpm)
0	127.50	922.99
100	125.22	906.51
200	122.91	889.78
300	120.56	872.79
400	118.18	855.53
500	115.75	837.97
600	113.28	820.09
700	110.77	801.87
800	108.20	783.29
900	105.58	764.29
1000	102.89	744.87
1100	100.14	724.97
1200	97.32	704.54
1300	94.42	683.54
1400	91.43	661.90
1500	88.34	639.54
1600	85.15	616.38
1700	81.82	592.31
1800	78.35	587.19
1900	74.71	540.85
2000	70.87	513.08
2100	66.80	483.56
2200	62.42	451.89
2300	57.67	417.47
2400	52.60	379.35
2500	46.40	335.90
2600	39.19	283.73

**Attachment 3 to DIT-B-00011-04:**

Two memos from Operations Department to ENSA. The first memo is 4 pages, dated 7/12/99 from Jim Abshire, EOP Project Manager to Gary Brassart, ENSA and Vance Vanderburg, ENSA, re: ES-1.3. The second memo is one page, dated 9/17/98 from Paul Cooper, EOP Coordinator to James Feinstein, subject: ECCS Switchover Times. There are 6 pages including the cover sheet in this attachment.

DIT-B - 00011-04  
Attach. 3

pg. 2 of 6

# Memo

**To:** Gary Brassart, ENSA,  
Vance Vanderburg, ENSA  
**From:** Jim Abshire, EOP Project Manager  
**CC:** Roger T. Rickman, EOP Program Manager  
**Date:** 07/12/99  
**Re:** ES-1.3

Analysis of the proposed final disposition of the steps contained in emergency procedure ES-1.3.

Item # 1 – The 5 minute maximum interruption of RHR flow to the RCS is acceptable to the EOP group as formerly agreed to and previously validated in 1998.

Item # 2 – The swapover sequence for realignment of the RHR pumps and CTS pumps suction from the RWST to the containment sump will remain the same as was previously validated on the simulator (This is Step 8 in the current draft of ES-1.3).

Item # 3 - Possible changes to the current draft of procedure ES-1.3 are as follows:

- |          |   |
|----------|---|
| Step 1C1 | This caution will remain as is to remind the operator that flow to the RCS is to be maintained at all times.  |
| Step 1C2 | This caution will remain as is to alert the operator that auto restart of the injection pumps may not occur under the listed conditions potentially causing interruption of flow to the RCS.  |
| Step 1C3 | This caution will remain the same to alert the operator to possible changing radiological conditions in the Auxiliary Building, allowing him to alert any personnel that may be sent out into the building to accomplish local tasks.   |
| Step 1   | This step will remain as is in accordance with the ERG  |
| Step 2   | This step will be changed to provide a quick check that CCW flow has been established to the RHR heat exchangers, and actions to establish this flow provided in the RNO, specific flow path (splitting of trains) verification will be moved to after the ECCS pumps have been aligned to the sump, to be consistent with the ERG. |

- Step 3 This Step will remain as is to provide the operator with a check that the equipment necessary to support the swapover to recirculation mode is available and operable, and to provide transition to the correct procedure in the event that the equipment is not available.
- Step 4 This step will be changed/or deleted to reflect the automatic operation of the CCP miniflow valves if and when the Seal Water heat exchanger is upgraded to a pressure great enough to prevent relief of contaminated water from the containment to the Auxiliary Bldg., via its relief to the VCT and the VCT relief to the HUT's. Once this is accomplished, the CCP miniflow valves can be allowed to operate in automatic mode. The portion of the step that uses the Pressurizer PORV for a miniflow valve for the CCP's will be eliminated due to its nature as an unresolved safety question. These leakoff valves should be closed during the recirculation phase, and the analysis concerning the deadheading of a CCP during a small break LOCA should be revisited to verify if this condition could occur (any LOCA large enough to empty the RWST will drop pressure enough to provide ample flow for pump protection, any leak small enough to hold pressure up far enough to deadhead a pump will allow SI termination criteria and reestablish normal charging and letdown).
- Step 5 This step may be deleted if the entry condition for the procedure can be changed to the maximum RWST level that will permit swap-over of the RHR pumps to the containment sump. Entry at this maximum level will ensure that sufficient water has been injected to the RCS make the swapover to recirculation mode necessary, while allowing sufficient time for the operator to accomplish the swapover prior to reaching minimum NPSH level in the RWST, and allow the operator to perform the procedure without any delays because the action level has been reached when the operator arrives here. (Operations would like to restore this number to 32% to allow more time to complete actions).
- Step 6 This step will remain as is to be consistent with the ERG and provide the correct order of priority for the emergency procedures. (under these conditions this instruction takes priority over the performance of the FRG's)
- Step 7 This step will remain as is to provide the proper indication to the operator that NPSH exists for the operation of the RHR pumps from the containment sump, to prevent vortexing at the pump suction, and provide transition to the proper instruction if the RHR pumps cannot be used.
- Step 8C1 This caution will remain as is to alert the operator of time constraint associated with the listed steps.
- Step 8 This step and all substeps will remain as is, and have been validated as performable in the prescribed time frame successfully on the simulator. The associated RNO's provide the proper contingency actions and transition points to account for equipment failures.
- Step 9 This step will remain as is to provide a check that the CTS portion of the swapover to recirculation has occurred and alignment of the cooling medium for the Heat exchangers is correct, in order to remove the maximum possible heat from the containment sump (this is plant specific).

- Step 10 This step will remain as is as part of the verification that the necessary heat sink for ECCS heat removal required to remove the heat generated in the RCS is available when entering the recirculation mode.
- Step 11 This step may be deleted (pending licensing direction) or will be reworded to check both RHR pumps running with CCW flow on their respective heat exchanger, and RNO to disable any non-operating pump or pump with no CCW flow to its heat exchanger, as well as the isolation of the injection line of the non-operating RHR pump to prevent injection flow from the operating train via the SI/CCP suction cross tie header.
- Step 12 This step will remain as is to provide verification that the maximum amount of water that is available has been injected to the RCS prior to swapover of the remaining injection pumps to the recirculation mode. A number for the minimum NPSH for operation of the high head injection pumps is needed here.
- Step 13 This step will remain as is (pending licensing direction) in order to provide train separation on the SI pumps and prevent runout conditions on one pump if the other should trip.
- Step 14C1 This caution will remain as is to alert the operator of potential damage to the SI and CCP's when available NPSH from the RWST is minimal, and to be consistent with the ERG. A setpoint for the minimum NPSH for high head pumps should be obtained from engineering and inserted here.
- Step 14 This step will remain as is to prevent transfer of any of the water from the containment sump to the RWST via the SI pump recirc line, and verify that RCS pressure is below shutoff head of the SI pumps in accordance with the ERG (small break LOCA or Secondary line break that allows pressure to remain above shutoff head). RNO will be changed to stop the pump instead of initiating a cooldown if RCS pressure is above shutoff head of the pumps.
- Step 15 This step will be deleted as redundant to step 14.
- Step 16 This step will be deleted as redundant to step 14.
- Step 17 This step will remain as is with the omission of substep "a." if the seal water heat exchanger is upgraded and the CCP miniflows are allowed to operate in the automatic mode, all other substeps remain in order to provide the proper instructions to complete the swapover to recirculation mode of the SI and CCP's.
- Step 18 This step will remain as is to indicate to the operator that monitoring of the Critical Parameter Status Trees and the FRP's are in affect.
- Step 19 Note This note and the associated step should be deleted (pending licensing direction) since the RHR pumps are each individually capable of supplying suction to all four high head injection pumps, (both SI and both CCP's) and there is no need to stop the operating pumps as long as one of the suction cross tie valves are open (established in step 17).
- Step 19 This step will be deleted (pending licensing direction) since one RHR pump is capable of providing the flow required by all four high head injection pumps when the SI/CCP suction cross tie valves are open which is verified in step 17 or the proper pumps are stopped if the suctions cannot be cross tied.





DIT-B-00011-04  
Attach. 3; pg. 5 of 6

- Step 20 This step will remain as is and is provided to restart ECCS pumps that may have been shutdown during the swapover process and that are now available.
- Step 21 This step will remain as is to complete the swapover to the recirculation mode by closing off the RWST as a suction source for any ECCS pumps.
- Step 22 This step may be deleted if the seal water heat-exchanger can be upgraded, or will remain as is to detect and isolate any backleakage through the VCT to CCP suction check valve that would be a core bypass path.
- Step 23C1 This caution may change to contain a specific value (if analysis allows) to alert the operator to the containment pressure that will require placing RHR containment spray in service.
- Step 23C2 This caution wording may change to alert the operator that a containment pressure spike will occur at some time after the event due to depletion of the ice bed.
- Step 23 This step may change to use crmt pressure instead of time (if analysis allows), and directs the operator in placing one train of RHR spray in service whenever crmt pressure reaches a preset value the event.
- Step 24 This step will remain as is and provides the proper transition to the procedure in effect at the completion of this procedure.

Preparer:

Mike E. Shultz 7/12/99

Reviewer:

[Signature] 7/12/99 EOP Manager

SRO Review:

[Signature] 7/12/99

Attachment to VanderBurg to Peck Letter, 9/18/98  
A-32

Call Jim Hawley

Marshall Hurst  
3284

Roger Rickman

AEP

AMERICAN  
ELECTRIC  
POWER

DIT-B-00011-04

Attach. 3

pg. 6 of 6

Date: September 17, 1998

Subject: ECCS Switchover Times

From: EOP Coordinator *Paul Coq 9/17/98*

To: James Feinstein

The information below for the no failure case was obtained from actual time validation data. The time provided is bounding for the data sets reviewed. The other time data was obtained by estimation except for valve stroke times which are ISI program maximum limits.

#### ES-1.3 Valve Manipulation Sequence:

Assumptions: 2 trains operating, no failures

Time (sec)	Event
0	RWST level drops to initiation setpoint (20%)
60	RHR and CTS pumps in 1st train are stopped
120	RHR and CTS pumps in 2nd train are stopped
300	RHR and CTS pumps in 1st train are started with suction on recirc sump
360	RHR and CTS pumps in 2nd train are started with suction on recirc sump

Same switchover event but new reference point for time:

0	RWST level drops to high-head switchover setpoint (11%)
300	CCP/HHSI get suction from recirc sump (i.e. IMO-340 and IMO-350 are open)

Assumptions: 2 trains operating, most limiting single failure [DC control power]  
[Loss of dc control power to 1st train is most limiting failure vs. operator response]

Time (sec)	Event
0	RWST level drops to initiation setpoint (20%)
75	Pumps in 1st train fail to stop but suction valves begin to close
135	RHR and CTS pumps in 2nd train are stopped
205	Suction valves for 1st train pumps are fully closed
230	Recirc sump suction valve for 1st train starts to open
275	Recirc sump suction valve for 1st train is full open
375	RHR and CTS pump in 2nd train are started with suction on recirc sump

Same switchover event but new reference point for time:

0	RWST level drops to high-head switchover setpoint (11%)
300	CCP/HHSI get suction from recirc sump

These times have been approved by Operations Department management:

*Amy Pollan*  
Signature

9-17-98

Date

K:\17532\WP04\TAM\MOT\ES1\MEMO.DOC

Attachment 4 to DIT-B-00011-04:

"Break Size/Location Matrix for the Resolution of the Containment Sump Issues Program"



# Break Size/Location Matrix for the Resolution of the Containment Sump Issues Program pg. 2 of 2

BREAK SIZE (Dia. or Area)	LOCATION	MODE 1 (HFP)	MODE 3 <sup>(6)</sup> (350°F)	MODE 4 <sup>(7)</sup> (235°)
0.61" <sup>(1)</sup>	Cavity	X	X	X
2.75" <sup>(2)</sup>	Cavity	X	X	X
1 ft. <sup>2</sup> <sup>(3)</sup>	Sump/Cavity	X	N/A	N/A
DECL <sup>(4)</sup>	Sump	X	N/A	N/A
6"	Sump	X	X	X
4"	Sump	X	X	X
3"	Sump	X	X	X
2"	Sump	X	X	X
1.5"	Sump	X	X	X
1"	Sump	X	X	X
0.5"	Sump	X	X	X
4" <sup>(5)</sup>	Sump/Cavity	X	X	X
3" <sup>(5)</sup>	Sump/Cavity	X	X	X
2" <sup>(5)</sup>	Sump/Cavity	X	X	X
1.5" <sup>(5)</sup>	Sump/Cavity	X	X	X
1" <sup>(5)</sup>	Sump/Cavity	X	X	X
MSLB 4.6 ft <sup>2</sup>	Sump	X	N/A	N/A
MSLB 1.4 ft <sup>2</sup>	Sump	X	N/A	N/A

- (1) The break occurs at the bottom of the reactor vessel.
- (2) The break occurs on the top of the reactor vessel and is a steam space break.
- (3) The break occurs on the cold leg and 72% of the break flow flows to the sump.
- (4) This break represents a Double-Ended Rupture on the Cold Leg.
- (5) The break occurs on the cold leg and the analysis should direct appropriate fractions of the break flow to the sump and cavity.
- (6) Run cases by reducing size until containment spray does not actuate; smaller cases not required to be run
- (7) Cases for Mode 4 not required to be run for FAI/99-77.

HFP Hot Full Power (100% Full Power)

HZP Hot Zero Power

Attachment 5 to DIT-B-00011-04:

"Single Failure Configuration for DC Cook Containment Sump Analyses"

## SINGLE FAILURE CONFIGURATION FOR DC COOK CONTAINMENT SUMP ANALYSES

The configuration of the Cook safeguards trains is such that each of the two emergency diesel generators provides power to:

- 1 High-Head Centrifugal Charging Pump
- 1 Intermediate-Head Safety Injection Pump
- 1 Residual Heat Removal Pump
- 1 Containment Spray Pump
- 1 Containment Air Recirculation (CEQ) Fan

Under normal Loss of Offsite Power conditions, both generators will start and load their assigned pumps and fans.

If there are no failures, two of each component listed above will function.

If a single failure of one diesel generator is assumed, an entire train is lost.

If offsite power is maintained, the equivalent failure would be the loss of one of the two vital busses.

If the limiting single failure of a specific component is assumed, either the entire train must be lost or only that single component is assumed lost.

Thus, if the configuration of 2 operating containment spray pumps and only 1 containment recirculation (CEQ) fan yields the most limiting single failure, both diesels and all their assigned pumps must be operating.

Assuming additional equipment lost besides the limiting configuration above would require more than one failure and is not required.

### RHR Operation

If both trains of RHR are operating, they provide suction to the SI and CCP pumps and inject directly into the RCS. When RHR sprays are actuated, one RHR would be re-aligned from RCS injection to RHR spray. The supply to the SI and CCP pumps is unchanged. The other RHR pump is unchanged.

If only one RHR pump is operating, it would (could) provide suction flow to all four SI/CCP and simultaneously inject into the RCS. When the RHR sprays are actuated, one set of SI/CCP pumps would be secured and the RHR pump's injection flow would be re-aligned to RHR spray. Supply to one set of SI/CCP pumps would not be changed.

This implies that one RHR pump cannot provide flow to all four SI/CCP pumps AND the RHR spray system.



Discussion of "Approved for Use" Design Input Values in DIT-B-00011-04

The entire set of "Approved for Use" design inputs provided in DIT-B-00011-04 have been reviewed relative to the design inputs used in FAI/99-77, Rev. 1 and correspondence between these documents has been found for all the design inputs with four exceptions. These four exceptions used in FAI/99-77, Rev. 1 have all been found to be representative of the "Approved for Use" design input values as discussed below. The four alternate input values used in FAI/99-77, Rev. 1 either have no impact on the minimum calculated recirculation sump water levels or provide additional conservatism in the reported results.

Maximum Containment Spray Flow Rate with 2 Trains (Item #'s 11, 12 and 13)

The total containment spray flow rate used in FAI/99-77, Rev. 1 was 7429 gpm and the "Approved for Use" value was 7400 gpm. The split fractions for spray flow delivered to the upper header and the lower headers inside and outside the crane wall are unchanged by the small (29 gpm) deviation in total spray flow. The impact of the deviation in the total flow is negligible and unobservable on the minimum sump level. If any change in sump level could be detected the deviation in the total spray flow rate would lead to slightly smaller melted ice masses. Less ice melt is conservative as it would reduce the minimum sump level.

Minimum Containment Ice Bed Mass (Item #19)

The initial ice bed mass used in FAI/99-77, Rev. 1 was 2.11 Mlbm and the "Approved for Use" value was 2.2 Mlbm. The inventory of melted ice credited in demonstrating compliance of the minimum sump levels with the Cook vortexing limit was significantly less than the initial ice mass for all cases. Since the credited melted ice mass was always less than the initial ice mass, an increase in the initial ice mass will have no impact on the minimum calculated sump levels.

Containment Air Recirculation - CEQ Fan-Capacity Curve (Item #23)

The total air recirculation (CEQ) flow rate used in FAI/99-77, Rev. 1 was 37,000 cfm and the "Approved for Use" value was 40,000 cfm. The recirculation flow rate equals the flow rate of gas delivered from the lower containment compartment to the upper compartment. This dictates the rate that steam in the lower compartment is delivered to the ice condenser where it condenses and melts ice. A lower air recirculation flow rate will result in a lower ice melt rate and less melted ice mass for maintaining the active sump level. The assessments provided in FAI/99-77, Rev. 1 based on an air recirculation flow rate of 37,000 cfm are conservative regarding the minimum sump water levels since smaller ice melt rates than would be produced by a 40,000 cfm air recirculation flow rate have been credited.

CCW Flow to RHR Heat Exchanger for Maximum UA Case (Item #28c)

The cooling water (CCW) flow rate to the RHR heat exchanger used in FAI/99-77, Rev. 1 was 4950 gpm and the "Approved for Use" value was 5500 gpm. RHR sprays were not actuated for any of the cases assessed in FAI/99-77, Rev. 1 since two trains of containment spray were always available. Cooling provided by the RHR heat exchanger only affected the temperature of the RCS injection flow during recirculation cooling. A lower RHR cooling water flow rate would produce a higher temperature injection flow rate at the RHR heat exchanger outlet. This could be expected to lead to higher temperature fluid leaving the core after decay heat addition and a corresponding higher steam release rate from the cold leg LOCA break. A higher steam release rate could lead to higher ice melt rates and higher minimum sump water levels. However, the conservative LOCA break mass and energy release rates used in FAI/99-77, Rev. 1 mixes the steam and water break flows which greatly reduces the steam in containment available to melt ice. The conservatism in the model for the LOCA break flow used in FAI/99-77, Rev. 1 greatly exceeds the impact of non-conservatively higher RHR heat exchanger outlet temperatures. No discernable impact on the minimum sump water level will result from using an RHR cooling water flow rate of 4950 gpm rather than 5500 gpm.

## APPENDIX B

### Flow Split for Postulated Ruptures in the Cold Leg Near the RPV

#### B.1 Introduction

Analyses for potential rupture locations must also consider those regions of the RCS pressure boundary near the RPV. Figure B-1 is a representation of a cold leg at the RPV nozzle and illustrates the relatively tight clearance between the cold leg and the biological shield as well as the fact that a break discharge into this region could result in flow being split into that which is directed toward the reactor cavity and that directed into the lower compartment. In this region, the postulated LOCA is considered to occur at the weld between the reactor vessel nozzle and the cold leg or within the cold leg itself. These small LOCAs are not considered in the vessel nozzles since these are a part of the qualified reactor vessel and the wall is substantially thicker than the cold leg as illustrated in Figure B-1. Also, since the effective break sizes are small compared to the vessel wall thickness and are undergoing a large radial expansion (discussed below) hence, these are not considered to be "directed" except radially outward. Consequently, the subsequent response to the flashing water jet will be almost uniform in the two directions available for expansion, i.e. into the region next to the RPV and through the biological shield into the lower compartment.

Given any postulated LOCA in this region with a break area of  $A_b$ , the two-phase critical flow rate can be estimated from the Henry-Fauske model (Henry and Fauske, 1971) as

$$W_b = C_d A_b (2 \rho_f P_o (1 - \eta))^{0.5} \quad (B-1)$$

where  $C_d$  is the break discharge coefficient,  $\rho_f$  is the density of saturated water,  $P_o$  is the RCS system pressure and  $\eta$  is the critical pressure ratio calculated by the model for subcooled and saturated conditions. For saturated conditions the critical pressure ratio is approximately 0.8 and for high subcooled conditions the pressure ratio can be approximated as the saturation pressure

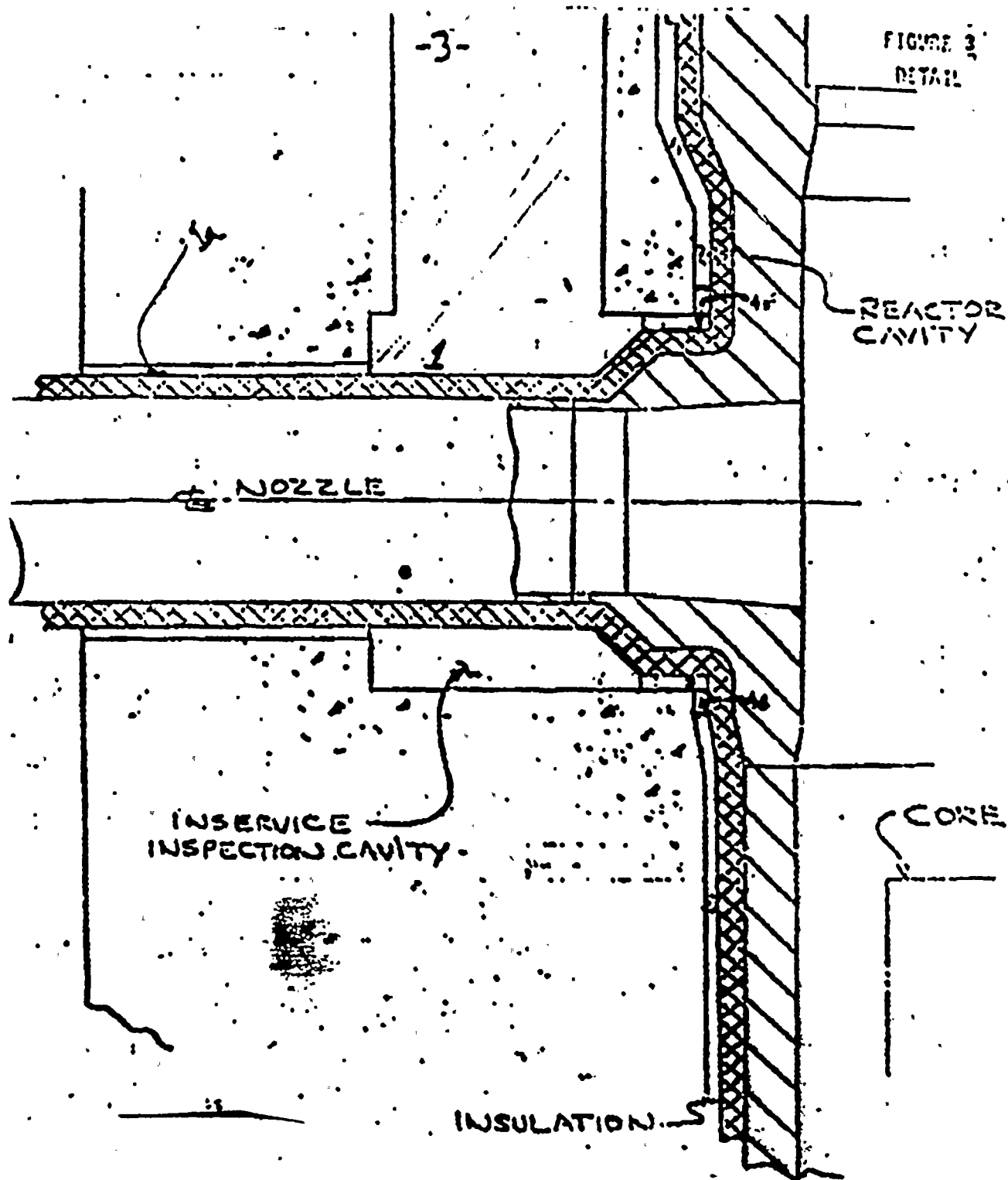


Figure B-1 Description of the region where small breaks may be considered in the RCS piping.

divided by the vessel pressure ( $P_{in}/P_o$ ). The Henry-Fauske model uses the minimum of these two conditions. For these small LOCA evaluations, the effective break area is the parameter modeled since a spectrum of effective break sizes are considered. The effective break area is that calculated using a discharge coefficient of unity to represent the product of the actual discharge coefficient and an assessment of a realistic break area. In this regard, the effective break area is a convenient and simplified means of addressing the important issue of potential sensitivities to the break area.

Given the break flow rate, the steam-water mixture discharge from the break will expand rapidly as the mixture depressurizes from the pressure at the break location to the containment ambient pressure. Considering the jet depressurization considered in the ANS standard for jet impingement (ANS, 1988) this depressurization is represented as being conical and having a half angle of  $45^\circ$ . This depressurization results in a further acceleration of the two-phase mixture as given by

$$(U_a - U_e) = \frac{(P_e - P_a)}{\rho_f U_e} \quad (B-2)$$

where  $U_e$  is the mixture velocity at the discharge plane with  $P_e$  and  $P_a$  being the respective exit plane and ambient pressures. Using the continuity equation to define the exit plane velocity results in an expression for the two-mixture velocity after expanding to the ambient conditions as given by

$$U_a = \frac{P_e - P_a}{G_e} + \frac{G_e}{\rho_f} \quad (B-3)$$

where  $G_e$  is the mass flux for the break. Using typical values such as saturated water at 1015 psia (7 MPa) the two-phase mixture velocity at atmospheric pressure would be about 560 ft/sec (171 m/sec) with the two-phase quality of about 0.3. Assuming a homogeneous mixture, the two-phase specific volume is expressed by

$$v_{2\phi} = (1-x) v_f + x v_g \sim x v_g \quad (B-4)$$

with the two-phase density being given by

$$\rho_{2\phi} = \frac{1}{v_{2\phi}} \quad (B-5)$$

In the above expressions,  $x$  is the two-phase quality,  $v_f$  is the specific volume of saturated water and  $v_g$  is the specific volume of saturated steam. Given this depressurization and flashing, the two-phase density would be about 0.35 lbm/ft<sup>3</sup> (5.6 kg/m<sup>3</sup>). Since this discharge flow is moving radially outward, it will impinge on the wall of the insulation and/or the biological shield creating a point of stagnation with the flow directed uniformly away from the stagnation point. This pressurization for the expansion of critical flow jets with impingement on a wall in the near vicinity of the break location has been investigated experimentally by Nguyen and Forrest (1980) as well as Kastner et al. (1978) and analytically by Epstein et al. (1983) and these observations have been captured in the ANSI standard. As this fluid flows radially outward and stagnates, the stagnation pressure can be estimated from the incompressible relationship

$$P_s = \frac{\rho_{2\phi} U_a^2}{2} + P_a \quad (B-6)$$

Using the two-phase mixture density and the expansion velocity, the local pressure increase above ambient is calculated to be 12 psi (82 KPa) which forces the flow equally in all directions. It should also be noted that the information in the ANS standard suggest that the depressurization to the ambient pressure for these rapidly expanding jets requires up to 3 effective rate diameters. Consequently, in this tight configuration it is possible that the local stagnation pressure is greater than that estimated through this approach. With an increased stagnation pressure the flow would have an increased tendency to be uniformly distributed.

The effective flow resistance for this discharge flow through the annular gap between the insulation and the biological shield wall is one means of assessing the capabilities for the flow to escape into the lower compartment. The pressure difference required for this flow can be expressed by



$$\Delta P = f \frac{L}{D_h} \left( \frac{W_1^2}{2 \rho_{2\phi} A_{BS}^2} \right) \quad (B-7)$$

where  $f$  is the turbulent friction factor (0.02),  $L$  is the effective length of the flow path to the lower compartment,  $D_h$  is the effective hydraulic diameter for this flow path,  $W_1$  is half of the discharge flow and  $A_{BS}$  is the flow area through the biological shield. For an effective break diameter of 1 inch (2.5 cm) the critical flow rate is 54 lbm/sec (24.5 kg/sec) such that  $W_1$  is 27 lbm/sec (12.3 kg/sec). Further assuming that the hole through the biological shield is 3 ft in diameter with a 1 inch clearance gives a flow area of 0.78 ft<sup>2</sup> (0.073 m<sup>2</sup>) and if the length of the flow path is 4 ft, the effective pressure difference required for the flow to move from the stagnation point to the lower compartment is about 0.3 psi (2000 Pa). This approximate evaluation shows that the flow resistance for discharge into the lower compartment is small compared to that pressure developed by the jet stagnation.

Two aspects of this jet stagnation flow are important in analyzing these results. The first is that once the jet is stagnated, the flow split is not generally determined by the respective loss coefficients for flow paths through the biological shield to the lower compartment and the competing flow path to the reactor cavity. This would only be the case when one or both of these flow paths could not transmit the flow given the jet stagnation pressure. Certainly the above analyses indicate that the flow path through the biological shield can easily transmit the flow. Evaluating the flow paths toward the RPV is more difficult due to the support blocks under two of the cold legs and two of the hot legs. These larger structures carry the weight of the vessel and also block much of the flow path toward the reactor cavity. Assuming that the break occurs in one of the cold legs without a support structure results in a conclusion that this path also could transmit one-half of the discharge flow given the jet stagnation pressure. Hence, once the flow is stagnated, there is no mechanism to cause the flow to deviate from a 50/50 split of the discharge flow.

A second feature to consider is that the discharge flow is generally a two-phase jet. With the steam evolved due to flashing of high pressure water, the steam velocity is sufficient to "flood" any local water accumulation. For example, consider the 1 inch diameter break considered above,



the two-phase discharge of 27 lbm/sec results in a homogeneous velocity of about 80 ft/sec (25 m/sec) which is well above any separation velocity for the two phases. Moreover, assuming that the phases do separate, the steam velocity approximately 300 ft/sec (100 m/sec) which is far greater than the entrainment velocity expressed by Kutateladze (1972) as

$$U_{ent} = 3.7 \sqrt[4]{\frac{g\sigma(\rho_f - \rho_g)}{\rho_g^2}} = 3.7 \sqrt[4]{g\sigma \left( \frac{1}{v_f} - \frac{1}{v_g} \right) v_g^2} \quad (B-8)$$

where  $g$  is the acceleration of gravity and  $\sigma$  is the steam-water surface tension. For pressure near one atmosphere, the entrainment velocity is about 58 ft/sec (18 m/sec). This shows that water could not separate out of "pool" in cross-sectional area changes. Thus, the two-phase flow pattern would be a homogeneous mixture of steam and water in thermodynamic equilibrium.

These analyses also consider substantial changes in the RCS pressure and temperature. As such, the temperatures could decrease to conditions in which the water temperature in the RCS would approach the normal boiling point, i.e., there would be little potential for flashing. Furthermore, the RCS pressure could also be substantially reduced. As an example of such conditions, let us consider that the RCS pressure is reduced to approximately 150 psig with cold water. Under these conditions, the discharge velocity for the water would be about 150 ft/sec (45 m/sec) which roughly corresponds to the conditions generated by a high pressure fire hose. Therefore, even under these depressurized and cold conditions the jet impingement behavior would be expected to produce an equal flow split between the water discharged to the reactor cavity and that directed to the lower compartment. With these additional features considered for the single-phase and two-phase behavior after jet stagnation, equal fractions of the discharge flow would be directed toward the lower compartment and the reactor cavity.

Given the best estimate behavior described above, the assessments for the minimum sump inventory have been addressed for the most limiting cases. To achieve the most limiting case, conservatism in this assessed flow split may be used by decreasing that contribution directed towards the lower compartment. For postulated breaks in the new vicinity of the reactor vessel, the larger the value of the flow directed to the lower compartment the greater the level in the

containment sump. As discussed above, basic analyses concludes that this flow split would be 50/50. Furthermore, no mechanistic process was identified that would significantly alter this equal flow split.

**APPENDIX C**  
**Ice Condenser Door Opening**



## ICE CONDENSER DOOR OPENING

### 1.0 INTRODUCTION

For ice condenser containments, the flow of steam and noncondensable gases into the ice condenser control the containment pressurization under postulated accident conditions. In addition, this also controls the rate of ice melting which is an integral part of the containment response. To assess this behavior, which includes uni-directional and counter-current flows, the containment description models the extent of opening for the spring loaded ice condenser doors which separate the containment lower compartment from the ice condenser. This subroutine describes this door model in terms of three different characteristic curves which are typically considered to assess the influence of uncertainties in the door response.

### 2.0 STRUCTURE AND INTERFACE

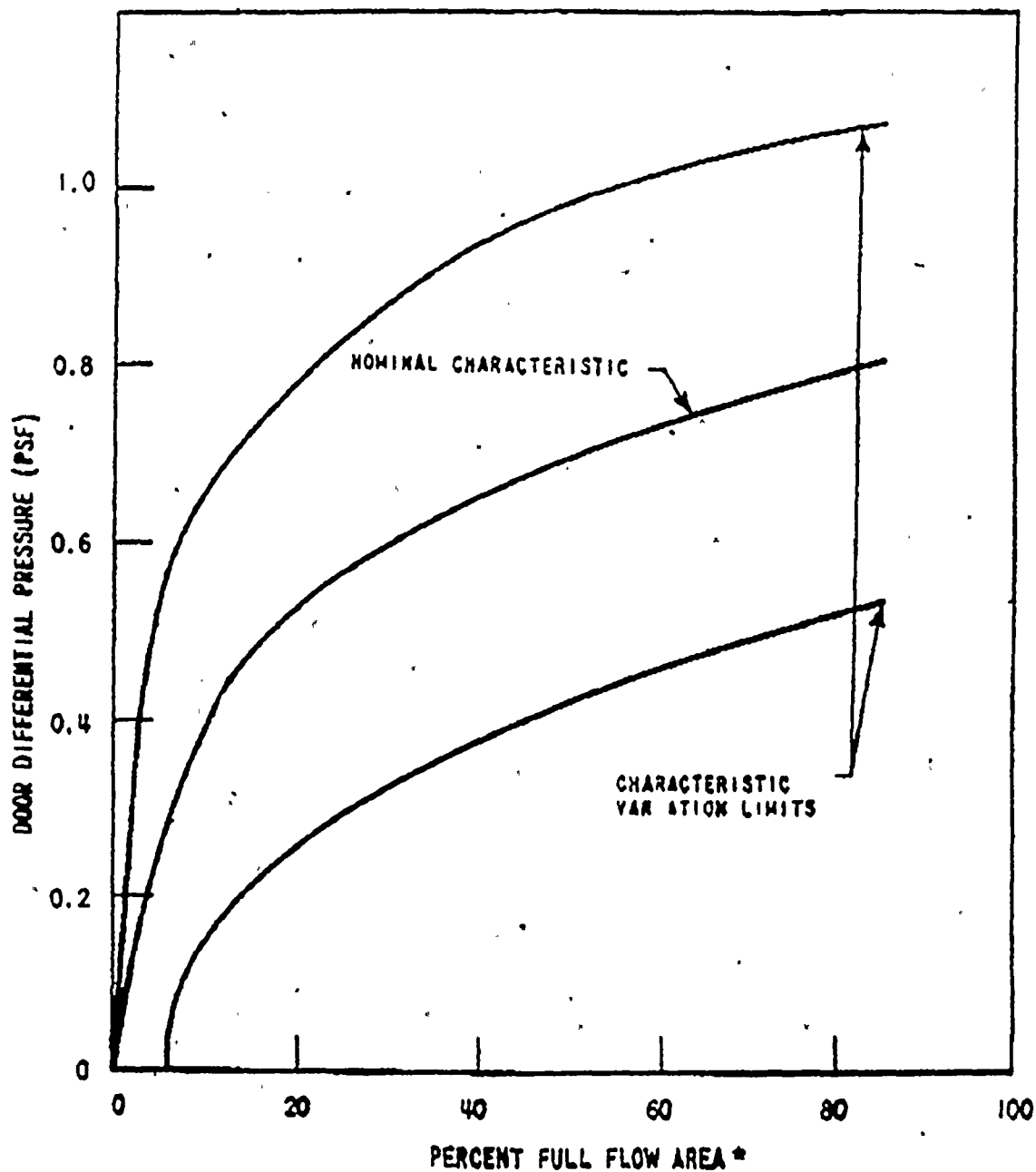
Subroutine ICDOOR is called by AUX EVT, which is part of the MAAP4 Generalized Containment Model (GCM). In particular, this is called to determine the extent of the junction area that would be held open as a result of the imposed uni-directional flow. This is then considered in assessing the flows to the other containment compartments as determined by the GCM.

### 3.0 PHYSICAL BASIS OF THE MODEL

The force required to open ice condenser doors is quite small with a typical value being less than 1 lbf/ft<sup>2</sup>. Figure 1 shows the typical characteristics for the fractional door flow area as a function of the differential pressure across the doors. This figure shows the nominal door characteristic behavior plus the variation limits for the typical characteristics that can be expected due to variations in the door hinges, static friction, etc. These variations are considered in the MAAP4 model to determine the potential influence, or lack thereof, of the different characteristic curves shown in Figure 1, which are taken from AEP [1999].

The MAAP4 model represents both once-through and counter-current flows through individual junctions, but the once-through flow is that which would determine the extent of the door open area. The extent of the door opening can be represented in terms of the pressure differential across the individual doors or this can be represented as the area that would be opened by a specified once-through flow. Since the once-through flow is more stable than the pressure differential across the door when considering differential pressures of the order of 10 Pa, and since the recirculating fans essentially deliver a specified flow rate, it is recommended that the model be characterized in terms of the imposed once-through flow rate. Such an approach is outlined below.

Figure 1: Flow Area - Pressure Differential



\*Full flow area is defined as door port area at maximum door opening

Consider that characteristic curves shown in Figure 1 can be represented by a cubic expression

$$A_o = K (\Delta P)^3 = FR \cdot A_{TOT} \quad (1)$$

where  $A_o$  is the door open area,  $A_{TOT}$  is the total door area,  $FR$  is the fractional opening characteristic shown in Figure 1,  $\Delta P$  is the total pressure differential accelerating the flow through the doors, and  $K$  is the constant of proportionality that is different for the three different curves shown in Figure 1. Considering that the flow through the open doors is represented by the Bernoulli equation with a discharge coefficient ( $C_D$ ) to treat the non-idealities of the flow, the pressure differential can be related to the once-through flow rate

$$\Delta P = \frac{1}{2 \rho_{gD}} \left[ \frac{W}{C_D FR \cdot A_{TOT}} \right]^2 \quad (2)$$

where  $W$  is the once-through mass flow rate, and  $\rho_{gD}$  is the gas density of the donor compartment, which is the lower compartment in this expression. Casting this in the form of the volumetric flow rate ( $\dot{Q}_V$ ) results in the following expression

$$\Delta P = \frac{\rho_{gD}}{2} \left( \frac{\dot{Q}_V}{C_D FR A_{TOT}} \right)^2 \quad (3)$$

Solving equation (1) for the pressure differential and substituting into equation (3) results in

$$\left( \frac{FR \cdot A_{TOT}}{K} \right)^{1/3} = \frac{\rho_{gD}}{2} \left( \frac{\dot{Q}_V}{C_D \cdot FR \cdot A_{TOT}} \right)^2 \quad (4)$$

or solving for the open area

$$(FR \cdot A_{TOT})^{7/3} = K^{1/3} \cdot \left( \frac{\rho_{gD}}{2} \right) \left( \frac{\dot{Q}_V}{C_D} \right)^2 \quad (5)$$

Since the area opened by the once-through flow is the desired result from the function, this is solved in terms of the area available as given by

$$FR \cdot A_{TOT} = K^{1/7} \left( \frac{\rho_{gD}}{2} \right)^{3/7} \left( \frac{\dot{Q}_V}{C_D} \right)^{6/7} \quad (6)$$

or for the fractional area opened by the imposed flow





$$FR = \frac{K^{1.7}}{A_{TOT}} \left( \frac{\rho_{gD}}{2} \right)^{3.4} \left( \frac{\dot{Q}_v}{C_D} \right)^{6.7} \quad (7)$$

The doors in the plant are tested at each outage in terms of the force required to prevent the doors from closing at a 40° open angle as well as other tests. A typical value for this is a torque of 145 in/lb with variations between about 110 and 180 in/lb. For a door that is partially opened and is acting as a nozzle ducting flow from the lower compartment through the door opening, the average differential pressure acting to open the doors is the average value of the lower compartment pressure and the ice condenser inlet plenum, minus the inlet plenum pressure as illustrated in Figure 2. Consequently, the average pressure differential then acts with a lever arm of one-half the door width, i.e. 21 in. (0.53 m). The force pressure difference corresponding to 145 in/lb is 6.9 lbf, or considering the door width to be 42 in and a height of 92.5 in (a cross-sectional area of 3885 in<sup>2</sup>/27.0 ft<sup>2</sup>/2.5 m<sup>2</sup>) the pressure difference required to hold the door open at a 40° opening angle is  $1.78 \times 10^{-3}$  psi or 0.26 psf. (This corresponds to 12.2 Pa in the SI system of units.) Using the information provided by AEP, which includes Westinghouse questions and answers on the basis for the tech spec surveillance on acceptance criteria for the ice condenser doors, a 40° door opening is equivalent to a fractional area of approximately 35%, which is taken to be 350 ft<sup>2</sup> for this analysis. (The full open area is assumed to be 1000 ft<sup>2</sup> (92 m<sup>2</sup>).) Considering that the average pressure difference is one-half of the total pressure difference, the required total pressure differential is 0.52 psf. Figure 3 compares this value with the characteristic curves of Figure 1 and also shows the boundaries represented by the high and low values of the measured torque to maintain the door open at a 40° angle [Henry, 1999]. As shown, a 35% full open area at a door differential pressure of 0.52 psf results in a value which is between the lower characteristic limits and that shown as the nominal characteristic. Hence, the plant measurements are consistent with the characteristic curves. To analytically represent the characteristic limits let us consider a cubic functional form which uses the following single points to evaluate the constants of proportionality for the three characteristic curves.

**Lower Limit Characteristic:** 35% full flow area achieved at a total door differential pressure of 0.35 psf.

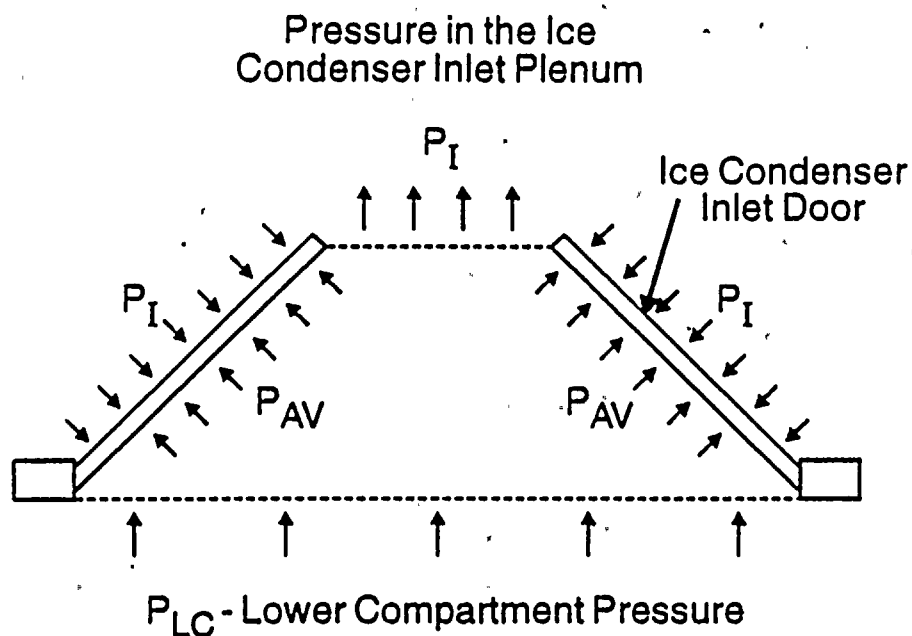
**Nominal Characteristic:** 35% full flow area achieved at a total door differential pressure of 0.60 psf.

**Upper Limit Characteristic:** 35% full flow area achieved at 0.85 psf.

For all the characteristic curves 35% full open area is taken as 350 ft<sup>2</sup> or 32.6 m<sup>2</sup>. For the lower limit total pressure difference of 0.35 psf corresponds to 16.8 Pa which results in a value for the constant proportionality of  $6.88 \times 10^{-3}$  for the open flow area such that the lower limit characteristic is given by

$$A_{OL} = 6.88 \times 10^{-3} (\Delta P)^3 \quad (8)$$

Figure 2: Schematic Illustration of the Average Pressure Acting to Open the Ice Condenser Inlet Doors

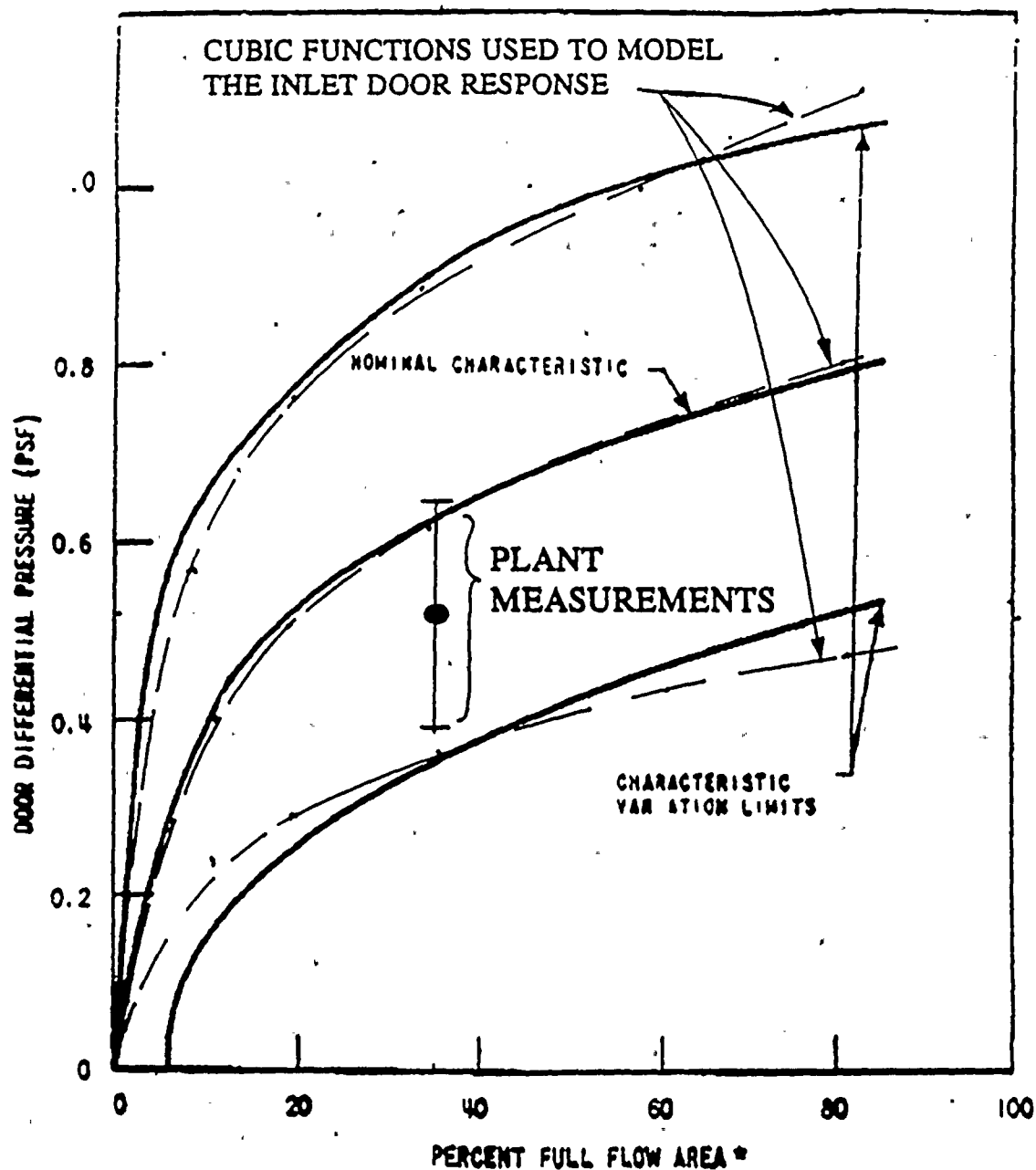


$$P_{AV} = \frac{(P_{LC} + P_I)}{2}$$

RH991017.CDR 1-12-99



Figure 3: Comparison of the Measured Plant Behavior for a 40° Door Opening and the Cubic Functions Used to Model the Door Response With the D.C. Cook FSAR Door Characterization



\*Full flow area is defined as door port area at maximum door opening

and the fractional opening is

$$FR_L = 7.4 \times 10^{-5} (\Delta P)^3 \quad (9)$$

Note that the constant proportionality is dimensional and the above values are for the international system units since the MAAP internal calculations are in this system. Following the same approach for the nominal characteristic line, the proportionality constant results in the expression

$$A_{ON} = 1.38 \times 10^{-3} (\Delta P)^3 \quad (10)$$

with the fractional opening expression being

$$FR_N = 1.5 \times 10^{-5} (\Delta P)^3 \quad (11)$$

Using the same methodology to determine the upper characteristic limits for the open flow area results in the expression

$$A_{OU} = 4.84 \times 10^{-4} (\Delta P)^3 \quad (12)$$

and the fractional opening is given by

$$FR_U = 5.2 \times 10^{-6} (\Delta P)^3 \quad (13)$$

The three expressions for the fractional opening are shown in Figure 3. Using cubic expressions for the three different door area characteristic curves provides an adequate representation of the uncertainties associated with the door response which are also consistent with the measurements in the D.C. Cook units. Moreover, this representation is consistent with the vendor characterization for the uncertainties and door behavior. Furthermore, it provides a means of evaluating of the influence of such uncertainties on the containment response for a realistic range in model parameters characterizing the door uncertainty behavior. As illustrated in this figure, the differences between the cubic behavior and the vendor information are small compared to the uncertainties between the nominal, lower limit and upper limit behavior.

The model also considers that once the doors are open there is a minimum opening area since the doors never return to a completely closed condition. This minimum opening area is specified in the MAAP parameter file and is used in the following manner:

$$A_{open} = \max (A_{o,min}, A_{model}) \quad (14)$$

In this expression  $A_{model}$  is the calculated opening area from the model-parameter selected from the three expressions given above. In this way, the influence of a minimally open area for the door behavior is included in the generalized containment evaluation.



#### 4.0 VALIDATION

The relationship of this model to the three door curves discussed in the D.C. Cook FSAR and the plant experience was discussed in Section 3.

#### 5.0 NOMENCLATURE

The nomenclature is defined in the text.

#### 6.0 REFERENCES

AEP, 1999, D.C. Cook Units 1 and 2 Updated Final Safety Analysis Report (UFSAR).

Henry, R. E., 1999, Personal Communication.





**APPENDIX D**  
**Representation of the Ice Condenser Outlet Temperature**

## REPRESENTATION OF THE ICE CONDENSER OUTLET TEMPERATURE

### 1.0 INTRODUCTION

The MAAP Generalized Containment Model (GCM) includes a representation of the ice condenser behavior used in this type of PWR containment. This is one of the containment compartments which in addition typically includes the reactor cavity, the lower compartment deadend volumes, and the upper compartment. Assessments related to uni-directional flows and counter-current flows are the same for all of the containment types given the differences in controlling features, such as the ice condenser inlet doors. One of the principle features controlling the extent of energy removal in the ice condenser is the temperature of gases leaving the ice condenser upper region and flowing into the containment upper compartment. This subroutine evaluates this gas temperature as a function of the dynamic conditions entering the ice condenser and the available ice mass to condense the steam.

### 2.0 STRUCTURE AND INTERFACE

Subroutine ICEOUT is called by subroutine HTICE to assess the temperature of gases leaving the top of the ice condenser. An energy balance combines the incoming steam and noncondensable gas energy fluxes with the output of this subroutine to assess the energy removed in the ice condenser by the composite process of condensing steam and melted ice.

### 3.0 PHYSICAL BASIS OF THE MODEL

A review of the available experimental results, such as the proprietary Westinghouse Waltz Mill experiments [Salvatori, 1974] and those from the PNL ice condenser tests [Ligotke, et al., 1991], show that for the different conditions there can be substantially different gas outlet temperatures. For example, Figures 1 and 2 are taken from Ligotke and show the measured gas temperatures near the exit of the ice condenser for tests with high and low incoming steam partial pressures, respectively. These experiments were representative of small break Loss-Of-Coolant Accident (LOCA) conditions and it is clear that the outlet temperature is low early in the transient and increases as ice melting occurs. In the Westinghouse experiments, large LOCA conditions were simulated and high exit temperatures are observed early in the blowdown and then decreases with decreasing blowdown flow. Since this exit temperature behavior differs from a constant, it is more realistic for the MAAP4 model to represent the differences in these temperatures than to model the outlet temperature as a user-specified constant value. The following is an approach to represent this information in a more mechanistic manner.

Figure 3 illustrates the ice baskets in the general configuration of an ice condenser containment and Figure 4 is a cutaway view showing the ice basket arrangement, as well as the steam/noncondensable entry point at the Lower Inlet Doors (LIDs), the turning vanes, the

Figure 1:  
Ice Basket Section Thermal Profiles Near the Exit for Test 11  
[Ligotke, et al., 1991].

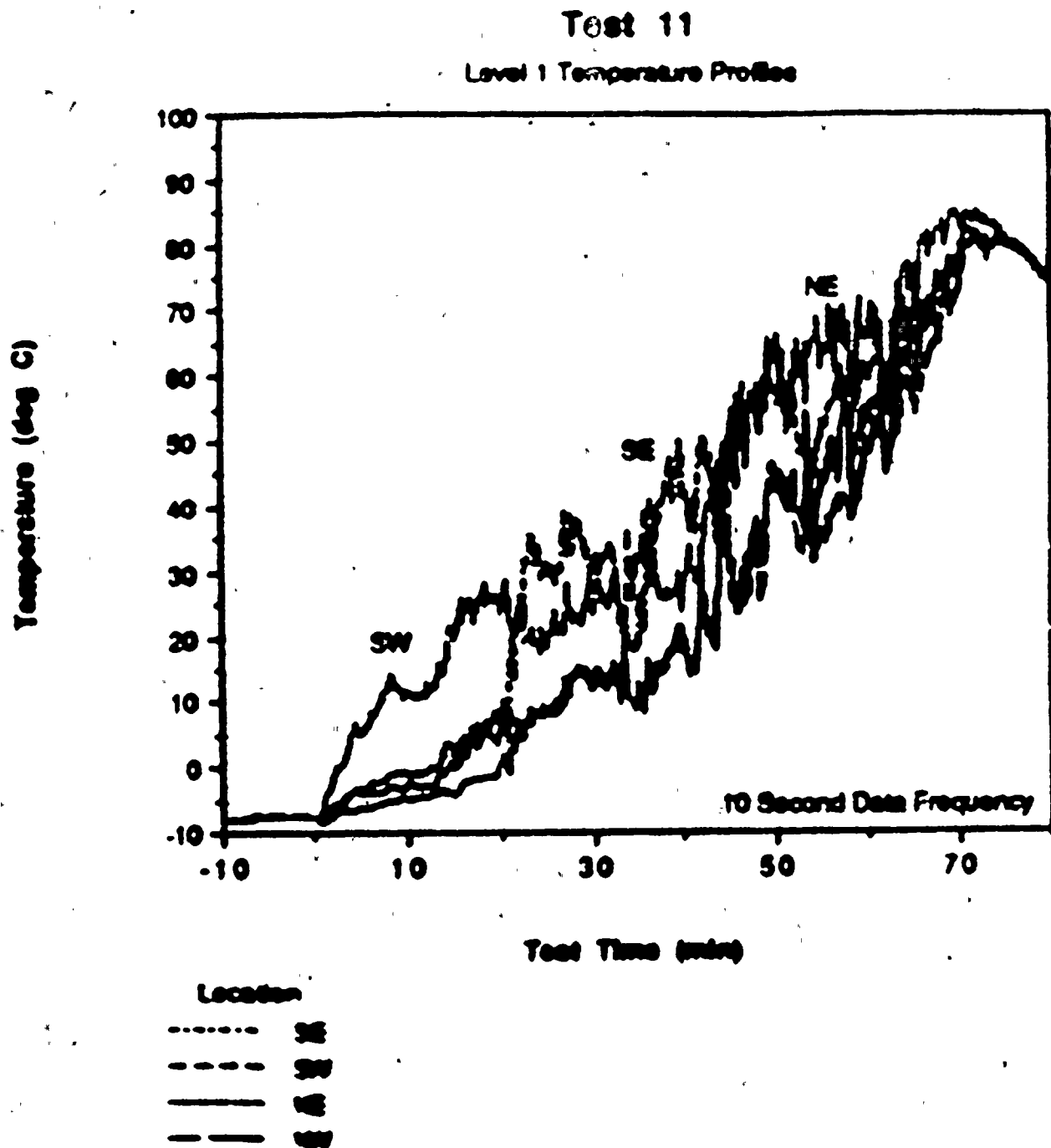


Figure 2:  
Ice-Basket Section Thermal Profiles Near the Exit for Test 13  
[Ligotke, et al., 1991].

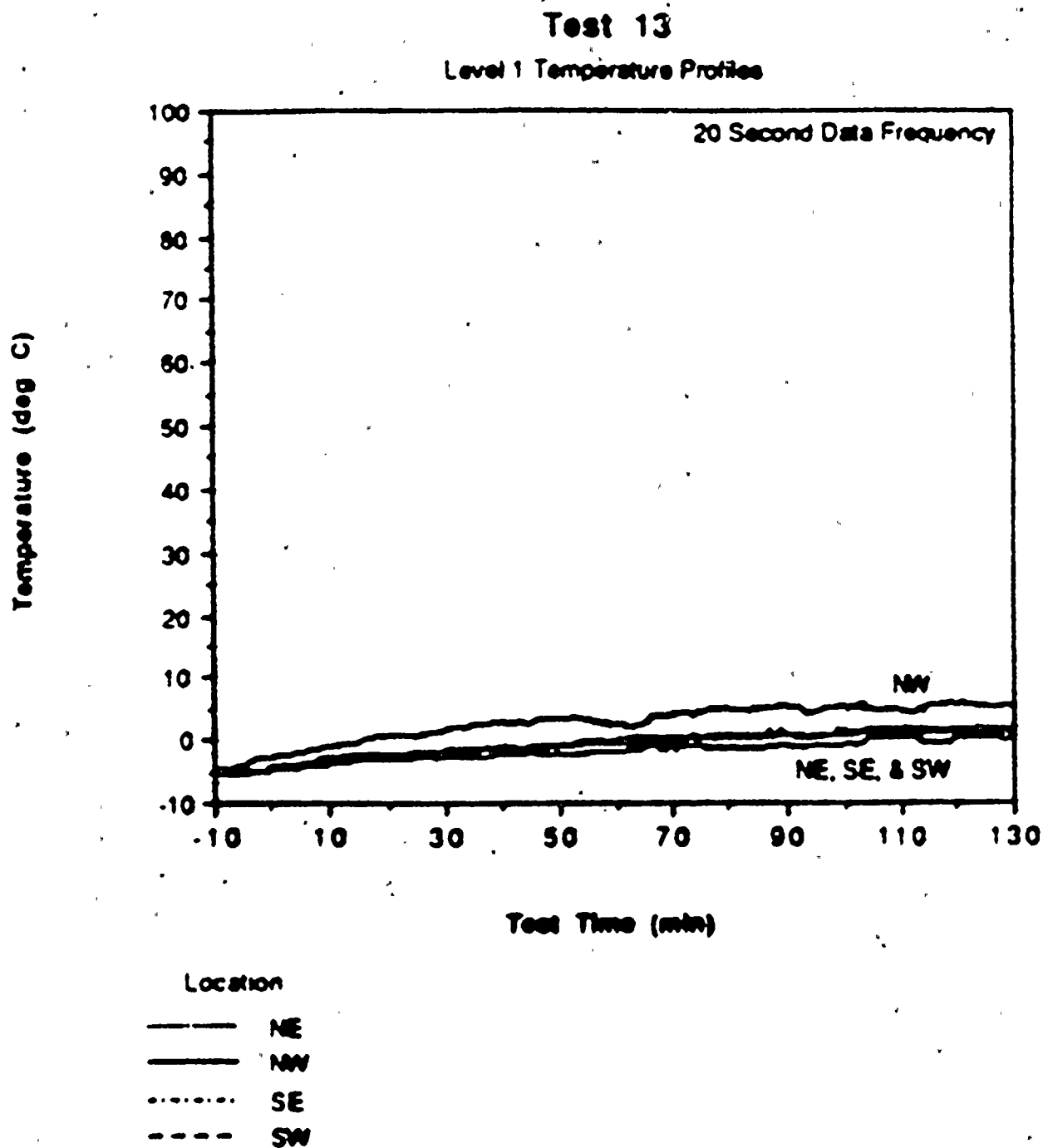
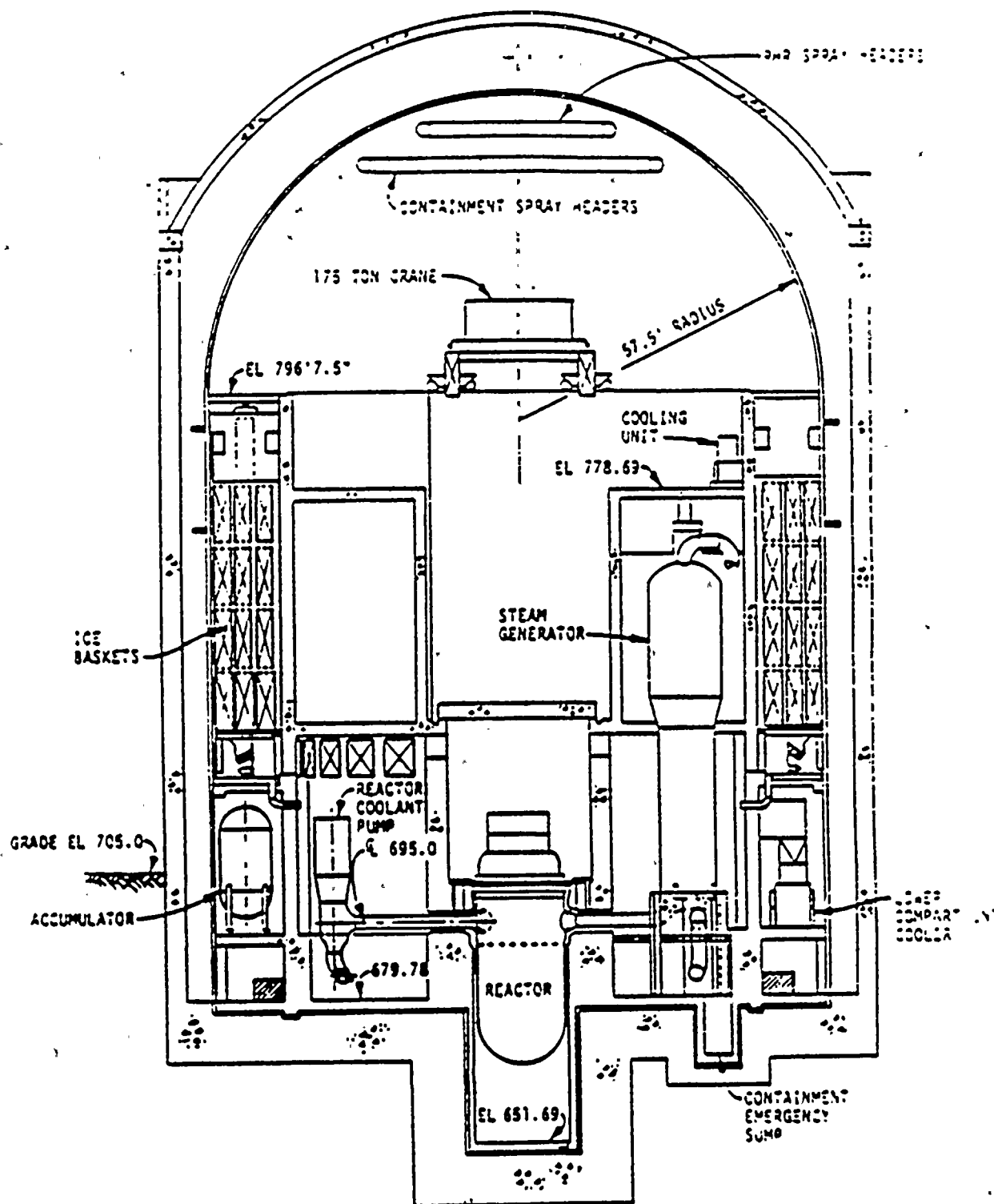




Figure 3: Containment Cross-Section.





intermediate deck doors, and the upper deck doors. Consider the gas/steam flow in the ice condenser as flow through a series of vertical cylinders with the energy transfer limited on the gas side by convection between the gas stream and the ice surface. Assume that this flow can be represented as parallel (inline) flow through the densely packed group of ice columns (the pressure suppression heat sink), as illustrated in Figure 5. Combining this with an additional assumption that the flow is turbulent, the energy transfer rate from the flowing steam and noncondensable gases can be expressed as

$$W_g c_{Pg} \frac{dT_g}{dz} = -(h_c + h_{add}) P_{ht} (T_g - T_{im}) \quad (1)$$

where  $W_g$  is the increasing gas/steam flow rate,  $c_{Pg}$  is the specific heat at constant pressure for the steam and noncondensable gas mixture,  $T_g$  is the gas temperature,  $h_c$  is the turbulent convective heat transfer coefficient,  $h_{add}$  is the effective heat transfer coefficient due to other processes such as natural convection and thermal radiation,  $P_{ht}$  is the heat transfer perimeter for energy transfer (the number of ice baskets (N) times the perimeter of a single basket), and  $T_{im}$  is the ice melting temperature. Representing the turbulent flow convective heat transfer coefficient using Reynolds analogy gives

$$h_c = \frac{f}{2} \rho_g c_{Pg} U_g \quad (2)$$

and substituting this into equation (1), along with the one-dimensional continuity equation for the gas flow rate, results in the following expression for the axial temperature gradient

$$\frac{dT}{dz} = - \left( \frac{f}{2} + \frac{h_{add} A_F}{W_g c_{Pg}} \right) \frac{P_{ht}}{A_F} (T - T_{im}) \quad (3)$$

Separating the variables and integrating yields an expression for dimensionless gas exit temperature ( $\theta$ ) in terms of the turbulent friction factor ( $f$ ), the effective heat transfer coefficient for additional heat transfer processes, the incoming flow, and the ice column geometry;

$$\theta = \frac{T_{g,exit} - T_{im}}{T_{g,in} - T_{im}} = \exp \left\{ \left( -\frac{f}{2} + \frac{h_{add} A_F}{W_g c_{Pg}} \right) \frac{P_{ht}}{A_F} L_I \right\} \quad (4)$$

where  $A_F$  is the cross-sectional flow area, with  $T_{g,exit}$  and  $T_{g,in}$  being the gas/steam exit and inlet temperatures, respectively. Note that the length of the ice column ( $L_I$ ) is in the exponential term for this quasi-steady approach. As the ice mass melts, this length decreases causing the exit gas temperature to increase (assuming all other parameters remain the same).



Figure 4: Ice Condenser Cutaway.

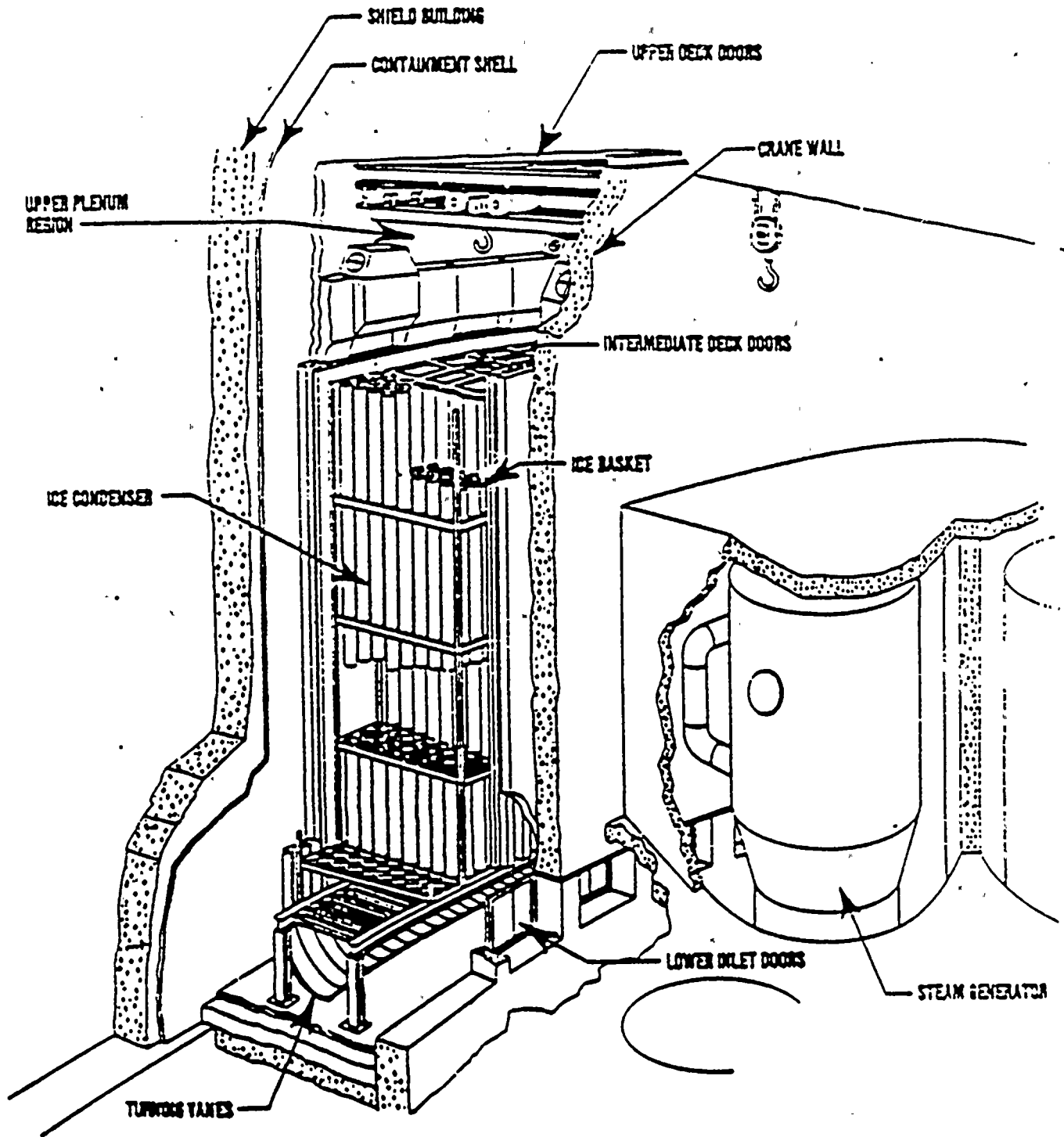
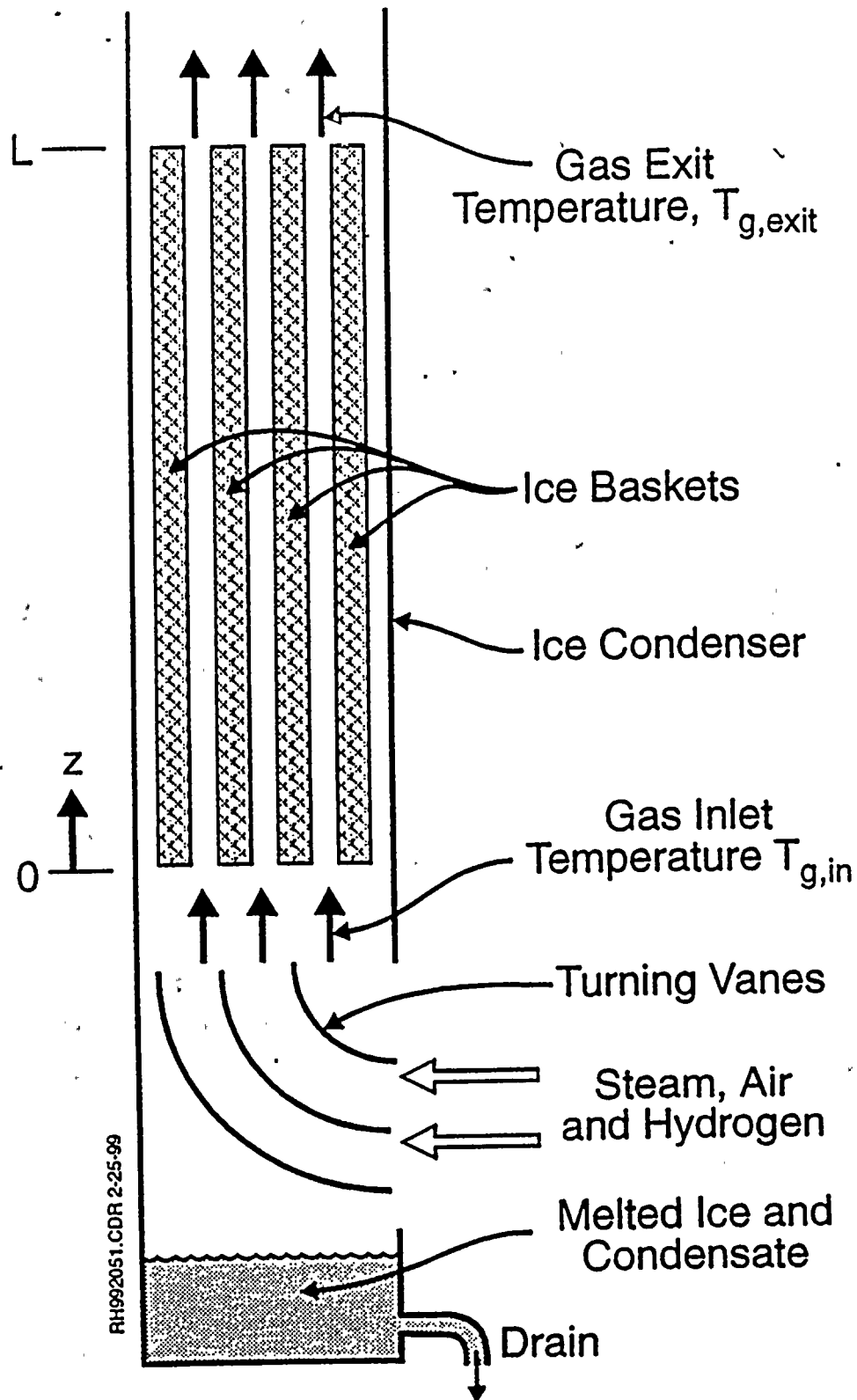


Figure 5: Steam and Noncondensable Flow Through the Ice Condenser.



#### 4.0 VALIDATION

The validation for this routine is through the dynamic benchmarks with the Waltz Mill Westinghouse and PNL ice condenser experiments. These are presented in Volume III of the MAAP User's Manual "Benchmarking". This section should be consulted with respect to the validation exercise.

#### 5.0 NOMENCLATURE

The applicable nomenclature is defined in the text.

#### 6.0 REFERENCES

Ligothe, M. W., et al., 1991, "Ice-Condenser Aerosol Test," NUREG/CR-5768, PNL-7765.

Salvatori, R., 1974, "Final Report: Ice Condenser Full-Scale Section Test at the Waltz Mill Facility," WCAP-8282.



**APPENDIX E**  
**Benchmarking of the MAAP4 Ice Condenser**  
**Model With Waltz Mill Experiments**



**BENCHMARKING OF THE MAAP4 ICE CONDENSER MODEL  
WITH WALTZ MILL EXPERIMENTS****1.0 INTRODUCTION**

Large scale experiments [Salvatori, 1974] were performed to investigate the response of the ice condenser compartment to a spectrum of LOCA conditions. Figure 1 is an isometric view of the experiment which includes:

- a boiler vessel to simulate the reactor coolant system,
- a receiver vessel which simulates the containment,
- a separation of the simulated containment into lower and upper compartments by a divider deck,
- an ice condenser compartment to condense steam entering the upper compartment, and
- eight full-size (diameter) ice baskets with a height which is 3/4 of that used in the D.C. Cook plant.

This integral experiment contains all of the necessary elements of the containment response to investigate the containment capabilities with respect to various LOCA events. Table 1 summarizes the major parameters for the experiment and compares these to a typical ice condenser plant configuration. For this benchmarking effort, various sizes of the LOCA are considered such that the performance of the MAAP4 ice condenser model can be evaluated for a spectrum of initiating events.

Note, due to the proprietary status of this experiment, numeric values have been removed from some of the following comparison plots. Organizations wishing to receive full disclosure of this information must first receive authorization from Westinghouse Electric Corporation.

**2.0 BOUNDARY CONDITIONS**

For these evaluations, it is important to test a variety of break sizes. In this regard, four experiments have been chosen:

- Test A - typical of a design basis large LOCA,
- Test C - a blowdown rate similar to a medium size LOCA,

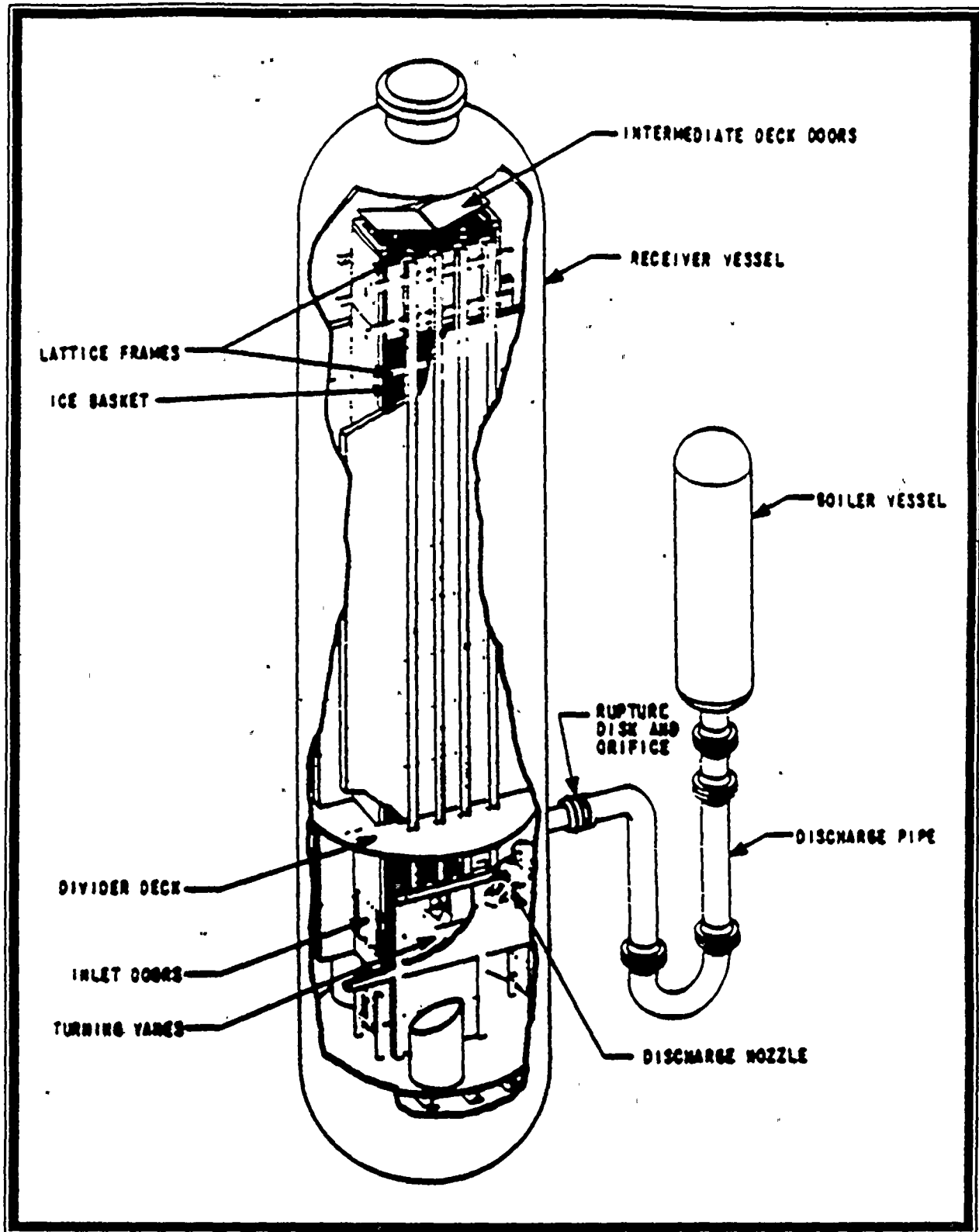


Figure 1 Isometric View of Boiler and Receiver Vessels at the Waltz Mill Test Facility.



**Table 1: Summary of Test Scale Factors Comparison  
With Typical Ice Condenser Plant Design**

Parameter	Plant	Test	Plant/Test Scale Factor
<b>Ice Condenser</b>			
Basket Height (ft)	48	36	1.33
Basket Diameter (in)	12.1	12.1	1.0
Basket Surface Area (ft <sup>2</sup> )	295,400	912	324
Basket Internal Volume (ft <sup>3</sup> )	74,500	230	324
Flow Area (ft <sup>2</sup> )	1,354	5.61	243
Hydraulic Diameter (ft)	0.88	0.88	1.0
Inlet Door Area (ft <sup>2</sup> )	1,064	4.5	236
Ice Weight (lbs)	$2.75 \times 10^6$	8490	324
DECL Blowdown Mass Rate (lbs/sec)	85,000	350	243
DECL Blowdown Energy Rate (BTU/sec) (average over first 1.5 seconds)	$47.5 \times 10^6$	$1.956 \times 10^5$	243
Total Energy Release (Btu)	$320 \times 10^6$	$9.88 \times 10^5$	324
<b>Volumes</b>			
Lower Compartment (ft <sup>3</sup> )	307,000	912	336
Ice Bed (net with ice) (ft <sup>3</sup> )	127,000	315	403
Upper Compartment (ft <sup>3</sup> )	746,000	2,412	309
Total Active Volume (ft <sup>3</sup> )	1,180,000	3,639	325
Compression Ratio	1.42	1.39	1.02

- Test F - a blowdown rate similar to a small LOCA, and
- Test K - a large LOCA followed by post blowdown energy release typical of decay heat.

Through this spectrum of accident conditions, the MAAP4 model can be benchmarked to assess the capabilities for representing the ice condenser response under a spectrum of LOCA conditions. Table 2 summarizes the pertinent initial and boundary conditions for these four experiments.

<b>Table 2: Tabulation of Pertinent Initial and Boundary Conditions For the Full-Scale Section Tests</b>				
	Test A	Test C	Test F	Test K
Date of Test	12/31/73	1/10/74	1/30/74	3/11/74
Initial Boiler Pressure (psig)	1302	1290	1308	1285
Subcooling (°F)	26	43	45	63
Orifice Diameter (in)	2.57	0.76	0.295	2.57
Percent Plant Blowdown Mass Rate	101	11	1.65	130
Percent Plant Blowdown Energy Rate	101	10	1.6	117
Percent Plant Blowdown Energy	137	132	114	Note (1)
Initial Upper Compartment Temp. (°F)	99	77	81	
Initial Lower Compartment Temp. (°F)	78	64	75	
Boiler Energy Discharge (Btu's x 10 <sup>6</sup> )	1.55	1.53	1.53	3.6
Net Energy Discharge (Btu's x 10 <sup>6</sup> )	1.35	1.30	1.13	
(1). Blowdown + post blowdown energy release.				

The necessary information for each of these experiments is contained in MAAP4 subroutine BCHICE, which is called from subroutine BENCH. This new subroutine characterizes the information necessary to perform each benchmark and this is performed in the following manner.

The following quantities are input to the code, either through the input deck or directly in BCHICE.

- vessel volume,

- discharge pipe volume,
- initial boiler vessel pressure,
- initial water subcooling in the discharge pipe,
- total energy available,
- measured blowdown pressure vs. time for the given experiment, and
- post blowdown steam flow rate vs. time for Test K.

With the information for each experiment the following calculations are performed:

- Mass of water in the discharge pipe equals the pipe volume divided by the specific volume of the subcooled water.
- The energy in the boiler vessel is equal to the total energy minus the energy in the subcooled water in the pipe.
- The combination of the vessel volume and energy are solved simultaneously to determine the mass of saturated steam and water in the boiler vessel.

Once the mass of subcooled and saturated water is determined, the MAAP4 subroutine WFLOW is called based on the measured pressure at a given time and the orifice break area. Subcooled blowdown calculations are performed until the mass lost equals the mass of subcooled water, at which point the remaining blowdown is assumed to be a saturated two-phase mixture. Once the blowdown transitions to steam alone, the specific volume of the steam is determined by the total volume divided by the calculated remaining mass and the steam enthalpy is assumed to be the saturated value based upon the measured pressure.

The MAAP4 containment model is set up with five nodes:

- the lower compartment bottom node,
- the lower compartment upper node,
- the ice condenser,
- compartment directly above intermediate deck doors, and
- the annular section of the upper compartment which surrounds the ice condenser.

The experimental report provides little information on the heat sinks for the test apparatus, other than to say that the surfaces were insulated. For the longer running tests, such



as the small LOCA case Test F, and the decay heat experiment Test K, small contributions of heat sinks are important. From these benchmarks, we assume steel mass of 3600 lbm for the ice baskets and their supports and a heat sink surface area of 200 ft<sup>2</sup> is assumed for the annular compartment attached to the upper compartment. These are minimal values for the heat sinks that would be available, but as is discussed later, are sufficient for these benchmarks.

There is a limited description available for the steam injection into the lower plenum for the different experiments, particularly that for the small break representation Test F and the long term decay heat injection for Test K. Since the principle means of pressurizing the test facility is displacement of noncondensable gases from the lower compartment and the ice condenser to the upper compartment, this displacement process is an important aspect of the numerical model. Since there is limited information available, the MAAP model divides the lower plenum into two nodes (the top node and the bottom node) and splits the incoming flow rate into contributions to the two different nodes. For Tests A and C, which represent large and medium size breaks, the incoming steam flow was divided into equal portions for the top and bottom node. Also, for Test K, since the recirculation fan was running during the long term steam release, the incoming flow rates were again divided into equal portions for the top and bottom node. For Test F, the small break LOCA, which was performed without any recirculation fan flow, the incoming steam flow is divided with 80% going to the upper node and 20% to the bottom node to represent the potential stratification of the low flowing steam discharge into the lower compartment resulting from this small break simulation. If additional information becomes available regarding the details of the lower compartment injection, in particular for the small break representation in Test F, this modeling aspect can be further refined.

Major parameters controlling the behavior in the ice condenser evaluations are FTWICE and FCONDP. The best estimate values for these are 0 and 2, respectively, with the former representing the condition in which the ice condenser drain temperature is the average of the steam inlet and the ice melt temperatures; and the latter configures the energy transfer between the lower compartment steam space and water masses in terms of an agitated pool with an agitated gas space. In particular, there is no significant condensation if a colder gas layer could be developed above a water pool which does not circulate. This is not to be expected since there is a large water drainage rate as the ice melts and this tends to induce a well-mixed circulation pattern between the two nodes in the lower compartment, as well as individually within the gas and water volumes. The other values for these two parameters that are considered include FTWICE = 1, which is a condition where the drain temperature is the average of the steam inlet temperature and the steam exit temperature. This is always used for conditions in which the noncondensable gas flow rate through the ice condenser is sufficient to "flood" the water drainage. However, this value can also be used in sensitivity analysis to show the influence of such an assumed behavior on the ice melt rate. Values of FCONDP = 0 and 1 are also possible with the former indicating no condensation on the water pool and a value of unity indicating that as condensation occurs a stable cold gas thermal layer develops next to the water pool which dramatically reduces the condensation rate. The results of these various model parameters are compared to the Waltz Mill experiments below.

### 3.0 DISCUSSION OF RESULTS

In the best-estimate evaluations, the MAAP4 ice condenser model uses values of  $FTWICE = 0$  and  $FCONDP(1) = 2$ , with the temperature of the air and steam leaving the top of the ice condenser being determined by the mechanistic model. Figure 2 compares the measured containment response and that calculated by the MAAP4 model for Test A. As illustrated, the MAAP4 model provides a good characterization of the containment pressurization, including the peak pressure achieved during the blowdown history, and the subsequent depressurization as the mass discharge rate decreases during later stages of the blowdown. It is not surprising that MAAP provides a reasonable characterization of the upper compartment pressure history since this is generally due to the displacement air from the lower compartment to the upper compartment, with a minor contribution due to the increased steam partial pressure in the upper compartment. Figure 2 shows that MAAP4 somewhat underestimates the upper and lower compartment pressures. This is likely due to the simplified view that the integral code has of the loss coefficients through the ice condenser inlet doors and through the ice mass itself, and also the result of not modeling small leakages past the divider plate for the upper compartment responses.

Figure 3 shows the remaining ice mass for the large break representation. MAAP4 provides an excellent characterization of the total ice mass melted in this experiment. Comparisons of this nature help determine the uncertainty bands to be considered in the integral containment model for parameters. This will be discussed further for the other tests considered at the end of this section.

Of particular interest for small break evaluations are those experiments with smaller effective break areas. Figure 4 illustrates the measured pressure history for Test C, which is representative of a medium size LOCA. As shown, there is good agreement between the pressurization of the simulated containment as well as good agreement between the pressure differential between the upper and lower compartment for this experiment. Furthermore, as illustrated in Figure 5, the MAAP calculation underestimates the melted ice mass. It is important to note in these calculations that the representation for pressure vs. time given in Test C still has a considerable pressure after 130 seconds, which is the value reported in the experimental test report. Hence, there was an additional blowdown of steam through the test facility and additional ice melting that would be typical of the value determined when the apparatus was disassembled at the end of the test. To examine the influence of additional blowdown energy, the MAAP4 benchmark was continued until the system was essentially depressurized, i.e., about 180 secs. At this time, the calculated ice mass available is 5000 lbm compared to the reported value of 4625 lbm. Thus, the MAAP model is in agreement with the results of the experiment and conservatively underestimates the ice melting rate.

Of particular interest for break evaluations are the results of Test F and Test K since these represent a blowdown of a typical small break (Test F) and the ice melt associated with long term decay heat steam generation added to the containment (Test K). The results for the measured upper and lower compartment pressures as a function of time are shown in Figure 6

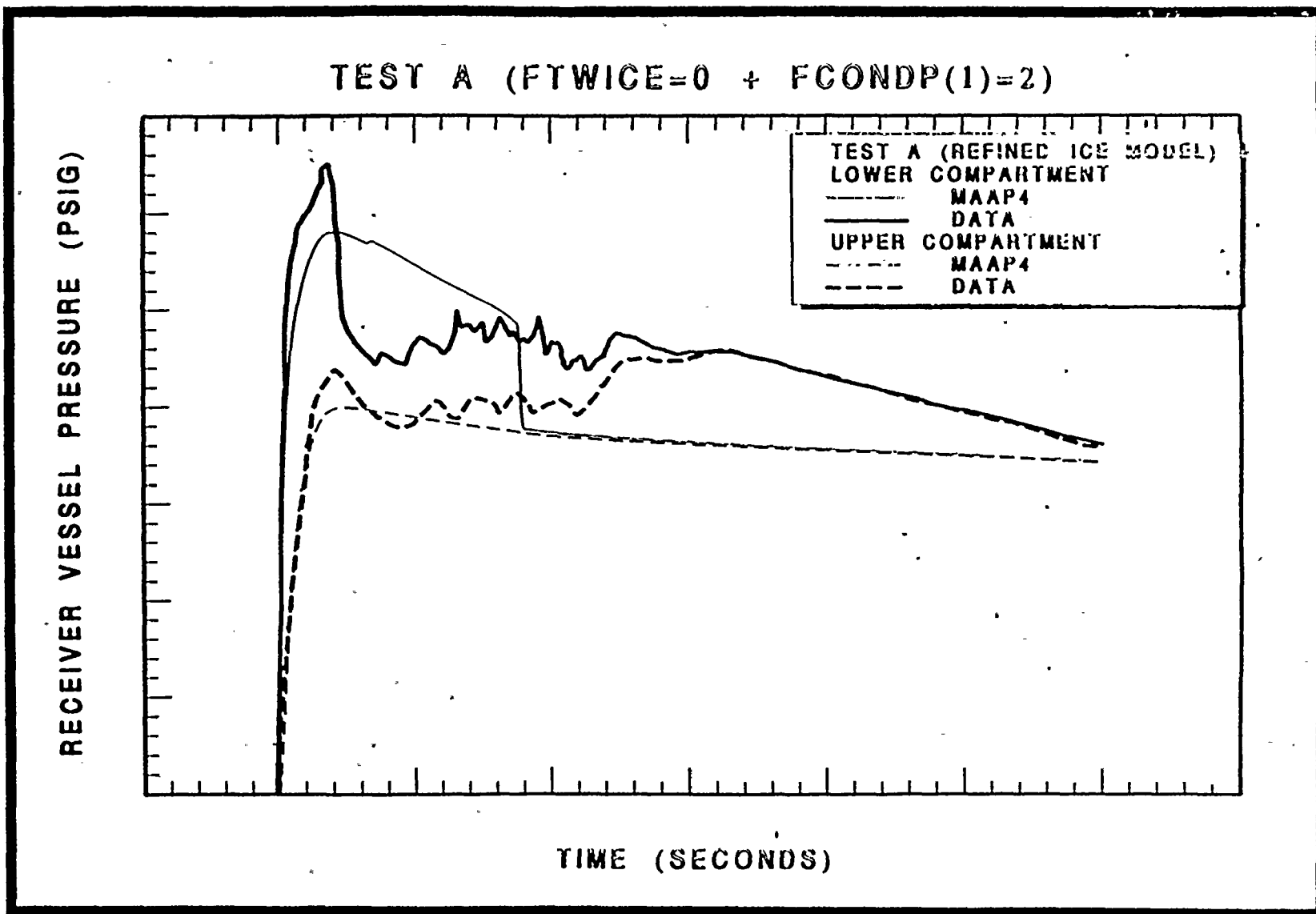


Figure 2: Comparison of the Upper and Lower Compartment Pressures for the MAAP4 Containment Model and the Experimental Data from Test A (large break LOCA) of the Westinghouse Ice Condenser Experiments.





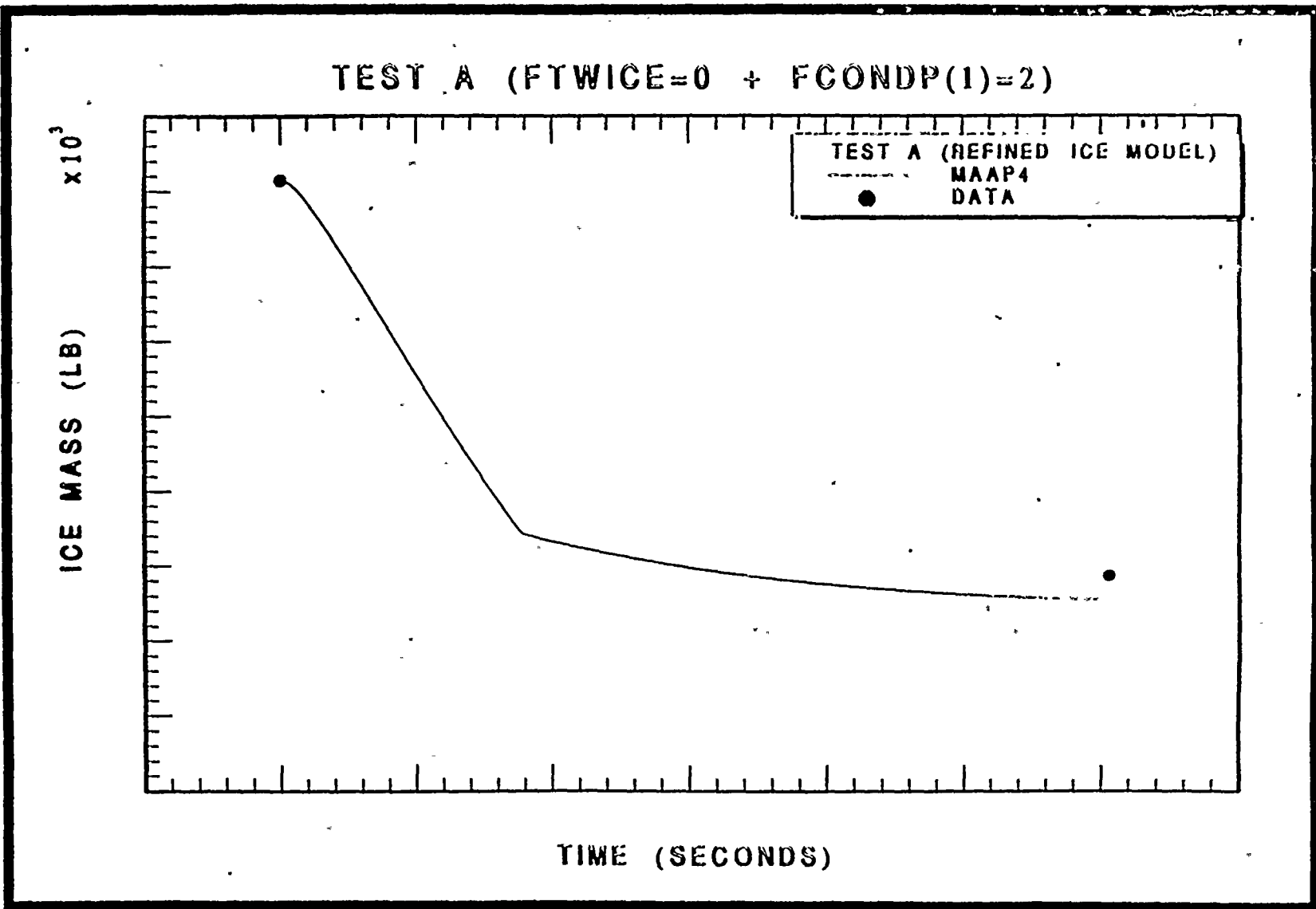


Figure 3: Comparison of the Calculation of Ice Melting for the MAAP4 Model and the End Point Remaining Ice Mass for Test A (large break LOCA).

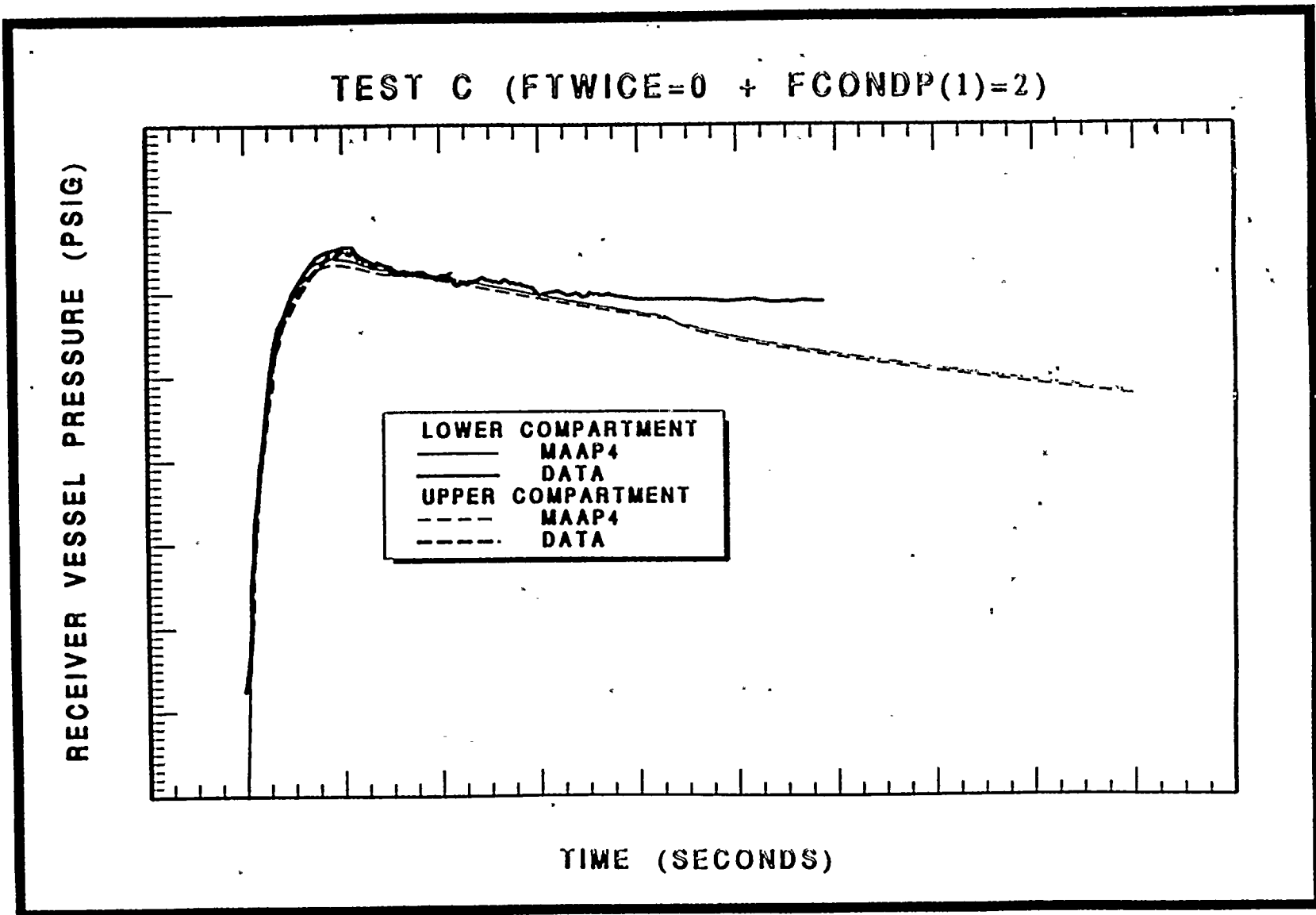


Figure 4: Comparison of the Upper and Lower Compartment Pressures for the MAAP4 Model With the Measured Behavior of Test C (medium LOCA).

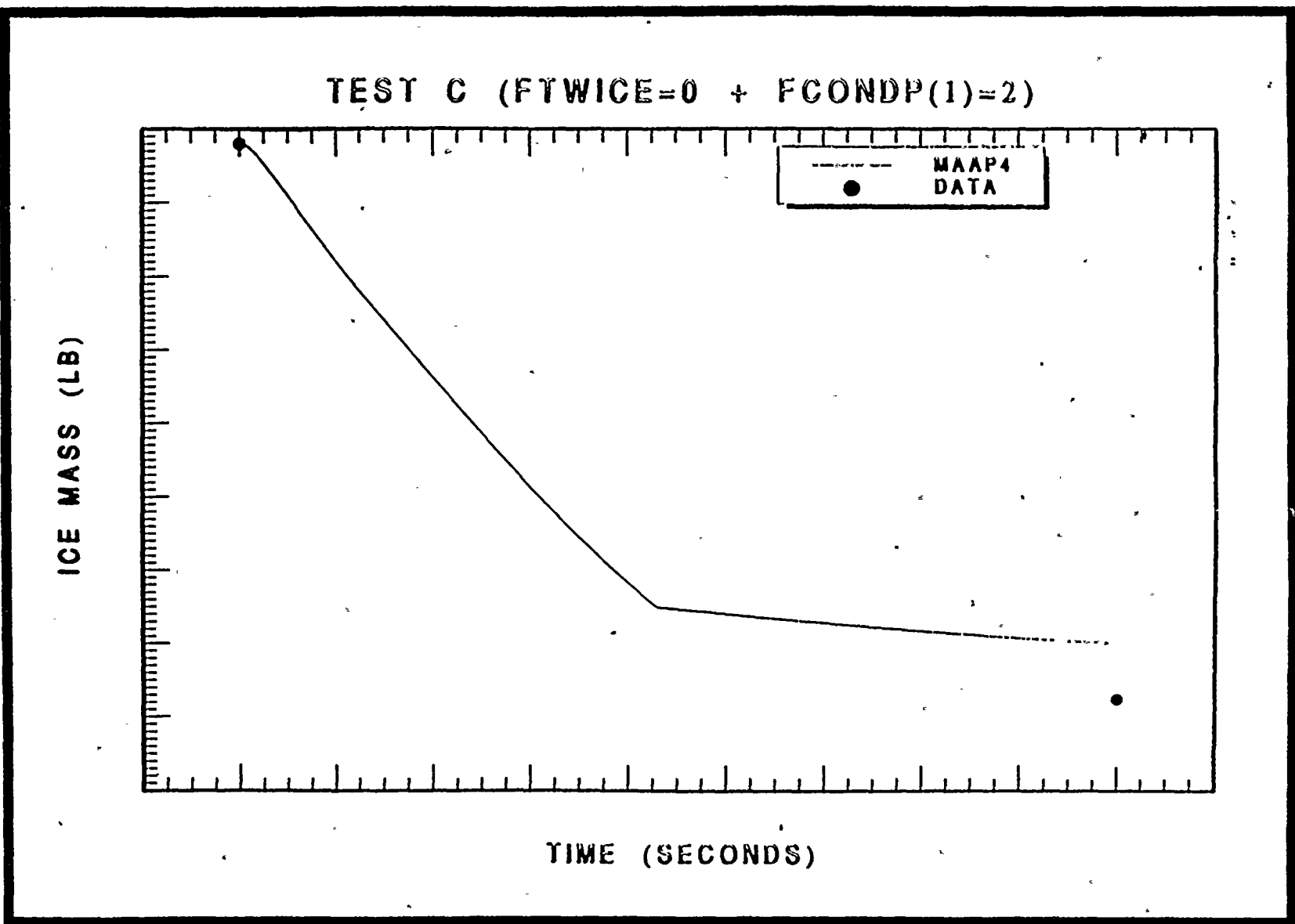


Figure 5: Comparison of the MAAP4 Ice Melt History With the Measured Ice at the End of Test C (medium LOCA).

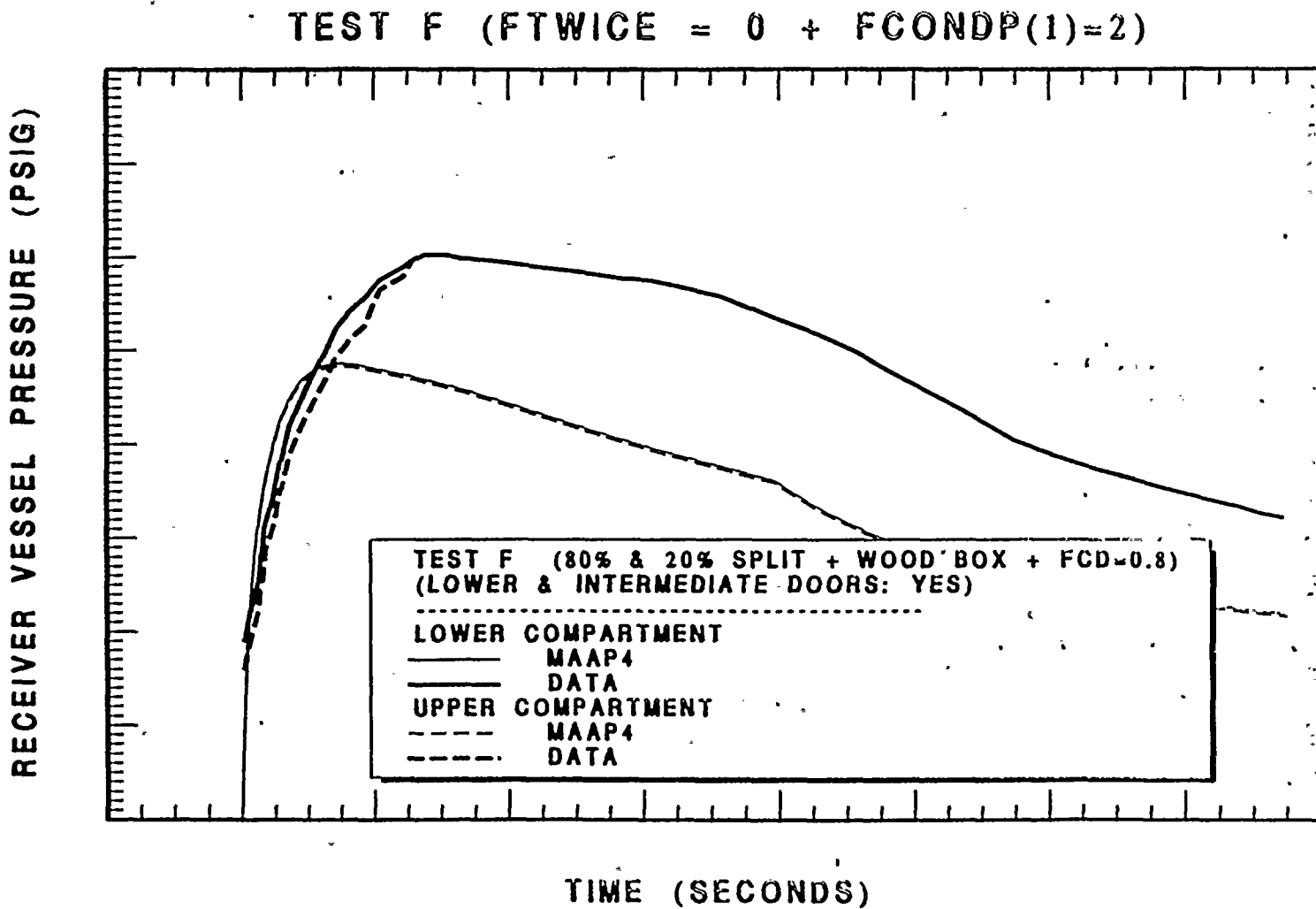


Figure 6: Comparison of the Measured Upper and Lower Compartment Pressures for Test F (small LOCA) and the MAAP4 Calculation.



for Test F. There is agreement with the rate of pressure increase developed in the test apparatus and the overall pressure transient. However, the peak pressure is somewhat underestimated, which is a function of the split imposed for the incoming steam flows into the lower compartment nodes. The remaining ice mass is illustrated in Figure 7 for Test F and it is shown that the MAAP4 model provides a reasonable representation of the ice mass melted during the test.

Test K had a different characterization from the previous experiments with the initial blowdown being that typical of a large break LOCA, similar to Test A. Subsequently, the steaming rate was decreased to that typical of decay heat to examine the longer term ice melt conditions. The steam was provided by an external boiler, with the steam being added to the lower plenum of the simulated containment. Since the steam rate was low, the details of the heat sinks in the apparatus become important, and as discussed above, these are only described in general in the test report. However, there is sufficient information to test the overall performance of the MAAP4 model. Since Test K is a large blowdown characterization, the initial phase was modeled in the same way as Test A, and at the end of the blowdown, a remaining ice mass of 5,776 lbm was input to the calculation to be consistent with the values described in the test report. Figure 8 illustrates the measured and calculated pressure histories for the long term behavior. As illustrated by Figure 9, the MAAP4 calculation melts the ice at about 4500 seconds which is preceded by some pressurization of the test vessel. The pressurization rate illustrated in the calculation compared to that from the experiment illustrates that the heat sinks in the experiments are more influential than those considered in the benchmark. However, further detailed representation in the heat sink model will only improve the comparisons illustrated for the other experiments, and in particular, will improve the agreement for Test A. For Test K, the recirculation fans are included such that the steam delivered to the apparatus in the benchmark flows into the lower compartment and thus to the ice condenser. If there are significant heat losses in the lower compartment, this decreases the net energy flow to the ice condenser and lengthens the experiment, which is the anticipated behavior given the comparison shown in Figure 8. However, the available benchmark is sufficient to show that the MAAP4 model can be used to characterize the ice condenser performance for a spectrum of plant conditions.

Figure 10 illustrates the incoming temperature to the ice condenser (TWSTI) throughout the Test K transient and the calculated exit temperature from the mechanistic model (TEX01). As is noted, the calculated exit temperature increases as the ice inventory is consumed and eventually approaches the incoming air-steam temperature when the ice melt is almost complete. Figure 11 compares the measured and calculated results for the melted ice drainage temperature in the bottom of the ice condenser. There is good agreement between the two with the long term MAAP calculation being somewhat higher than the measured data. A similar comparison for the water temperatures in the lower compartment is shown in Figure 12 which illustrates excellent agreement between the MAAP calculation and the measured behavior. With these good comparisons of the calculated ice melt rate and the water temperatures, the MAAP model is demonstrated to give a good representation of the energy transfer processes in this large scale ice condenser experiment.

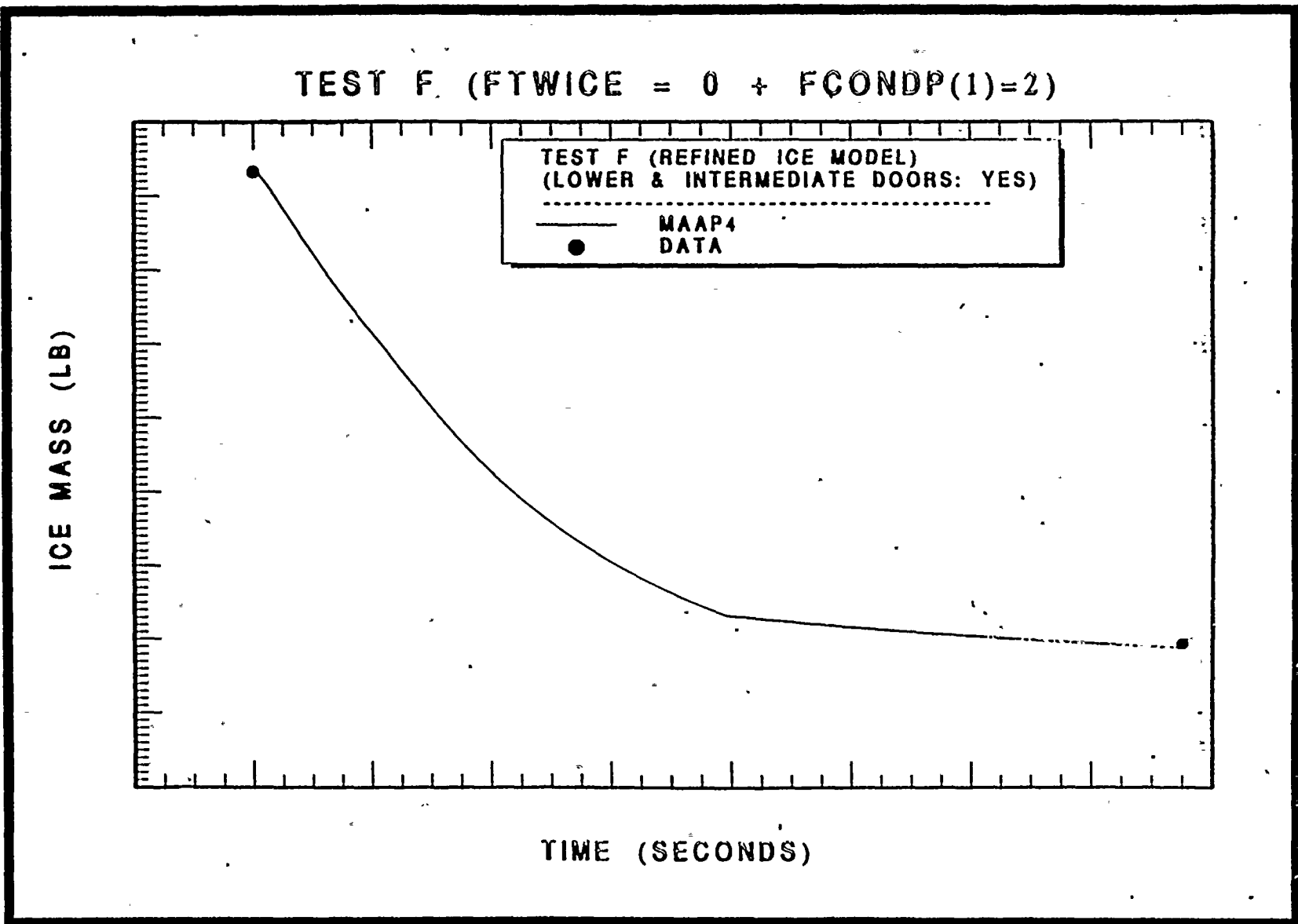


Figure 7: Comparison of the Measured Remaining Ice Mass With that Calculated from the MAAP4 Model for Test F.

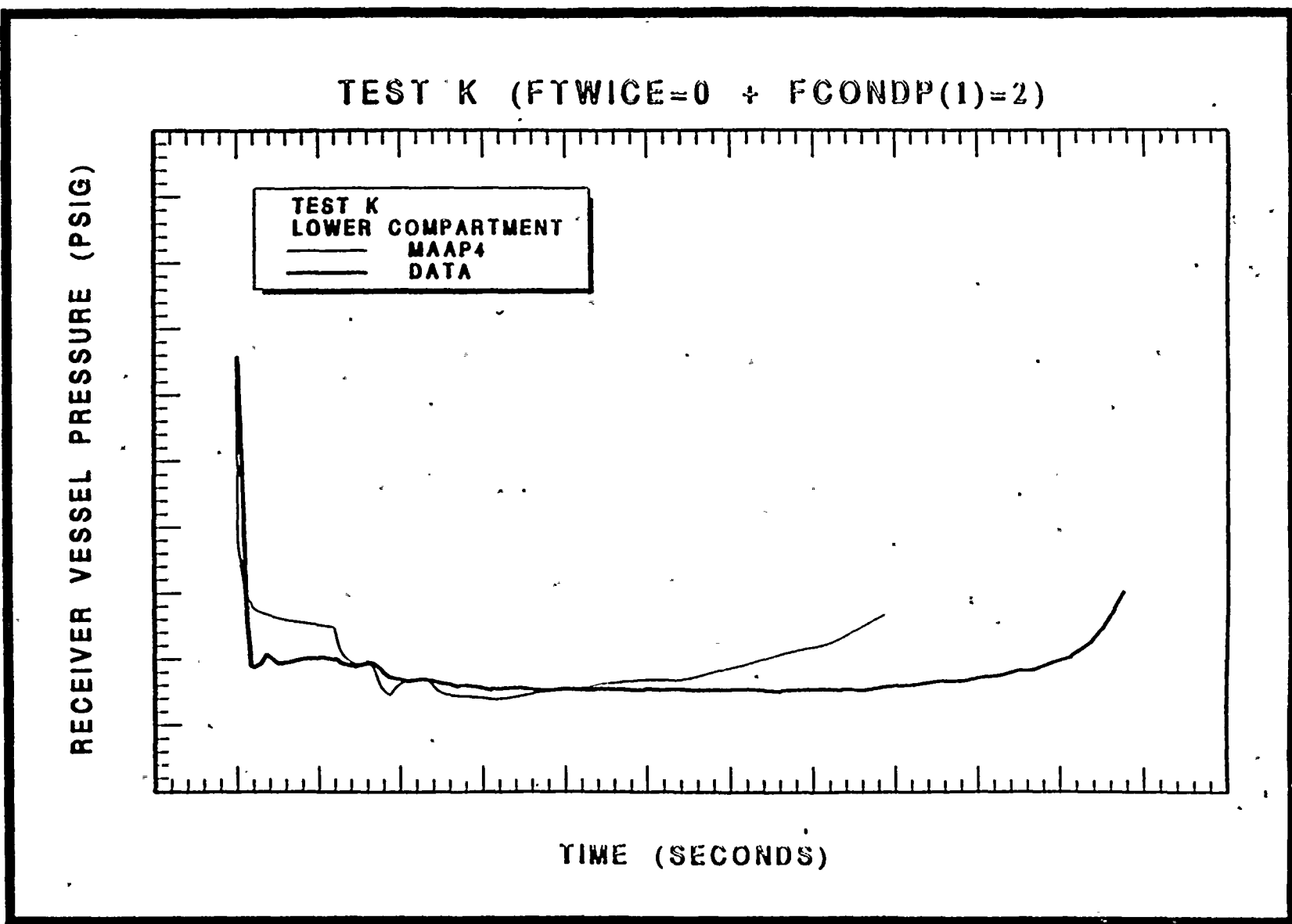


Figure 8: Comparison of the Measured Upper and Lower Compartment Pressures for Test K and the MAAP4 Calculation.



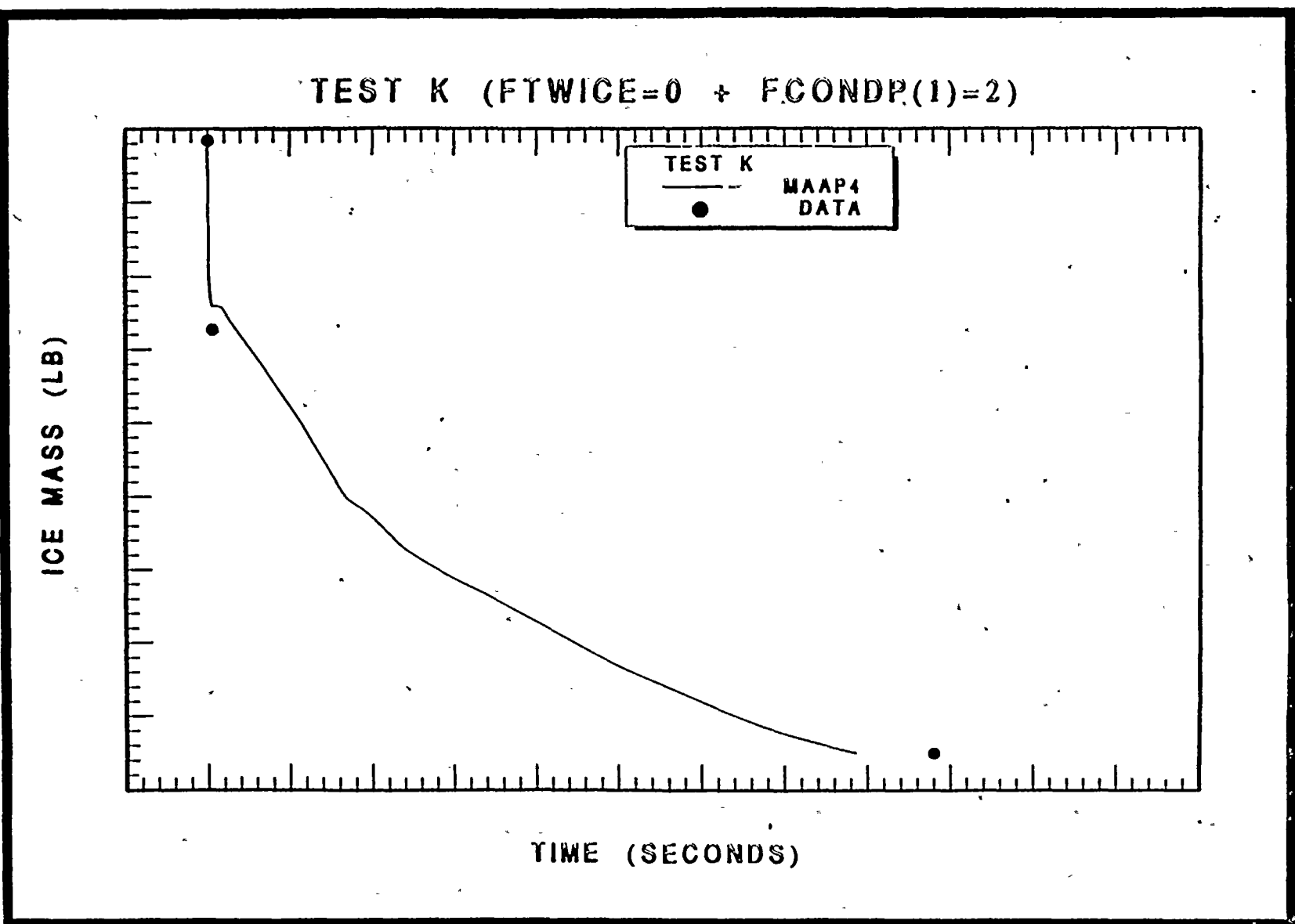
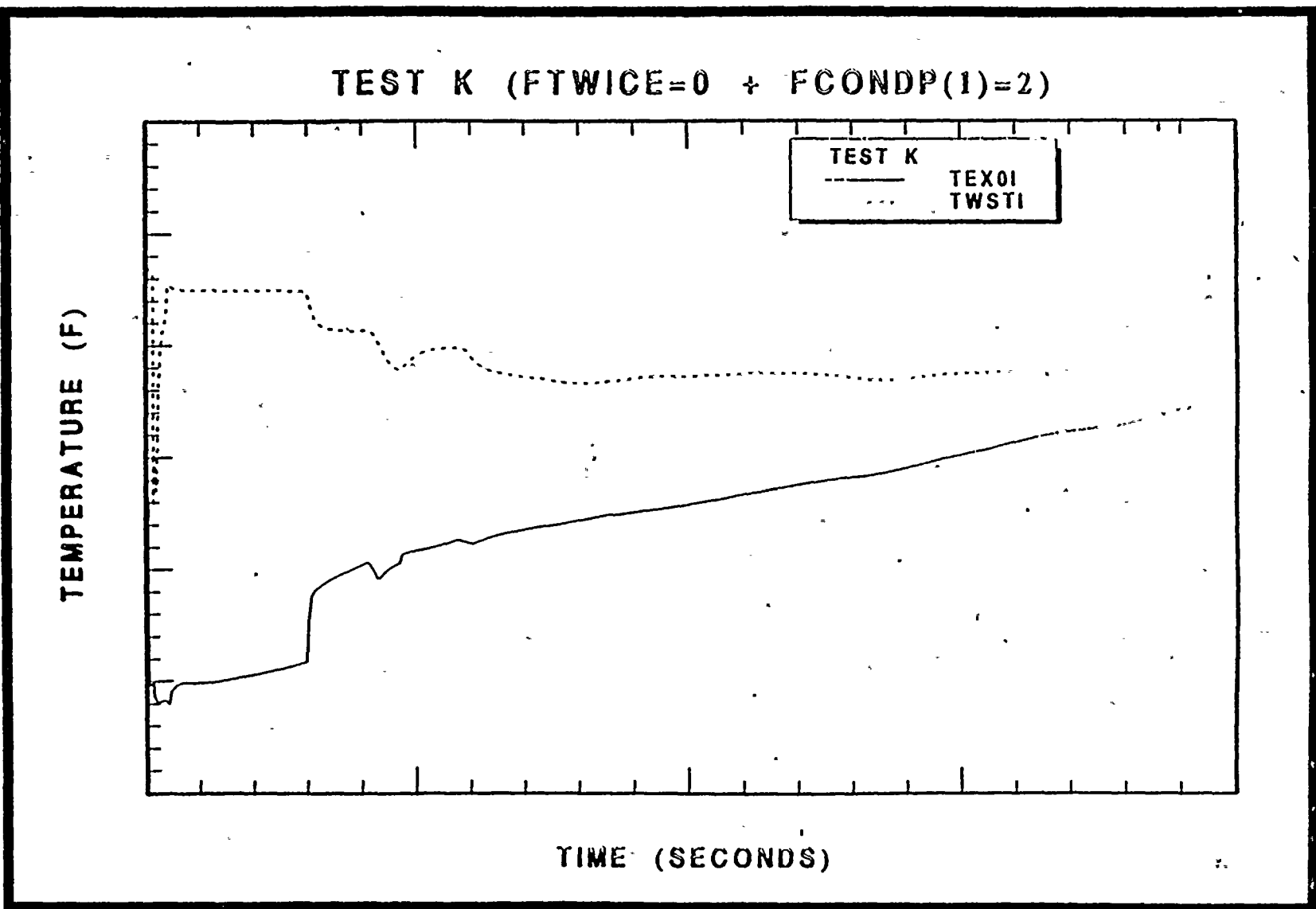


Figure 9: Calculated Ice Mass Melting History for Test K.





**Figure 10:** Calculated Values of the Incoming Steam Temperature and Ice Condenser Exit Temperature Using the Mechanistic MAAP Model.



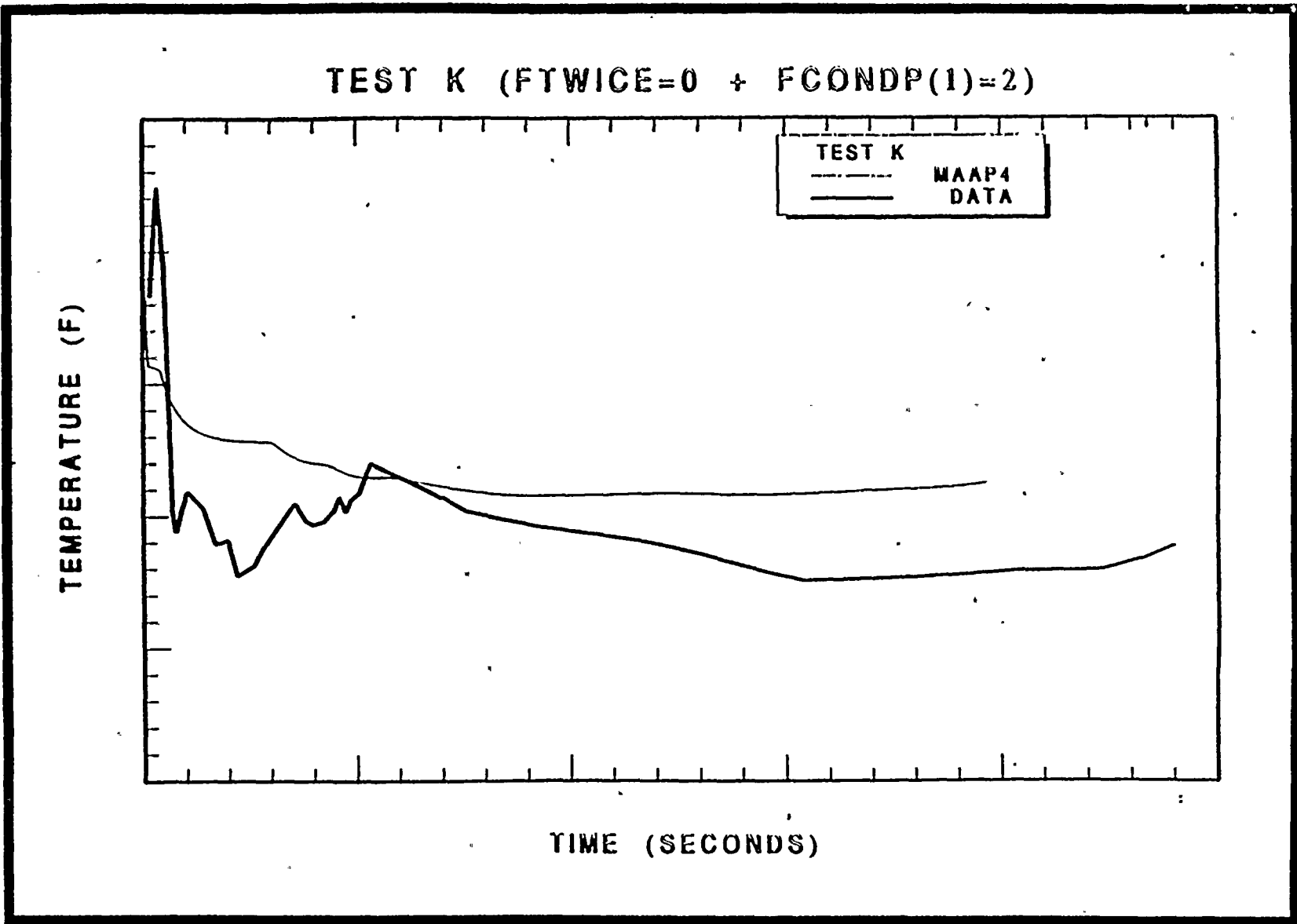


Figure 11: Comparison of the Measured Calculated and Measured Ice Melt Drainage Temperatures for Test K.



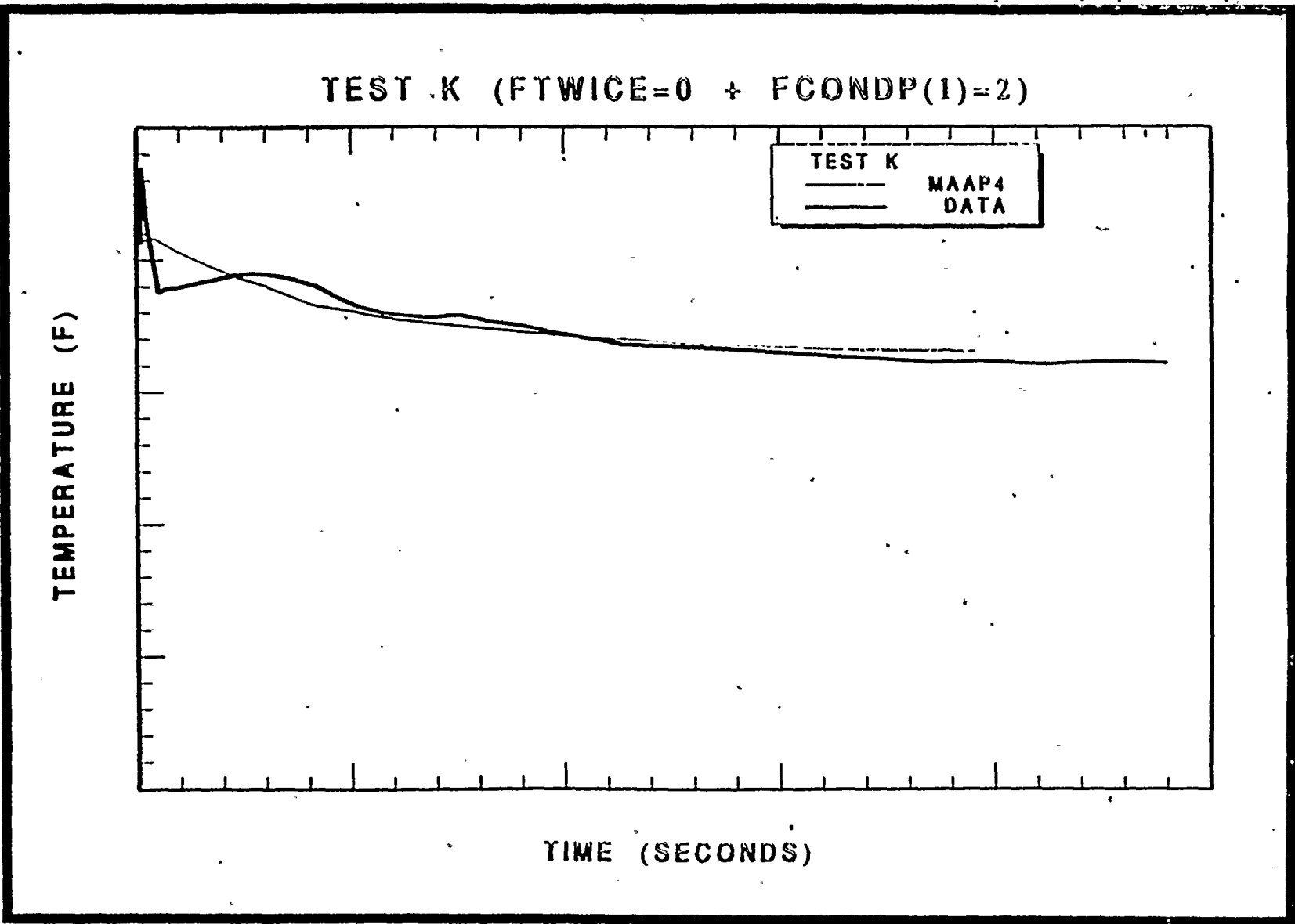


Figure 12: Comparison of the Calculated and Measured Temperatures of the Water in the Lower Compartment for Test K.

#### 4.0 SENSITIVITY STUDIES

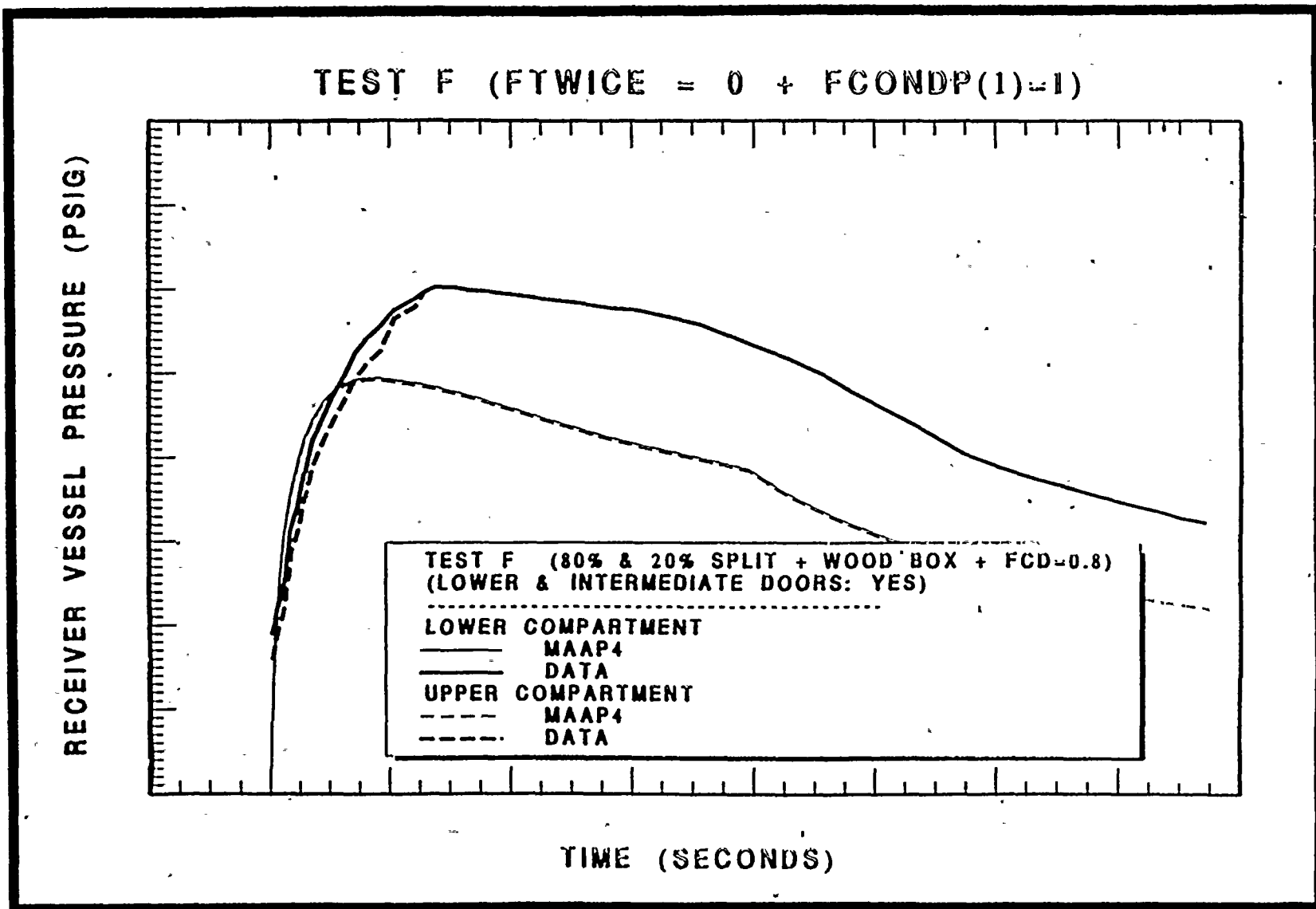
The most sensitive parameter in the evaluation with the Waltz Mill experiments is the potential for condensing steam on the water surface in the lower compartment. If such condensation does not occur, the steam mass flow rate into the ice condenser is significantly increased and the ice melting rate is accelerated. Furthermore, the measurement of the water temperatures in the lower compartment is also affected. This change has little influence on the large break sequences such as that represented by Test A, but for the small break in long term steaming behavior as depicted in Tests F and K, respectively, the influence of steam condensation in the lower compartment is important. Figures 13 and 14 compare the calculated pressure and ice mass remaining for Test F if the condensation in the lower compartment is evaluated as if a stable thermal layer develops next to the water surface. As illustrated, this results in an increased ice melting rate compared to that shown in Figures 6 and 7. Furthermore, the calculated performance of Test K (see Figures 15, 16, 17, and 18) compare the calculated performance for Test K with this model parameter variation with the measured data. As illustrated in Figure 16, the ice is melted out approximately 1,000 sec. earlier and the comparison with the measured temperature in the lower compartment (Figure 18) does not have the same level of agreement, as is shown in Figure 12. Hence, while this is a variation in the modeling behavior, comparisons with the experimental results indicate that the gas space in the lower compartment is well agitated, as is the water pool, as a result of the drainage from the ice condenser. Hence, the recommended values for condensation on such water pools is with the parameter  $FCOND(1)=2$  is the preferred model configuration.

Another sensitivity examined is the influence of the imposed flow split for the incoming steam flow in Test F. Figures 19 and 20 illustrate the influence of using a 50-50 split for this test. It is observed that the rate of pressure increase is much faster than the experimentally measured pressure, but the peak pressure is close to the measured value. Comparing the calculated ice mass melted with that shown in Figure 7 shows that an equal split of the imposed flow melts slightly less ice than observed in the experiment.

#### 5.0 CONCLUSIONS

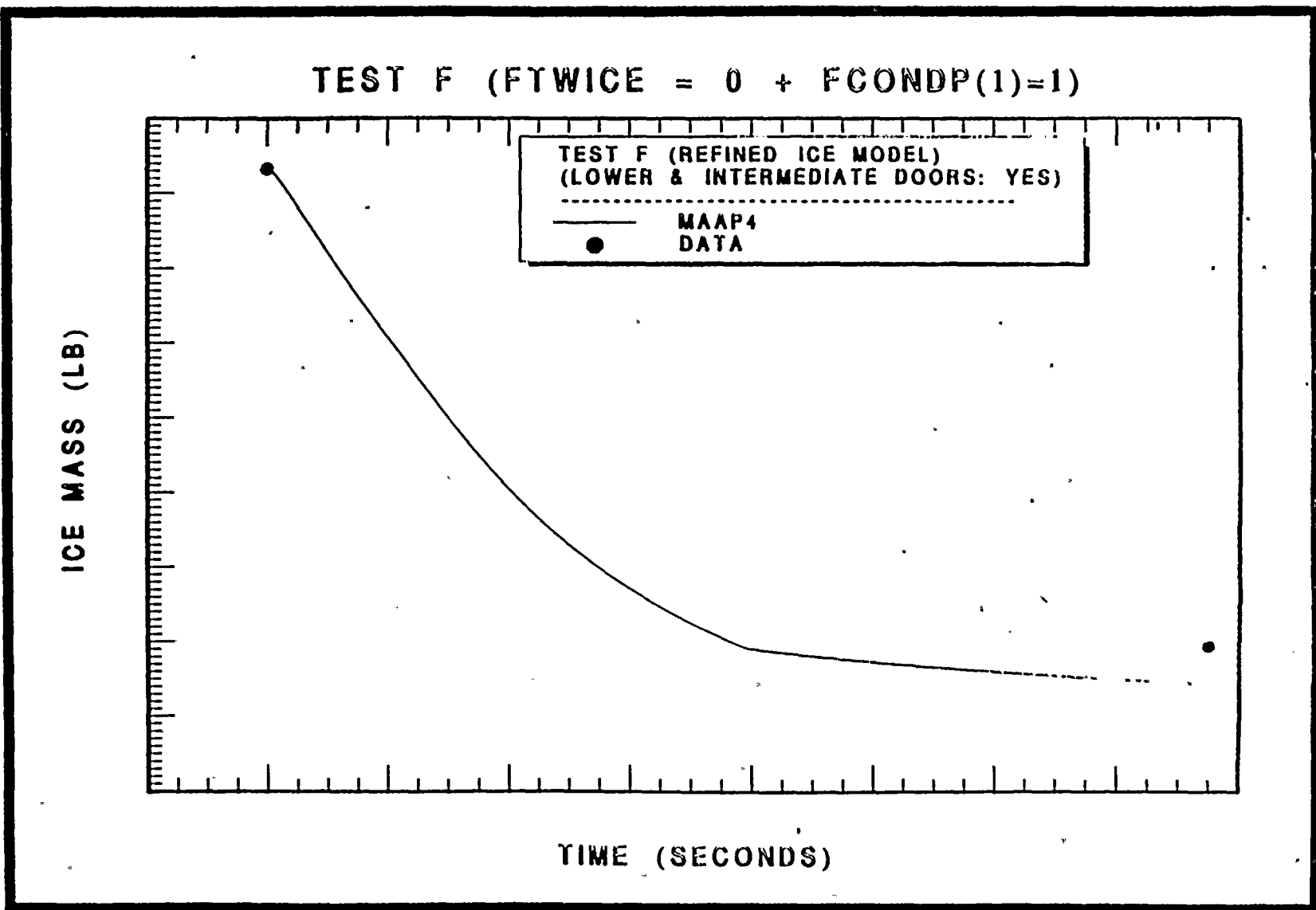
Comparing the MAAP4 ice condenser containment model with a spectrum of LOCA experiments shows that the MAAP4 characterization provides good agreement with the behavior for the various size LOCA conditions investigated, including long term decay heat added to the containment atmosphere. Furthermore, it shows that the MAAP4 mechanistic ice melt model provides a good characterization of the ice melt for a wide spectrum of accident conditions, including long term decay heat steam release. The model also provides a good representation of the ice melt drain temperature and lower compartment water temperature.



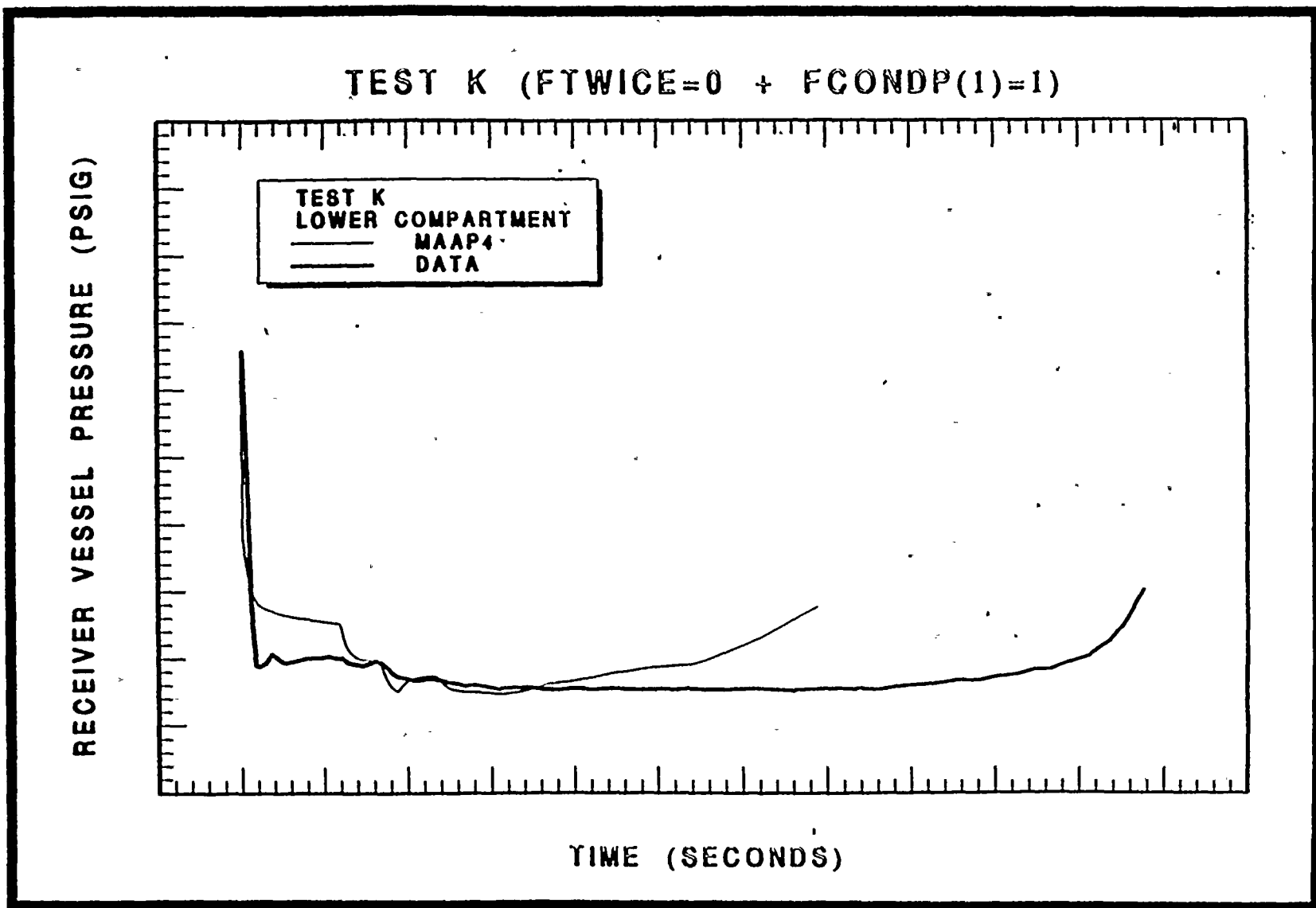


**Figure 13:** Comparison of the Calculated and Measured Vessel Pressure for Test F Assuming No Agitation in the Lower Compartment Gas Space.

1. The first part of the document is a list of names and addresses of the members of the committee.



**Figure 14:** Comparison of the Calculated and Measured Ice Mass Remaining for Test F Assuming No Agitation in the Lower Compartment Gas Space.



**Figure 15:** Comparison of the Calculated and Measured Vessel Pressure for Test K Assuming No Agitation in the Lower Compartment Gas Space.



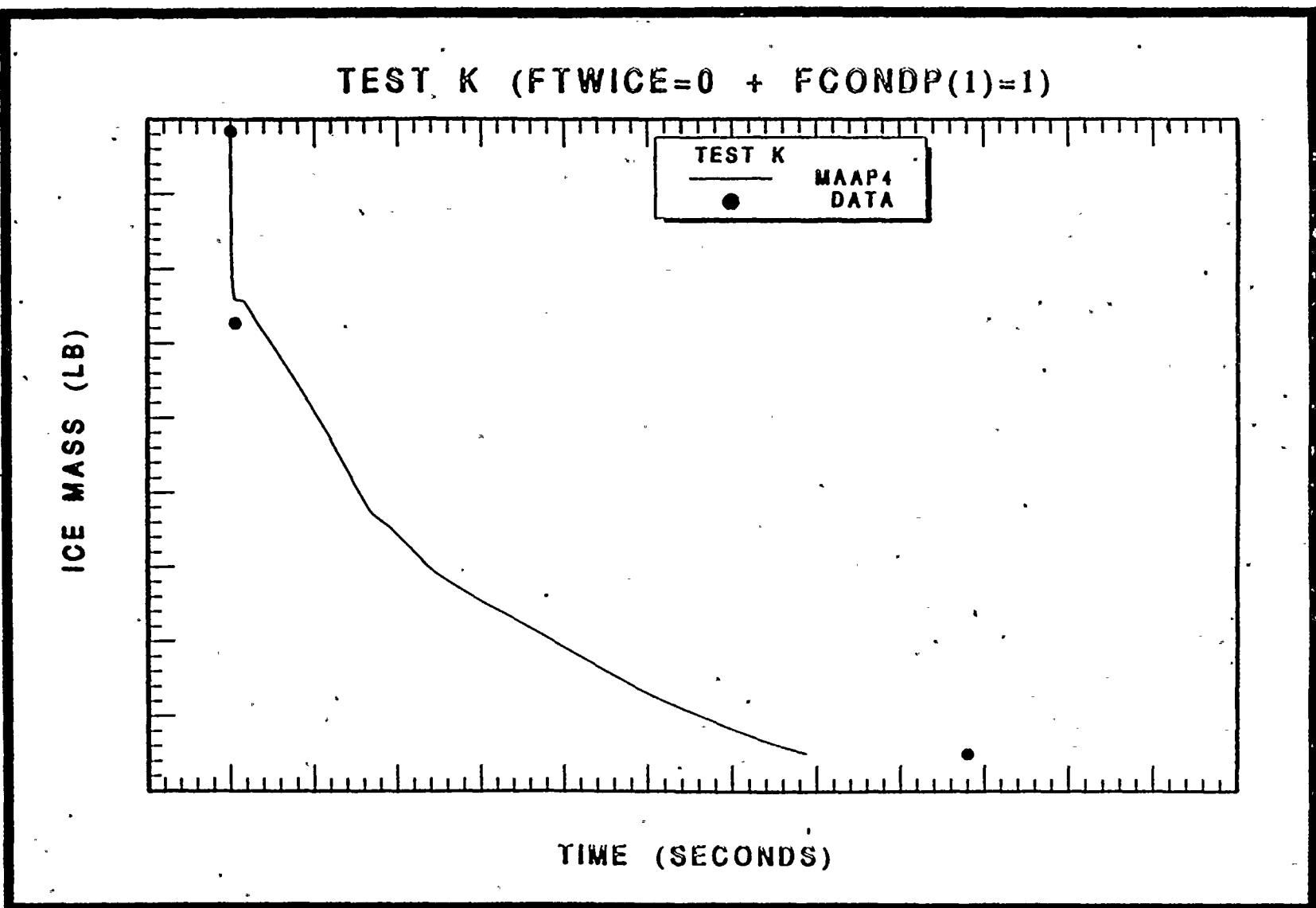


Figure 16: Comparison of the Calculated and Measured Ice Remaining for Test K Assuming No Agitation in the Lower Compartment Gas Space.



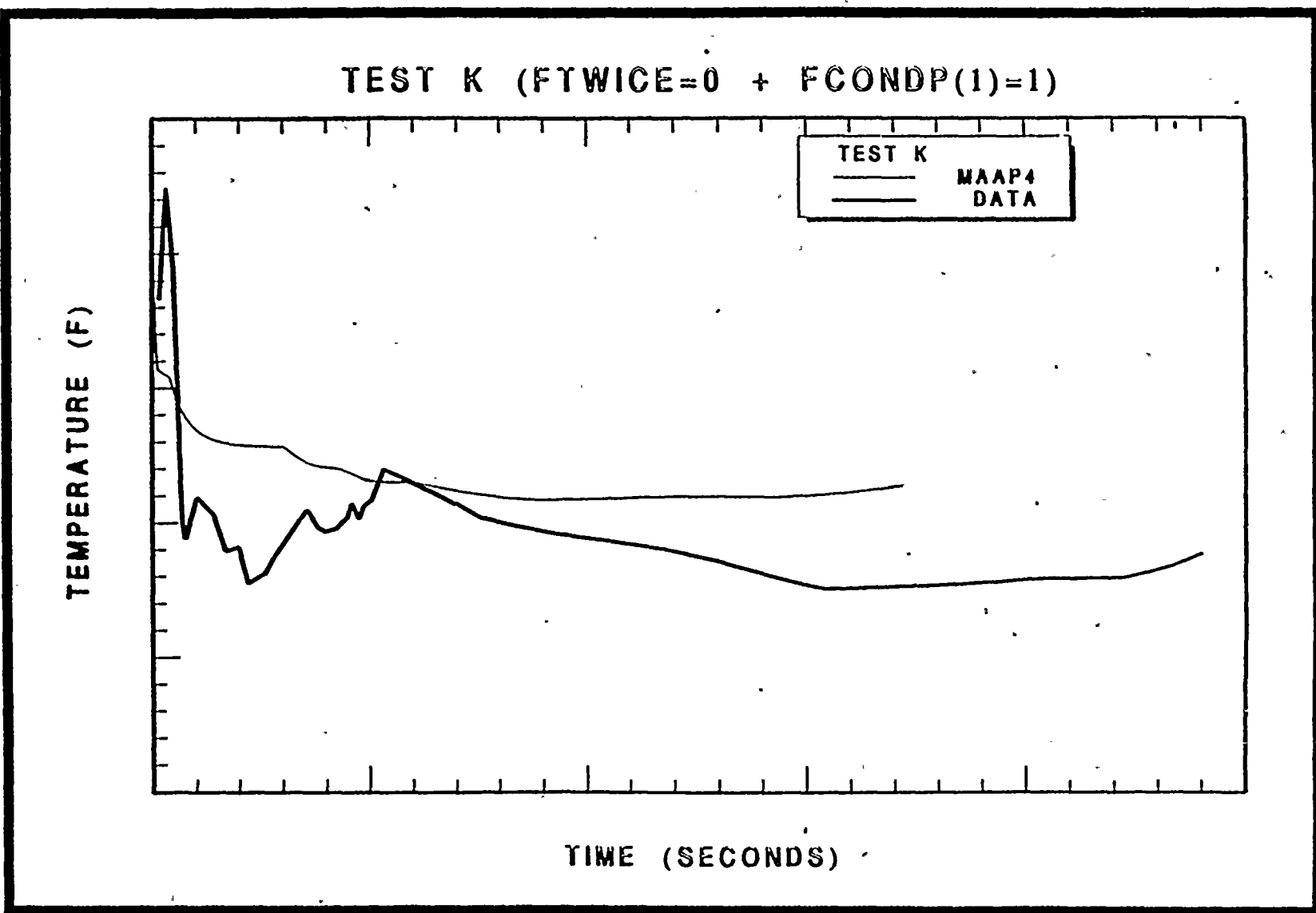


Figure 17: Comparison of the Calculated and Measured Ice Melt Drainage Temperatures for Test K Assuming No Agitation in the Lower Compartment Gas Space.



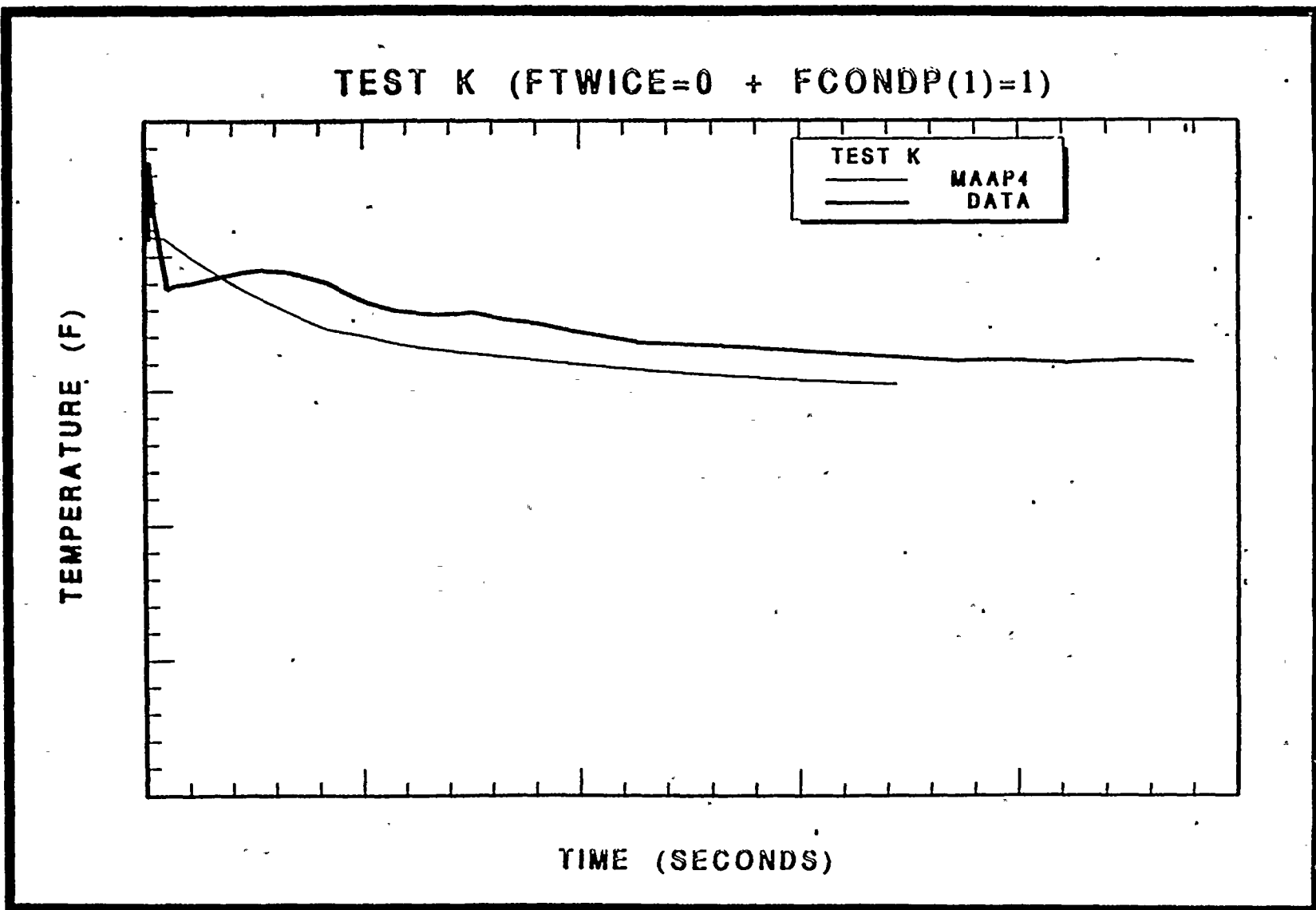


Figure 18: Comparison of the Calculated and Measured Lower Compartment Water Temperatures Assuming No Agitation in the Lower Compartment Gas Space.



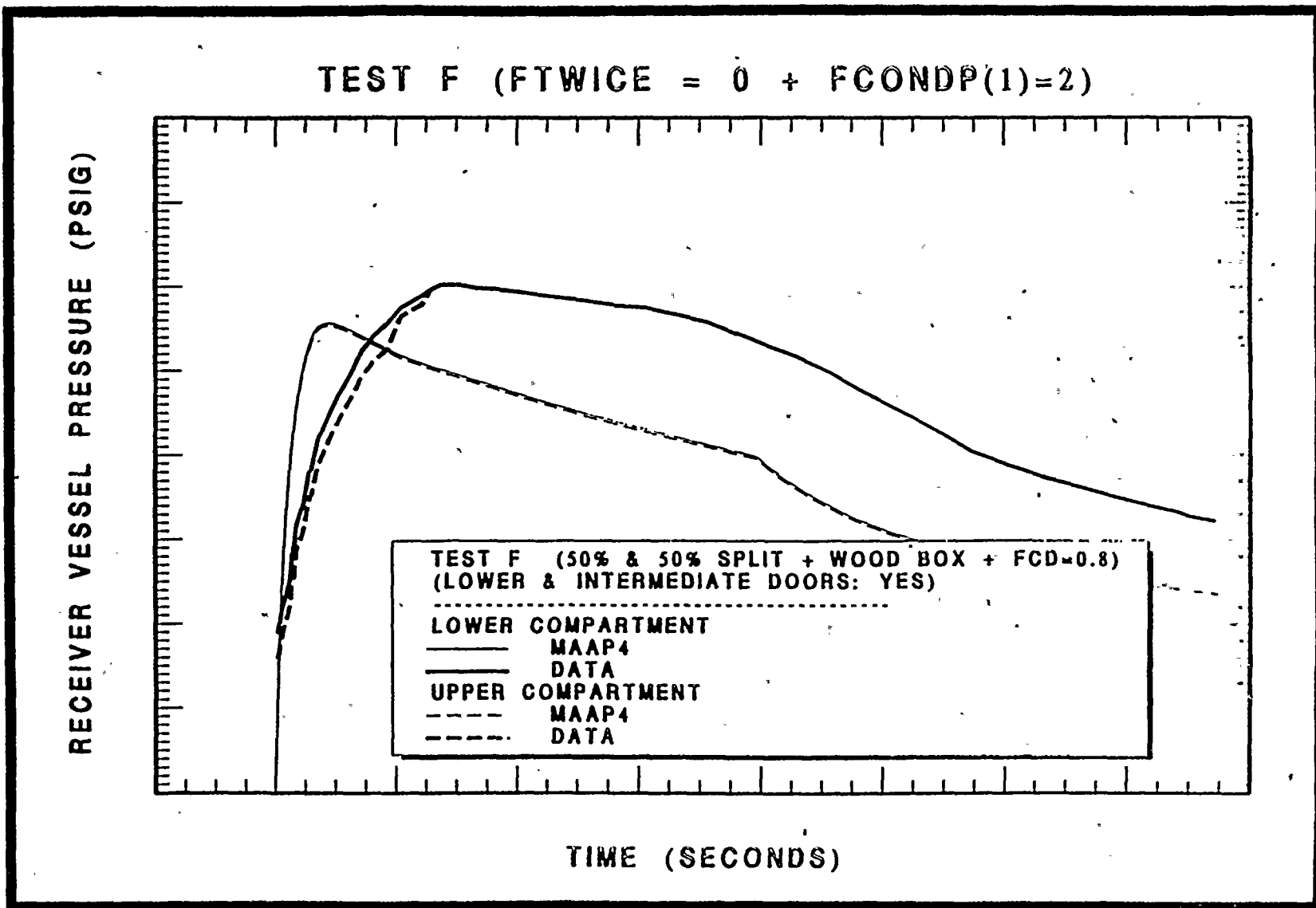


Figure 19: Comparison of the Calculated and Measured Vessel Pressure for Test F With an Equal Partitioning of the Incoming Steam Flow.



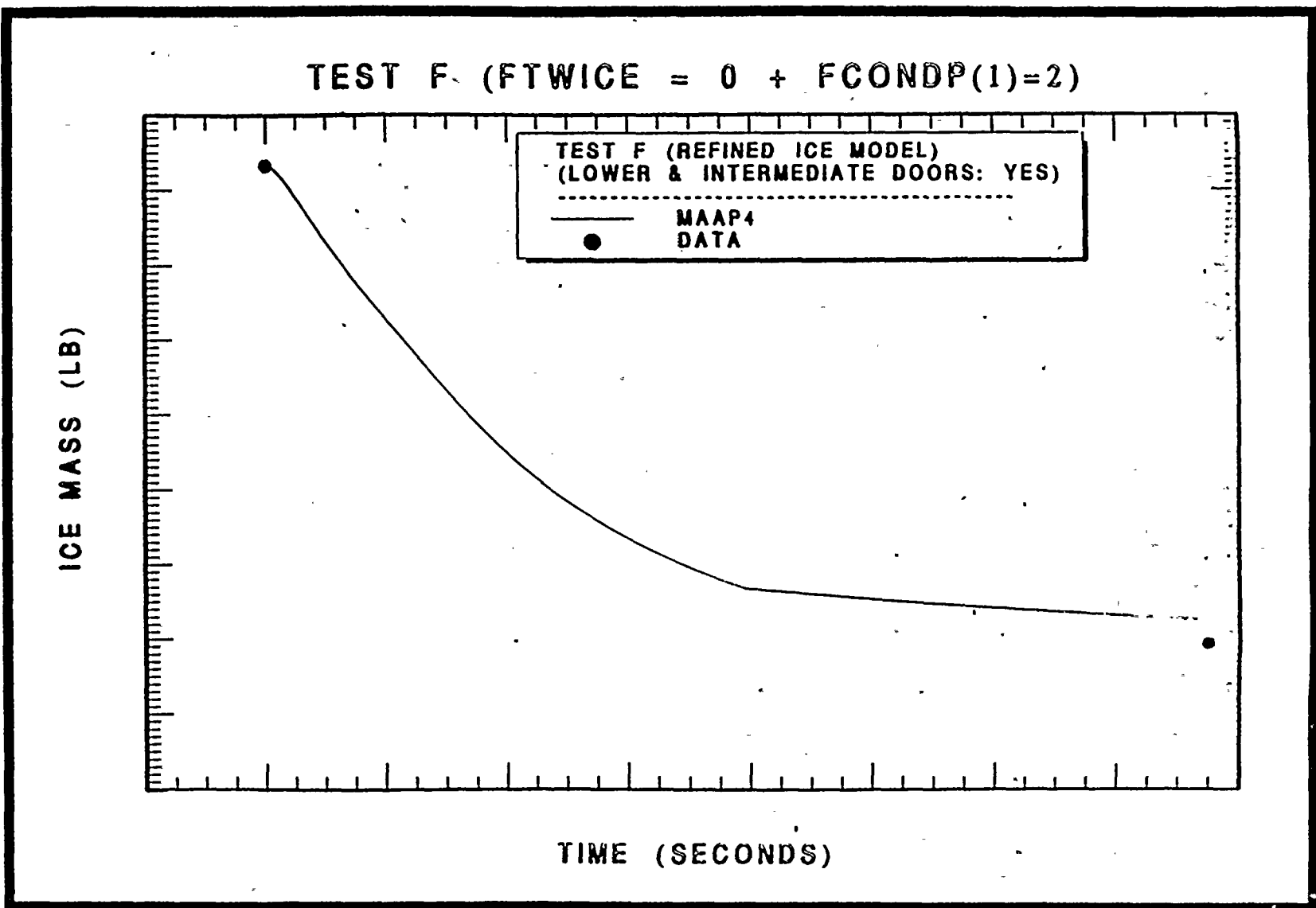


Figure 20: Comparison of the Calculated and Measured Remaining Ice Mass for Test F With an Equal Partitioning of the Incoming Steam Flow.



**6.0 REFERENCE**

Salvatori, R., 1974, "Final Report: Ice Condenser Full-Scale Section Test at the Waltz Mill Facility," Westinghouse Proprietary Class 2 Report, WCAP-8282.

**APPENDIX F**  
**Benchmarking of the MAAP Ice Condenser Model**  
**With the PNL Ice Condenser Experiments**



**BENCHMARKING OF THE MAAP ICE CONDENSER MODEL  
WITH THE PNL ICE CONDENSER EXPERIMENTS****1.0 INTRODUCTION**

Large scale experiments were performed at the Pacific Northwest Laboratory (PNL) to assess the ice condenser response to aerosol particle capture in ice condenser compartments [Ligothe, et al., 1991]. As part of these experiments, thermal hydraulic test were performed to investigate the extent of condensation in the ice beds for different inlet conditions representative of long term steam generation resulting from the reactor core decay power. Figure 1 is a schematic of the test apparatus, taken from Ligothe, et al. [1991], and shows the vertically oriented ice basket test section being supplied with heated air and superheated steam. Figure 2 is an elevation view of this test apparatus showing that the hot air and steam are ducted downward to a diffuser section in which the aerosol particulates are added for the aerosol test. The ice basket configuration is shown in Figure 3 with four major coolant channels being defined by one full size diameter ice basket, 4 half diameter baskets and 4 quarter cross-sectional area baskets. The gas temperatures are measured in the different quadrants and provide assessments for the temperature increase of the air-steam mixture as it moves axially through the test section.

This integral representation of the ice condenser behavior provides important insights with respect to the temperature of gases leaving the ice condenser as a function of the mass of ice remaining for different inlet flow conditions.

A simulation of the ice condenser Lower Inlet Doors (LIDs) was not included in this experimental apparatus. As a result, there were a number of experiments which encountered substantial natural circulation between the cold ice condenser and the warm air steam mixture temperatures in the inlet diffuser. These particular tests are not of relevance to the MAAP4 ice condenser model since the Lower Inlet Doors (LIDs) do not permit substantial natural circulation unless there is a means for one or more doors to be held open. Therefore, the tests of interest in this dynamic benchmark are those performed with higher gas flows through the test section to minimize, or prevent (by "gas flooding") this counter-current natural circulation flow capability.

**2.0 BOUNDARY CONDITIONS**

The important boundary conditions for these experiments are listed in Table 1 in terms of the tests examined, the volumetric steam flow entering the test section, the accompanying volumetric air flow, and the temperature at the entrance to the test apparatus. Considering that the ice basket simulation represents four baskets and that the plant has approximately 2000 baskets, the volumetric air flow shown in Table 1 (0.04 m<sup>3</sup>/sec) scales to an air flow rate in an ice condenser containment of approximately 40,000 scfm (standard cubic feet per minute) which is a typical value for one train of air recirculation fans in operation. Such a flow rate is the value



-Figure 1:  
Schematic of Ice-Condenser Test Facility as taken from Ligothke, et al., [1991].

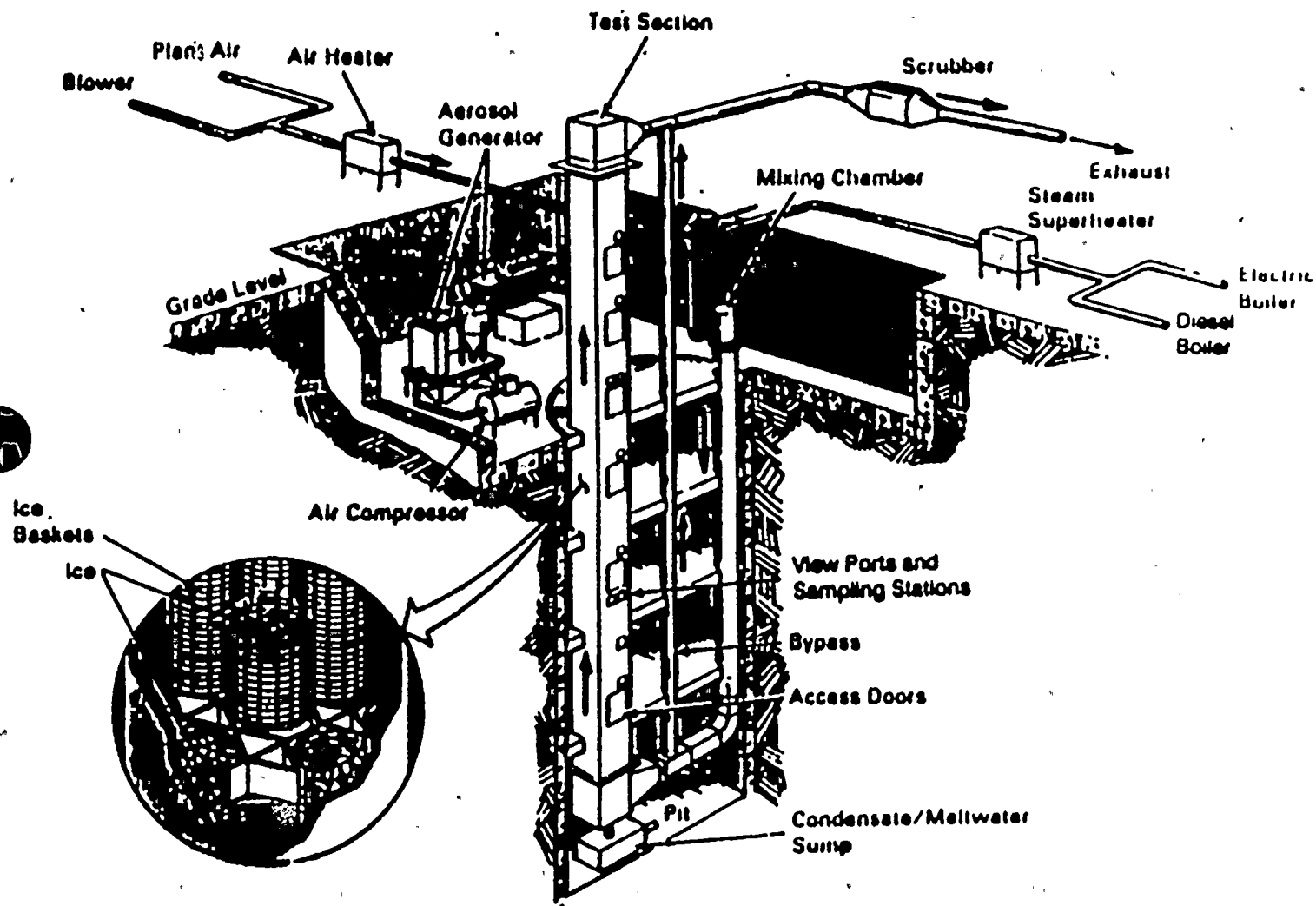




Figure 2:  
Elevation View of the West Face of the Test Section with Identification of Penetration Locations as taken from Ligotke, et al., [1991].

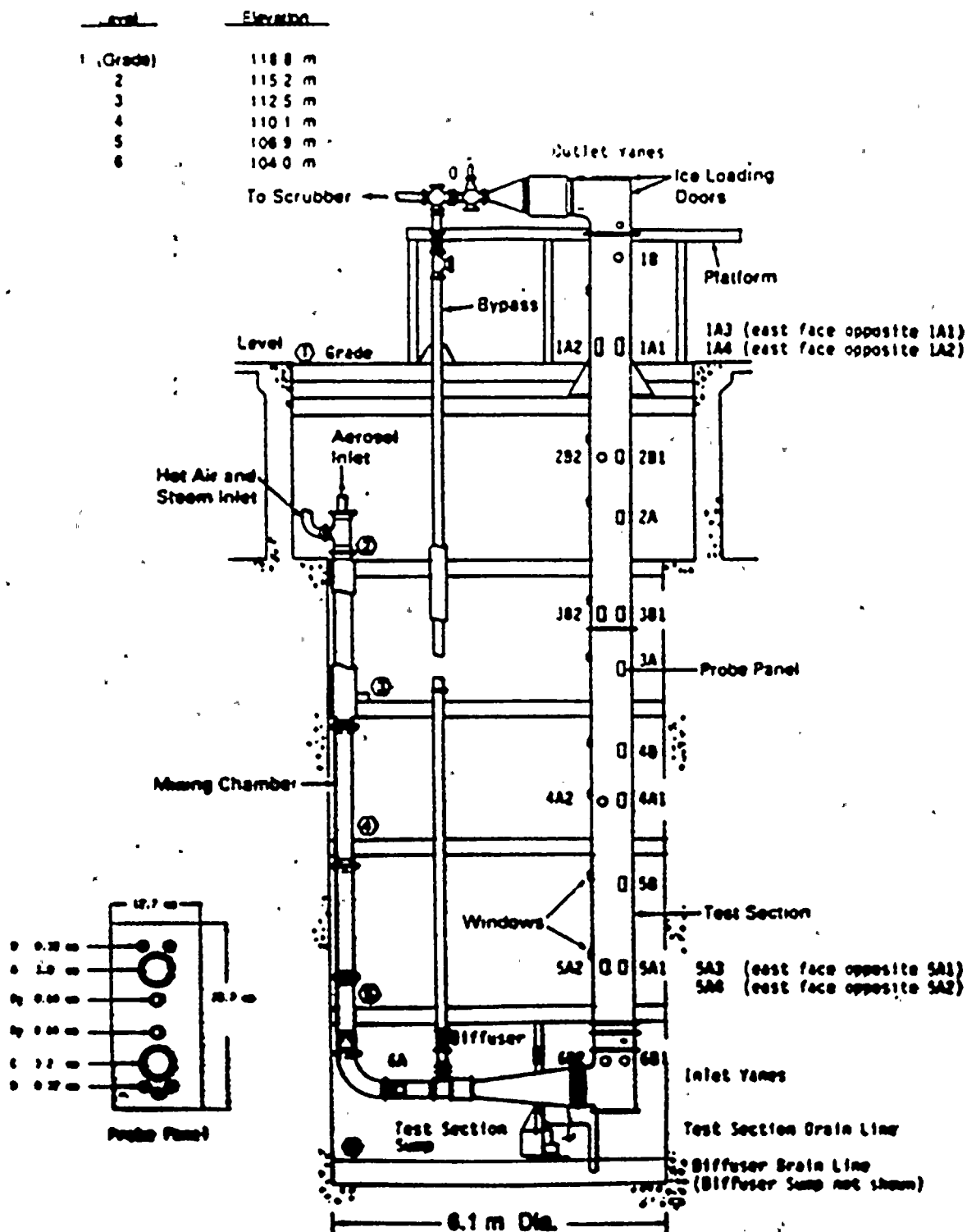




Figure 3: Test Section Cross-Section as taken from Ligotke, et al., [1991].

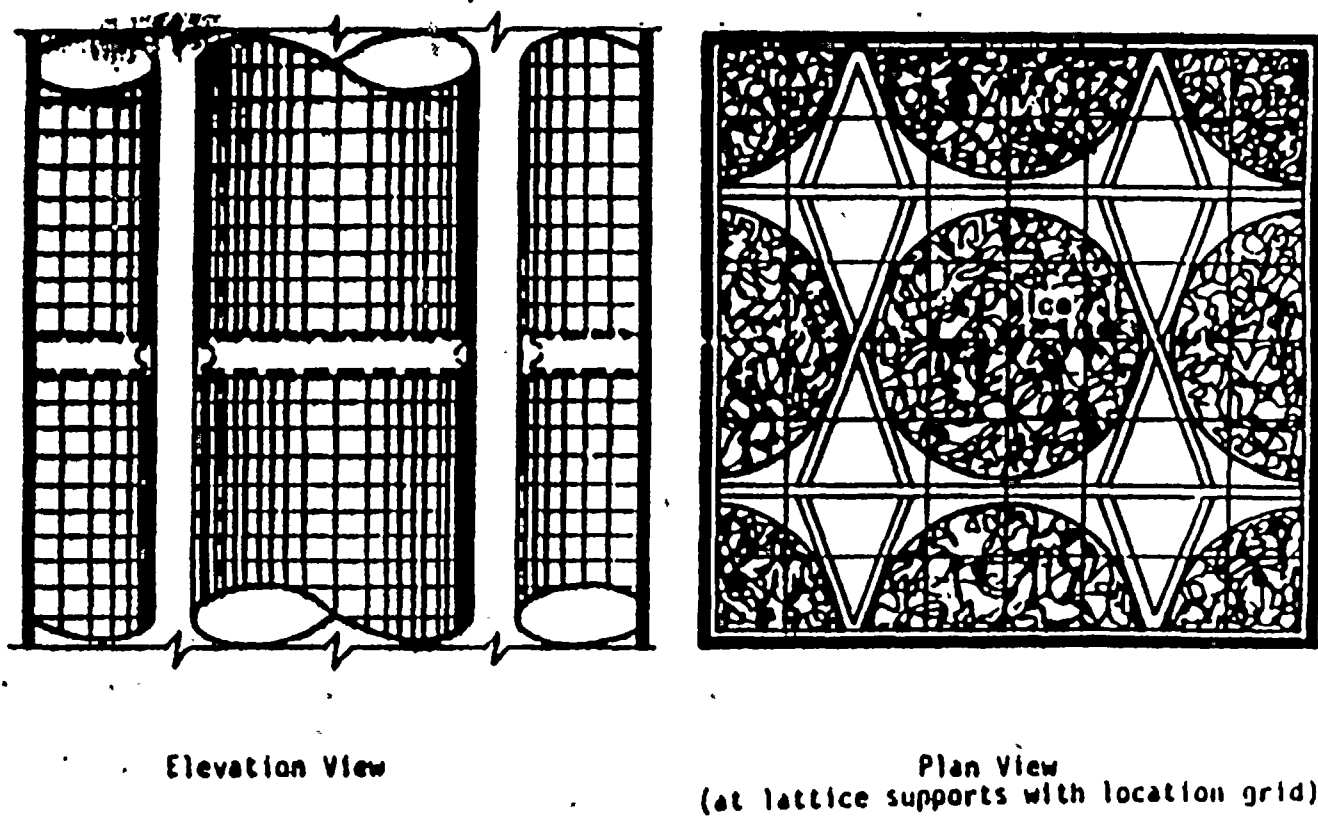






Table 1				
Test	Steam m <sup>3</sup> /s	Air m <sup>3</sup> /s	Total m <sup>3</sup> /s	T630 °C
8	0.10	0.12	0.22	126
9	0.35	0.04	0.39	112
10	0.40	0.04	0.44	121
11	0.34	0.04	0.38	105
12	0.017	0.057	0.07	92
13	0.02	0.05	0.07	111
14	0.02	0.09	0.11	115
	0.08	0.04	0.12	121

that is usually assumed for containment evaluations with a single failure being the failure of the second train of recirculation fans.

This benchmark is performed by inputting the measured ice condenser inlet temperatures (see Figures 4, 5, and 6 for the Level 5 temperature (inlet) for Tests 9, 11, and 13, respectively). Furthermore, the flow rates listed in Table 1 are input to the MAAP model which then calculates the ice condenser exit temperature and the corresponding ice melt rate associated with the available ice inventory. For this comparison, the results associated with Tests 9, 11, and 13 are explored since these provide the necessary insights associated with those conditions with a high steam partial pressure and those with a very low steam partial pressure. Using this spectrum of conditions provides the necessary assessment for the response of the representation of the gas exit temperature for the spectrum of inlet conditions. In formulating the inlet conditions for the three different experiments investigated, Test 11 experienced a boiler transient early in the test sequence. This causes the inlet temperatures to be lower than the desired value for approximately 10 minutes. This was represented in the benchmark by using the measured inlet temperatures at the level 5 location over the first 10 minutes to develop a representative inlet air-steam mixture temperature during this period. This then constitutes the boundary condition being supplied to the MAAP routines representing the extent of melting given the remaining ice inventory and the inlet conditions.

### 3.0 DISCUSSION OF THE RESULTS

Measured temperatures near the exit to the ice condenser are the most important aspect of the experimental investigation. Specifically, these provide a detailed representation of the gas exit temperatures as a function of experimental time. Given that the experimental time can be translated into the ice mass remaining, this provides an important test of the model representation for the extent of energy transfer ongoing in the ice condenser given the remaining ice mass. This is the important variable since it determines the energy balance within the ice condenser; specifically the ice melting rate.



Figure 4:  
Ice-Basket Section Thermal Profiles, Test 9 as taken from Ligothke, et al., [1991].

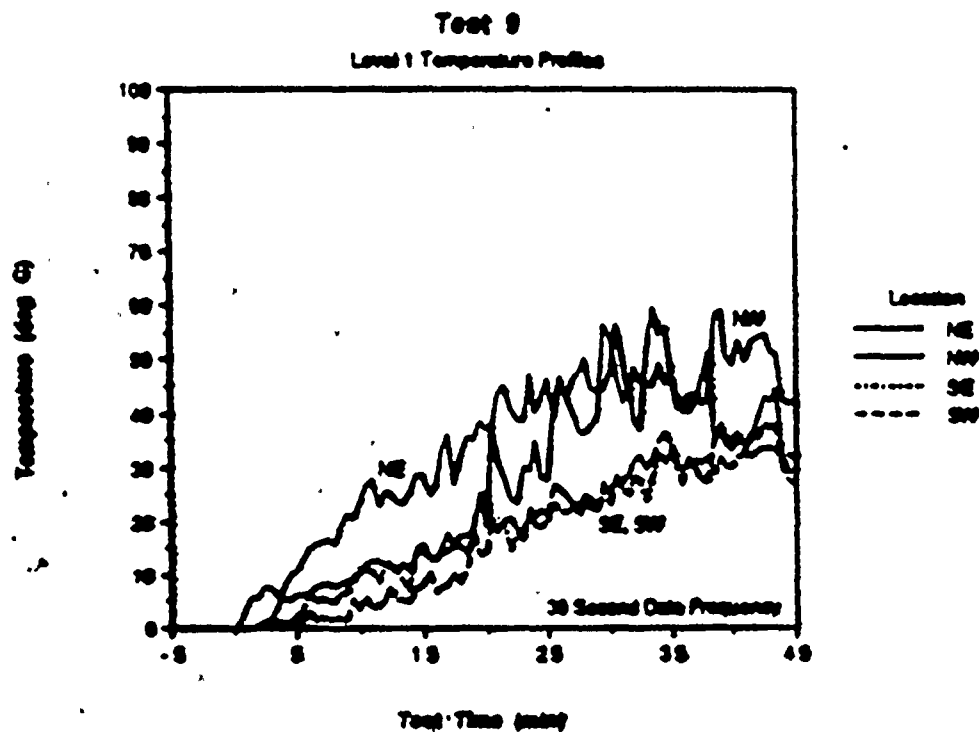
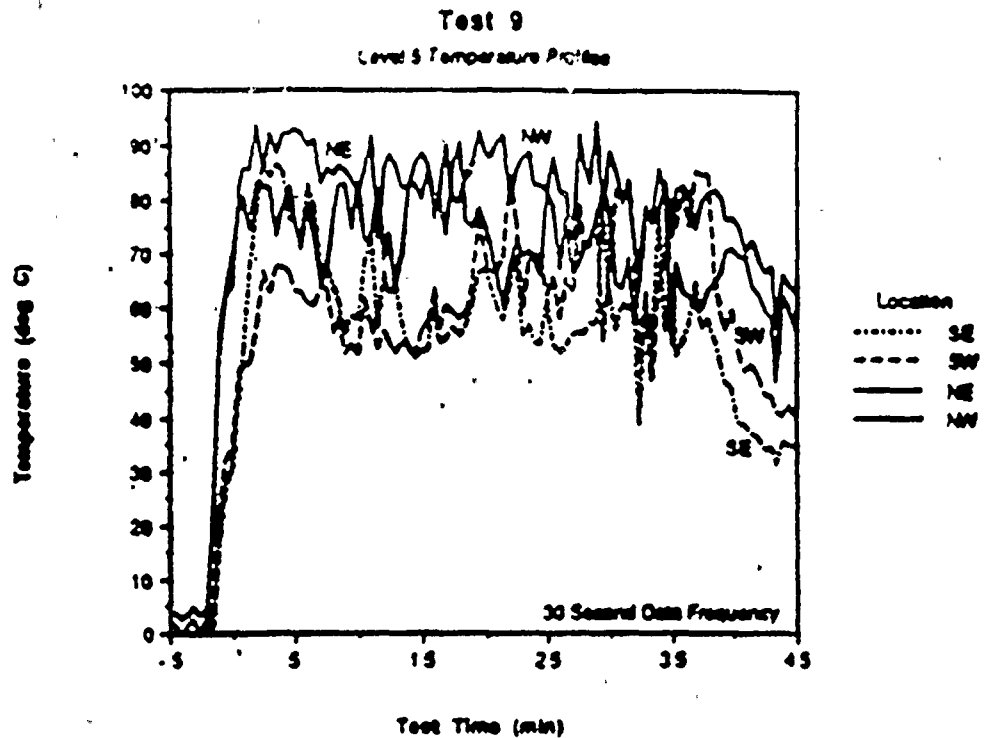


Figure 5:  
Ice-Basket Section Thermal Profiles, Test 11 as taken from Ligothke, et al., [1991].

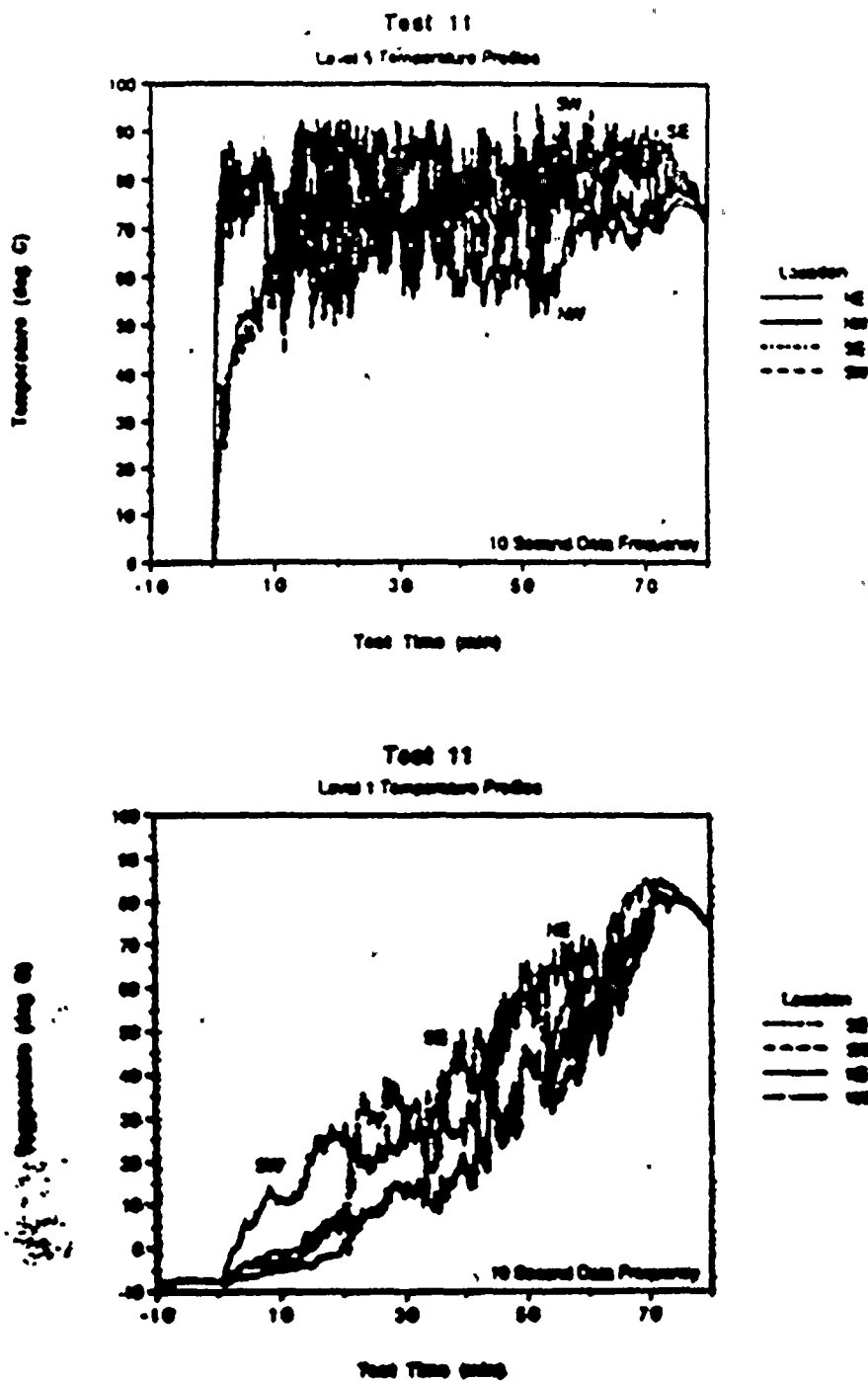
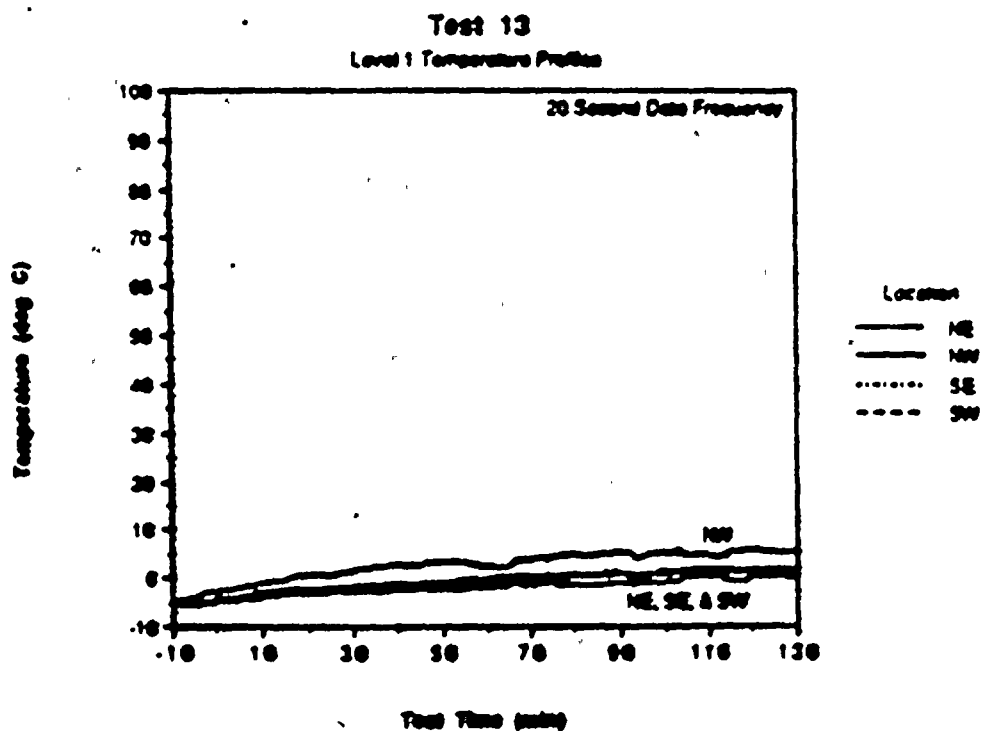
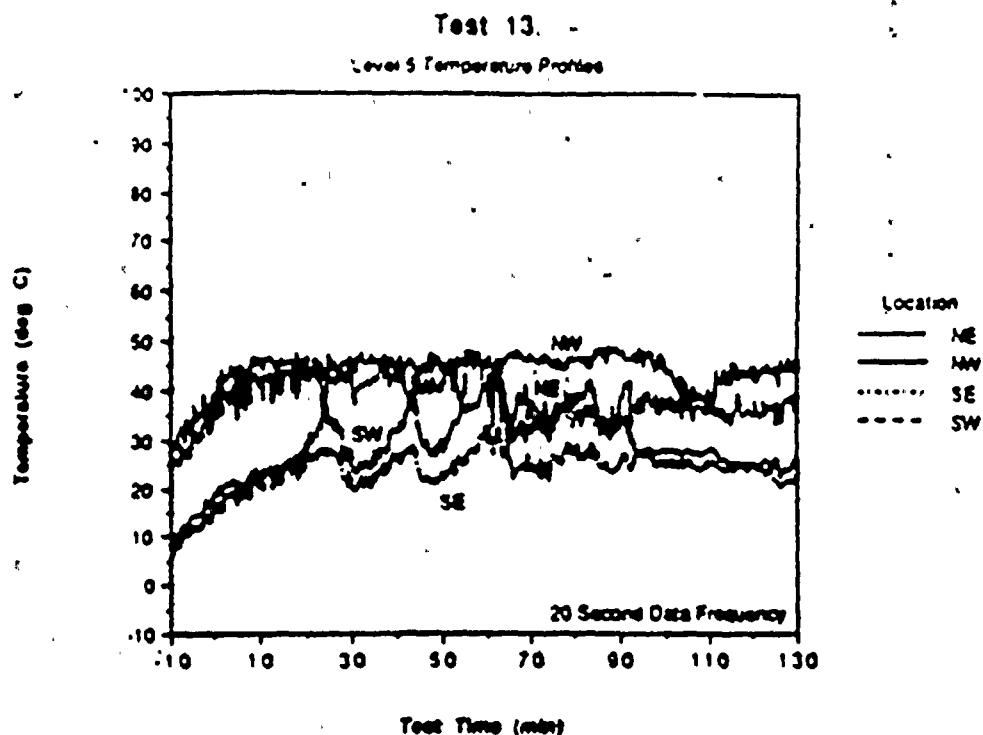


Figure 6:  
 Ice-Basket Section Thermal Profiles, Test 13 as taken from Ligotke, et al., [1991].





### 3.1 Test 9

With the input given for Test 9, the resulting comparison of the gas exit temperatures with the measured behavior is illustrated in Figure 7 and shows that there is good agreement between the measured exit temperature and that represented by the MAAP model for gas temperature exiting the ice condenser. The major reason for the increase of the temperature is the melt out of the ice bed. As illustrated in this representation, the MAAP uncertainty parameters varied in the representation is the heat transfer coefficient representing the additional energy transfer processes of natural convection and radiation (HTADDI) which is varied between a value of 0.5 and 2. The representation in Figure 7 shows that this variation adequately characterizes the increase in the exit temperature from the ice bed and also generally represents the variations between the two different thermocouples at the same axial location which are shown in the figures as THIGH and TLOW, i.e., the highest and lowest measured temperatures at location 1 which is near the top of the ice bed (see Figure 2). Hence, this parameter variation captures the increasing exit temperature as a function of time (representative of the progressive melt out of the ice bed) as well the variations in the temperatures at the same location.

### 3.2 Test 11

A similar comparison for the data of Test 11 is given in Figure 8 and again shows the measured temperature increasing as the ice melts out over approximately 1 hour. Again, there is good agreement between the measured behavior in the PNL test and the calculated behavior for the MAAP model. Given this agreement, the time for complete ice melting should also be in agreement. This illustration shows that ice melt is complete in the experiment after approximately 70 minutes whereas the MAAP model calculates this after about 60 minutes. Again this is a good characterization of the behavior in the test apparatus, particularly since the additional heat losses associated with the energy transfer to the ice box and the structural heat sinks associated with the test apparatus walls, etc. are not represented currently in the dynamic benchmark. The uncertainty variations treated for the variable HTADDI again encompasses the differences between the thermocouple measurements at level 1 for this experiment early in the transient. Hence, these variations clearly show the influence of uncertainties in the additional energy transfer early in the process when there is substantial ice remaining in the test apparatus.

### 3.3 Test 13

In this experiment there is very little steam flow associated with the measured air flow rate. Consequently, the melting rate is substantially less and the gas exit temperatures are essentially the ice temperature over the duration of the test (see Figure 9). This is also represented by the MAAP ice condenser gas exit temperature model and the comparison of the two shows good agreement between the measured and calculated behavior. This is important since it provides confidence that the MAAP model can adequately represent the various conditions that might be experienced in the spectrum of accident sequences for the ice condenser containment behavior.

Figure 7:  
Comparison of the Calculated and Measured Temperatures  
for the Ice Condenser Exit in the PNL Test 9.

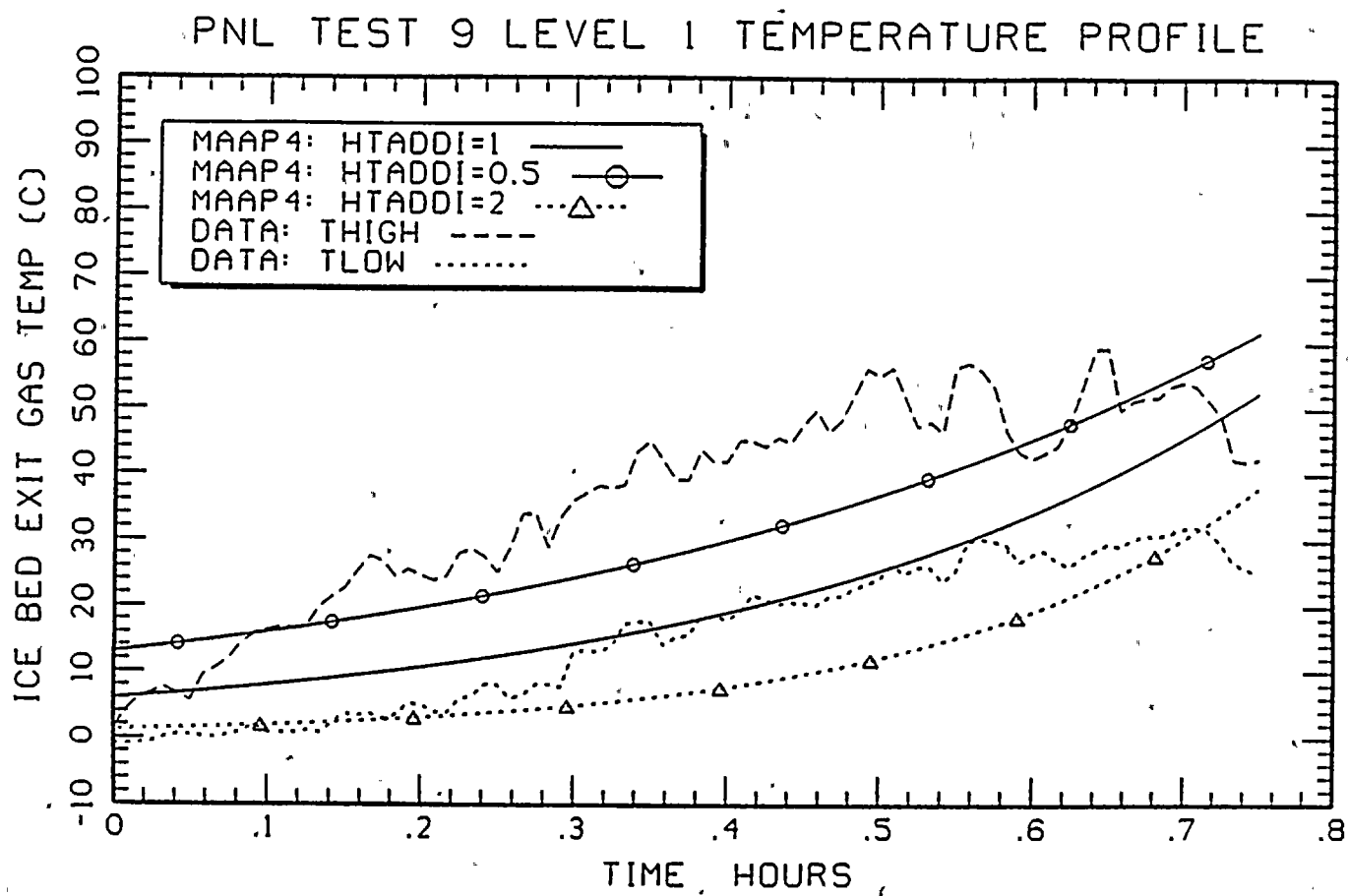




Figure 8:  
Comparison of the Calculated and Measured Temperatures  
for the Ice Condenser Exit in the PNL Test 11.

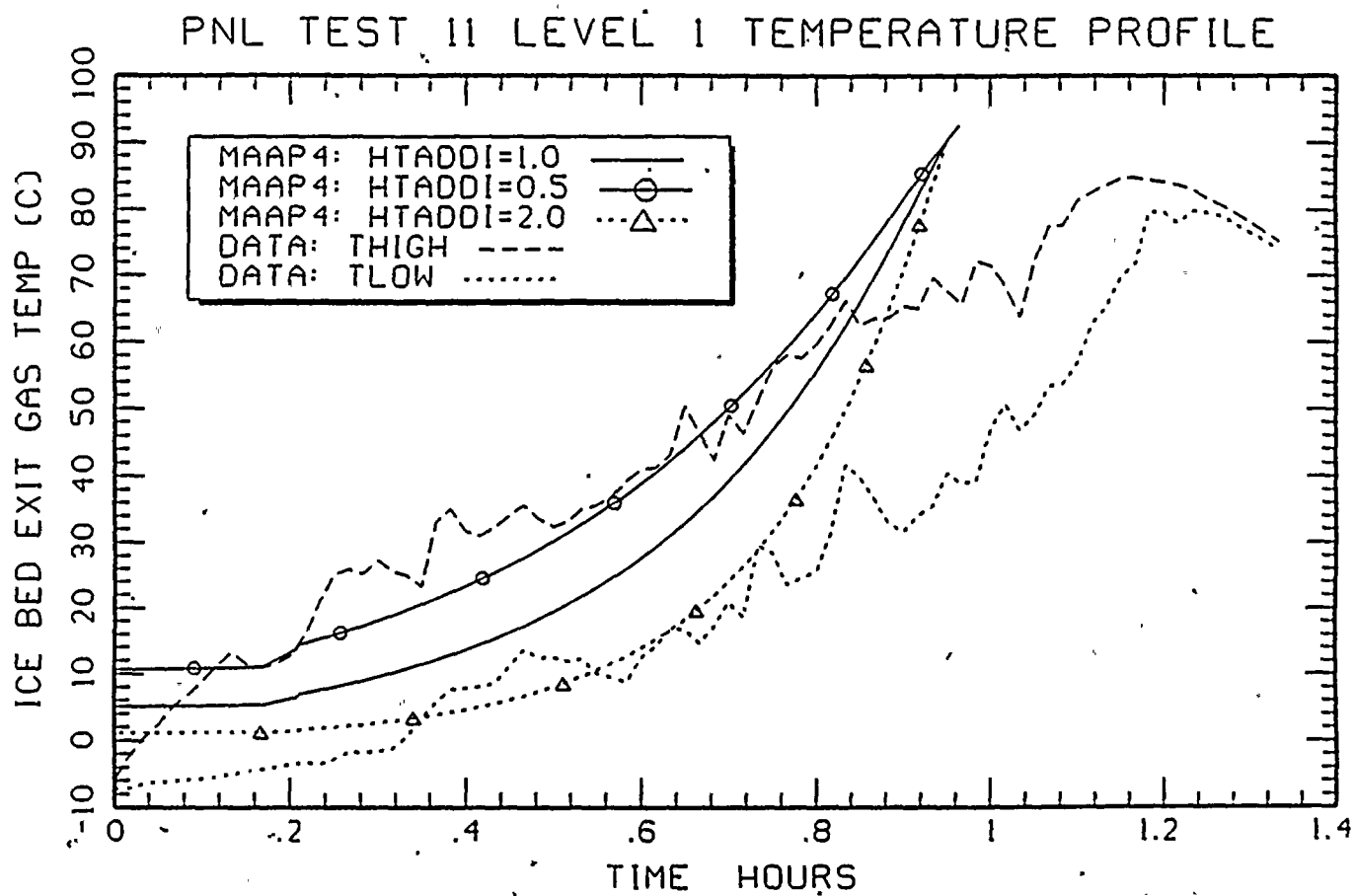
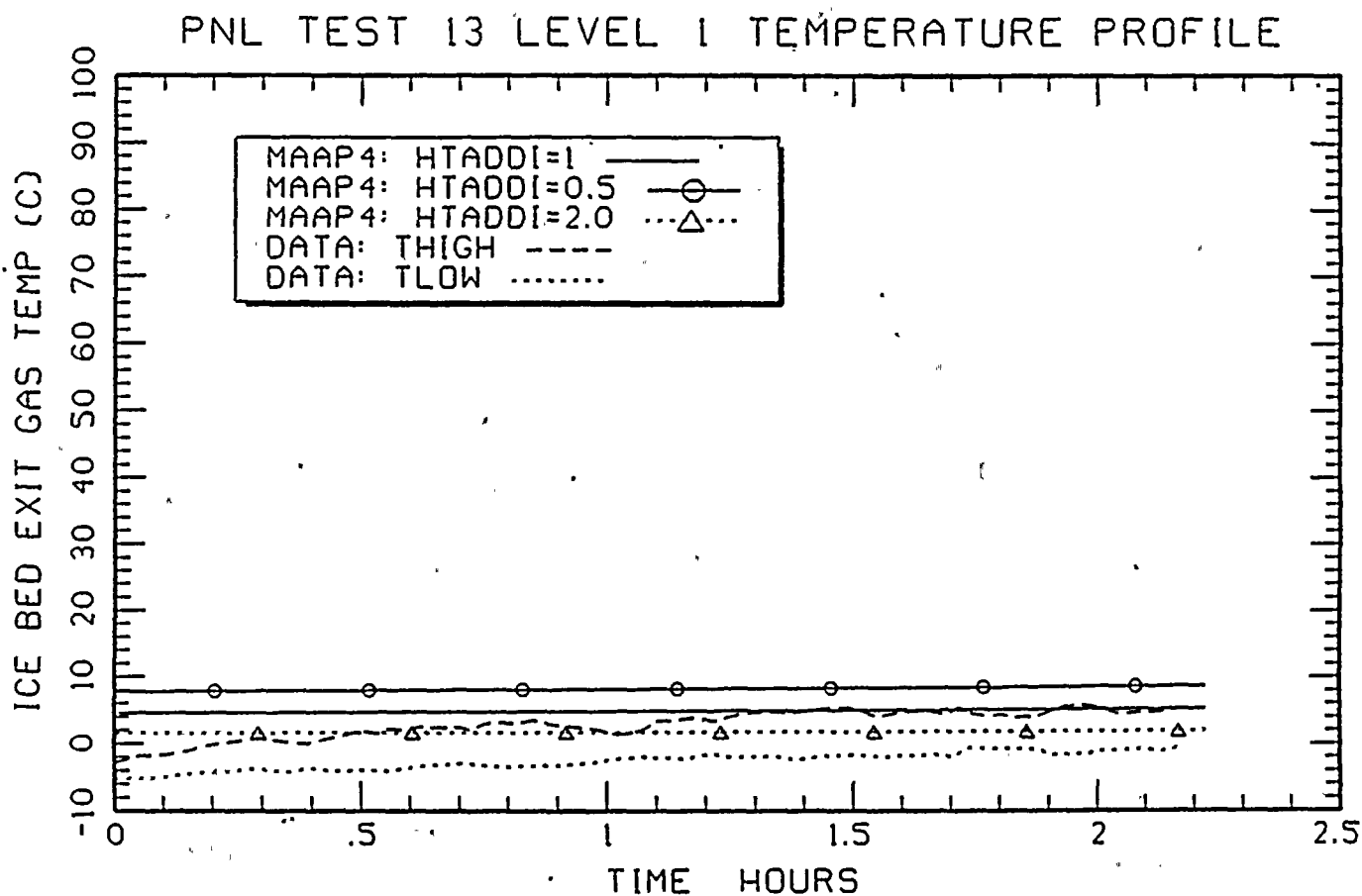


Figure 9:  
Comparison of the Calculated and Measured Temperatures  
for the ice Condenser Exit in the PNL Test 13.



The variations in the uncertainty parameter HTADDI shows that there is only a minor influence associated with the uncertainties in this low steam flow case. This illustrates that the uncertainties provide a reasonable characterization of the differences that can be expected between lean steam flow conditions and those in which the steam flow rate is the major component of the flow through the ice condenser.

#### 4.0 SENSITIVITY STUDIES

Sensitivity/uncertainty studies are discussed in Section 3.0.

#### 5.0 CONCLUSIONS

Comparison the MAAP ice condenser containment model with a spectrum of inlet conditions to the ice condenser shows good agreement for the thermal hydraulic response of the test performed. This is true for those experiments utilizing high steam partial pressures as well as those with a low steam partial pressure. Furthermore, the imposed gas flow rate is equivalent to the velocity through the ice bed that would be promoted by a single train of ice condenser recirculation air fans. Therefore, the behavior observed in these experiments, and the good agreement observed between the experimental measurements and the MAAP model develop a level of confidence that the MAAP calculation is a good representation of the containment response for a spectrum of accident sequences.

#### 6.0 REFERENCE

Ligothe, M. W., et al., 1991, "Ice-Condenser Aerosol Tests," NUREG/CR-5768, PNL-7765, R1.

**APPENDIX G**  
**Benchmarking of the CSTF**

**BENCHMARKING OF THE CSTF****1.0 INTRODUCTION**

This dynamic benchmark is controlled by subroutine which calls CSTFPF to develop a CSTF parameter file. These values are developed from the dynamic benchmarking file CSTF.DYB which documents information given in the experimental report [Bloom, et al., 1983]. This routine also performs any unit conversions necessary to be consistent with the MAAP internal computations. As a portion of the EPRI-sponsored research programs addressing hydrogen control in containments following a postulated severe accident at a nuclear plant, the Hanford Engineering Developing Laboratory Containment Systems Test Facility (CSTF) was used to investigate hydrogen concentration and mixing for ice condenser containment configurations. Specifically, these experiments investigated the degree of mixing and the potential for either "pocketing" of hydrogen or stratification of hydrogen-rich mixtures. Hydrogen-steam and helium-steam mixtures were investigated on a scaled basis for the releases from a small pipe break in the Reactor Coolant System (RCS) or from the pressurizer relief tank through a failed rupture disk. For all but one of these experiments, helium was used as a simulant for hydrogen. In the other test, hydrogen was used with a nitrogen atmosphere in the CSTF vessel.

The CSTF is a coded vessel 20.4 meters high, 7.6 meters in diameter with a total volume of 850 m<sup>3</sup> and has a rated pressure of 0.52 MPa at 160°C. Sub-compartments characterizing the containment lower compartment and the upper compartment were fabricated inside of the CSTF vessel along with representations of partially opened ice condenser doors and the air recirculation fans. Experiments were performed with and without forced circulation flow to investigate the potential for hydrogen accumulation for different accident scenarios.

**2.0 BOUNDARY CONDITIONS****2.1 Containment Compartments****2.1.1 CSTF Description**

The final report for this study [Bloom, et al., 1983] contains the following description of the test compartment fabricated inside of the CSTF vessel.

The test compartment, which simulated a simplified lower compartment area of an ice condenser plant, was fabricated in the lower area of the CSTF vessel. The test compartment conformed to the modeling criteria; but did not contain any geometrical objects, such as pipes, tanks, or structural elements. The linear scale factor between test compartment and reference plant design was 0.3. The test vessel outer wall simulated the plant crane wall, and the height to diameter ratio of the test compartment was equal to that for the reference plant design. Figures 1 and 2 are schematics of the annular test

Figure 1: Test Compartment Geometry, (taken from [Bloom, et al., 1983]).

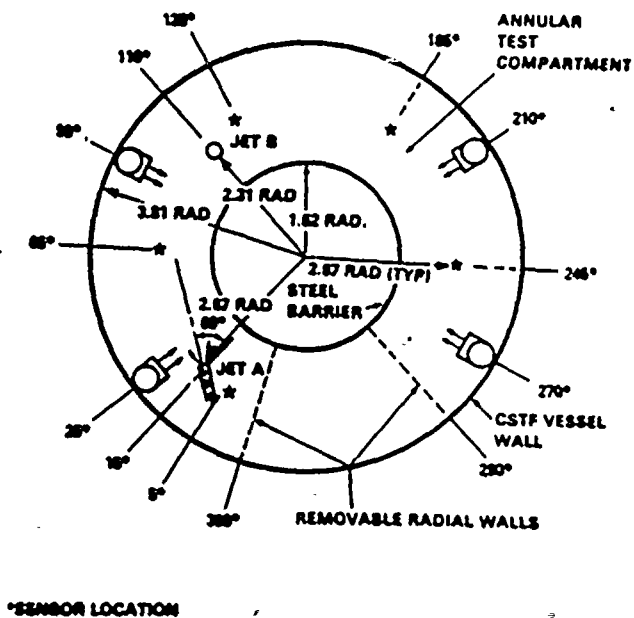
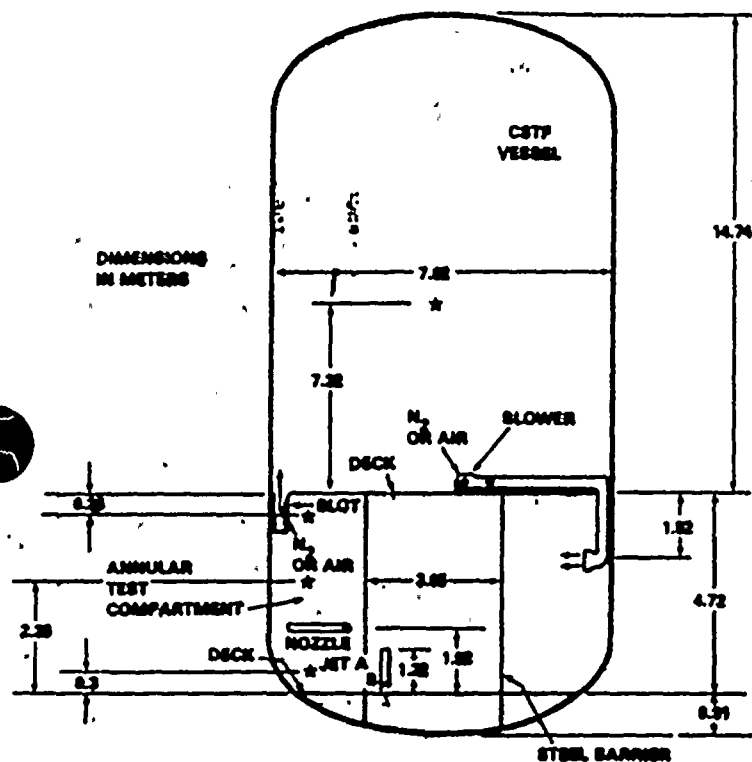
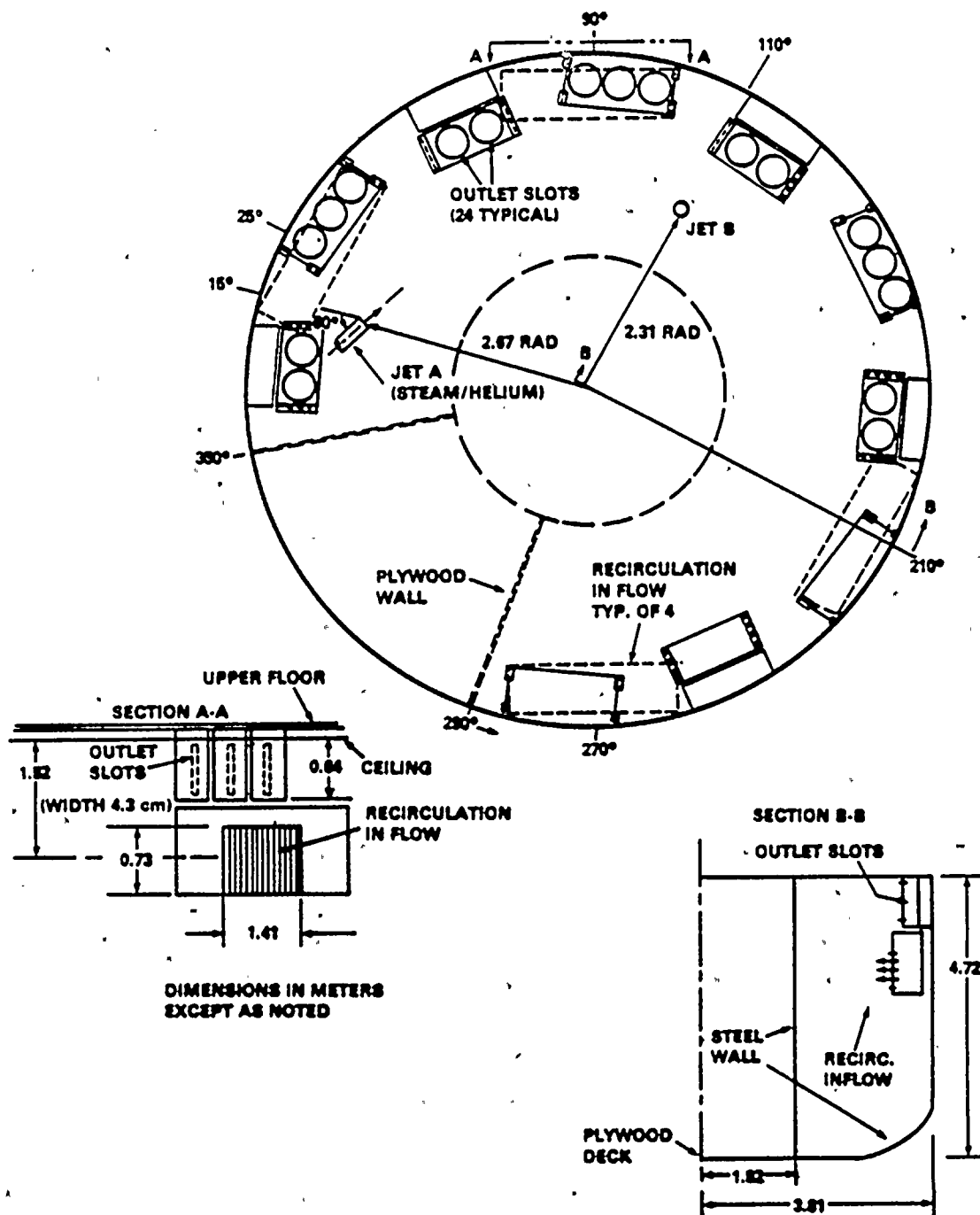


Figure 2: Test Compartment Air Recirculation Details  
(taken from [Bloom, et al., 1983].)



compartment whose outer diameter was 7.6 m (25 ft). The inside annulus was 3 m (10 ft) in diameter by 4.7 m (15.5 ft) high and was fabricated of corrugated steel sheet. A deck was provided inside the test vessel to act as the floor of the annular compartment, and on top of the annular compartment to represent the floor of the upper containment area. The test compartment occupied 300° of the annulus, leaving a 60° sector to represent the refueling area of the referenced plant.

The horizontal jet nozzle was located 25° from one radial wall of the annulus, and was at a height equal to one-third of the compartment height. The nozzle simulated a postulated break of a 5-cm (2-in) pipe and was directed 60° to the radius, as shown schematically in Figure 2.

The vertical jet nozzle simulating the release from the 25 cm (10 in) rupture disk on a pressurizer relief tank was directed vertically up into the test compartment. The nozzle location was 120° from the radial wall and 12 cm (47 in) from the lower deck. The radial distance from the nozzle to the vessel wall was 150 cm (59 in). A blower was used to simulate air recirculation from the upper to the lower compartment atmospheres. The size and location of the air inlet ducts were scaled, as far as possible, from the reference plant design, except the air register was internal to the vessel walls. The inlet ducts were arranged, as shown in Figure 1, at 25°, 90°, 210°, and 270°, to represent the openings in the crane wall which forms the outer cylindrical wall of the room. In the reference plant air flow is from the fan rooms to the lower compartment. The air flow rate, determined by the modeling criteria to be 104 m<sup>3</sup>/min (3730 ft<sup>3</sup>/min), was distributed through four openings each 0.73 m (2.4 ft) in height by 1.41 m (4.63 ft) wide at a velocity of 0.43 m/sec (140 ft/sec).

The outlet air flow passages, which represented the partially opened ice compartment doors, were 24 vertical slots 0.64 m (2.1 ft) high by 4.3 cm (1.7 in) wide. The slots were made in the wall of circular duct segments suspended from the ceiling of the compartment. The slots were equally spaced along the periphery of the compartment, over the 300° segment.

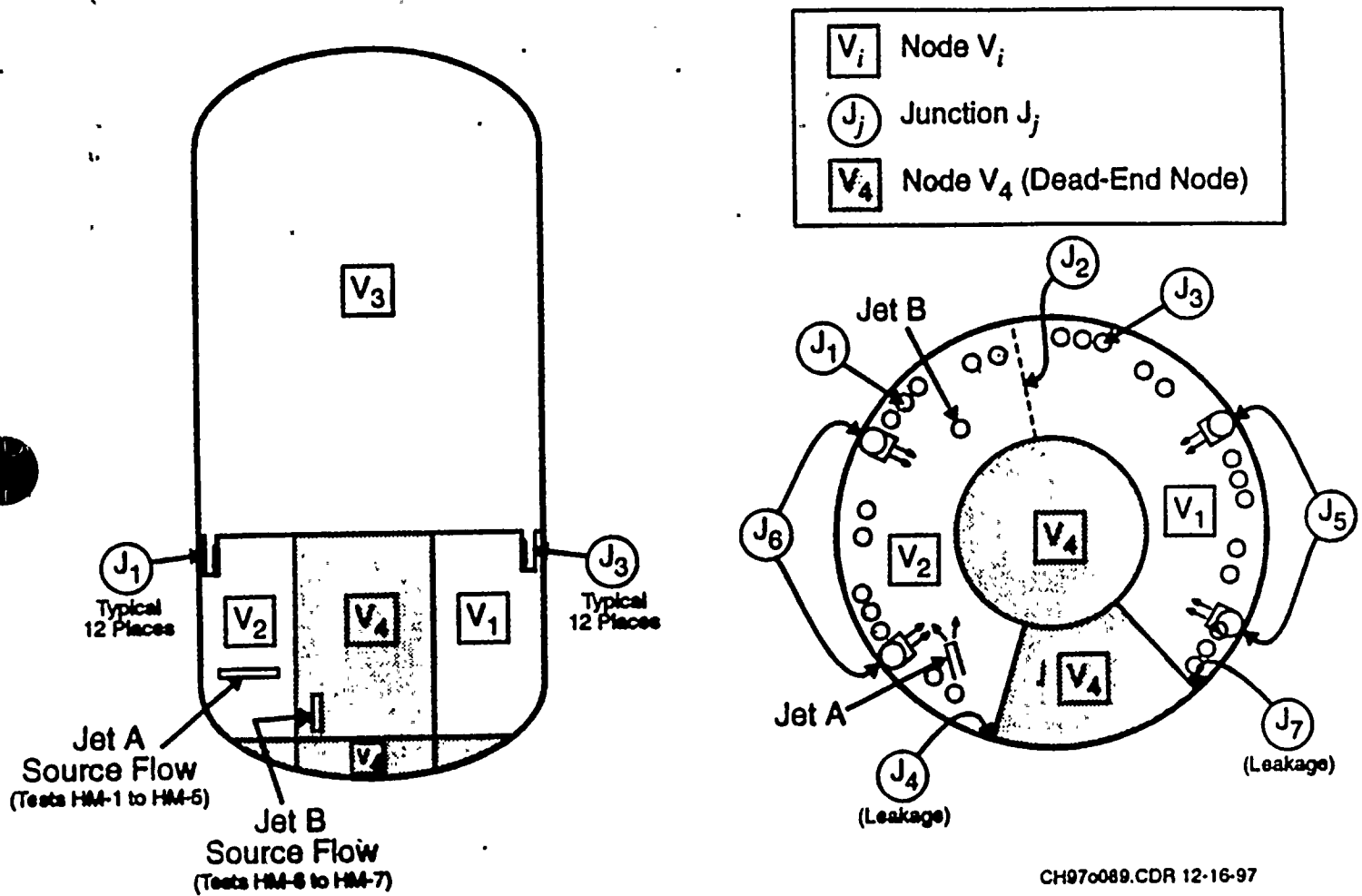
### 2.1.2 MAAF4 Modeling

The MAAF4 parameter file for CSTF defines a 4-node containment model, as shown in Figure 3. Node 3 is devoted to the entire upper volume. Since this volume is not comprised of sub-compartments, a presumption of homogeneity is made unless justified otherwise by the experiment.

The lower volume outside of the shield wall and refueling cavity mock-up is divided into Nodes 1 and 2 residing side-by-side and separated by a vertically-oriented (horizontal flow) junction. The balance of the lower volume resides inside the shield wall and refueling cavity



Figure 3: MAAP4 Nodalization for the CSTF Ice Condenser Experiments.



mock-up. Since leakage paths existing between these regions and Nodes 1 and 2, the mock-ups are consolidated into a single dead-end, Node 4.

## 2.2 Junctions

### 2.2.1 CSTF Description

As discussed above, the principal junctions of interest for these experiments are the 24 vertically oriented slots in the floor junctions representing the partially open doors of the ice condensers. These are modeled in the MAAP4 code with the appropriate opening area and the representative loss coefficient for this slot configuration. Other junctions are relatively large areas, as illustrated in Figures 1 and 2. Furthermore, the dominant facet of these experiments is one of the air recirculation operating to establish a forced mixing behavior. These are also explicitly modeled in the MAAP4 representation.

The partially open Lower Inlet Doors (LIDs) for the ice condenser, is the expected configuration in response to a small RCS break with decay heat steaming into containment. However, the fixed size of these junctions only partially represents the door response, since the plant doors are designed to vary in position depending upon the imposed pressure differential. Furthermore, the volumes simulating the lower doors do not have a significant volume. Hence, in this simulation the ice condenser volume is part of the upper volume, therefore, no dedicated ice condenser compartment, nor any ice mass, is modeled in this facility.

In addition to the lower door junctions, the main recirculation fans are modeled to take suction from the upper volume inventory and deliver the flow to the lower volume, as shown by the four vents in the lower volume in Figure 2. As will be discussed, usage of these fans is test-specific.

### 2.2.2 MAAP4 Modeling

An open vertically oriented junction, Junction 2, resides between Nodes 1 and 2. The junction is not imposed by a physical constriction. Rather, the junction is located to evenly divide the lower volume among the two nodes.

The ice condenser lower door mock-ups are modeled as two distinct open junctions with the doors between Nodes 1 and 3 comprising Junction 3 and doors between Nodes 2 and 3 comprising Junction 1. These junctions are intended to facilitate the potential for global circulation between Nodes 1, 2, and 3 in response to the preferential source flow location in Node 2. By consolidating several doors into only two distinct single junctions, it is presumed that the flow through the doors comprising a single junction is identical. This is sufficient unless the benchmark results justify a refinement to the number of junctions between the upper and lower volumes.

Junctions 4 and 7 define the leakage paths between Node 4 and Nodes 2 and 1, respectively. The size of the leakage paths are not known. However, an order of magnitude approximation for leakage size is probably sufficient to represent the minimal influence of Node 4.

Junctions 5 and 6 define the active recirculation fans between Node 3 and Nodes 1 and 2, respectively. In MAAP4, fan flow can be defined for any of the junction types (open, failure, check valve, or loop seal), but an open junction is conventionally used. Parameter PFAN(j) specifies the desired volumetric flow rate for Junction j.

Manual control of open/closed status for a junction containing a fan flow, and in general any junction, is accomplished by setting parameter JFRB(j) = 1/0 for "on" and "off", respectively. Recirculation fans are enabled at the appropriate sequence time, as dictated by the specific CSTF test. Furthermore, open Junctions 1 and 3 are also manually controlled. They are initially closed during the initial segment of the test to prevent natural convection, since the lower volume is pre-heated. They are then opened immediately prior to the gas injection phase.

It is noteworthy that a desired fan flow may not be achieved identically. Rather, the actual flow may be different since volumetric flow specified by PFAN(j) imposes a prescribed pressure differential across the junction necessary to achieve the desired flow rate. However, as containment-wide balance of pressure and flow is approached, the actual pressure differential may change, altering the intended fan flow rate. In the case of CSTF, it is presumed that the reported fan flow rates are actual measured quantities. To replicate the flow rates, the prescribed PFAN(j) values are adjusted so that the reported flow rates are achieved.

## 2.3 Structural Heat Sinks

### 2.3.1 CSTF Description

Since steam is injected into the CSTF vessel for these tests, the potential for steam condensation is also represented since part of the simulated containment configuration is steel and part is fabricated from plywood. The operating deck and refueling cavity mock-ups are wood, and the shield wall mock-up is corrugated steel. The condensation potential for the various heat sinks are represented in terms of their thickness, the heat transfer area, and the material of the individual structures.

As stated in the experimental report, the vessel shell is rated for a design pressure of 0.52 MPa at 160°C. Assuming a design hoop stress of 124 MPa, based upon one-half of a typical yield stress, the approximate thickness of the vessel wall is 1.6 cm (0.63 in.). Furthermore, the report mentions that the wall is insulated on the outside; this is also represented in the CSTF parameter file as documented in the benchmark specific subroutine CSTFPF.



### 2.3.2 MAAP4 Modeling

The heat sinks for the various compartments represented in the MAAP4 CSTF representation are:

- a 12.7 m (0.5 in) thick steel wall,
- a 2.4 mm (3/32 or 0.094 in) thick corrugated steel wall, and
- a 25.4 m (1 in) thick plywood sheet.

These heat sinks are distributed through the various regions and are the only considerable heat sinks acting during the experiment.

## 2.4 Initial Conditions

### 2.4.1 CSTF Description

The final report for this set of experiments [Bloom, et al., (1983)] contains the following information.

Gas mixing and distribution characteristics of an ice condenser lower containment region were determined from three general types of tests. The test parameters are listed in the Test Matrix of Table 1. The types of tests performed were "preliminary", high velocity horizontal jet release, and high velocity vertical jet release. The preliminary tests involved air only, while a helium-steam release into air or a hydrogen-steam release into nitrogen were incorporated with the jet release tests. Hydrogen or helium concentrations, gas velocities, and temperature profiles were measuring during simulations of two hydrogen release scenarios. Mixing and distribution were determined from the concentration, velocity, and temperature profiles. The test objective was to determine the maximum release gas concentration difference between spatial locations in the compartment during two simulated hydrogen releases.

The objective of the four preliminary tests (HMP-1 through HMP-4) was to determine the separate and combined effects of natural and forced air recirculation on gas mixing in the test compartment. Tests HMP-1 and HMP-2 had relatively lower natural convection effects due to the smaller temperature difference between the bulk air and the vessel wall. Tests HMP-3 and HMP-4 were conducted with the bulk air temperature elevated which increased the temperature difference across the air boundary layer next to the wall and increased natural convection buoyancy effects on gas mixing. Tests HMP-2 and HMP-4 were provided with forced air recirculation scaled to simulate the air recirculation provided



Table 1: Hydrogen Mixing Test Matrix.

Table 1: Hydrogen Mixing Test Matrix.										
Test No.	Cont. Gas	Recirculation Flow Rate		Source Gas	He or H <sub>2</sub> Flow Rate		Steam Flow Rate		Initial Lower Vol. Gas Temp.	
		m <sup>3</sup> /min.	ft. <sup>3</sup> /min.		kg/min.	lb./min.	kg/min.	lb./min.	°C	°F
Preliminary Tests										
HM-P1	Air	0	0	-	-	-	-	-	29	85
HM-P2	Air	104	3700	-	-	-	-	-	29	85
HM-P3	Air	0	0	-	-	-	-	-	66	150
HM-P4	Air	104	3700	-	-	-	-	-	66	150
High Velocity Horizontal Jet Tests										
HM-1	Air	0	0	He-Steam	0.41	0.9	12.3	27	66	150
HM-2	Air	0	0	He-Steam	0.82	1.8	24.5	54	66	150
HM-3	Air	104	3700	He-Steam	0.41	0.9	12.3	27	66	150
HM-4	Air	104	3700	He-Steam	0.82	1.8	24.5	54	66	150
HM-5	N <sub>2</sub>	104	3700	H <sub>2</sub> -Steam	0.41	0.9	24.5	54	66	150
High Velocity Vertical Jet Tests										
HM-6	Air	104	3700	He-Steam	0.41	0.9	12.3	27	66	150
HM-7	Air	104	3700	He-Steam	0.82	1.8	24.5	54	66	150





to the ice condenser plant lower containment region. Test parameters measured were local air velocity magnitude, air temperature, wall temperature, and air recirculation flow rate.

The objective of the jet release tests was to determine the maximum hydrogen concentration difference in the ice condenser lower containment compartment. A secondary objective was to characterize the relative importance of the high momentum jet, forced air recirculation, and natural convection mixing processes. Helium was a simulant for hydrogen in six of seven tests. One of the six helium tests and the one hydrogen test used identical conditions to determine if helium was a valid simulant for hydrogen.

Mixing tests HM-2 through HM-5 were all simulations of a steam-hydrogen release from a 5 cm (2-inch) pipe break. Tests HM-1 and HM-2 were cases without air recirculation normally provided during an accident scenario for an ice condenser lower containment region. Tests HM-3 and HM-4 were conducted with modeled air recirculation flows. Tests HM-1 and HM-3 were conducted with helium-steam release rates arbitrarily set at one-half the reference release rate to determine the effect of reduced jet momentum on mixing in the test compartment volume. Mixing test HM-5 was modeled to be "similar" to HM-4 with the difference that hydrogen was used as the source gas and nitrogen was used as the containment gas. This test was conducted to determine whether helium was a valid simulant for hydrogen in these tests.

The final tests HM-6 and HM-7 simulated a vertical hydrogen-steam jet release directed upward from a location geometrically similar to that of a pressure relief tank rupture disk vent. The helium-steam source rates were identical to those of tests HM-3 and HM-4, respectively. These flow rates were also representative of the releases from a 5 cm (2-inch) pipe break as well as a rupture of the pressure relief tank rupture disk.

#### 2.4.2 MAAF4 Modeling

The initial pressure and temperature of each node is specified in the parameter file or as a local parameter change in the input deck. The initial gas constituents (air or nitrogen) are also specified in the parameter file or input deck.

### 2.5 Time-Dependent Conditions

#### 2.5.1 CSTF Description

At a test-specific time prior to source flow initiation, covers on the lower door junctions are removed. Due to the relatively hot gas in the lower volume, buoyancy-driven counter-current flow is initiated through the door junctions, manifested by a drop in the lower volume temperature as cold upper volume gas begins to exchange with hot lower volume gas.



If recirculation fans are part of a specific test, they are actuated at some point between the opening of the lower door junctions and the initiation of the break source flow. Generally, the fans are initiated at the same time as the removal of the covers from the lower door junctions. It should also be noted that this is representative of the plant behavior since one train of the recirculation fans is sufficient to open the LIDs. Moreover, this assumption is justified by the lower volume temperature history. The noted decrease in temperature at the time of door junction opening is much more pronounced for those tests with fan recirculation, indicating that fan flow must exist to account for the enhanced mixing of the cold upper volume gas with the hot lower volume gas.

The break mass flow rate temperature histories for steam and hydrogen simulant are documented in Bloom, et al., [1983] for each test. A sample history is shown for Test HM-1 in Figure 4. The nominal values of recirculation fan volumetric flow rate and steam and hydrogen simulant mass flow rate as shown in the test matrix, Table 1. These injection histories are input by reading the CSTF.DYB file.

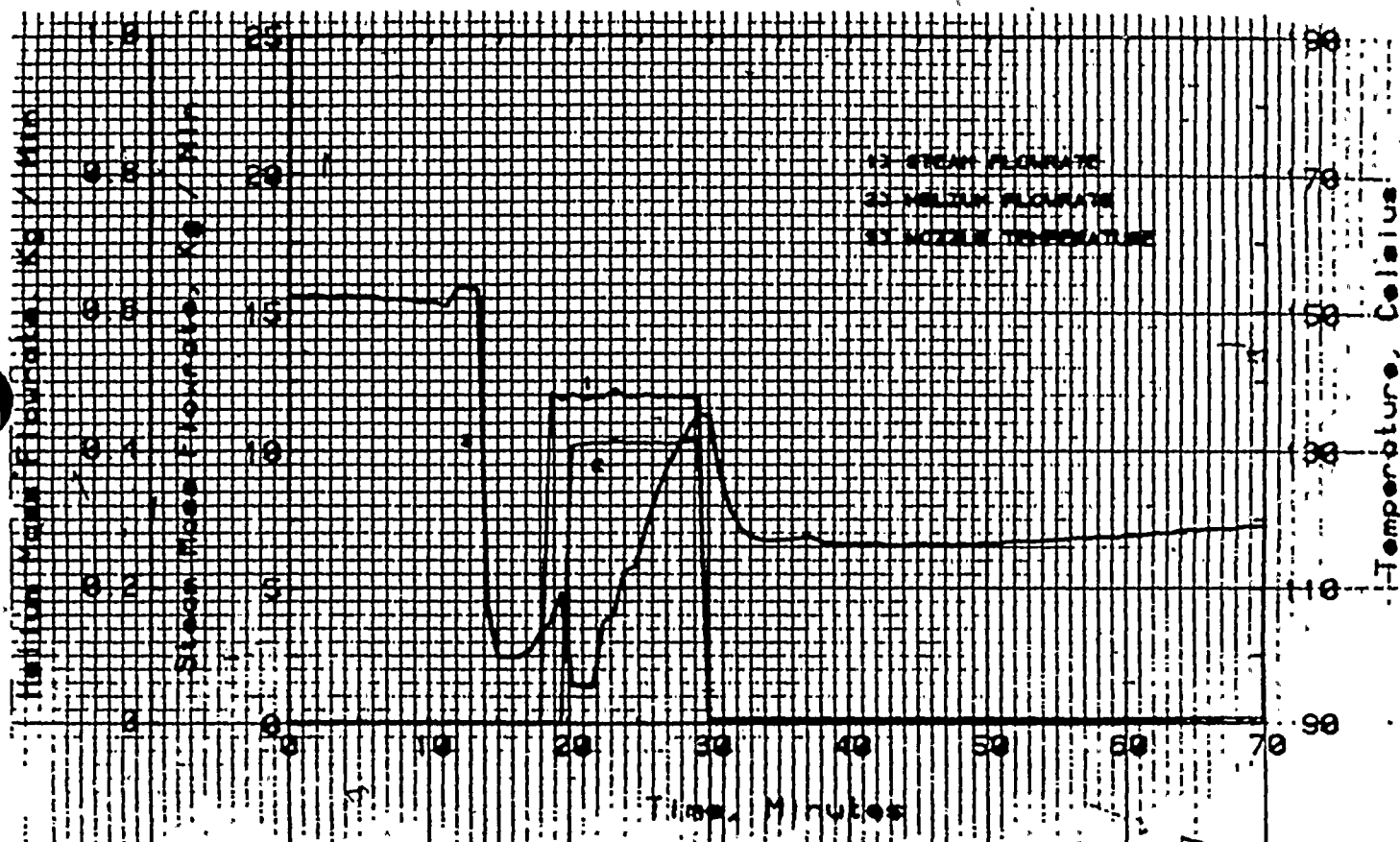
After termination of steam and hydrogen simulant injection, test data acquisition was continued until the system stabilized. This always coincided with full dissipation of concentration and temperature gradients, demonstrating that substantial mixing of the upper and lower volumes yielded a homogenized state. No hydrogen stratification nor pocketing occurred.

### 2.5.2 MAAP4 Modeling

Lower door junction covers, Junctions 1 and 3, are modeled by setting JFRB(1) = 0 and JFRB(3) = 0, respectively, to close these junctions at initiation of the code run. Removal of these covers at the time indicated in the test is accomplished by setting JFRB(1) and JFRB(3) equal to 1 to open these junctions. If recirculation fans are activated for a test, Junctions 5 and 6 are initially closed and then opened at the indicated time using the appropriate values for JFRB(5) and JFRB(6).

Time history for mass and energy flow rates of steam and hydrogen simulant into Node 2 is implemented by digitizing the mass flow rate and temperature from the test, a sample of which is provided in Figure 4. This is read into the calculation through the dynamic benchmark file CSTF.DYB. The data is added to corresponding look-up tables in the input deck. This allows the code to interpolate values from the tables during the transient. After being processed through the input deck, the data is ultimately transmitted to the MAAP4 containment regional routines, AUXREG, via the CSTF-specific benchmark routine, BCSTF.

Figure 4: Test: HM-1A Nozzle Gas Flowrates and Temperature  
(taken from [Bloom, et al., 1983]).



**2.6 Instrumentation****2.6.1 CSTF Description**

The lower volume of the facility is instrumented to determine if local hydrogen accumulation is possible. Such an investigation is particularly relevant for ice condenser containments since the segregation between the upper and lower volumes could result in hydrogen accumulation below the operating deck. Instrumentation arrays are located in the axial direction, to determine the extent of stratification, and in the azimuthal direction, to investigate concentration gradients in this direction due to the preferential location of source jets A and B in Figure 2.

Specifically, Table 2 defines the designations of "top", "mid-plane", and "bottom" in terms of the respective axial locations for the instrument arrays. Table 3 then provides a summary of the instrument arrays, including the axial and azimuthal location of each sensor and the instruments at each location. These included gas velocity probes (anemometers), gas sample probes, and thermocouples. Figure 2 shows these locations at the star (\*) symbol.

**Table 2: Instrument Location Definitions.**

Designation	Location	Elevation (relative to grade elevation (0 m))
Top	0.2 m (9 in.) below the upper deck	- 3.97 m (- 13 ft.)
Mid-Plane	2.36 m (7.75 ft.) up from the lower deck	- 6.1 m (- 20 ft.)
Bottom	0.3 m (1 ft.) up from the lower deck	- 8.2 m (- 26.8 ft.)

**Table 3: Instrumentation in Lower Volume.**

Sensor Location	Point No.	Gas Velocity Probe	Gas Sample	Thermocouple
5°, Top	1	Yes	Yes	Yes
65°, Top	2	Yes	Yes	Yes
125°, Top	3	Yes	Yes	Yes
185°, Top	4	Yes	Yes	Yes
245°, Top	5	Yes	Yes	Yes
5°, Mid-Plane	15	No	No	Yes
65°, Mid-Plane	16	No	No	Yes
125°, Mid-Plane	8	Yes	Yes	Yes
185°, Mid-Plane	17	No	No	Yes
245°, Mid-Plane	18	No	No	Yes
5°, Bottom	6	Yes	Yes	Yes
65°, Bottom	14	No	No	Yes
125°, Bottom	7	Yes	Yes	Yes
185°, Bottom	9	Yes	Yes	Yes
245°, Bottom	10	Yes	Yes	Yes



Using these instruments and additional instrumentation, the following data types were collected:

- Helium, or hydrogen, concentrations,
- Gas temperatures,
- Gas velocities,
- Oxygen concentration (H<sub>2</sub> test only),
- Test vessel wall temperatures,
- Atmospheric pressure,
- Steam flow rate,
- Helium or hydrogen flow rate, and
- Air recirculation fan flow rate

The upper volume had substantially less instrumentation since the focus was lower volume concentrations. As shown by Figure 2, it may have been limited to one sensor location in the middle due to the presumption of homogeneity in the upper volume.

### 2.6.2 MAAP4 Modeling

The noted CSTF instrumentation is not influential to specification of input boundary conditions for MAAP4. However, an output consideration is noteworthy. CSTF gas sample probe measurements were reported in terms of "dry" simulant content. That is, the sampled steam was condensed prior to determining the simulant mole fraction. Of course, the balance of the non-condensable was either normal air constituents (with helium as simulant) or pure nitrogen (with hydrogen as simulant).

In contrast, steam is included in the MAAP4 calculation of gas constituents, which inhibits a comparison of conventional code output with experiment data. This difficulty is easily resolved through the use of the user-defined function feature within the MAAP4 input deck. The mole fraction of "dry" simulant in each compartment can be calculated at each time step with the following function:

$$x_j = \left[ 1 + \frac{\sum_i \frac{m_i}{MW_i}}{\frac{m_j}{MW_j}} \right]^{-1} \quad (1)$$

where  $j$  = index for the simulant,  
 $i$  = index for all other non-condensable constituents,  
 $m$  = mass,  
 $MW$  = molecular weight, and  
 $x$  = mole fraction.

$x_j$  can then be included in a plot file. In addition, the time scale for the digitized experiment data is expressed in minutes. Therefore, a user definition function of time in minutes is included in this plot file for easy comparison with the data.

### 3.0 DISCUSSION OF RESULTS

#### 3.1 Test HM-1

Test HM-1 was executed with the parameters shown in Table 1. No recirculation fans were utilized. Therefore, the contributors to mixing were forced flow, imposed by the helium-steam source flow, and natural convection, imposed by the lighter gas in the lower compartment due to the elevated initial temperature. It was necessary to perform some tests in the series without recirculation fans since these are actuated only after containment pressure exceeds the setpoint defined in the plant technical specifications. Therefore, it is conceivable that a sufficiently small break in the RCS would liberate steam and hydrogen to containment without actuating the fans.

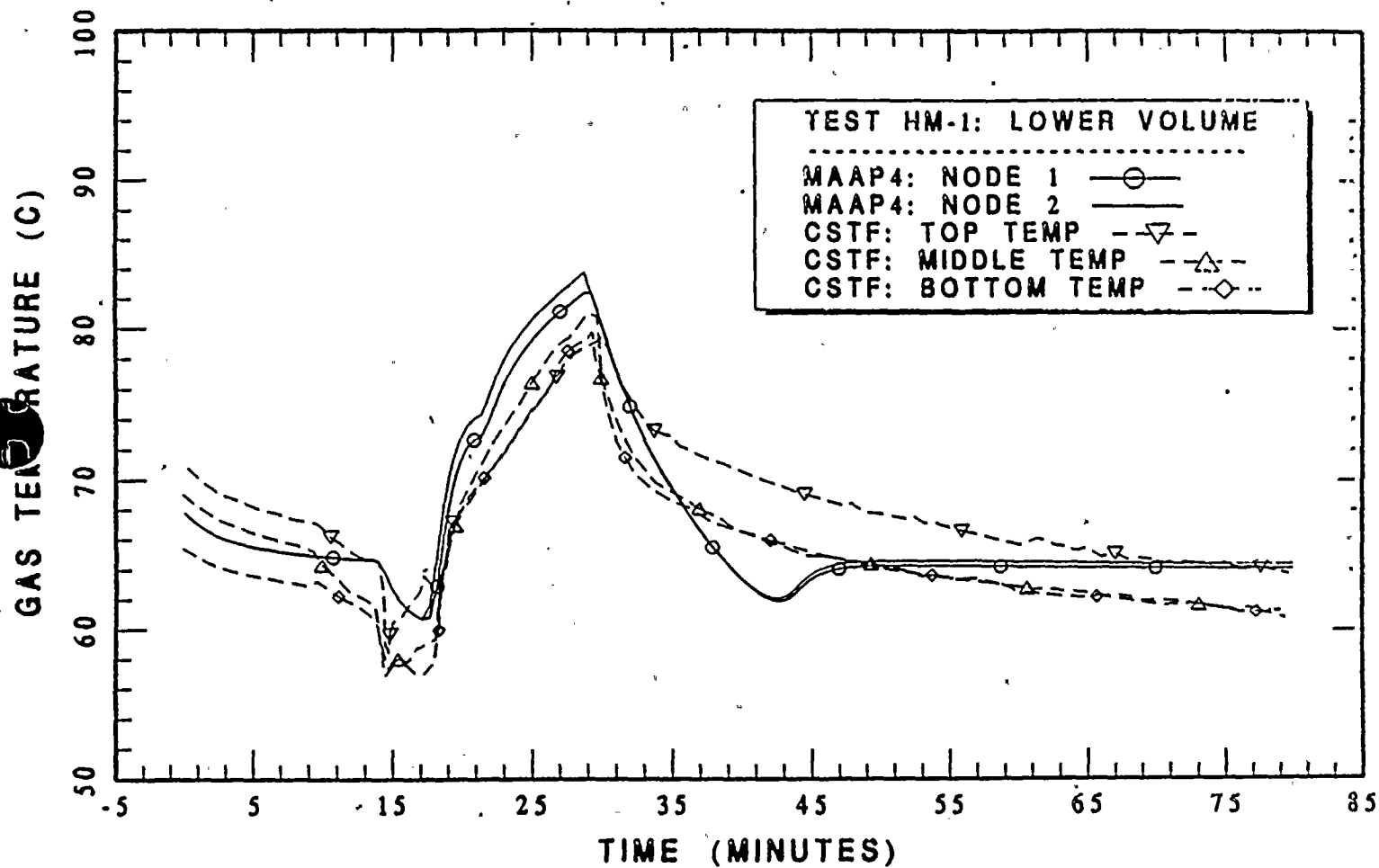
Figure 5 shows a comparison of lower volume gas temperature thermocouples with the predicted temperature for Nodes 1 and 2. Both MAAP and the data show a shallow temperature decrease, ostensibly due to the influences of heat sinks. At roughly 14 minutes, there was a substantial drop in temperature. This was presumed to be the opening of the junctions representing the ice condenser lower doors, followed by the onset of natural convection between relatively hot lower-volume and the relatively cold upper volume ( $\approx 30^\circ\text{C}$ ). Therefore, Junctions 1 and 3 were opened at this time. Indeed, MAAP also predicted a similar temperature decrease.

Upon initiation of the source flow, both the data and MAAP ascend in a similar manner until termination of the source flow. At this point, the data and MAAP decrease in an asymptotic manner as natural convection promotes continued mixing, approaching a homogenized system.

In the first ten minutes after source flow termination, MAAP shows a somewhat more rapid decrease. In contrast, the data shows a more gradual, smooth decrease. Furthermore, the top temperature separates from the corresponding mid-plane and bottom values. Such behavior is shown in the data at other azimuthal locations. This signifies a small but sustained stratification. Most likely, counter-current flow at Junctions 1 and 3 feeds cold gas as a plume



Figure 5:  
Comparison of MAAP4 Calculated Lower Volume Temperature  
and the CSTF Data for Test HM-1.



into the middle and lower regions of the lower volume. The top region remains hotter due to the stratification. It feeds the relatively hot gas participating in the counter-current flow at Junctions 1 and 3.

The current MAAP nodalization of the lower volume does not accurately predict these details since Nodes 1 and 2 are horizontally oriented, not vertically. If further resolution is needed, additional vertical nodes would provide a better representation of these details. However, this difference in rates is secondary to the overall agreement in temperature at the end of the test.

Figure 6 shows the comparison between hydrogen simulant concentration for the data and MAAP. As shown, there is good agreement between the measured and calculated responses.

### 3.2 Test HM-2

This experiment also had no recirculation fans with a high velocity horizontal jet of a helium-steam mixture being injected into the lower compartment. Here again the major contributors to mixing were the forced flow imposed by the injection source and natural convection due to the lighter density of the incoming gaseous source flow. Figure 7 illustrates the measured and calculated gas temperatures in the lower volume with Figure 8 presenting the measured and calculated values for the helium concentration in this region. As shown by the comparisons, the MAAP models for natural circulation between compartments provides a good representation of the system transient response in terms of both temperature and light gas concentrations.

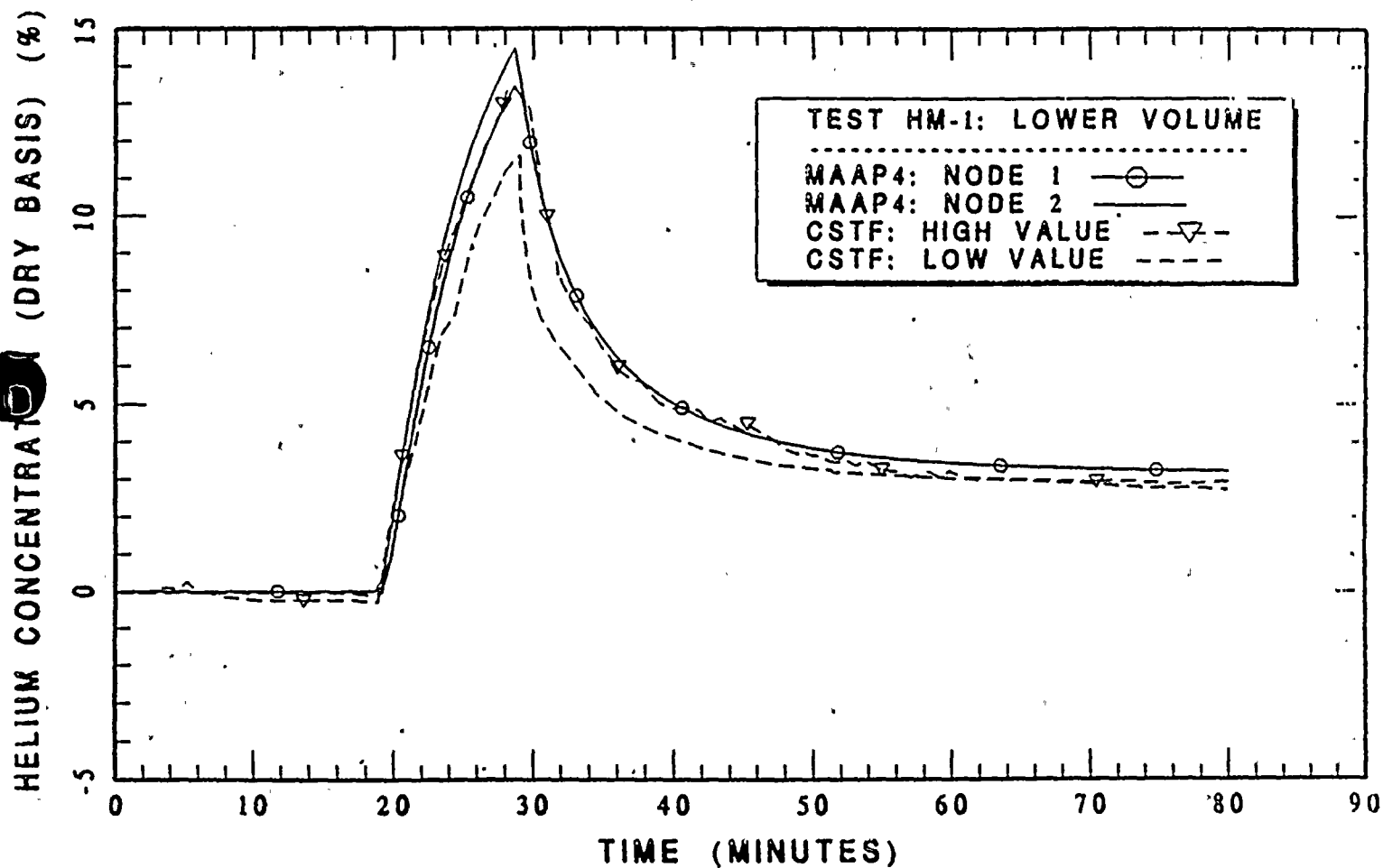
### 3.3 Test HM-3

As listed in Table 1, this was the first experiment with a recirculation flow rate combined with an injection flow of a steam-helium mixture. Figure 9 compares the MAAP calculation with the recorded measurements in the lower volume for the gas temperature, while Figure 10 shows a similar comparison for the helium concentrations in the lower volume. Since there is a forced recirculation flow in this experiment, it is expected that there would be agreement between the measured and calculated values and the figures show that this is the case.

### 3.4 Test HM-4

This experiment used a recirculation flow rate equal to that used in Test HM-3, but had a higher helium injection rate. Figure 11 compares the measured results with the MAAP calculation for the gas temperature in the lower volume, with Figure 12 illustrating the comparison of a measured and calculated helium concentrations in this lower volume. Here again the MAAP calculation provides a good representation for the measured values.

Figure 6:  
Comparison of MAAP4 Calculated Lower Volume Helium Concentration  
and the CSTF Data for Test HM-1.



11/11/11



Figure 7:  
Comparison of the Calculated and Measured Gas Temperatures in the Lower Volume  
for CSTF Test HM-2.

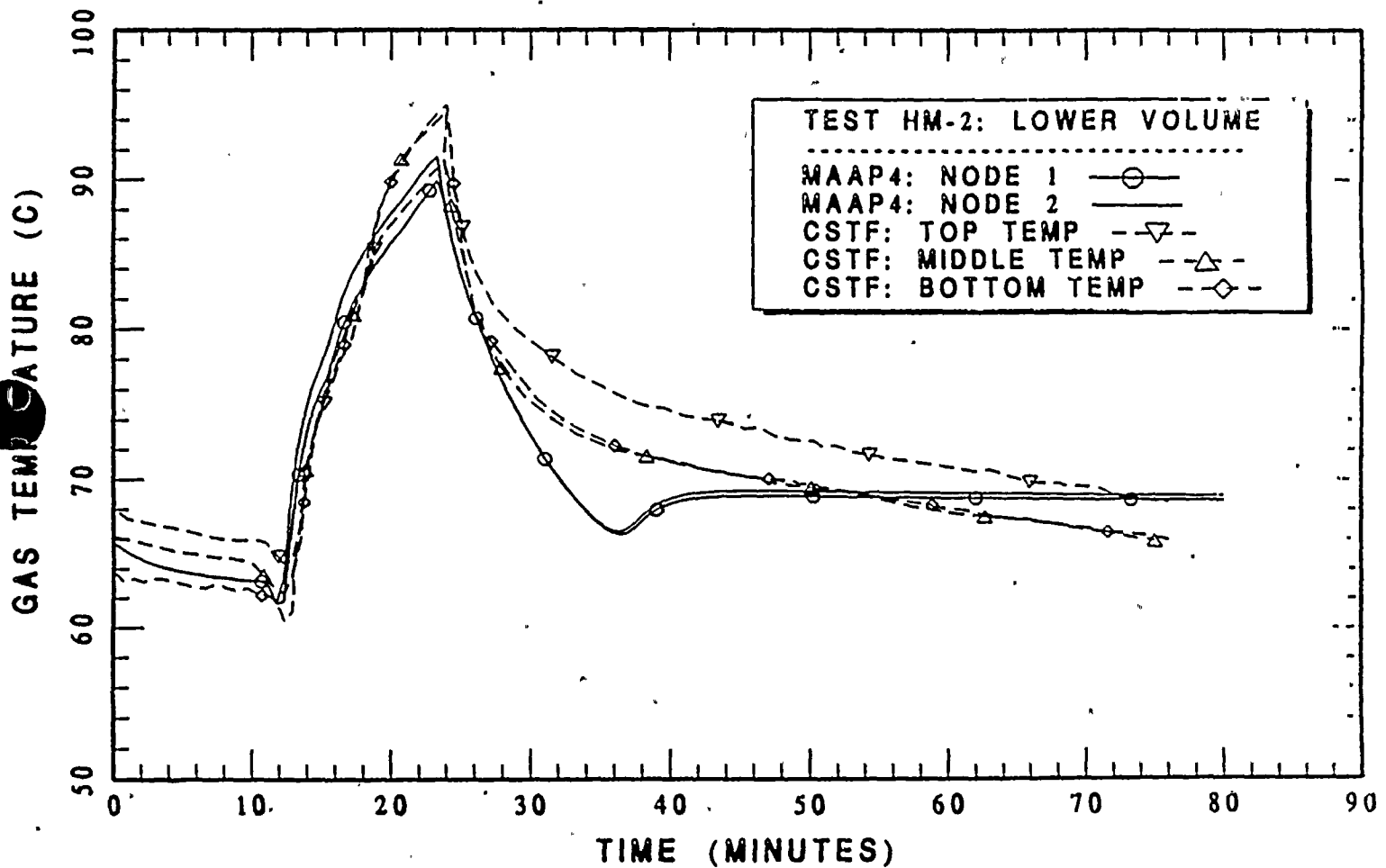


Figure 8:  
Comparison of the Calculated and Measured Heating Concentrations  
in the Lower Volume for CSTF Test HM-2.

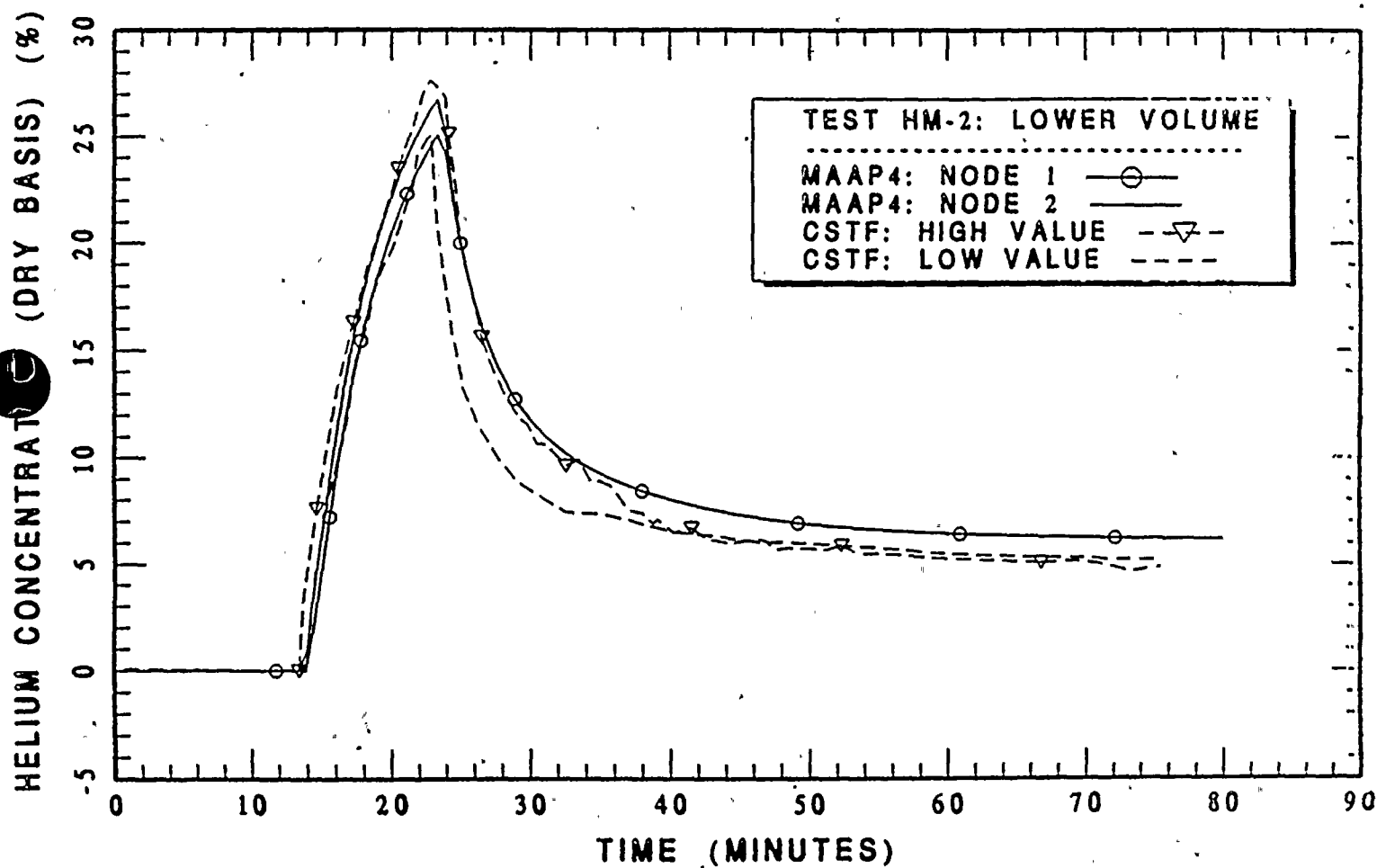


Figure 9:  
Comparison of the Calculated and Measured Gas Temperatures in the Lower Volume  
for CSTF Test HM-3.

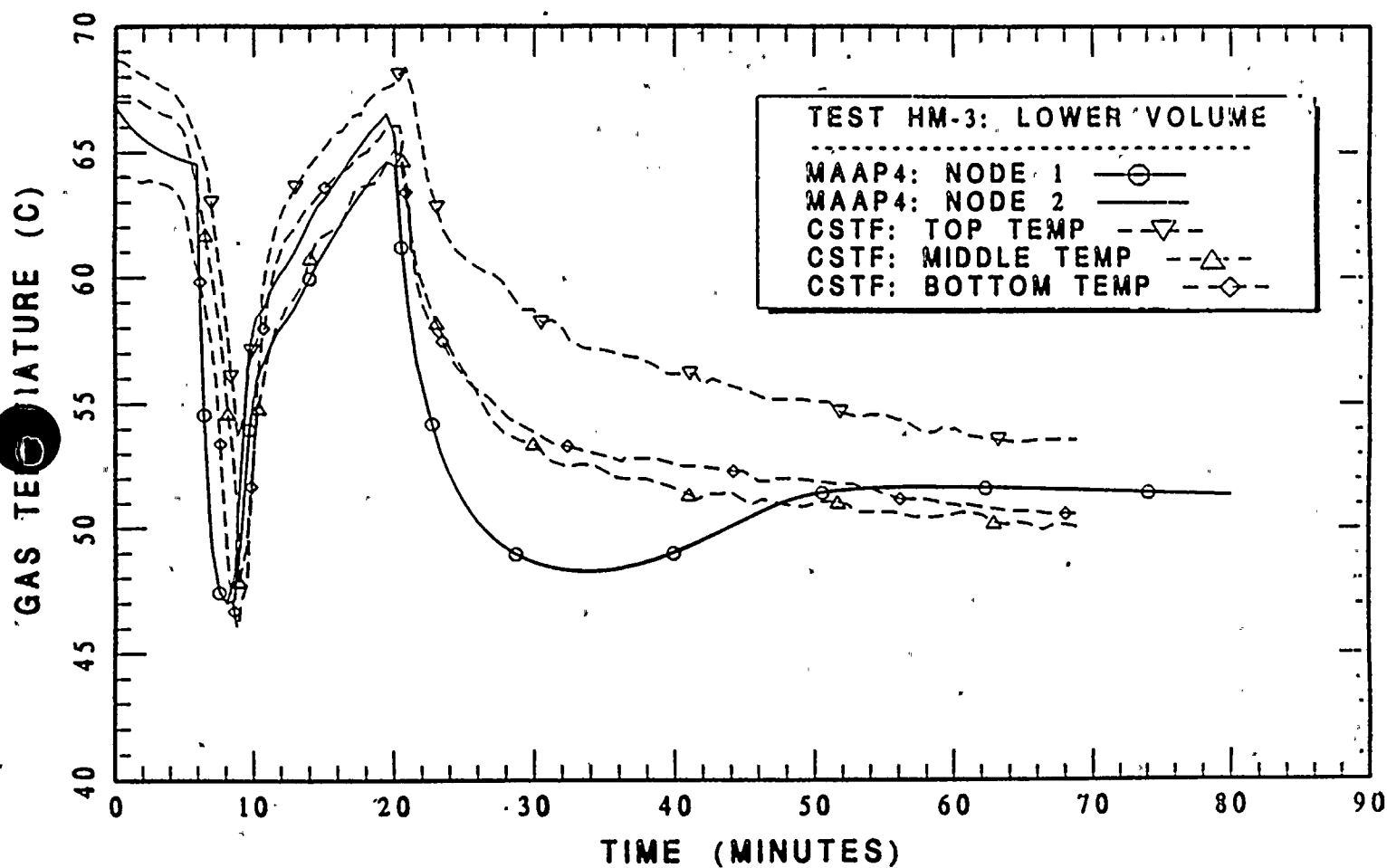


Figure 10:  
Comparison of the Calculated and Measured Heating Concentrations  
in the Lower Volume for CSTF Test HM-3.

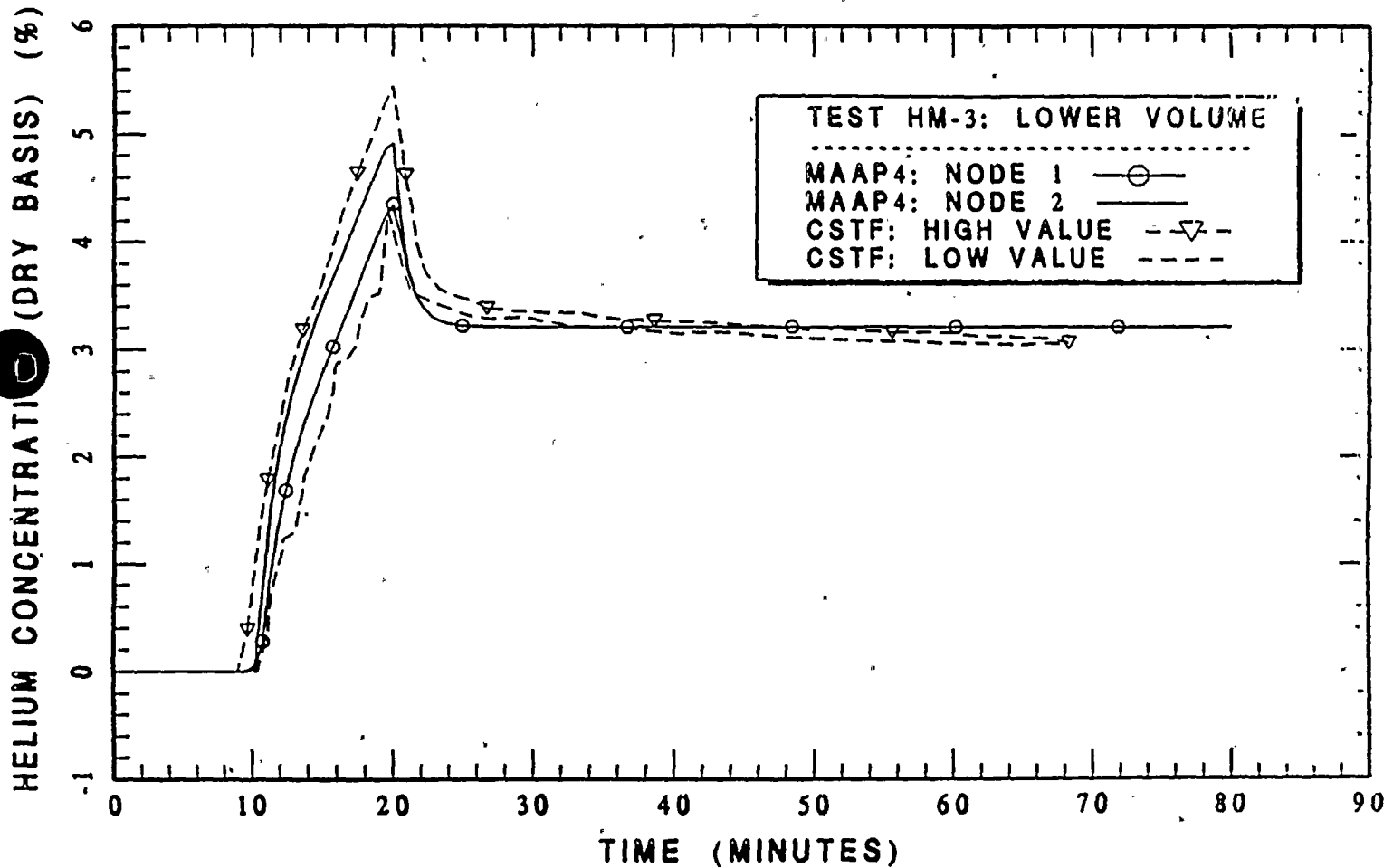






Figure 11:  
Comparison of the Calculated and Measured Gas Temperatures in the Lower Volume  
for CSTF Test HM-4.

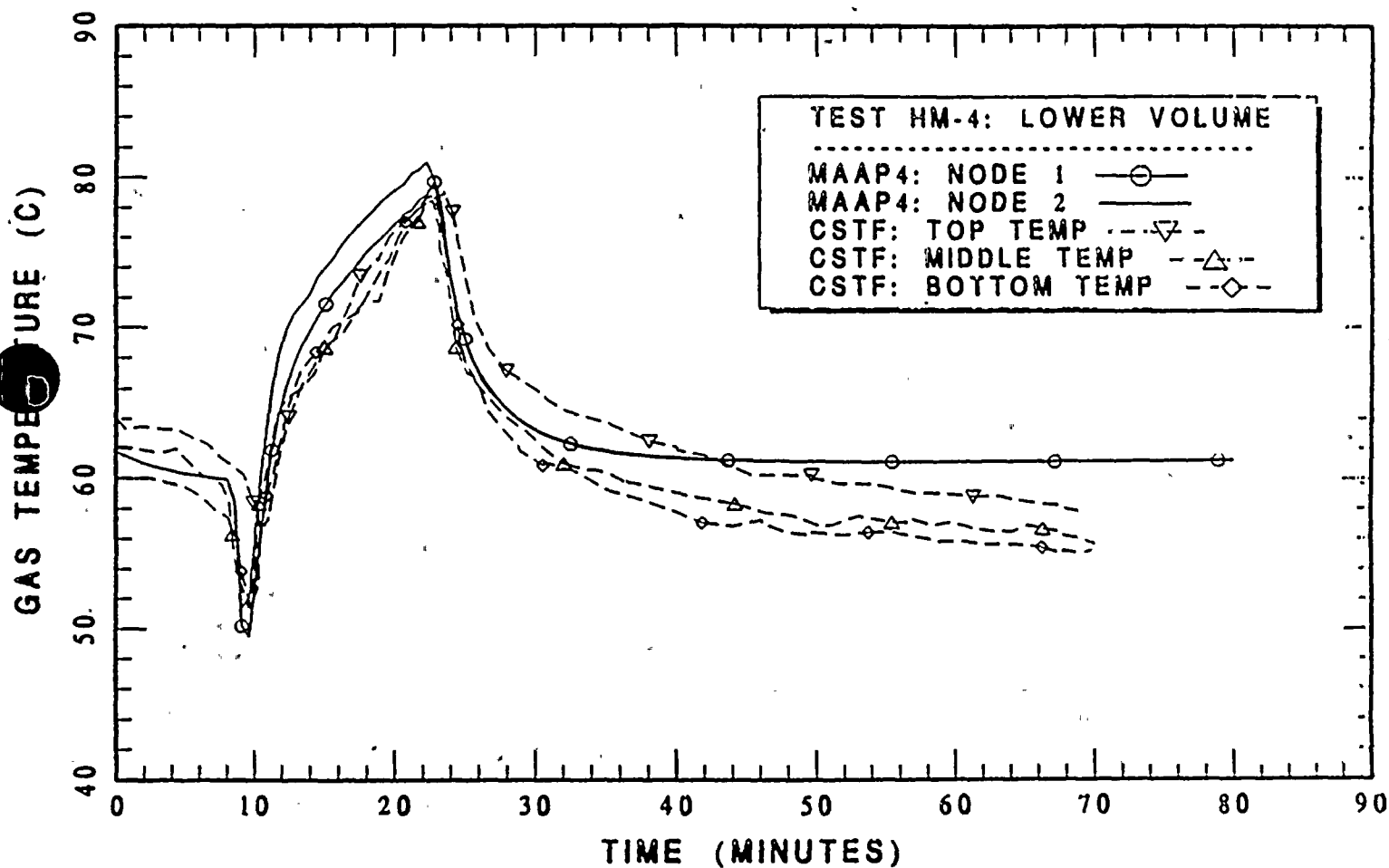
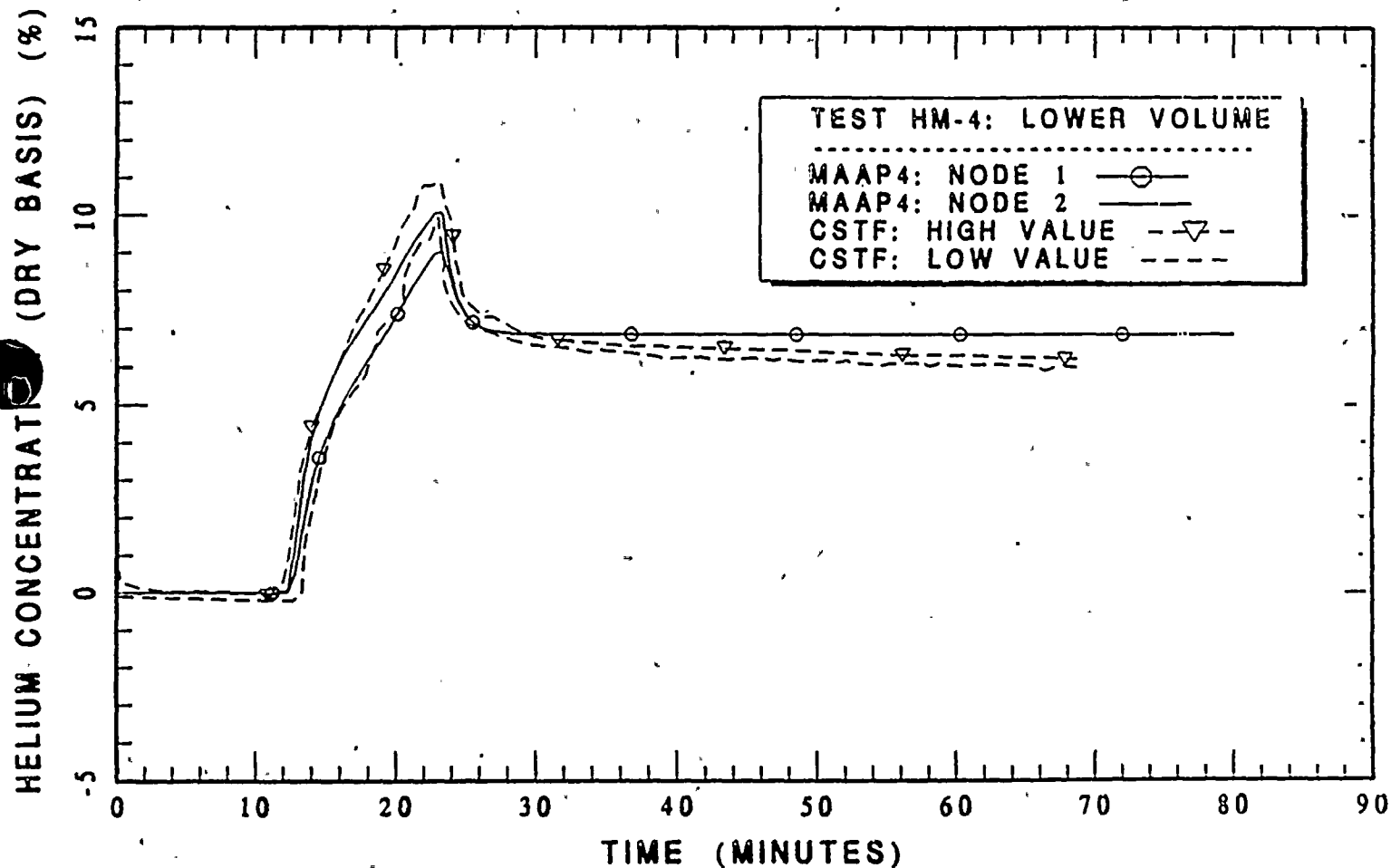


Figure 12:  
Comparison of the Calculated and Measured Heating Concentrations  
in the Lower Volume for CSTF Test HM-4.



### 3.5 Test HM-5

Hydrogen was used as the light gas injection for this experiment and the CSTF vessel was filled with nitrogen instead of air prior to initiating the experiment. This provides a test of the calculational capabilities for the light gas of interest in reactor safety analyses. Figure 13 compares the calculated and measured gas temperatures in the lower volume for this set of conditions and Figure 14 illustrates the comparison for the measured and calculated helium concentrations. As was the case with the previous comparisons, the MAAP response is in good agreement with the measured behavior for both of these parameters.

### 3.6 Test HM-6

A high velocity vertical jet was used in this experiment with the injection gas being a mixture of helium and steam and the CSTF atmosphere being air, as listed in Table 1. Figure 15 compares the measured and calculated gas temperatures for the lower volume with Figure 16 illustrating the comparison of measured and calculated temperature in the upper volume. A comparison of the measured and calculated helium concentrations in the lower volume is given in Figure 17. The comparisons provided in these three figures show that the MAAP representations for combined free and forced convection provide a good characterization of the measured CSTF behavior.

### 3.7 Test HM-7

For this test, a helium-steam mixture was injected into an air atmosphere with the helium injection rate being twice that used in Test HM-6. Figure 18 compares the measured and calculated gas temperatures in the lower volume with Figure 19 illustrating a similar comparison for the upper volume. Figure 20 compares the measured and calculated helium concentrations in the lower volume. As demonstrated by these comparisons, the MAAP containment model provides a good characterization of the light gas behavior in the containment, as well as the gas temperatures in the containment volumes.

## 4.0 SENSITIVITY STUDIES

The principal difference between the various experiments is whether or not forced circulation flow is imposed between the upper and lower compartments in the simulated ice condenser containment. In this regard, the major difference in the flow behavior is whether counter-current natural circulation flows are modeled between the compartments and whether these flows can be "flooded" by the imposed recirculation flow. To illustrate the importance of these counter-current natural circulation flows in two of the experiments, test HM-1 was calculated with the counter-current natural circulation flow removed from the model. Figure 21 shows the calculated and measured gas temperatures for the lower volume with Figure 22 comparing the

Figure 13:  
Comparison of the Calculated and Measured Gas Temperatures in the Lower Volume  
for CSTF Test HM-5.

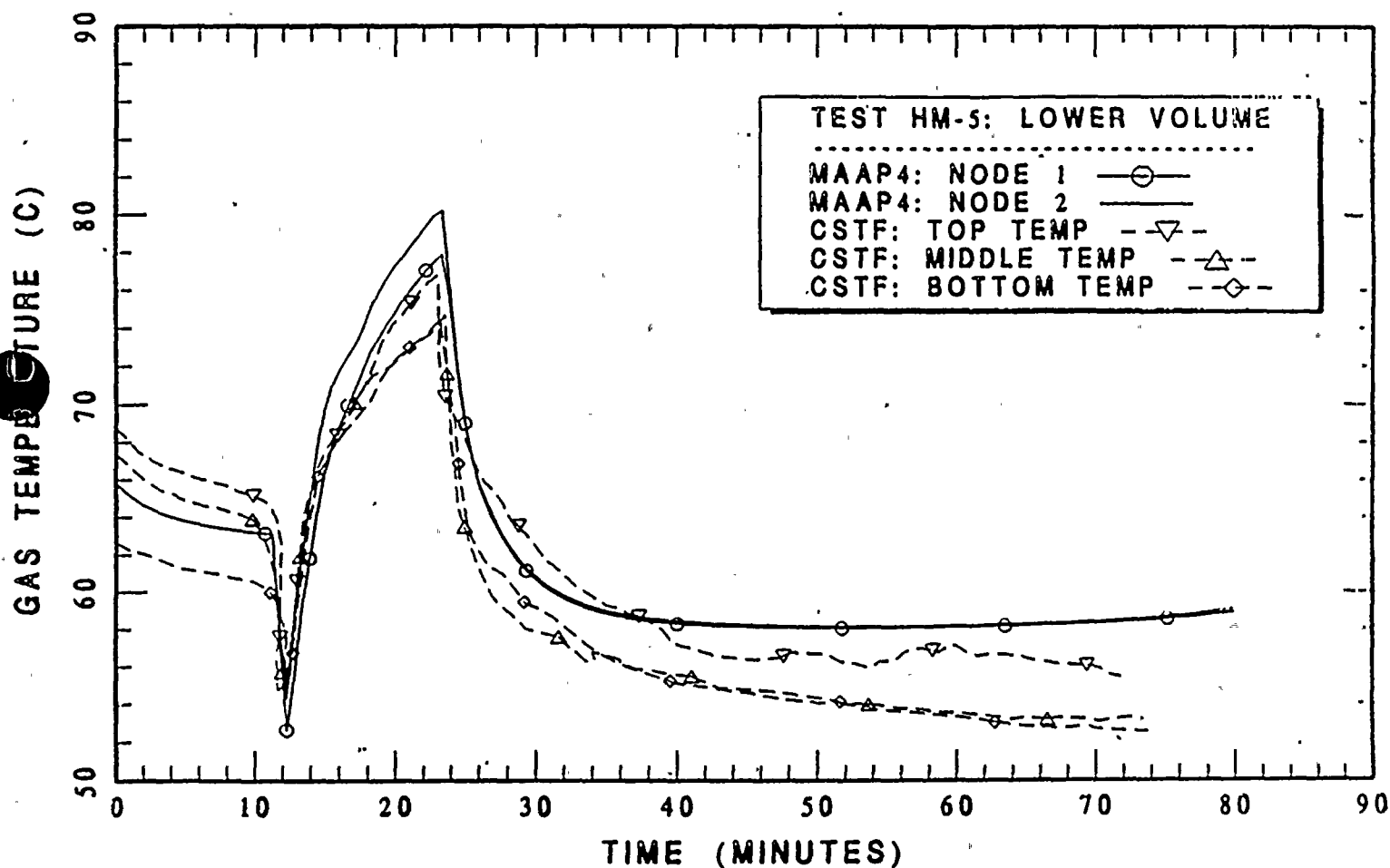


Figure 14:  
Comparison of the Calculated and Measured Heating Concentrations  
in the Lower Volume for CSTF Test HM-5.

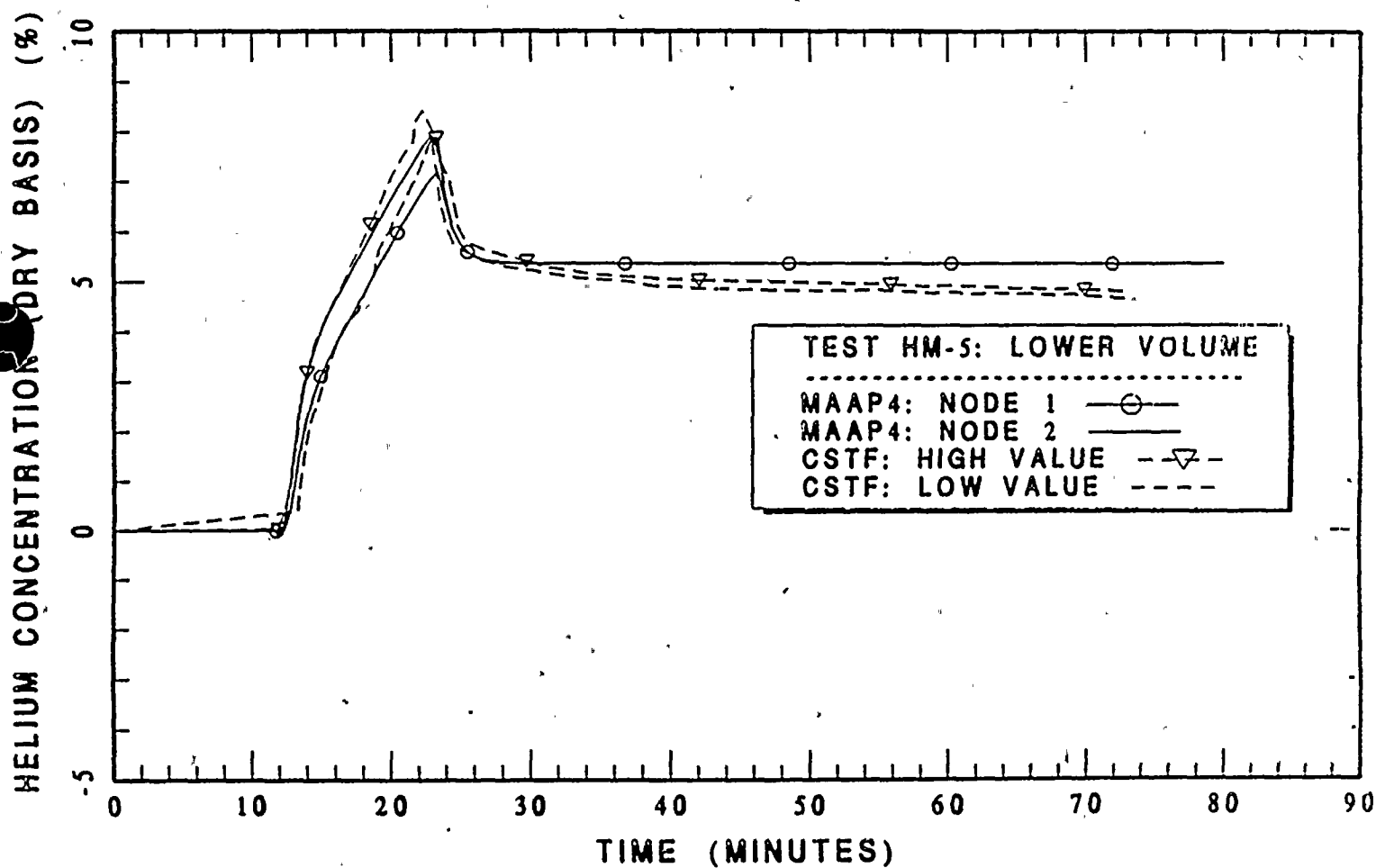




Figure 15:  
Comparison of the Calculated and Measured Gas Temperatures in the Lower Volume  
for CSTF Test HM-6.

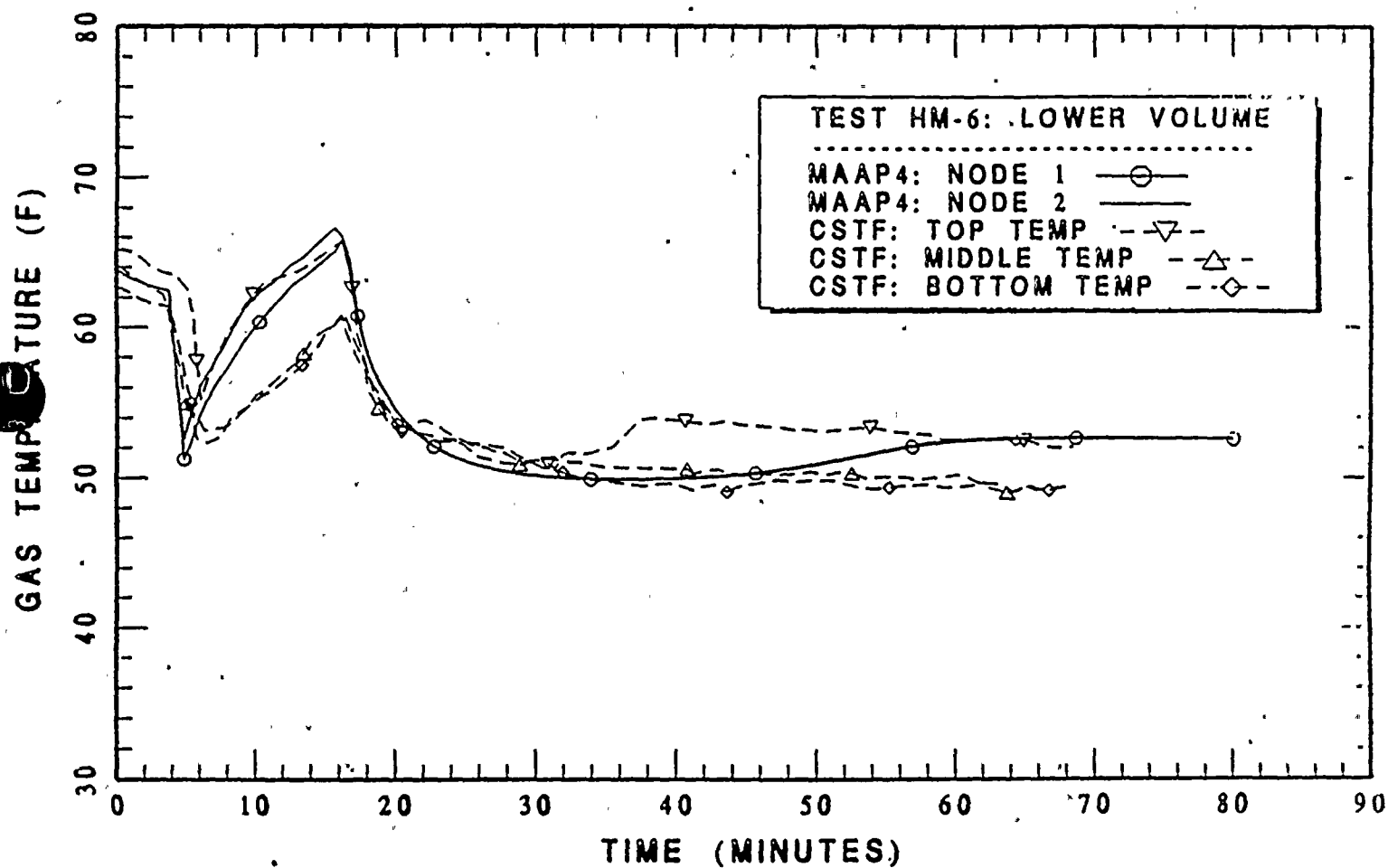




Figure 16:  
Comparison of the Calculated and Measured Heating Concentrations  
in the Upper Volume for CSTF Test HM-6.

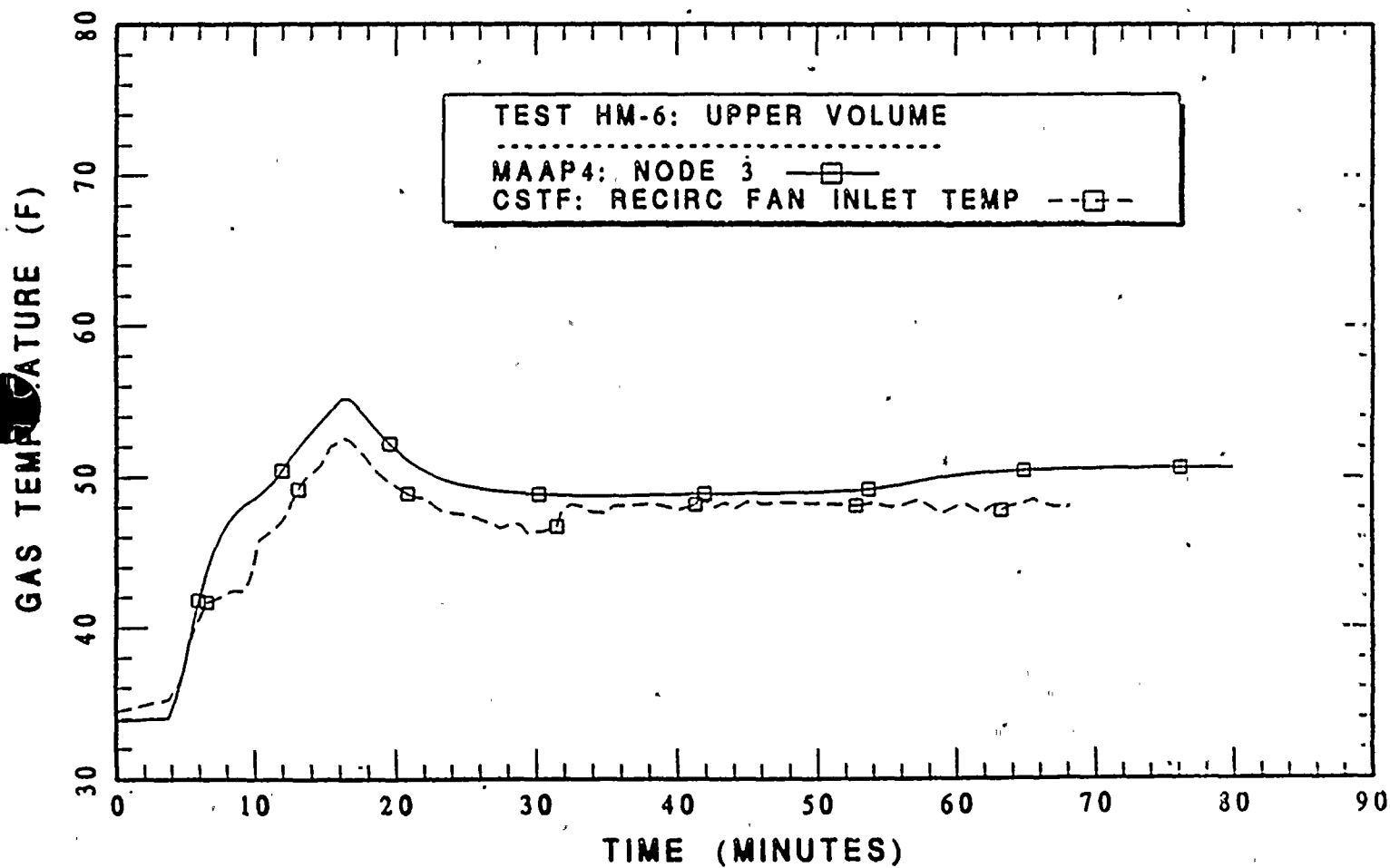


Figure 17:  
Comparison of the Calculated and Measured Heating Concentrations  
in the Lower Volume for CSTF Test HM-6.

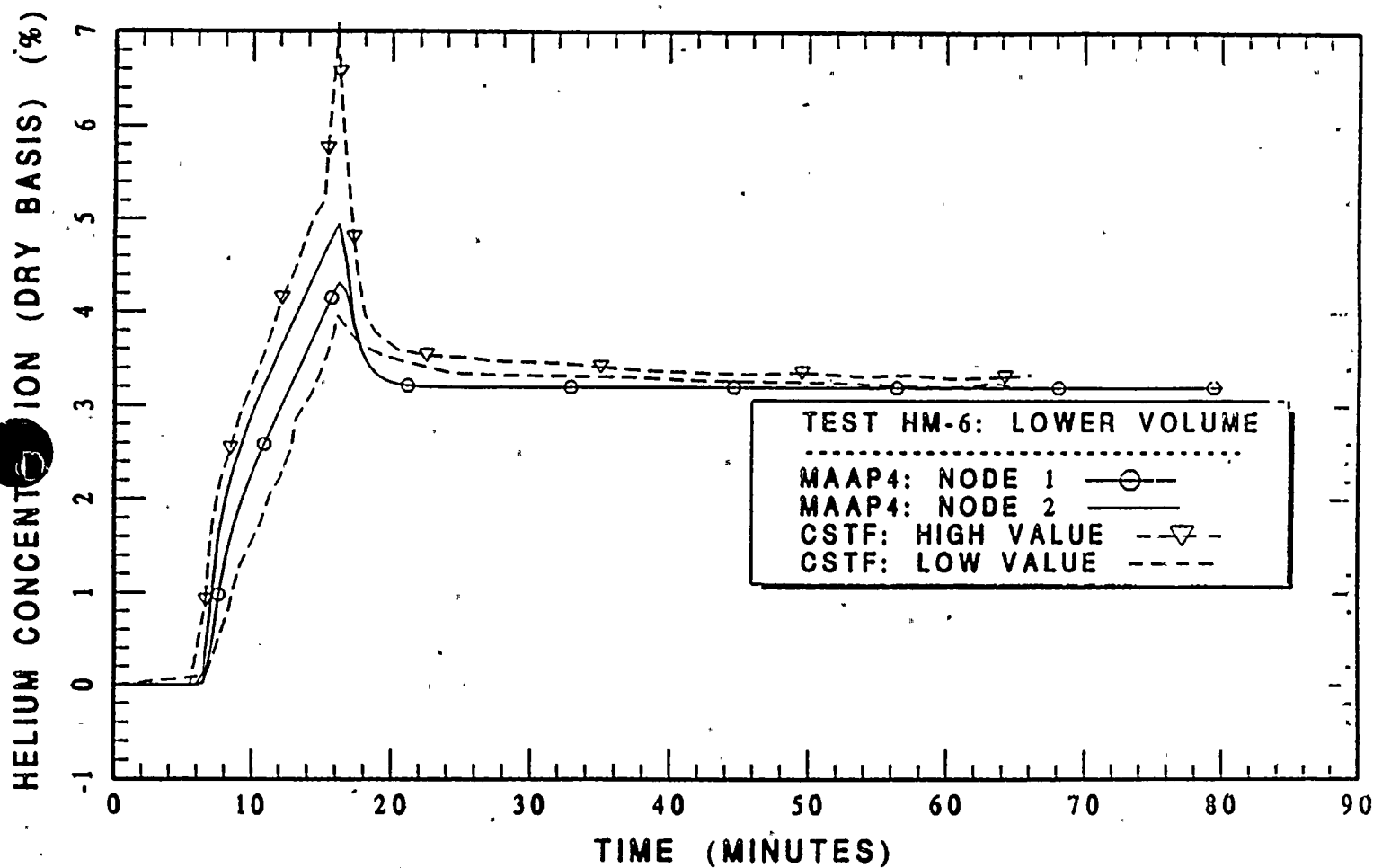


Figure 18:  
Comparison of the Calculated and Measured Gas Temperatures in the Lower Volume  
for CSTF Test HM-7.

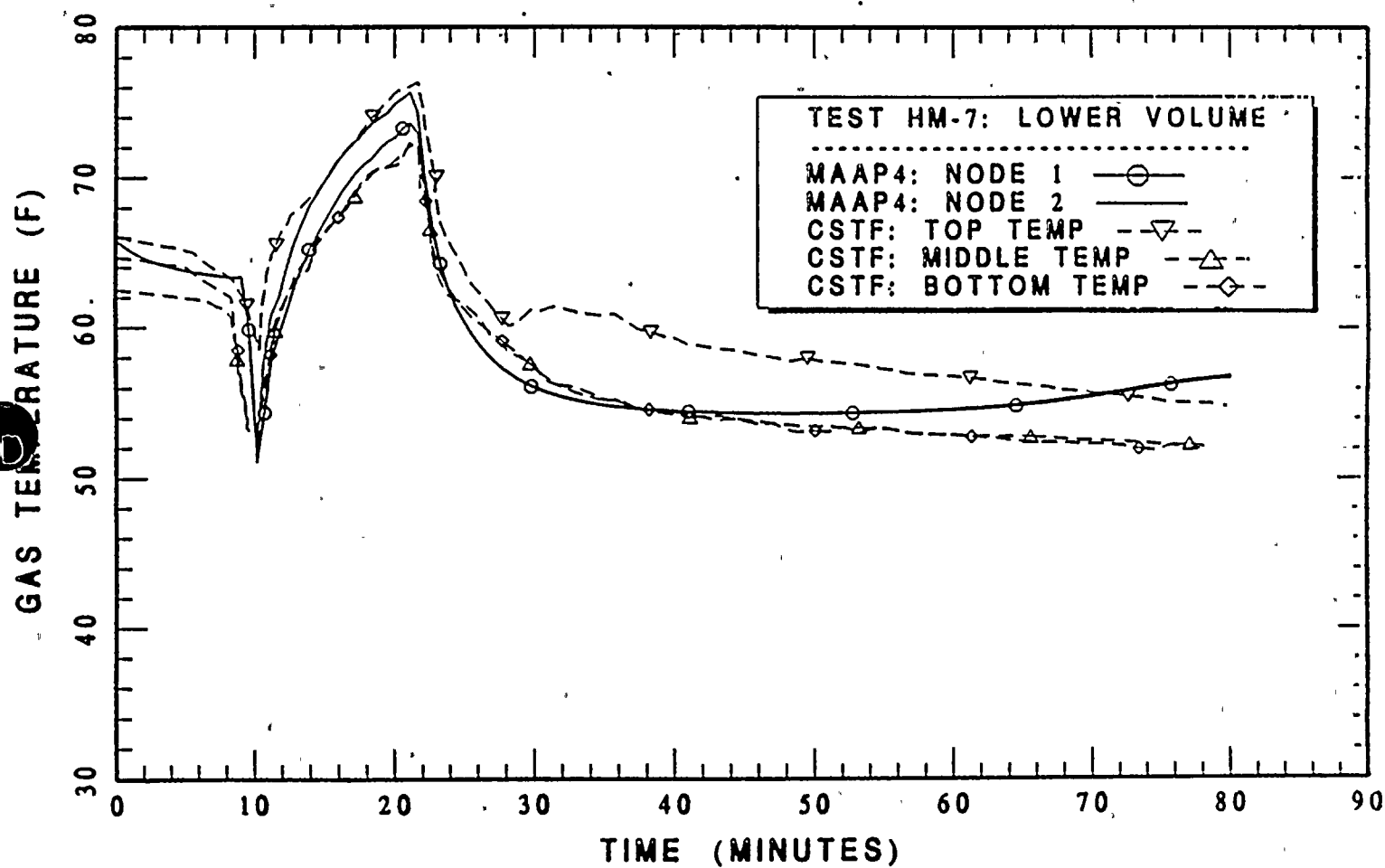


Figure 19:  
Comparison of the Calculated and Measured Heating Concentrations  
in the Upper Volume for CSTF Test HM-7.

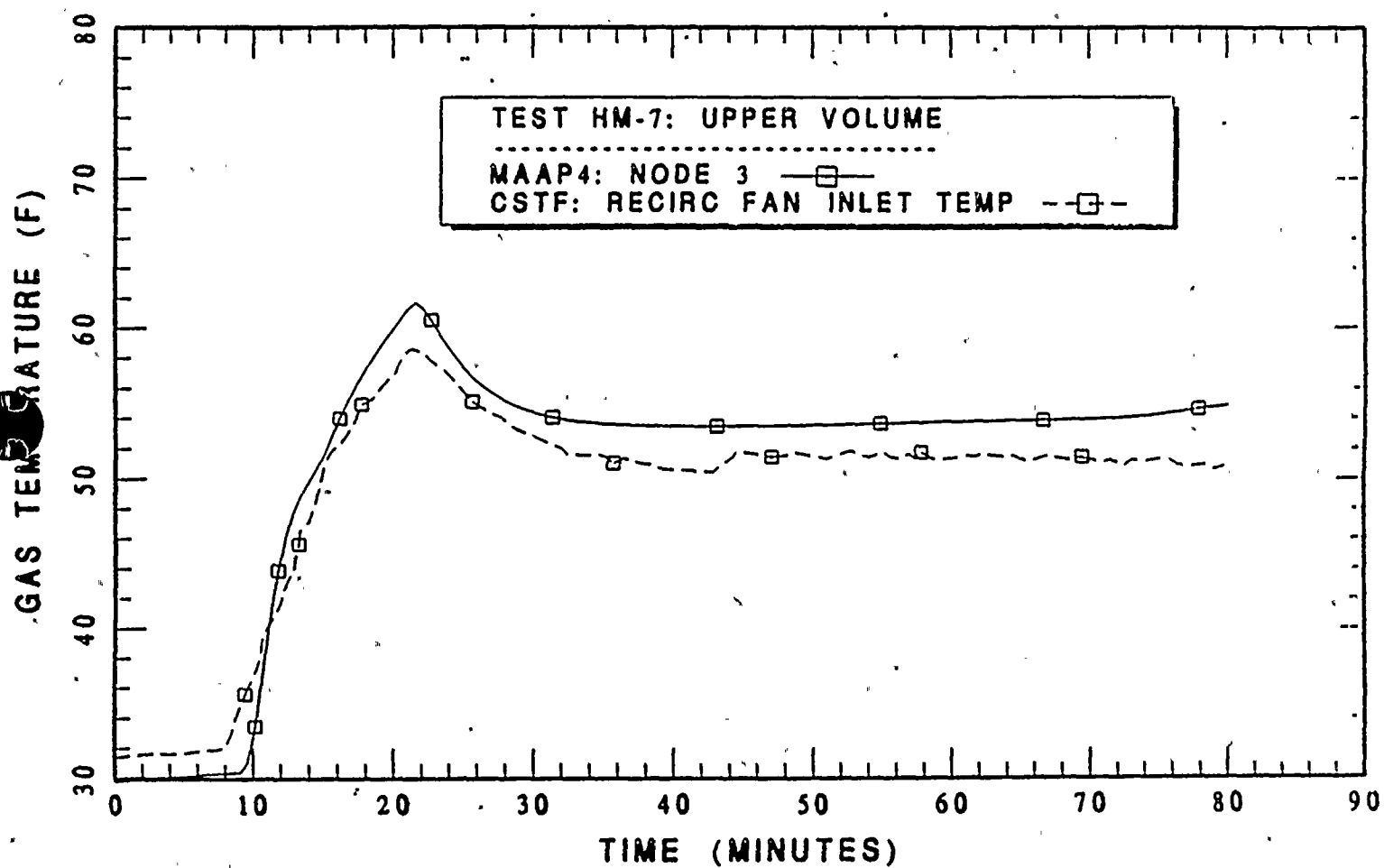




Figure 20:  
Comparison of the Calculated and Measured Heating Concentrations  
in the Lower Volume for CSTF Test HM-7.

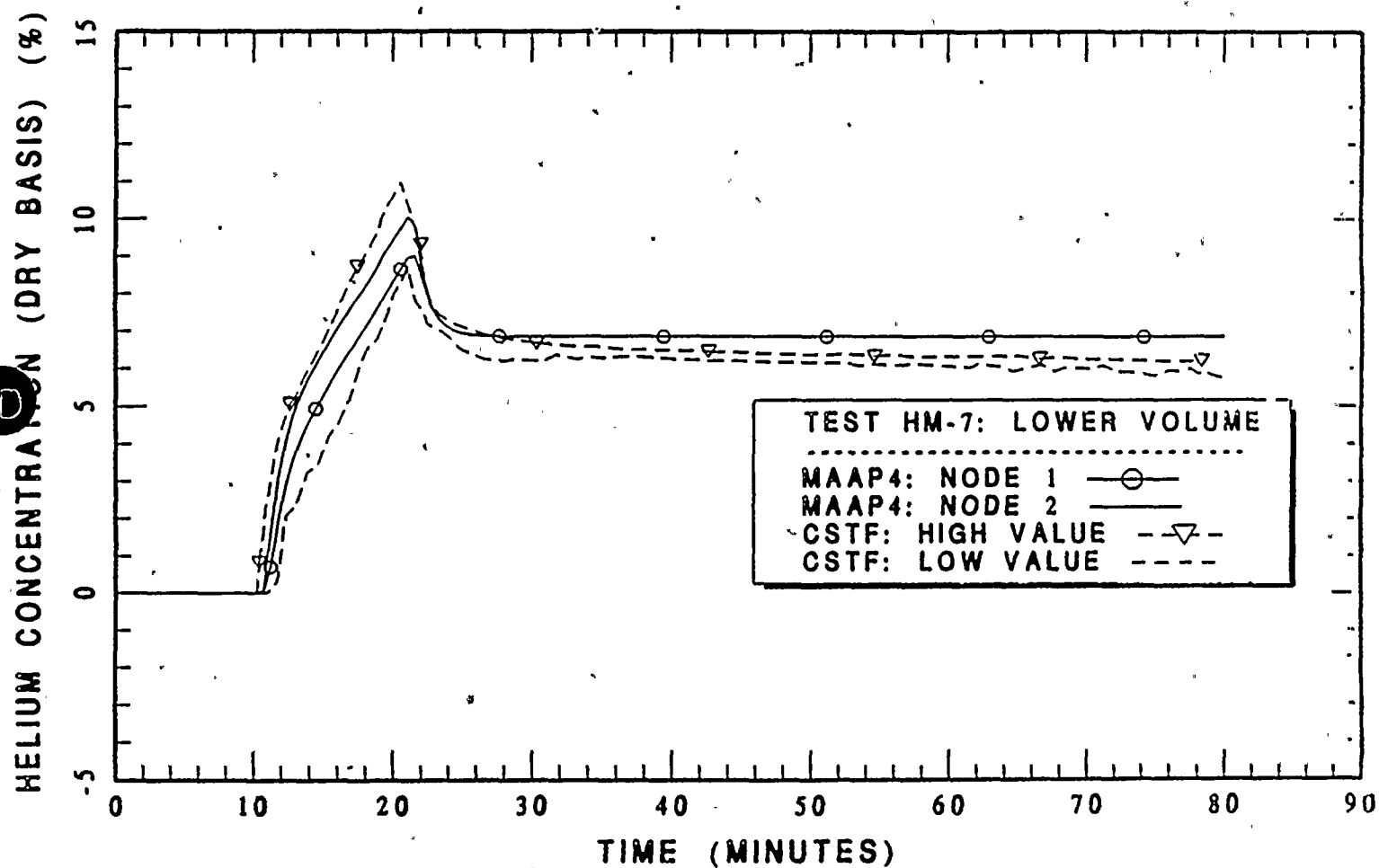




Figure 21:  
Comparison of the Calculated and Measured Gas Temperatures for the Lower Volume  
in CSTF Test HM-1 With Counter-Current Natural Circulation Flows Ruled Out.

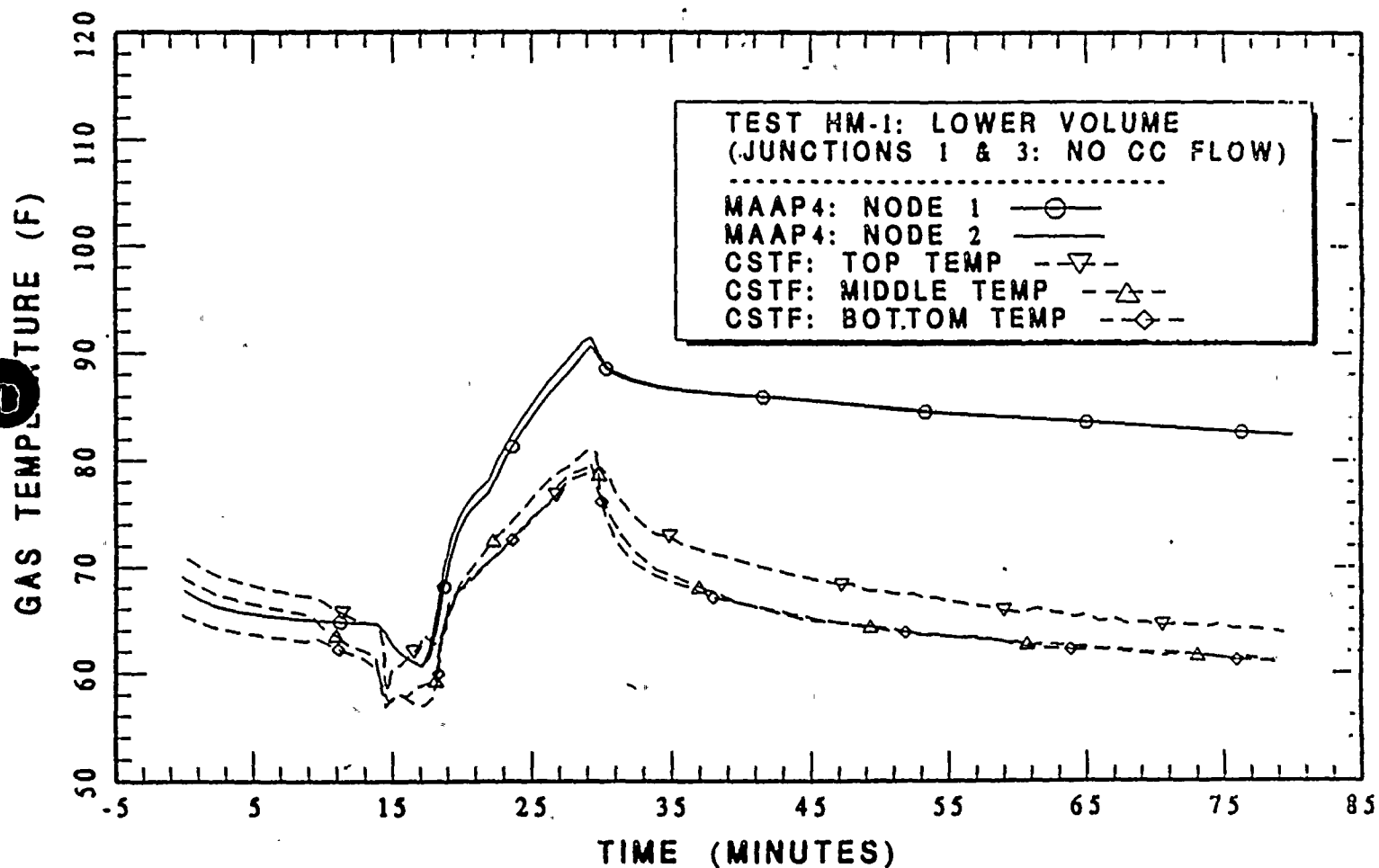
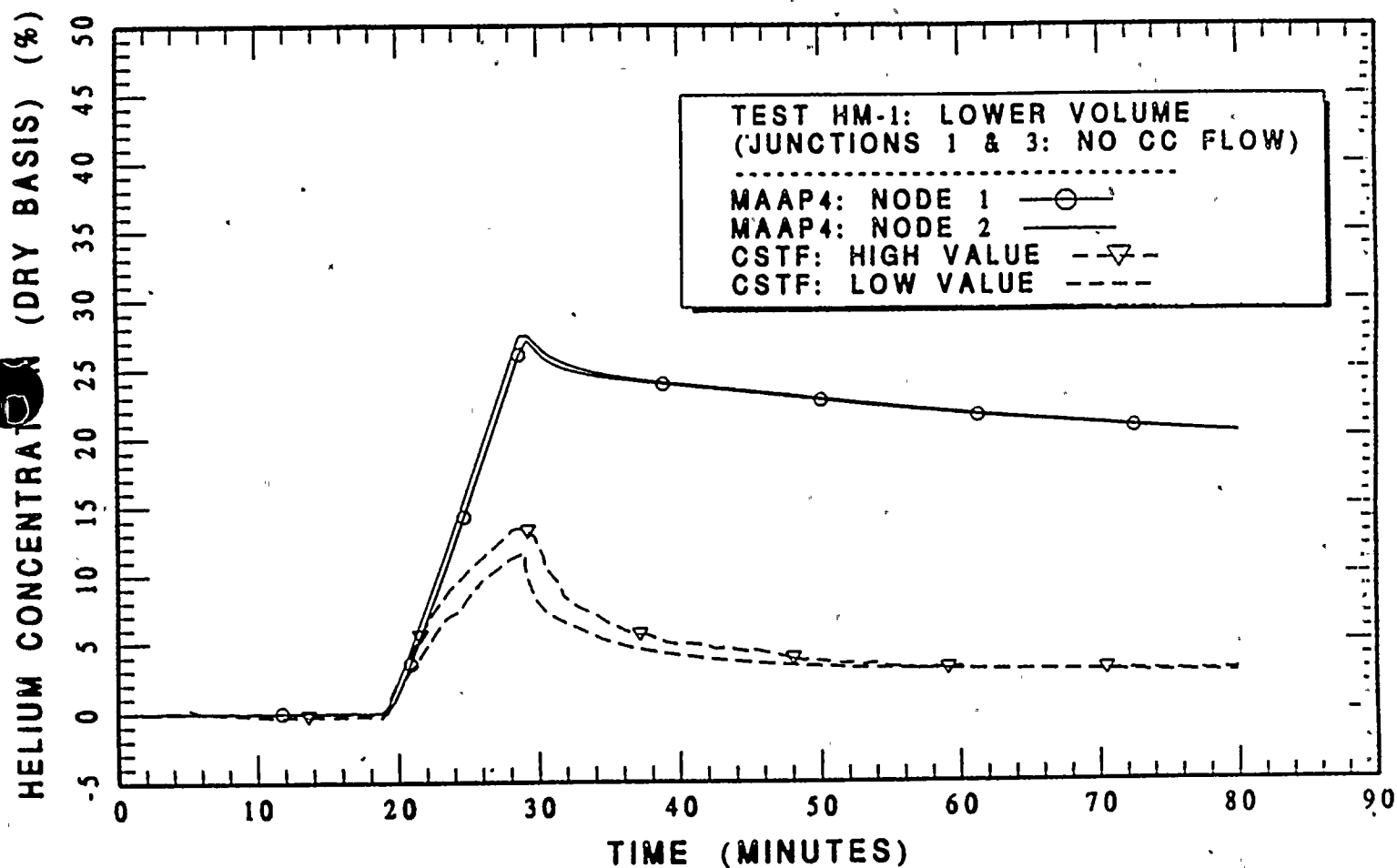




Figure 22:  
Comparison of the Calculated and Measured Helium Concentration in the Lower Volume  
for CSTF Test HM-1 With Counter-Current Natural Circulation Flows Ruled Out.





calculated and measured helium concentration in this lower volume. Contrasting these results with those shown in Figures 5 and 6 demonstrate that the representation of counter-current natural circulation flows is essential to the good agreement illustrated by the comparisons in Section 3. In particular, when there is no forced flow by the recirculation fans, which is the case for CSTF test HM-1, the major mechanism for distributing light gases and energy between the upper and lower volumes is through counter-current natural circulation flow. This is further enforced by the comparisons of the MAAP model without counter-current natural circulation flows for test HM-7, shown in Figures 23, 24, and 25. In this test, there is forced flow imposed by the recirculation fans and it is sufficient such that the counter-current natural circulation flows are calculated to be "flooded" in the representation of the partially opened lower inlet doors of the ice condenser. As shown by these comparisons, the counter-current natural circulation flow plays no role in distributing the energy (gas temperature) and light gas concentration between the lower and upper volumes.

This sensitivity illustration clearly demonstrates the importance of including a representation for counter-current natural circulation flows in containments, especially during the portion of the accident when the air recirculation fans are not active. Without this representation, the containment evaluation under-estimates the potential for distributing light gases through connected volumes.

## 5.0 CONCLUSIONS

These comparisons of the MAAP Generalized Containment Model with the spectrum of test conditions considered for the simulated ice condenser containment in the CSTF vessel show that the MAAP model provides an effective representation of the containment response under both natural circulation and forced flow conditions. Good agreement between the calculated and measured behaviors are obtained for all of the test conditions examined in the CSTF test program and therefore the user has the confidence that the MAAP model can follow the influences of light gas, such as hydrogen, being released to the containment as a consequence of postulated accident sequences. Furthermore, the sensitivity studies performed illustrate the importance of including representations for both forced and natural circulation flows between the containment compartments, including natural circulation counter-current flows through the partially opened doors in the CSTF simulation. Since the expected ice condenser response to small break LOCA conditions is to have lower inlet doors only partially opened, this potential for examining both the forced flow and natural circulation flow is important. Furthermore, it is particularly important to assess the potential for experiencing "flooding" of the gas flow in the partially opened doors as a result of the imposed recirculation flow by the air return fans.

## 6.0 REFERENCE

Bloom, G. R., Muhlestein, L. D., Postma, A. K., and Claybrook, S. W., "Hydrogen Mixing and Distribution in Containment Atmospheres," EPRI Report NP-2669, 1983.

Figure 23:  
Comparison of the Calculated and Measured Gas Temperatures for the Lower Volume  
in CSTF Test HM-7 With Counter-Current Natural Circulation Flows Ruled Out.

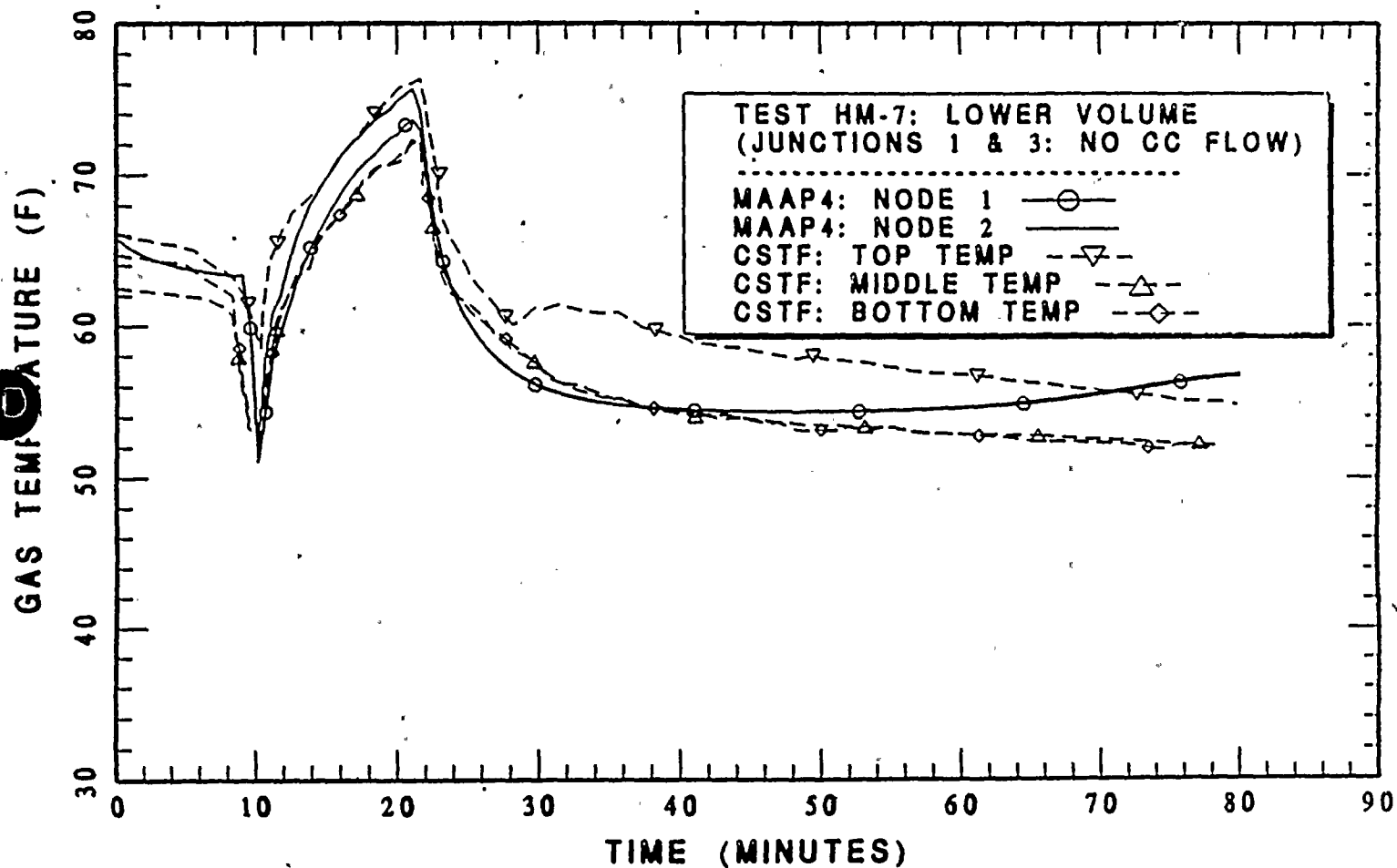


Figure 24:  
Comparison of the Calculated and Measured Gas Temperatures for the Upper Volume  
in CSTF Test HM-7 With Counter-Current Natural Circulation Flows Ruled Out.

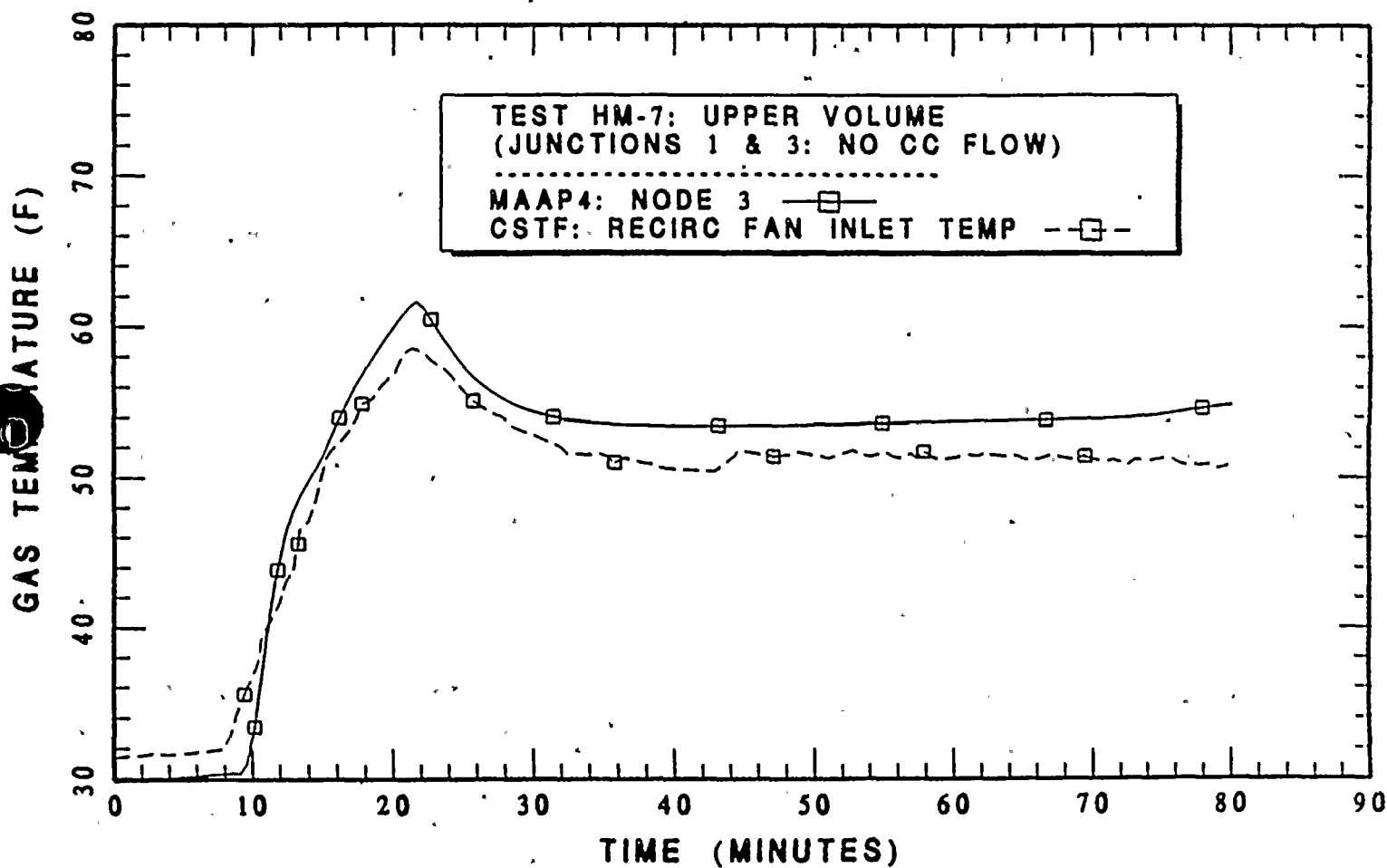
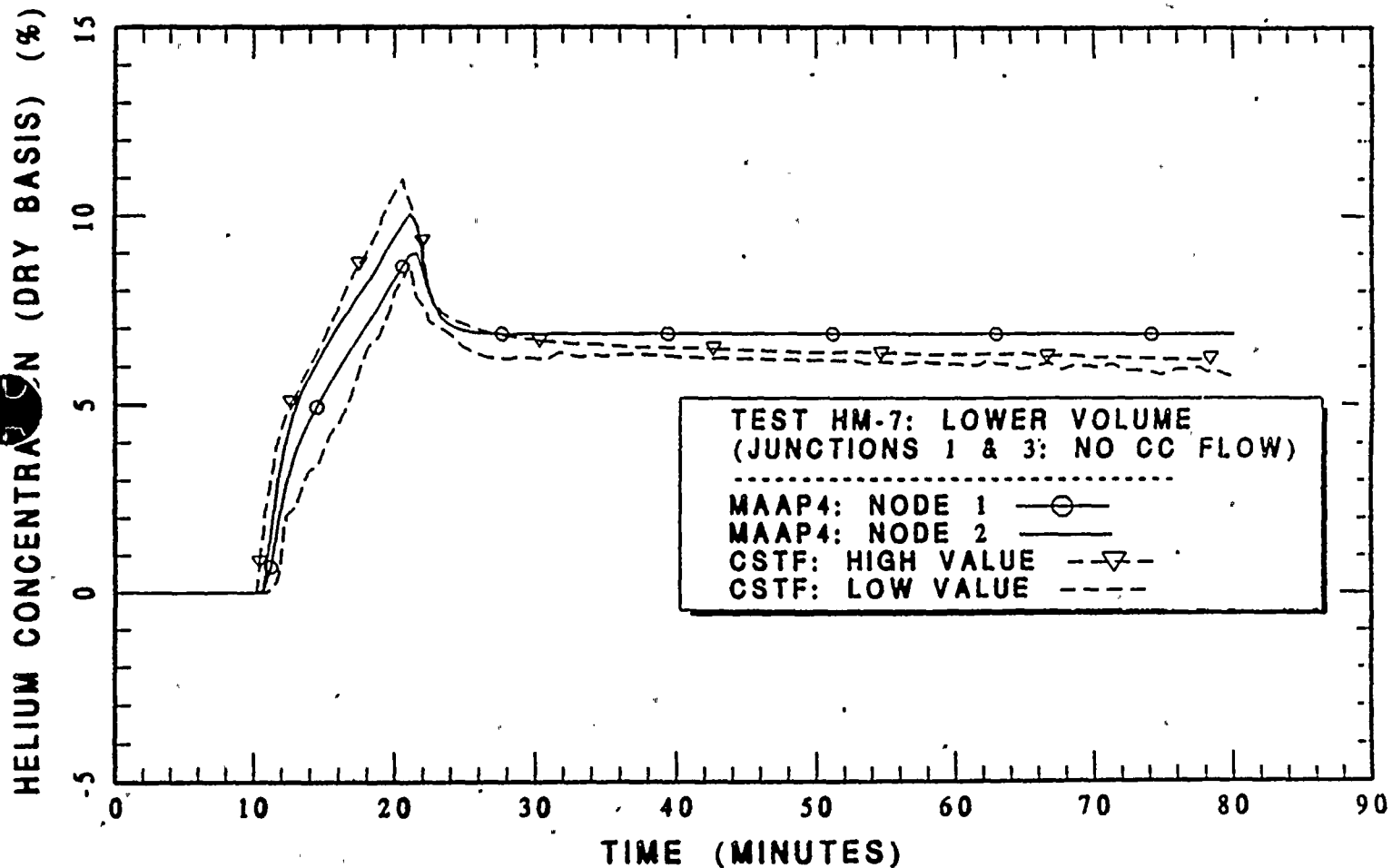




Figure 25:  
Comparison of the Calculated and Measured Helium Concentration in the Lower Volume  
for CSTF Test HM-7 With Counter-Current Natural Circulation Flows Ruled Out.







## APPENDIX H Droplet Fall Velocity

The terminal velocity for a water drop falling through gas can be determined by equating the mass of the droplet with the drag. This is given by

$$(\rho_w - \rho_g) \frac{4}{3} r g = C_D \frac{\rho_g V^2}{2} \quad (H-1)$$

where the terms are defined as

- $\rho_w$  is the water density,
- $\rho_g$  is the gas density,
- $r$  is the droplet radius,
- $g$  is the acceleration of gravity,
- $C_D$  is the drag coefficient, and
- $V$  is the droplet terminal velocity.

Solving for the terminal velocity results in

$$V = \left[ \frac{8}{3} \left( \frac{\rho_w - \rho_g}{\rho_g} \right) \frac{r g}{C_D} \right]^{1/2} \quad (H-2)$$

Note that this equation must be used with a consistent set of units. The drag coefficient is a function of the terminal velocity as indicated by the curve shown in Figure H-1 which is taken from Vennard (1959). Since the drag coefficient is a function of the velocity (Reynolds number  $N_R = Vd \rho_g / \mu_g$ ) this has to be solved in an intricate manner (the term  $\mu_g$  is the gas dynamic viscosity). For the 700 micron spray droplet size given in the D.C. Cook FSAR, it is found that the terminal velocity is approximately 10 ft/sec and the drag coefficient is unity. This corresponds to a terminal velocity of 600 ft/min, which is a convenient value since the typical volumetric water flow rates are specified in gpm. Hence, the airborne water mass from a given containment spray



# FLUID FLOW ABOUT IMMERSED OBJECTS

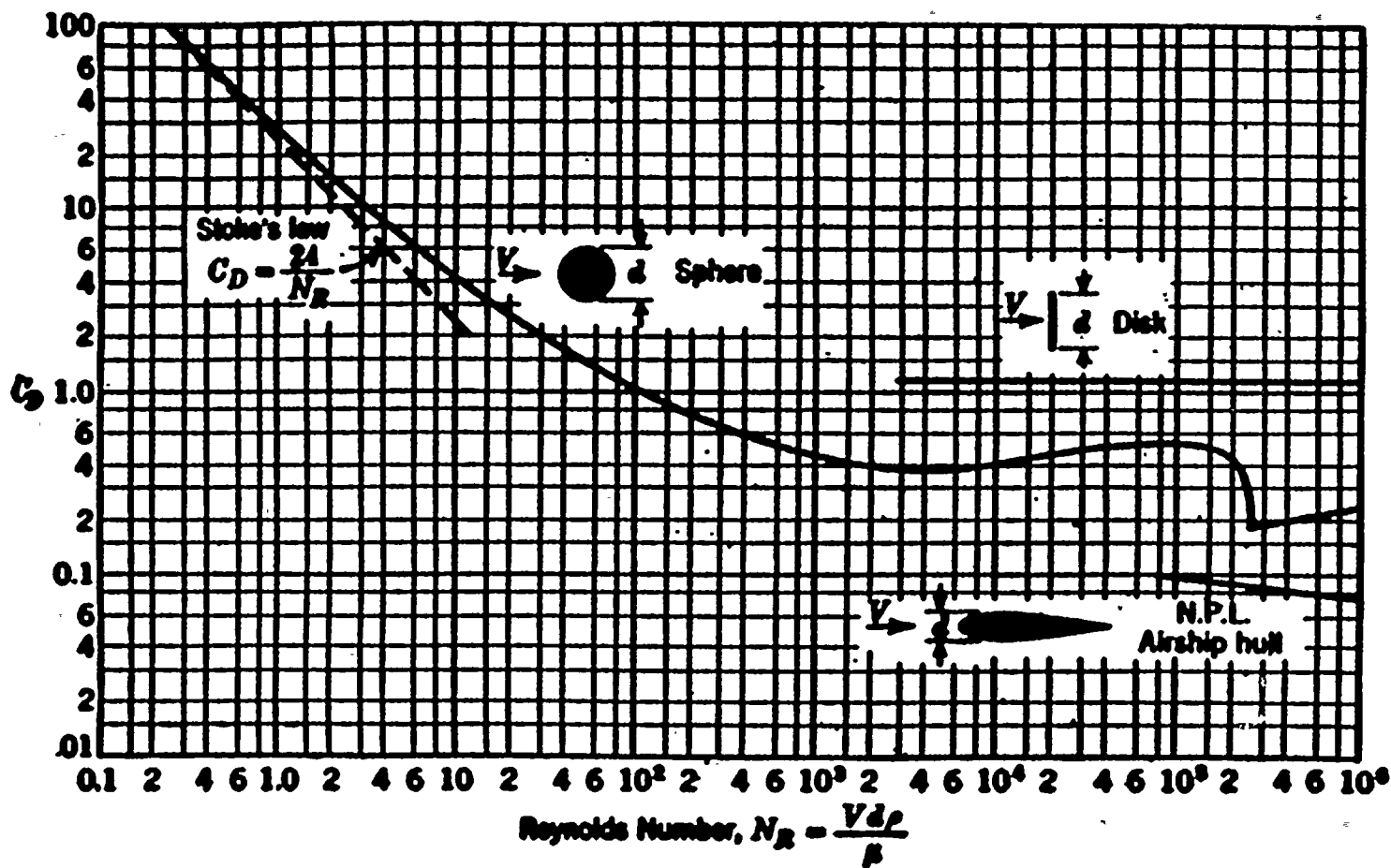


Figure H-1 Drag coefficient for sphere, disk, and streamlined body as represented in Vennard (1959).

is dependent upon the fall height for the spray and can be estimated from the equation

$$Q \text{ (gal)} = \dot{Q}_v \text{ (gpm)} \cdot h/V_1 \quad (\text{H-3})$$

where the terms have the following definitions

- $h$  is the droplet fall height for the compartment,
- $Q$  is the airborne water volume in gallons,
- $\dot{Q}_v$  is the spray flow rate in that compartment in gpm, and
- $V_1$  is the droplet terminal velocity in ft/min.

This is the approach used to assess the airborne water volumes due to the spray flow actuation for the three different compartments of interest.

#### Reference

Vennard, J. K., 1959, Elementary Fluid Mechanics, Third Edition, John Wiley & Sons, Inc., New York.

## APPENDIX I Water Film Drainage Analysis

As part of the evaluation for water holdup in containment, this analysis considers that some of the spray flow rate in each compartment would impinge upon structure walls and undergo holdup due to film drainage on these walls. This is addressed through a Nusselt laminar film calculation for the drainage, which is conservative (overstates the water mass) since this dynamic interaction would tend to promote turbulent film drainage.

The maximum laminar flow drainage film thickness is given by

$$\delta_{\max} = \left[ \frac{3 \dot{m}_L \mu_w}{\rho_w^2 g} \right]^{1/3} \quad (\text{I-1})$$

as represented by Kreith (1960). The variables in this equation are:

- $g$  is the acceleration of gravity,
- $\dot{m}_L$  is the drainage flow rate per unit length (perimeter) of wall,
- $\rho_w$  is the water density, and
- $\mu_w$  is the water dynamic viscosity.

As indicated by this expression, the film thickness on the wall is weakly dependent upon the water flow rate. Hence, this is not particularly sensitive to the evaluation of how much of the spray flow rate contacts the available walls in a compartment. This expression represents the maximum film thickness at the bottom of the compartment. The average film thickness is approximated as two-thirds of the maximum value. For the parameters of interest here, a typical film thickness for laminar drainage would be about  $200 \mu\text{m}$  (0.008 in). This average film thickness is then applied to the wall area in each of the three compartments to determine the holdup that should be considered in each compartment. These are then summed to determine the water mass that is assumed to remain in the RWST in the MAAP4 analyses.

**Reference**

Kreath, F., 1960, Principles of Heat Transfer, International Textbook Company, Scranton, PA.



ATTACHMENT 8 TO C1099-08

MPR ASSOCIATES, INCORPORATED

"CONTAINMENT SUMP LEVEL DESIGN CONDITION  
& FAILURE EFFECTS ANALYSIS  
FOR POTENTIAL DRAINDOWN SCENARIOS"